PhD degree in Molecular Medicine

European School of Molecular Medicine (SEMM),

University of Milan and University of Naples "Federico II"

Faculty of Medicine

Settore disciplinare: BIO/11

Mechanisms controlling the integrity of converging forks during replication termination

Ramveer Choudhary

IFOM-IEO Campus, Milan

Supervisor:

Prof. Marco Foiani

IFOM-IEO Campus, Milan

Anno accademico 2017-2018

Table of contents

I) Acknowledgments

II) List of Abbreviations

II) Figures Index

1. Abstract …… 1

2. Introduction…… ……2

2.1 The yeast *Saccharomyces cerevisiae* cell cycle and the DNA damage checkpoint……2

2.2 DNA replication initiation and S-phase dynamic. ……3

2.3 Lagging and Leading strand DNA synthesis:……4

2.4 The topology of replicating chromosomes. ……8

2.4.1 Topoisomerases in DNA repl**ication.……8**

2.4.2 Termination and chromosome segregation**……**10

2.4.3 Topoisomerases and transcription……10

2.5 Condensin complex and topology during transcription……12

2.6. Natural impediments to DNA replication……15

2.6.1 Transcription……15

2.6.2 Coordinating Transcription and Replication……16

2.6.3* Activities controlling R loops *in vivo……18

2.6.3.1 Removal of R loops by ribonucleases and helicases**……18**

2.6.3.2 Negative DNA supercoiling facilitates R-loop formation**……19**

2.6.3.3: mRNP biogenesis protects against R-loop formation. **……20**

2.6.4 Transcription Termination and R-loop Resolution ……21

2.6.5 Gene gating, R-loop Resolution and Replication fork collision. ……23

2.6.6 Replication-Associated Mechanisms to Overcome Conflicts ……25

2.6.6.1 Auxiliary Helicases **……25**

2.6.6.2 S-phase Checkpoint **……25**

2.6.6.3 Replication Restart and DNA Repair **……28**

2.7 Pathological Outcomes of the Topological Interference between Replication and Transcription ……30

2.8 Replication Barriers Associated with Repeat DNA and Protein–DNA Complexes……31

2.8.1. Telomeres……31

2.8.2 rDNA Repeats……32

2.8.3 Centromeres ……32

2.8.4 tRNA Genes and LTR Retrotransposons……32

2.8.5 DNA Barriers of Repetitive DNA and Secondary Structures……33

2.9. Replication stress and fragile site expression……33-35

2.9.1 CFSs are late replicating due to hard to replicating nature……34

2.9.2 CFSs are enriched in large genes transcribing even during S phase…34

2.10 Under-replicated genome in S-phase and Mitosis at CFSs:……35

2.11. Targeting DNA replication stress for cancer therapy:……38

2.12. Conclusions and perspectives……39

3. Results Chapter 1:

Natural chromosomal pausing sites are endogenous fragile sites prone to accumulate CNVs under replication stress. ……(40- 52)

1.2 Genome wide mapping of CNVs under mild replication stress in wild type cells……42

1.3 Reduced level of DNA Pol α make TERs fragile……44

1.3. Tel1 and Mec1 control CNVs at natural chromosomal pausing sites, RFBs and TERs……45

1.3.1 Rad53 suppresses CNVs in proliferating cells under replication stress……45

1.3.2 *rad53 sml1* and *tel1 mec1 sml1* experiencing mild replication stress (25mM HU) showed major genomic CNVs……47

1.3.3 Tel1p/Mec1p control the fragility of Replication Termination Zones (TERs)..49

1.4 Topological constrain at TERs accumulate replication intermediates and breaks in Replication checkpoint deficient strains under replication stress…50

1.5 Conclusion……52

Results chapter 2: Condensins control the integrity of natural fork pausing elements and TERs……(53-61)

2.1 Bnr1 enriches at natural chromosomal pausing sites, highly transcribing ORFs and TERs……54

2.2 Bnr1p interacts with transcribed genes……55

2.3 Brn1p localizes at different natural chromosomal pausing sites including TERs……56

2.4 Depletion of condensin complex subunits (Ycg1p or Ycs4p1) causes chromosomal segregation defects and replication checkpoint activation……57

2.5 Mapping genome-wide fragile sites in *Ycg1^{dg} and Ycs4^{dg}* strains in the presence of mild replication stress……58

2.6 TERs are fragile in the absence of Condensin subunits (Ycg1p and Ycs4p)..60

2.7 Conclusion……..61

Results chapter 3: ……..(62-75)

PIF1 family helicase Rrm3p counteracts the accumulation of RNA-DNA hybrids at natural chromosomal pausing sites and TERs……

3.1 RRM3 showed strong binding pattern, at natural chromosomal pausing sites (CPSs) and replication fork barriers (RFBs)……..64

3.2 Rrm3 suppresses RNA-DNA hybrid accumulation at different pausing elements……65

3.3 Transient RNA-DNA hybrid accumulation during S-phase in Δrrm3 at TERs……..66

3.4 Genome wide CNVs analysis in *rrm3* strain along natural chromosomal pausing sites, replication fork barriers and TERs……..68

3.5 Replication termination zones accumulate all features associated with fork pausing and stalling in *Δrrm3* strains……..69

3.6 Cell cycle progressions is not impaired in *Δrrm3* mutants……71

3.7 Termination zone accumulate Unusual Replication intermediates in *Δrrm3*……72

3.8 Rrm3 and Rad53 interact to resolve unusual replication intermediates at TERs and suppress breakages at TERs……..73

3.9 Conclusion…… 73

Results: chapter 4: ……(75-89)

Senataxin-1 (Sen1p) suppresses genomic copy number variations at transcribing natural chromosomal pausing sites and TERs

4.1 Sen1p is required for recovery from HU……78

4.2 Sen1p expression though-out cell cycle……..79

4.3 Depletion of Sen1p causes replication checkpoint activation and G2/M arrest under replication stress……79
4.4 Different transcribing natural chromosomal pausing sites exhibit enrichment for Sen1p under replication stress……80
4.5 Genome wide enritchement of R-loops in the absence of Sen1p…… 82
4.6 CNVs mapping in sen1^{dg} under mild replication stress……83
4.7 CNVs in sen1^{dg} strains localize at Sen1-FLAG binding sites and R-loops in sen1^{dg} mutants……84
4.8 Termination Zones accumulate R-loops in sen1^{dg} strains……85
4.9 TERs are fragile in sen1^{dg} strains under replication stress……86
4.10 Sen1p suppresses breaks at TERs during mitotic phase of cell cycle under replication stress……87
4.11 Conclusion……89

Results: chapter 5:……(90-111)
Rrm3 and Sen1 assist replicon fusion at Termination Zones
5.1 Double mutant *sen1^{dg}* rrm3Δ exhibit a first cell cycle arrest in G2/M…..90
5.2 Double mutant sen1^{dg}rrm3Δ showed arrest from metaphase to anaphase with lagging chromosomes mimicking anaphase bridges……91
5.3 sen1^{dg}rrm3Δ do not alter replication initiation at ARSs……92
5.4 Double mutant *sen1^{dg}rrm3Δ* strains accumulate unresolved replication termination intermediates……93
5.5 *sen1^{dg}rrm3Δ* mutants accumulate RNA-DNA hybrids at different chromosomal pausing sites, RFBs and TERs……94
5.6 DRIP-pPCR captures transient RNA-DNA hybrids accumulation at TERs during S-phase in absence of Sen1p and Rrm3p……96
5.7 Common interactors between Sen1 and Rrm3 helicase indicates different pathways might be involved in replication fork metabolism at TERs……97
5.8 Origin firing is not affected in *sen1^{dg}rrm3Δ* strain under replication stress……98
5.9 sen1^{dg}rrm3Δ mutants accumulate copy number variations……99

5.10 Mild replication stress accumulates DSBs at TERs in sen1^{dg}rrm3Δ during the S-phase……101
5.11 Characterization of replication intermediates in *sen1^{dg}rrm3Δ* by EM…103
5.12 Depletion of Condensin complex subunits Ycg1p and Ycs4p rescues cell cycle arrest of sen1^{dg} rrm3Δ……105
5.13 Depletion of Condensins subunit Ycg1p or Ycs4p rescues G2/M arrest and resolves unusual replication intermediates at TERs in sen1^{dg}rrm3Δ……106
5.14 Absence of Condensins suppresses R-loop accumulation at TERs in sen1^{dg}rrm3Δ……107
5.15 Absence of Condensins suppresses DSBs accumulation at TERs in double mutant sen1^{dg}rrm3Δ under mild replication stress……109
5.16 Conclusion……111

4. Materials and methods ……(109-139)
4.1 *S. cerevisiae* strains……112
4.2 Growth media and buffers composition for *S. cerevisiae*……113
4.3 Buffers……113.

4.4 Yeast transformation (PCR cassette or plasmid)……114

4.5 Cell cycle arrest……114

4.6 Total protein extract with TCA……115

4.7 Western blot protocol (SDS-PAGE)……115
4.8 FACS (Fluorescence activated cell sorter) analysis……116
4.9 Spot assay……117

4.10 DAPI and tubulin staining ……117
4.11 ChIP-on-chip……117

4.12 DRIP with DNA:RNA hybrids precipitation……126

4.13 GIP analyses and statistical methods……129

4.14 In-vivo psoralen crosslinking of the DNA……129

4.15 Genomic DNA extraction with the Qiagen genomic Kit……131

4.16 Analysis of replication intermediates by two-dimensional agarose gel electrophoresis (2D gel)……132

4.17 PFGE procedure……138

4.18 Scoring Copy number variation with Next generation sequencing……140

5. Discussion:……(143-148)

5.1. Checkpoint kinases counteract fragility of endogenous natural pausing elements and TERs……143

5.2 Condensin complex control fragility at natural chromosomal pausing sites and TERs……145

5.3. Rrm3 is required for fork protection at natural pausing sites and TERs……145

5.4. Sen1 prevents R-loop accumulation at TERs and collaborates with Rrm3 in mediating replication termination……146

5.5. Programmed fork pausing and resolution of R-loops are key processes for TER integrity……146

6. References:……149-162

I) Acknowledgments

I dedicate this thesis to my mother **Jaina Devi** for her unconditional love and support. She taught me importance of hardworking and believing in yourself when nothing working (Typical scenario for PhD life).

I would like to express my sincere gratitude and respect to **Prof. Marco Foiani**, for the having faith in me and providing opportunity to work with him in fun and intellectual atmosphere while doing research. He has been great example of being humble and respectful towards colleagues and pursuing novel ideas in the field.

I owe special thanks to my admirable all friends in campus and all **MF research group members** for amazing scientific and social environment.

II) List of Abbreviations

2D-gel Two Dimensional Agarose Gel Electrophoresis

ARS Autonomously Replicating Sequence

ATR Ataxia Telangiectasia and Rad3-related protein

BSA Bovine Serum Albumin

BrdU 5-bromo-2'-deoxyuridine

BPB Bromophenol blue

ChIP-on-chip Chromatin Immunoprecipitation on chip

DAPI 4',6-diamidino-2-phenylindole

DDT DNA Damage Tolerance

ddH2O double-distilled H2O

DMSO Dimethyl Sulfoxide

dsDNA double-stranded DNA

DTT Dithiothreitol

DSB Double Strand Break

DRIP DNA-RNA hybrid Immunoprecipitation

EDTA Ethylen Diammino Tetraacetic Acid

Gal Galactose

Glu Glucose

GIP Genomic ImmunoPrecipitation

HJ Holliday Junction

HR Homologous Recombination

HU Hydroxiurea

MOPS 3-morpholinopropane-1-sulfonic acid

mRNA messenger RNA

NGS next generation sequencing

NSE:Non Smc Element

O/N Overnight

ORF Open Reading Frame

PEG Polyethylene glycol

PFGE Pulse Field Gel Electrophoresis

PRR Post Replication Repair

RFB: Replication Fork Barrier

rcf relative centrifugal force

rpm revolutions per minute

RNAPII RNA polymerase II

RT Room Temperature

SDS Sodium Dodecyl Sulphate

SDS-PAGE SDS-Poly-Acrylamide Gel Electrophoresis

SSC Saline-Sodium Citrate

ssDNA single-stranded DNA

SUP Supernatant

SCIs Sister Chromatid Intertwinings

SCJs Sister Chromatid Junctions

SGA Synthetic Genetic Array

SMC Structural Maintenance of Chromosome

STR Sgs1-Top3-Rmi1

TBS Tris-buffered saline

TBST TBS + Tween 20 0.1%

TdT Terminal deoxynucleotidyl transferase

TE Tris-EDTA **TER** Termination zone

Triton X-100 polyethylene glycol p-(1,1,3,3-tetramethylbutyl)-phenyl ether

Tween 20 Polyoxyethylene (20) sorbitan monolaurate

TLS Translesion synthesis

TS Template Switching

Wt wild-type

YNB Yeast Nitrogen Base

YPD (YEPD) Yeast Extract Peptone Dextrose

YPG (YEPG) Yeast Extract Peptone Galactose

III) Figures Index

Introduction :……..(2-39)

Model 1: Schematic representation of the DNA replication initiation and elongation process……
Model2: Functions of topoisomerases at different steps of DNA replication.
Model 3: Topoisomerases and interplay with transcription.
Model 4: A model for the loading of condensin at gene promoters.
Model 5: Head-on and Co-directional Transcription-Replication Conflicts
Model 6: Cellular activities limiting R-loop accumulation in defective RNA biogenesis
Model 7: the association of promoter and terminator regions establishes Gene Gating and Replication Forks collision in loops
Model 8: Replication-Associated Mechanisms to Prevent and Resolve TRCs.
Model 9. Pathological Events Caused by Replication and Transcription Interference
Model 10. Replication stress, genomic instability and fragile sites expression.
Model 11: Examples of DNA structures arising in S-phase under replication stress that may cause problems for chromosome segregation in mitosis unless resolved
Model: 12 Therapeutic agents that enhance replicative stress.

Results: Chapter 1: ……..(40- 52)

Figure 1. Mild replication stress accumulates Genome wide CNVs (deletion and amplification) at affecting most of natural chromosomal pausing sites.
Figure 2: Replication Termination Zones are fragile sites.
Figure 3: Mapping genome wide CNVs in Rad53K227A strain under replication stress.
Figure 4: Mapping genome wide CNVs in *rad53 sml1* and *tel1mec1 sml1* strains under replication stress.
Figure 5: Replication Checkpoints (Mec1p/Tel1p) suppresses fragility and higher molecular weight Replication Intermediates at TERs in presence of mild replication stress.
Figure 6: Top2p and Replication Checkpoint proteins interact to preserve DNA breaks and Replication Intermediates at TERs.

Results: Chapter 2: ……..(53-61)

Figure 2.1 Bnr1 enriches at natural chromosomal pausing sites, highly transcribing ORFs and TERs.
Figure 2.2. Dynamic nature of Brn1p along ORFs forms TSS to TTS.
Figure 2.3. Different natural pausing sites showed increased association with Brn1P under replication stress.
Figure 2.4. Depletion of Condensin subunits -Ycg1p and Ycs4p caused segregation defects and replication checkpoint activation.
Figure 2.5. Mapping genome wide CNVs in *Ycg1^{dg} and Ycs4^{dg}* strain with mild replication stress.
Figure 2.6. Distribution of CNVs along different genomic regions and their significant association with amplifications and deletions in *Ycg1^{dg} and Ycs4^{dg}* strains.
Figure 2.7. DSBs accumulation at TER302 in ycg1^{dg} and ycs4^{dg} stain under replication stress.

Results: Chapter 3: ……..(62-74)

Figure 3.1. Rrm3p-FLAG (Chip) binding at different natural chromosomal pausing sites and replication fork barriers under physiological condition.
Figure 3.2. R-loop accumulation at different natural chromosomal pausing sites and Replication termination in absence of rrm3.
Figure 3.3: Transient hybrid accumulation during S-phase in Δrrm3 at TERs
Figure 3.4: Mapping genome wide CNVs under mild replication stress in Δrrm3 cells.
Figure 3.5: Different Features associated with functional Rrm3p at TERs.
Figure: 3.6. Cell cycle progression profile Δrrm3 strain at physiological condition and replication stress induced by HU.
Figure: 3.7. Not Origin firing but Replication termination was impaired in Δrrm3 cells under replication stress.
Figure 3.8: Rrm3p and Replication Checkpoint proteins interact to preserve fragility at TERs including Replication intermediates.

Results: Chapter 4:……..(75-89)
Figure 4.1: Cell cycle progression profile of sen1^{dg} strain in physiological condition and replication stress induced by HU.
Figure 4.2: Sen1p expression during different stage of cell cycle.
Figure 4.3: sen1^{dg} showed increased Checkpoint activation presence of mild replication stress (25mM HU)

Figure 4.4 Different transcribing natural chromosomal pausing sites exhibit enrichment for Sen1p under replication stress.
Figure 4.5. R-loop accumulation at natural pausing sites, RFBs and Replication termination
Figure: 4.6 Meta-analysis of genome wide CNVs in *Sen1^{dg}* strain with mild replication stress.
Figure 4.7: CNVs in sen1^{dg} strains are strongly associated with Sen1p-FLAG protein binding sites and R-loop prone genomic loci
Figure 4.8: replication termination zones (TERs) are strongly associated with Sen1p-FLAG protein binding and R-loop prone genomic loci in sen1^{dg}
Figure4.9: Sen1p preserve fragility at TERs including Replication intermediates.
Figure 4.10: Sen1p suppresses breaks at TERs during mitotic phase of cell cycle under mild replication stress

Results: Chapter 5:……(90-111)
Figure 5.1: Double mutant *sen1^{dg}* rrm3Δ showed G2/M arrest immediately after the first cell cycle under physiological condition.
Figure 5.2: Double mutant sen1^{dg}rrm3Δ shows an arrest from metaphase to anaphase transition with lagging chromosomes, mimicking anaphase bridges phenotype.
Figure5.3: No aberrant replication intermediates accumulation at ARS during gross chromosomal replication in sen1^{dg}rrm3Δ.
Figure 5.4: Double mutant sen1^{dg}rrm3Δ strains accumulate replication termination intermediates during physiological cell cycle.
Figure 5.5. R-loop accumulation at TERs and different natural chromosomal pausing sites in *sen1^{dg}rrm3Δ* during S-phase.
Figure 5.6: DRIP-pPCR captures transient R-loop accumulations at TERs during the S-phase in absence of Sen1p and Rrm3p.
Figure 5.7: Common interactors between Sen1 and Rrm3 helicases indicated that different pathways are involved in the replication fork metabolism.
Figure 5.8: Origin firing at ARS305 was not impaired in absence of sen1^{dg}rrm3Δ under replication stress.
Figure 5.9: Mapping genome wide CNVs under mild replication stress in sen1^{dg}rrm3Δ.
Figure 5.10: Mild replication stress accumulates DSBs at TERs in sen1^{dg}rrm3Δ during S-phase of cell cycle.
Figure 5.11. sen1 rrm3 cells accumulate TERs with long ssDNA regions at the fork fusion point

Figure 5.12: Depletion of Condensin complex subunits Ycg1p and Ycs4p rescues physiological cell cycle arrest of sen1^{dg}rrm3Δ.
Figure 5.13: Condensin subunits Ycg1p and Ycs4p caused accumulation of aberrant replication intermediates at TERs in sen1^{dg}rrm3Δ.
Figure 5.14.1: DRIP-pPCR captures transient R-loop accumulations at TERs during S-phase in sen1^{dg}rrm3Δ, but is rescued by depletion of Ycg1p.
Figure 5.14.2: Spot assay based viability in different genotypes.
Figure 5.15: Absence of Condensin complex suppresses DSBs accumulation at TERs in double mutant sen1^{dg}rrm3Δ under mild replication stress, and epistasis interaction with replication checkpoints.

Materials and methods: ……..(112-142)

Table 1. Genotypes of the strains used in this study……..

Model 4.1: Schematic representation of the replication and repair intermediates analyzed by 2D gel electrophoresis.

Model 4.2: CNV-seq, a new method to detect copy number variation using high-throughput sequencing

Discussion: ……..(140-145)

Model 5.1: Different steps of events at TERs preserving genomic integrity……..

1. Abstract

Mechanisms controlling the integrity of converging forks during replication termination

During S phase, natural fork pausing elements including replication termination zones (TERs) and transcribed genes, can easily lead to genotoxicity and chromosome fragility at fragile sites (CFs), known as hotspots for DNA breaks and chromosomal rearrangements, particularly in cancer cells. However, the key factors and pathways protecting the integrity of CFSs are not well understood. In order to elucidate these mechanisms, we used yeast as a model system, and combined genetic and genomic studies aimed at identifying fragile sites genome-wide.

We found that centromeres, rDNA, telomeres and TERs represent hot spots for copy number variation (CNV) in wild-type yeast cells exposed to replication stress. We found that top2 contributes to relieve the topological stress and extensive fork pausing during termination at TERs. We also observed that fragility at these sites is greatly enhanced in checkpoint mutants ($Tel1^{ATM1}$ and $Mec1^{ATR1}$), likely due to their inability to uncouple transcription from gene gating, thus leading to topological stress in front of replication forks. TER fragility in checkpoint defective cells can be partially rescued by Top2 and Condensin complex inactivation.

We further demonstrated that Pif1 family helicase, Rrm3, regulate extensive fork pausing at TERs and endogenous pausing sites by suppressing RNA-DNA hybrid (R-loops) accumulation. Alongside, a RNA-DNA helicase Senataxin1 (Sen1) coordinates replication and transcription collision at TERs and endogenous fork pausing. Absence of Sen1 accumulates CNVs at TERs and double-strand DNA breaks. We show that programmed fork pausing and resolution of R-loops are key processes for TER integrity. Accordingly,, *sen1 rrm3* double mutants, accumulate gaps and RNA-DNA hybrids at TERs and fail to fuse replicons; moreover, these mutants exhibit unscheduled condensation events at *TERs* leading to chromosome entangling. Taken together, our data strongly suggests that, the replication checkpoint, Sen1 and Rrm3, coordinate replication termination to prevent accumulation of unsolved topological constrains and premature recruitment of Condensins and Top2.

2. INTRODUCTION

2.1 The yeast *Saccharomyces cerevisiae* cell cycle and the DNA damage checkpoint.

The cell cycle is an ordered succession of events that subsequently occur in proliferating cells. Two daughter cells are generated from a mother cell during the cell division that possesses all the information to repeat the process. Thus, during cell division, all cellular components must be duplicated and transmitted correctly to the daughter cells. The most important element is the genetic information (DNA), which must be accurately duplicated in a process called DNA replication. The two copies are then packed and segregated carefully to the two daughter cells. DNA synthesis and chromosome segregation take place in two distinct phases of the cell cycle, the first during S-phase, while the latter occurs during mitosis (or M phase), where the cells physically divide in a process termed cytokinesis. Those two phases are separated by two additional gap phases, called G1 and G2, in which cells undertake all the metabolic reactions necessary for the next cell cycle stage. The cell cycle can be therefore divided in four phases, the G1 (synthesis of cytoplasmic proteins takes place) the S-phase (DNA replication), the G2 phase (the preparation of the mitotic apparatus) and the M phase, (where chromosomes segregate and cells divide).

Defective replication or unbalanced segregation of the chromosomes that lead to mutations and chromosomal aberrations causing genetic diseases and cancer (Hartwell and Kastan 1994, Roche and Lowndes 2007). To preserve the integrity of the genome, cells have developed surveillance mechanisms that regulate the order and timing of cell cycle transitions, and coordinate the cellular response to DNA damages and/or events that perturb replication, referred to as DNA damage checkpoint (Hartwell and Weinert 1989, Weinert and Hartwell 1989, Elledge 1996). The checkpoint pathways were initially described as limited to the transduction of a signal required to arrest the cell cycle progression, thus providing time for the cells to repair DNA lesions (Hartwell and Weinert, 1989). However, the current scenario is that the checkpoint acts as a much more complex response that cooperates with multiple cellular pathways to modulate the cellular physiology with the final objective to sustain cell viability and genome integrity (Branzei and Foiani 2009, Labib and De Piccoli 2011). The checkpoints pathway is very

well conserved throughout eukaryotes and acts in late G1, in S and in G2/M, different phases of the cell cycle.

2.2 DNA replication initiation and S-phase dynamic.

Eukaryotic cells initiate DNA synthesis from hundreds of replication origins distributed over the different chromosomes covering whole genome. The temporal and spatial program of origin activation (firing); is imposed by well-defined cis-acting sequence features. The chromosomal sequences required for an origin of replication are different between different eukaryotic organisms with few key similarities. In the unicellular eukaryote *S. cerevisiae*, three to four DNA sequences of 10–15 base pairs spread over 100–150 bp act as an origin and include the highly conserved and essential **A**utonomously **R**eplicating **S**equence (ARS) (Newlon, Collins et al. 1993, Newlon and Theis 1993).

Pre-replicative complex (pre-RC) select DNA replication initiation regions, ARSs in the G1 phase of the cell cycle. ARSs recruits pre-RC complex in sequential events. The pre-RC is composed complex of initiator proteins: origin recognition complex (ORC) (Bell and Stillman 1992, Stillman, Bell et al. 1992), Cdc6, Cdt1, Cdc7-Dbf4 and the MCM complex (Mechali 2010). ORC is a six-proteins (Orc1-6) complex and all proteins are present in an equal stoichiometry. The complex is conserved throughout evolution but the sequence of all subunits is very different among eukaryotic organisms. The ORC remains bound to the replication origin during the entire cell cycle (Liang, Weinreich et al. 1995, Weinreich, Liang et al. 1999). Cyclin-dependent kinases (CDKs) regulate phosphorylation of the ORC subunits and their binding to chromatin in cell cycle dependent manner. Doing so CDKs prevents the re-replication of the genetic material during the same cell cycle (Nguyen, Co et al. 2001).

After DNA double helix unwinding, the pre-RC complex is disassembled and replaced by another set of proteins initiating DNA synthesis process that form pre-Initiation Complex (pre-IC). Removal of Cdc6 and Cdt1 lead to the transition between Pre-RC and Pre-IC, which is followed by the recruitment of replication initiation proteins: Mcm10, Cdc45, Sld3, Dpb11 and GINS in sequential manner and phosphorylation status can be regulated.

Mcm10 has been found in the same screen together with MCM2-MCM7 genes in *Saccharomyces cerevisiae*. Mcm10 is tightly associated with the nuclear chromatin and the

MCM complex (Merchant, Kawasaki et al. 1997). The timing of recruitment of Mcm10 to the chromatin differs among organisms and highly linked to genomic landscape. In *Saccharomyces cerevisiae* Mcm10 acts as a pre-RC component and anchors the Mcm2-Mcm7 complex to the replication origin during G1 phase (Kawasaki, Hiraga et al. 2000). In contrary, in *Xenopus laevis* the Mcm10 recruitment occurs after the MCM complex loading onto DNA.

Cdc45 is essential gene and play main function of DNA replication initiation in yeast (Mimura, Masuda et al. 2000). Cdc45 associates with pre-RC in G1 phase and binds to the MCM complex (Aparicio, Weinstein et al. 1997). This interaction is stable association with total chromatin and connected with S-CDKs activation at the G1/S transition (Zou and Stillman 1998). Cdc45 physically interacts with Mcm2 and serves as a linker between the pre-RC and the pre-IC. The loadings of Cdc45p and DNA Polα onto late origins are inhibited in a Rad53-dependent manner (Aparicio, Weinstein et al. 1997). The association of RPA with late origins is similarly blocked (Tanaka and Nasmyth 1998). These interactions maintain as spatial and temporal origin firing pattern that can be modified depending on physiological and pathological cellular proliferation.

Throughout the cell cycle in *Saccharomyces cerevisiae*, Cdc45 interact with Sld3 and form a complex, this interaction is essential for its association with the MCM complex (Kamimura, Tak et al. 2001). Sld3-Cdc45 binds to ORIs through MCM proteins and the complex is crucial for origin unwinding in the initiation step of DNA replication after recognition of ARSs (Kamimura, Tak et al. 2001).

Dpb11 suppresses mutations of two essential subunits in DNA polymerase II (ε) in budding yeast. It senses stalled replication forks in S phase and transmits the signals to the checkpoint machinery (Araki, Leem et al. 1995). Another component of the pre-IC is GINS complex, which is composed of four proteins: Psf1, Psf2, Psf3 and Sld5. This multi-protein complex is required during replication initiation and most probably during DNA synthesis (Takayama et al., 2003). GINS complex affects Sld3-Cdc45, Dpb11 and Pol ε binding onto DNA. These proteins assembling occur in a mutually dependent manner to initiate DNA duplex synthesis.

2.3 Lagging and Leading strand DNA synthesis:

Antiparallel orientation of the leading- and the lagging-strand in DNA duplex challenge highly conserved principles of DNA replication direction. The DNA template unwinding followed with polymerization of the daughter strands in 5' to 3' direction are the main two processes that DNA replication is based on. The enzymes responsible for uncoupling the DNA duplex are protein helicases associated with replisome , whereas the DNA strand synthesis reaction is carried by DNA replicative polymerases. The DNA unwinding in both directions generates ssDNA, which is immediately bound by RPA proteins (Tanaka and Nasmyth 1998). RPA complex is composed of three subunits: Rfa1, Rfa2 and Rfa3. RPA mediates binding of Dpb11 protein, which is essential for DNA polymerases loading onto DNA. Thus, the coordinated action between DNA helicases and polymerases allows the generation of two copies of the parental genome.

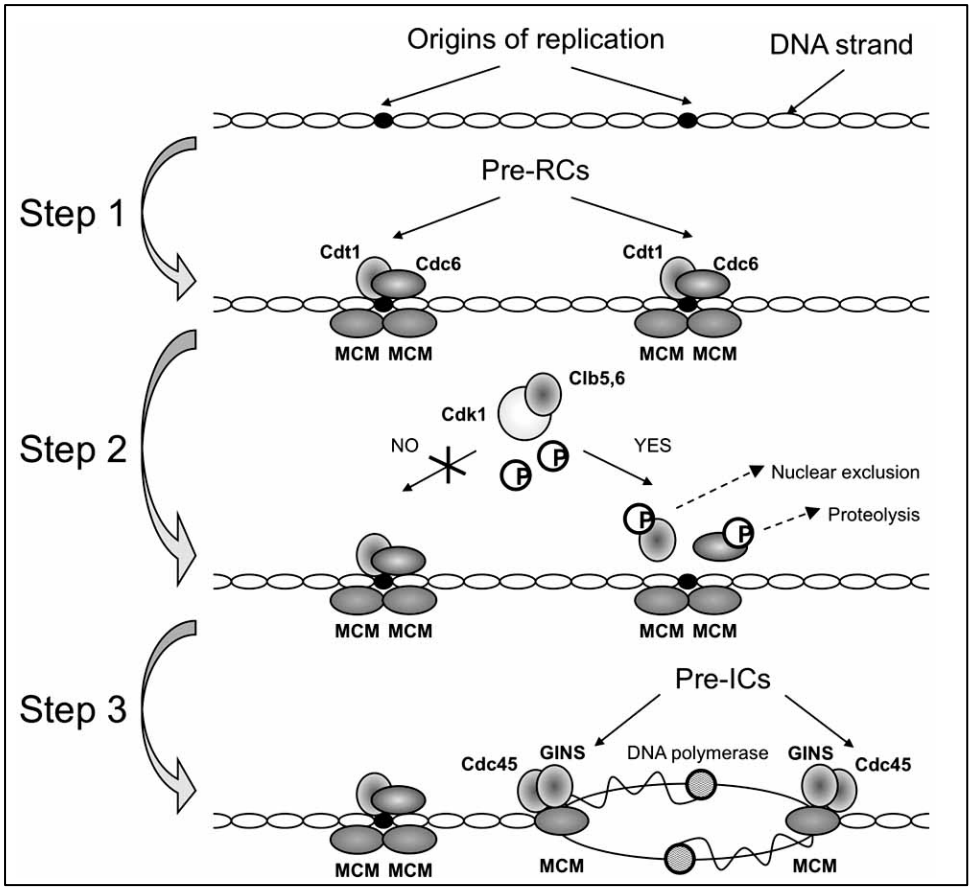
DNA polymerases are highly specialized enzymes that processed along a single-stranded DNA molecule and recruit free dNTPs to hydrogen bond with their complementary dNTP on the single parental DNA strand. In Eukaryotes, the main players in the canonical mode of DNA synthesis are five DNA polymerases: α, β, δ, ε and γ. Polymerase γ is responsible for the mitochondrial DNA synthesis while the others are located in the nucleus and are essential in the nuclear DNA duplication during S-phase. Because DNA polymerases require a primer from which the DNA synthesis reaction initiates, polymerase α (Pol α) functions as a replicative primase (Fisher et al., 1979) and it is the only eukaryotic polymerase that can start DNA synthesis *de novo*. Pol α is composed of four subunits that create a complex, which is essential in the DNA replication initiation and Okazaki fragments synthesis on the lagging strand of the replication fork. The P180 subunit is required for the polymerase activity, P58 and P48 control the primase activity and the forth B subunit plays an essential role at the early stages of DNA replication (Foiani, Liberi et al. 1995, Marini, Pellicioli et al. 1997). The primase synthesizes a primer containing a short ~10-nucleotide RNA stretch onto which the DNA polymerase adds 10 to 20 DNA bases (Nethanel et al., 1992). This priming process occurs both during replication initiation of the leading-strand synthesis and at the 5' end of each Okazaki fragment formation on the lagging strand. The RNA stretches priming Okazaki fragments are degraded, and extended DNA segments are linked to form a continuous DNA fragment. The process is called "Okazaki fragments maturation" and is mediated by RPA protein

binding, stabilizing DNA:RNA primers and stimulating Dna2 and Fen1 endonuclease activity. By extent of the strand displacement, maturation proceeds by the short or long flap-processing pathway. Fen1 and Dna2 degrade initiator RNA in a short and long flap pathway, respectively (Garg, Stith et al. 2004, Pike, Burgers et al. 2009).

Although Pol α is indispensable in priming DNA synthesis both on the leading- and the lagging strand, it is not able to continue DNA replication. After polymerase switch, Pol ε completes the leading strand replication. Pol δ generates Okazaki fragments during lagging-strand synthesis (Pursell, Isoz et al. 2007, Nick McElhinny, Gordenin et al. 2008)).

Replication forks are encircled by specialized clamps, which are called PCNA (Proliferating Cell Nuclear Antigen). PCNA loading does not occur frequently on the leading strand due to continuous DNA replication since its initiation. In contrary, constant initiation of Okazaki fragment synthesis on the lagging strand requires continual PCNA loading. Replication factor C (RF-C) serves as a clamp loader and consists of five subunits forming a stable ATP- dependent complex with PCNA (Tsurimoto and Stillman 1991), 1990). RF-C recognizes the primer-template junctions, where it loads PCNA. Importantly, when replication must be terminated, clamp loaders unload PCNA from DNA (Yao et al., 2006).

The faithful synthesis of leading- and lagging-strand relies on coordinated action and stable association of DNA polymerases with replication forks. Despite its role in genetic information duplication, DNA synthesis is also needed during DNA repair processes including recombination and lesions-bypass at the damaged DNA site(Conde and San-Segundo 2008). Thus, the polymerases involved in DNA amplification face the immense task to keep the genome intact.



Model 1: Schematic representation of the DNA replication initiation and elongation process. Pre-RC components are recruited to the replication origins during late M and early G1 phases of the cell cycle. At the origins, ORC recruits Cdc6 and Cdt1, which are required for the subsequent loading of the Mcm2–7 complexes.

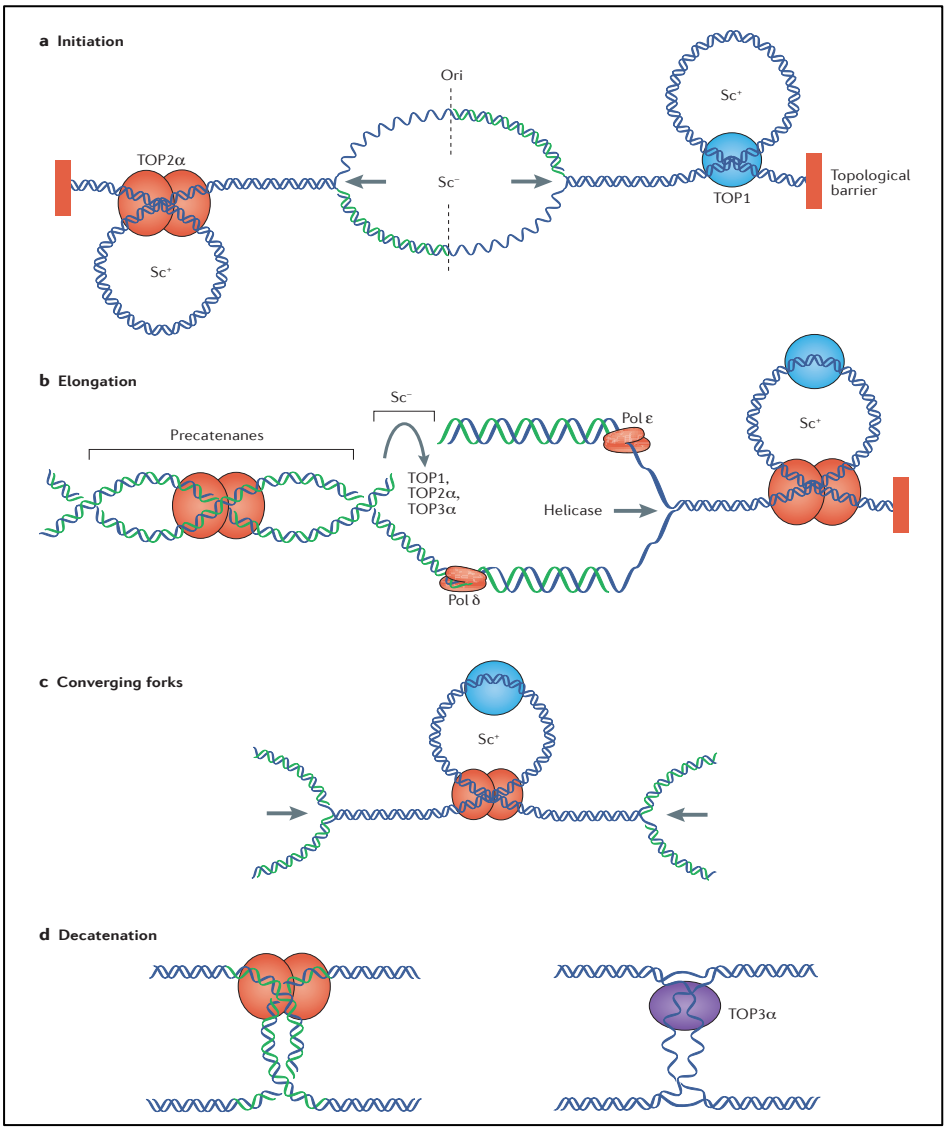
After pre-RC has assembled, its activation during S phase involves the assembly of a second step of factors like Cdc45 and GINS as well as the activity of Cdk1-Clb5,6, which phosphorylates and determines the fate of specific components of the replication machinery. Origin firing and DNA replication then start bi-directionally for leading and lagging strand synthesis **(modified and adapted from Barberis and Klipp, *Genome Inform.* 2007 and *Curr. Genomic*. 2010).**

2.4 The topology of replicating chromosomes.

The DNA double helix contorts and supercoils when is unwound by helicases (Olavarrieta, Hernandez et al. 2002, Fierro-Fernandez, Hernandez et al. 2007, Mayan-Santos, Martinez-Robles et al. 2008) and various topological constraints act on replicating DNA molecules (Postow, Crisona et al. 2001, Postow, Ullsperger et al. 2001). The replicating DNA generates pre-catenanes (+), which intertwine the daughter DNA, and positive supercoils ahead of the replication fork. If those structures are not resolved, the physical link between sister chromatids is established that impedes the accurate chromosome segregation during mitosis (Postow et al., 2004 (Postow, Crisona et al. 2001).

2.4.1 Topoisomerases in DNA replication

The roles of topoisomerases in replication derive extensively from work carried out in *Escherichia coli,* which has shown that topological constraints during replication elongation are managed by the concerted actions of DNA gyrase, which relaxes positive supercoils ahead of the replication fork, and the DNA de-catenation activity of Topo IV(Sissi, Vazquez et al. 2010). Our initial understanding of topoisomerase functions in eukaryotic replication (and chromosome segregation) was based on studies in yeast, in which budding and fission yeast have provided contrasting perspectives. Early experiments in topoisomerase- deficient mutants suggested that neither Top1 nor Top2 was absolutely required for replication initiation or elongation, whereas Top2 was absolutely required for the separation of fully replicated chromosomes. Cells lacking both Top1 and Top2 activities were severely but not entirely deficient in replication elongation(Brill, DiNardo et al. 1987, Brill, DiNardo et al. 1987, Kim and Wang 1989, Kim and Wang 1989), leading to Rad53-dependent DNA damage checkpoint activation (Bermejo, Doksani et al. 2007). These observations led to a model in which either topoisomerase could relieve positive supercoiling arising from replication fork progression. As discuss below, the function of individual topoisomerases during ongoing replication and how topoisomerases are recruited to sites of replication initiation and elongation turned out to be subtler than originally described.



Model2: Functions of topoisomerases at different steps of DNA replication.
A). Initiation of DNA replication requires separation of the two parental strands, which generates negative supercoiling (SC-) at the origin of replication and positive supercoiling (SC+) in the flanking regions owing to topological barriers, such as nuclear matrix attachment sites, insulators, Natural pausing sites, replication fork barriers and Termination zones where the DNA is not free to rotate around its axis. Positive supercoiling is resolved by TOP1 and TOP2α to allow replication fork progression (indicated by the arrows). **B)** Replication elongation generates positive supercoiling ahead of the replication fork and negative supercoiling behind it. Positive supercoiling is removed by TOP1 and TOP2α, whereas negative supercoiling can be removed by TOP1, TOP2α or TOP3α. TOP2α can also remove pre-catenanes, which are formed when the fork rotates during elongation and at Termination. **C)** Converging forks generate high positive supercoiling between them. **D)** Upon replication completion, catenanes are removed by TOP2α (left) and hemi-catenanes are removed by TOP3α (right). **(Modified and adapted from, (Pommier, Sun et al. 2016)**

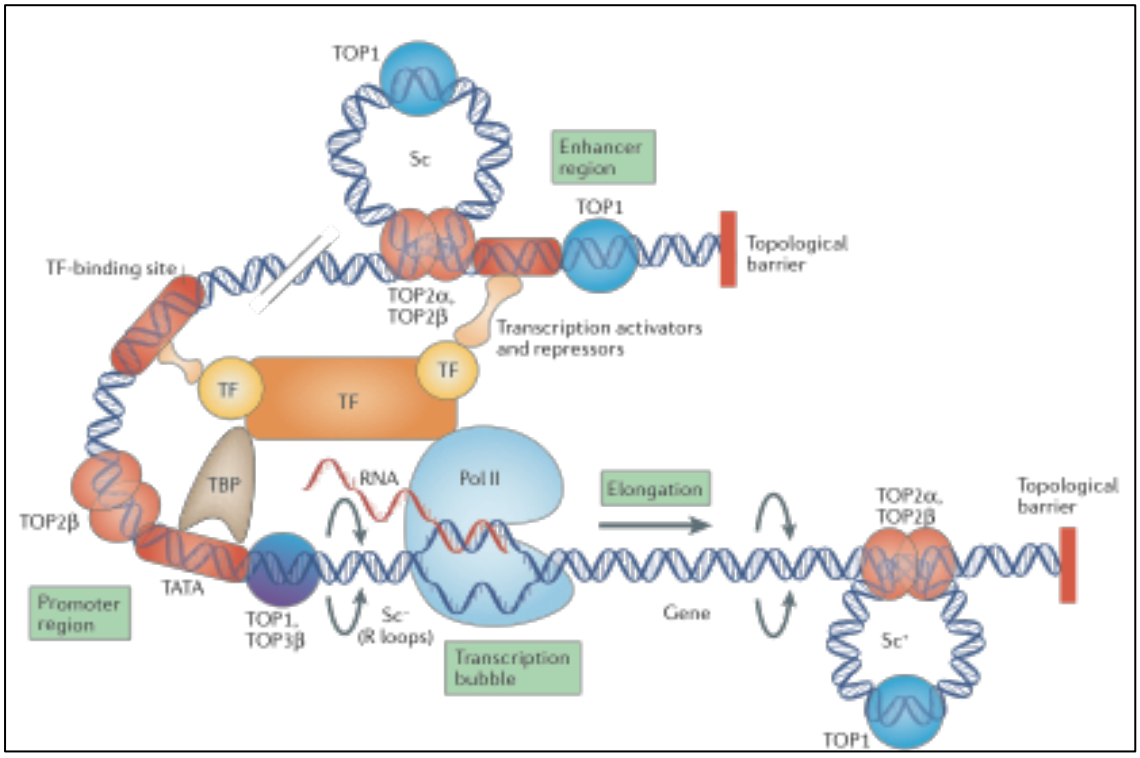
2.4.2 Termination and chromosome segregation

Several studies implicate both TOP2 and TOP3 enzymes in replication termination and sister chromatid separation (DiNardo, Voelkel et al. 1984, Baxter and Diffley 2008, Cuvier, Stanojcic et al. 2008, Falaschi 2009, Lee, Siaw et al. 2013), (Model 2D). TOP2 is required particularly at the point where replication forks converge(Fachinetti, Bermejo et al. 2010). It should be noted that type 1A topoisomerases probably contribute to de-catenation following replication termination at least in some contexts, but type 2 topoisomerases are probably the most important de-catenases. In yeast, Top2 was present at sites of replication termination and catalytically inactive Top2 interfered with the completion of replication. Subsequently, Top2 was found to bind to yeast termination region (TER) sites before the arrival of replication forks, to promote fork fusion (Fachinetti, Bermejo et al. 2010). Top2 was thus proposed to de-catenate sister chromatids following fork fusion, as its activity is required to preserve genome integrity and suppresses DSB formation at TER, presumably by allowing completion of replication, and to prevent breakage of chromosomes at subsequent steps of cell division. In addition to the recruitment of Top2 to replication fork barriers and TER sites, Sgs1, the yeast orthologue of the human BLM helicase, promotes Top2-mediated decatenation(Watt, Louis et al. 1995). RECQL5, a mammalian RecQ helicase, also facilitates human TOP2α-dependent separation of interlocked sister chromatids by interacting with TOP2α during S phase(Ramamoorthy, Tadokoro et al. 2012, Singh, Popuri et al. 2012, Popuri, Huang et al. 2013). The interaction of BLM with TOP2α seems to be important for BLM function during homologous recombination(Russell, Bhattacharyya et al. 2011), and it has also been suggested to be relevant for chromosomal decatenation(Rouzeau, Cordelieres et al. 2012).

2.4.3 Topoisomerases and transcription

Topoisomerases are required during transcription to manage the DNA supercoiling that accumulates ahead and behind the transcription machinery (Liu and Wang 1987). Experiments in yeast suggested that either Top1 or Top2 could efficiently provide the topoisomerase activities required for transcription (Brill, DiNardo et al. 1987, Bermejo, Capra et al. 2009) and that either could enhance the recruitment of RNA polymerase II (Pol II) to promoters (Sperling, Jeong et al. 2011). Recent results in yeast suggest that

topoisomerases are required for initiating the transcription of a subset of regulated genes such as *GAL* and *PHO* (regulated by galactose and inorganic phosphate, respectively); the requirements for topoisomerases differ depending on the detailed mechanism of gene activation (Ju, Lunyak et al. 2006, Ju and Rosenfeld 2006, Pedersen, Fredsoe et al. 2012, Roedgaard, Fredsoe et al. 2015). Importantly, these studies showed that topoisomerase activity is required for transcription initiation but not for elongation or re-initiation. Conversely, another study found that highly expressed genes require both Top1 and Top2, whereas Top1 alone can support genes with low transcription levels (Kouzine, Gupta et al. 2013).



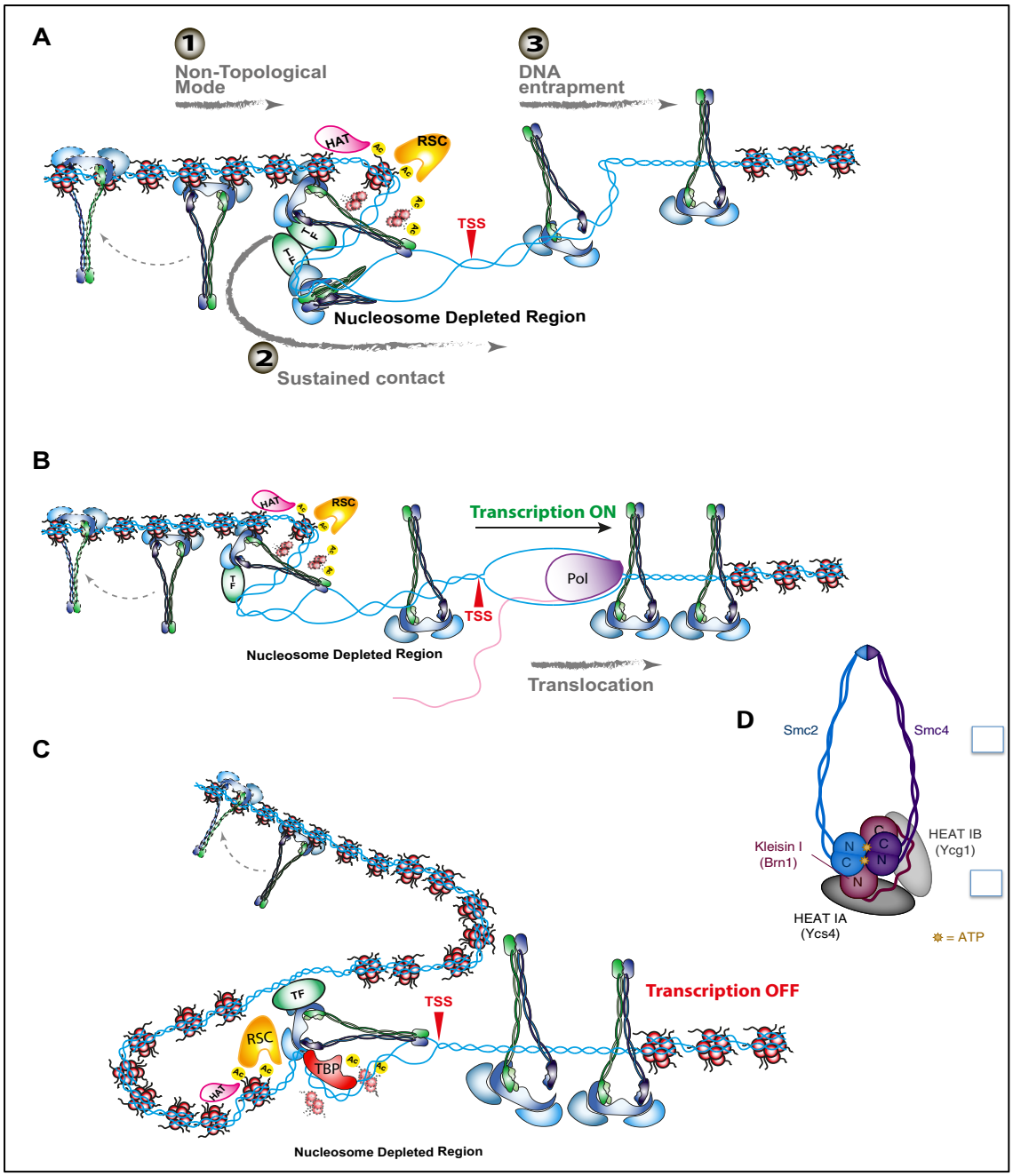
Model 3: Topoisomerases and interplay with transcription. Transcription imposes topological constraints that result from the progression of RNA polymerase II (Pol II). Positive supercoiling (Sc+) of the DNA template takes place ahead of the transcription bubble, which in turn obstructs further Pol II movement, and negative supercoiling (SC-), which promotes the formation of RNA–DNA hybrids (R loops), accumulates behind it. TOP2 and especially TOP1 enzymes function ahead of Pol II to remove positive supercoils, whereas relaxation of negative supercoils behind the transcription apparatus relies on TOP1 and TOP3. In addition, TOP1 regulates the activity of the transcription factor TATA-box-binding protein (TBP) at promoter TATA boxes independently of its catalytic activity. The formation of TOP2-mediated transient DNA double-stranded breaks at promoter regions in certain genes is crucial for transcription activation. TOP1 is also recruited to certain enhancer regions to promote (ligand-dependent) enhancer activation by

generating transient DNA single-stranded breaks. Topological barriers are genomic regions where the DNA is not free to rotate around its axis and require TOP1 and TOP2 to relax supercoils (Sc). **Modified and adapted from, (Pommier, Sun et al. 2016)**

2.5 Condensin complex and topology during transcription.

Several studies have determined the positions occupied by condensin along chromosomes in bacteria, budding and fission yeasts, *C. elegans*, chicken, mouse and human cells (D'Ambrosio, Kelly et al. 2008, D'Ambrosio, Schmidt et al. 2008); Gruber and Errington 2009; Schmidt et al. 2009; Dowen et al. 2013; Kim et al. 2013; Kranz et al. 2013; Nakazawa et al. 2015; Sutani et al. 2015; Kim et al. 2016). These studies revealed two remarkable and recurrent features in the localization pattern of condensins .The first one is the enrichment of condensin complexes at or near specialized genomic elements, such as the centromere-like sites in *Bacillus subtilis*, or at centromeres, telomeres and repetitive rDNA in eukaryotes. The second feature of condensin localization pattern is its enrichment in the vicinity of tRNA genes, and more generally of all highly expressed genes, regardless of whether they are transcribed by RNA Pol I, Pol II or Pol III.

In fission yeast, the profile of condensin along chromosome arms consists of a broad basal association punctuated by hotspots that coincide with genes actively transcribed by RNA Pol II during mitosis (Leonard, Sen et al. 2015, Nakazawa, Sajiki et al. 2015, Zhang, Paulson et al. 2016). Condensin accumulates at the transcription start site (TSS) and towards the 3'end of these mitotically active genes, and its enrichment increases with the level of transcription of the occupied genes (Leonard, Sen et al. 2015, Nakazawa, Sajiki et al. 2015, Sutani, Sakata et al. 2015). In human cells, condensin I is enriched at the promoter of highly expressed genes. It is absent from the body and/or the 3′ end of genes and its peak of association are centred on the TSS (Sutani et al. 2015). This difference might stem from the fact that transcription by all three RNA polymerases is inhibited during mitosis in human cells, like in most eukaryotes (Gottesfeld and Forbes 1997). Loaded at gene promoters, condensin might be displaced towards the 3′end of genes by active transcription in fission yeast, in a manner reminiscent of the translocation of the cohesin ring (Lengronne et al. 2004; D' A mbrosio et al. 2008; Ocampo-Hafalla et al. 2016; Davidson et al. 2016).



Model 4: A model for the loading of condensin at gene promoters. A) Condensin makes first contacts with nucleosomes through electrostatic interactions between non-SMC subunits and histone tails and/ or DNA. This preloaded mode of association can lead to the entrapment of the chromatin filament albeit with low efficiency. At active gene promoters, histone acetyltransferases (HAT) and ATP-dependent chromatin remodeling enzymes (RSC) evict nucleosomes, increasing the accessibility of genomic DNA. Additional contacts between non-SMC subunits and DNA-bound transcription factors (TF) and/ or non-nucleosomal DNA, plus other possible contacts between the hinge domain and ssDNA increase the residency time of condensin in the vicinity of free DNA, allowing the stimulation of ATP hydrolysis by the SMC heads, the transient opening of the ring and the capture of DNA. **B).** In fission yeast, active RNA polymerases (Pol) might subsequently

displace condensin rings towards the 3′ end of genes. **C).** In mammals, RNA polymerases are eliminated from chromatin during mitosis, but transcriptional bookmarks persist at the promoter of formerly active genes. Condensins might interact with TF bound to enhancers and non-nucleosomal DNA at gene promoters. In the absence of active transcription, topologically engaged condensin rings accumulate at gene promoters. TSS (Transcription Start Site) **Modified and adapted from (Robellet, Vanoosthuyse et al. 2017)**

The abundance of human condensin I over the TSS of genes that are transcriptionally silent during mitosis was found to be proportional to their transcription levels during interphase (Sutani et al. 2015). Furthermore, it was shown that condensin II is recruited *de novo* at a reporter gene in a transcription-dependent manner (Dowen et al. 2013), suggesting that all condensin complexes somehow respond to *cis*-acting transcription-dependent cues for their localisation. The fact that the rate of transcription impinges both on the localisation and the enrichment of condensin complexes and that this has been observed in evolutionarily distant organisms implies that one or several features associated with transcription must play a crucial and conserved role in the recruitment and/ or the positioning of condensin complexes along chromosomes (Bernard and Vanoosthuyse 2015).

2.6. Natural impediments to DNA replication.

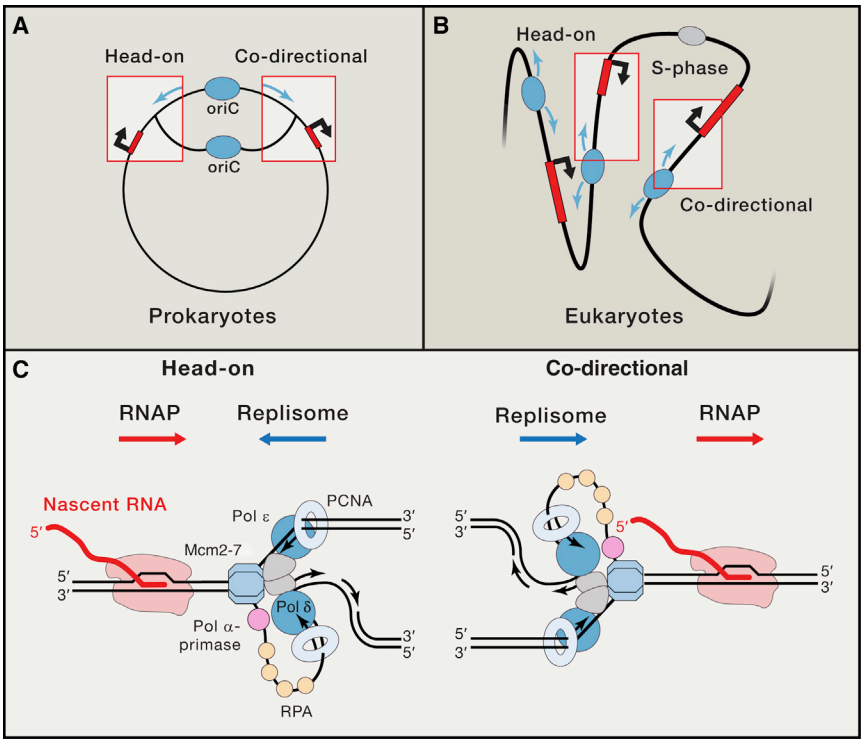
Numerous factors with exogenous, genetic and/or intrinsic origin hinder the replication fork passage along the genome and can jeopardize its integrity leading to genomic rearrangements hallmarks of cancer and in many human pathological scenarios.

Exogenous factors interfering with DNA replication are the source of DNA damage and/or nucleotide pools depletion (Iyer and Rhind 2017, Iyer and Rhind 2017). In the first matter, DNA replication is blocked at the sites of damage caused by, for example, UV light irradiation, DNA-damaging agents or topoisomerase inhibitors. In the second matter, replication fork progression is impaired by the lack of the deoxynucleoside triphosphates (dNTPs) essential for DNA amplification. Hydroxyurea is one of the drugs that affect the dNTPs pool (Kumar, Viberg et al. 2010, Giannattasio and Branzei 2017). Mutations of genes that inhibit replication fork progression by affecting S phase dynamics, the replisome components or factors contributing in nucleotide pool control, are a genetic threat that affect the accurate replication of the whole genome.

The integrity of S phase processes is threatened by the intrinsic factors that are the natural impediments to DNA replication. Those hindrances can be classified into five main replication-threatening groups: transcription, recombination and DNA repair, DNA binding proteins, replication slow zones and topologically altered DNA structures.

2.6.1 Transcription

Transcription complexes are one such endogenous impediment to replication, and a long-standing question has been how replication forks cope with the transcription machinery engaged on the same DNA template. In prokaryotic cells, a single origin is used to assemble two replisome complexes that duplicate the circular chromosome in opposite directions. Moreover, DNA replication and transcription initiate on the same DNA template without spatial or temporal separation (Model 5A). Because bacterial replisomes move more than 10-fold faster than RNA polymerase (RNAP) (Helmrich et al., 2013), encounters between transcription and replication complexes are unavoidable. Indeed, transcription-replication conflicts (TRCs) are routine in bacteria, and several highly orchestrated processes minimize their negative impact on genome stability and cell viability (Merrikh et al., 2012).



Model 5: Head-on and Co-directional Transcription-Replication Conflicts. (A) In prokaryotes, a single origin (oriC) is used to initiate replication in opposite directions along the single circular chromosome. (B) In eukaryotes, multiple origins initiate DNA synthesis during S-phase along the linear chromosomes. In both prokaryotic and eukaryotic genomes, head-on conflicts occur when a gene is encoded on the lagging strand, whereas co-directional encounters occur when a gene is encoded on the leading strand. (C) Schematic representations of the replisome and ternary RNAP complexes converging on the template DNA in head-on or co-directional orientations. Some key eukaryotic replisome components needed for DNA synthesis are indicated, including the replicative helicase (Mcm2-7, or DnaB in prokaryotes), leading- and lagging-strand DNA polymerases (Pol ε/d), DNA primase (Pol a-Primase), single-strand DNA- binding protein (RPA), and clamp loader complex (PCNA). **Modified and adapted from (Hamperl and Cimprich 2016)**

2.6.2 Coordinating Transcription and Replication

Although prokaryotes cannot avoid Transcription-Replication Conflicts (TRCs) on their circular chromosome, bacterial genomes have evolved a simple strategy to minimize their impact: highly transcribed and essential genes are preferentially co-oriented with the replisome (Model 5A). This bias is conserved in all known bacteria studied (Guy and Roten 2004) and especially important at highly transcribed and essential genes, as reversing the orientation of rRNA clusters, for example, disrupted replication and resulted in genome instability, activation of the SOS response, and cell death (Srivatsan et

al., 2010). Interestingly, such a co-orientation bias is not obvious in *S. cerevisiae*, whereas it may be present in the human genome (Petryk, Kahli et al. 2016). This difference may be explained by the compact nature of the yeast genome, which increases the likelihood that a replication fork meets a transcription complex in either orientation (McGuffee, Smith et al. 2013). With the discovery of pervasive transcription, however, analyses focusing solely on canonical genes may present an incomplete picture.

Although the orientation of replication and transcription is generally random in the yeast genome, certain regions may be protected from head-on TRCs. The multicopy rRNA gene cluster contains repeats of the heavily transcribed 35S rRNA gene, separated by an intergenic spacer encoding an autonomous replicating sequence (ARS). Although replication is initiated bi-directionally at the ARS, a polar replication fork barrier down-stream of active 35S rRNA genes prevents frequent head-on collisions by blocking forks from progressing in the direction opposite to RNAP I transcription (Model 5C) (Linskens and Huberman, 1988). Transcription-dependent replication-fork pause sites have also been described at yeast tRNA genes and at the ribosomal gene arrays of other organisms (Labib and Hodgson, 2007). These conserved regulatory elements in genomic regions with exceptionally high transcriptional activity may help reinforce co-directionality and minimize the more deleterious consequences of head-on TRCs.

Another mechanism by which TRCs may be minimized involves the redistribution of replication initiation factors on chromatin prior to their activation. In yeast, Mcm2–7 complexes loaded on DNA in G1-phase are repositioned by RNA polymerase outside of new transcription zones formed in transcription termination mutants (Gros et al., 2015).

During S-phase, eukaryotes compartmentalize replication of their genomes so that DNA replication and transcription machineries occupy distinct nuclear territories and act at distinct times (Model 5B) (Wei et al., 1998). More generally, a nascent RNA capture assay showed a global anti-correlation between transcription and replication timing (Meryet-Figuiere et al., 2014). Thus, higher eukaryotes coordinate transcription and replication in the nucleus spatially and temporally and thereby minimize interference between both processes. Nevertheless, there appear to be certain places in the genome where these safeguards are difficult to implement. For example, conflicts are unavoidable at the longest human genes, which undergo transcription for longer than one cell cycle. Some of these genes overlap with common fragile sites (CFSs), loci that replicate late in S-phase and are hotspots for chromosomal instability. The highly recurrent association of CFSs

with large genes suggests a functional relationship between transcription and fragility, but the mechanisms underlying this association are not understood (Le Tallec, Millot et al. 2013, Le Tallec, Koundrioukoff et al. 2014, Pentzold, Shah et al. 2017). R-loops may aggravate the fragility of a small subset of CFSs (Helmrich et al., 2011), but the majority of large genes are not fragile (Le Tallec et al., 2013). Interestingly, neural stem and progenitor cells have recurrent DSB clusters, which are also found in long, transcribed, and late-replicating genes (Wei et al., 2016), suggesting that such conflicts may be more common than previously anticipated.

Another class of fragile sites is known as early-replicating fragile sites (ERFSs). As these are found at actively transcribed genes replicated in early S-phase, it is tempting to speculate that the interference of transcription and replication machineries at genes in proximity to these ERFSs may account for their fragility (Barlow et al., 2013).

Although it is currently unclear whether the high levels of oncogene expression in many cell models are comparable to the levels observed in vivo in cancer cells, the connections between replication, origin firing, and transcription highlight the possibility that TRCs represent a potent source of genomic lesions that drive instability in different cancer types based on differential transcription of the regions involved (Barlow et al., 2013; Stork et al., 2016).

2.6.3 Activities controlling R loops *in vivo*

Short RNA–DNA hybrids form during natural processes such as replication, in which they prime DNA synthesis, or transcription at the active site of the RNA polymerase during ribonucleotide triphosphate incorporation. They are more stable than double-stranded DNA (dsDNA) and adopt different conformation that is intermediate between the B form of dsDNA and the A form of double-stranded RNA (dsRNA)(Roberts and Crothers 1992). A longer form of RNA–DNA hybrid can be generated by hybridization of the nascent RNA molecule with the template DNA strand. Such RNA–DNA hybrids and the resultant displaced single-stranded DNA (ssDNA) is collectively known as R loops (Model 6)

2.6.3.1 Removal of R loops by ribonucleases and helicases.

R loops can be removed by degradation of the RNA strand. This is achieved by RNase H enzymes, which specifically degrade the RNA moiety of RNA–DNA hybrids (Cerritelli and

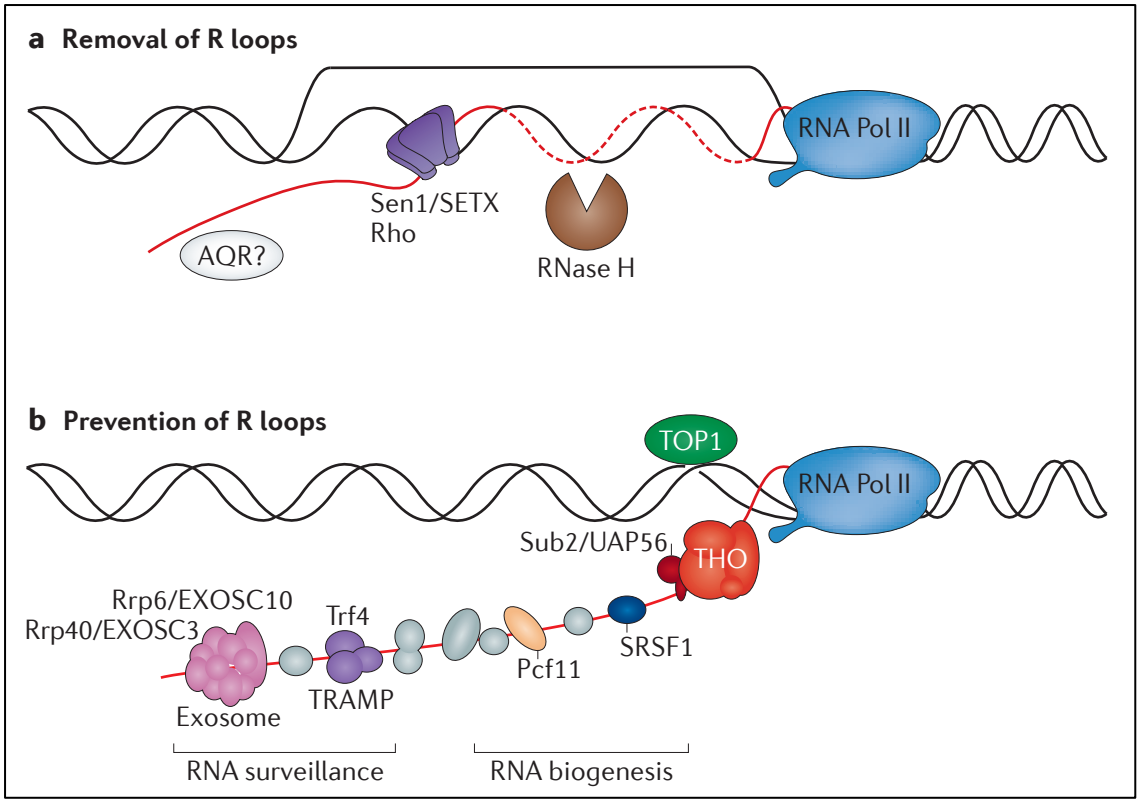
Crouch 2009) (Model 6). There are two types of RNase H enzymes, which differ in structure and substrate specificity. Both types of RNase H enzyme have the ability to remove RNA–DNA hybrids in addition to having different specialized roles (Skourti-Stathaki, Kamieniarz-Gdula et al. 2014). The yeast protein Sen1 and its human homologue senataxin (SETX) have also been implicated in R-loop homeostasis. *Schizosaccharomyces pombe* Sen1 was initially identified as a DNA and RNA helicase with 5′–3′ RNA–DNA unwinding activity (Kim, Choe et al. 1999). More recently, it was shown *in vivo* that *Saccharomyces cerevisiae* Sen1 helicase-inactive *sen1-1* mutants accumulated R loops at highly expressed loci and that inactivation of human SETX leads to increased occurrences of R loops at transcription termination pause sites. Furthermore, *Setx−/−* mice also accumulate R loops (Arning, Schols et al. 2008). The results suggest a role for Sen1/SETX in the dissolution of R loops, in particular during transcription termination. The human aquarius (AQR) protein, which is an RNA helicase of the same family as Sen1/SETX32, may also participate in R-loop removal *in vivo*, but we currently know little about this protein (Sollier, Stork et al. 2014).

2.6.3.2 Negative DNA supercoiling facilitates R-loop formation.

In yeast, the loss of both Top1 and Top2 increases R-loop accumulation at the rDNA locus (model 6B), causing RNA Polymerase I stalling and defects in precursor ribosomal RNA (pre-rRNA) synthesis (Arlt and Glover 2010, El Hage, French et al. 2010). Higher levels of R loops are seen in cells additionally lacking RNase H enzymes. Indeed, apart from mitochondrial DNA, the rDNA locus, located in the nucleolus, is the genomic region where most R loops accumulate in eukaryotic cells, as can be seen directly by immunofluorescence with the S9.6 RNA–DNA-specific hybrid antibody in yeast and human cells. Top1-deficient cells accumulate stalled replication forks and chromosome breaks in S phase, and that breaks occur preferentially at gene-rich regions of the genome (French, Sikes et al. 2011). Notably, these phenotypes were suppressed by preventing the formation of RNA-DNA hybrids (R-loops) during transcription. Moreover, these defects could be mimicked by depletion of the splicing factor ASF/SF2 (alternative splicing factor/splicing factor 2), which interacts functionally with Top1. This indicated that Top1 prevents replication fork collapse by suppressing the formation of R-loops in an ASF/SF2-dependent manner (Kim, Choe et al. 1999, Tuduri, Crabbe et al. 2009).

2.6.3.3: *mRNP biogenesis protects against R-loop formation.*

The nascent mRNA is key for the formation of R loops at genes, and deficiencies in messenger ribonucleoprotein particle (mRNP) assembly can strongly stimulate R-loop formation. This may be due to the direct or indirect protection of the nascent mRNA by specific RNA-binding proteins (RBPs) that would prevent its hybridization with the transcribed DNA strand (Model 6)(Dominguez-Sanchez, Barroso et al. 2011, Gomez-Gonzalez, Garcia-Rubio et al. 2011, Salas-Armenteros, Perez-Calero et al. 2017). R loops were detected physically in yeast mutants of the THO complex (which is involved in mRNP biogenesis) by purification of RNase H1-sensitive nucleic acids and genetically by suppression of their hyper-recombination phenotype by RNase H1 over- expression.



Model 6: Cellular activities limiting R-loop accumulation in defective RNA biogenesis. A). Removal of R-loops occurs by distinct but complementary mechanisms. RNase H enzymes can degrade the RNA moiety. Additionally, R loops can be unwound by helicases such as Rho in bacteria, Sen1 in yeast and senataxin (SETX) in humans, all of which have a role in transcription termination. Other putative helicases, such as aquarius (AQR), may also play a main role in R-loop dissolution. B). R-loop formation is prevented by topoisomerase 1 (TOP1), which resolves the local negative supercoiling behind the elongating RNA Pol II transcribed mRNA and by specific RNA-binding proteins that are

involved in RNA biogenesis (including the THO complex, serine/arginine-rich splicing factor 1 (SRSF1) and Pcf11) or in RNA surveillance (including the exoribonucleases exosome component 3 (EXOSC3) and EXOSC10 (Rrp40 and Rrp6 in yeast, respectively). TRAMP, Trf4– Air2–Mtr4p polyadenylation complex; UAP56 (56 kDa U2AF65-associated protein-also known as DDX39B; known as Sub2 in yeast). **Adapted and Modified (Santos-Pereira and Aguilera 2015, Sollier and Cimprich 2015)**

2.6.4 Transcription Termination and R-loop Resolution

Rapid removal of transcription complexes at the ends of genes can also reduce potential interference between transcription and replication. In bacteria, read through is prevented by transcription termination, one form of which involves Rho, a homo- hexameric helicase that triggers the dissociation of RNAP from RNA and the template (Peters et al., 2011). Inhibition of Rho- dependent transcription termination induces replication fork arrest and DNA DSBs, suggesting that a critical function of termination factors is to prevent RNAP complexes from blocking DNA replication (Washburn and Gottesman, 2011). Termination of eukaryotic protein-coding genes involves pausing of RNAPII and mRNA processing by components of the cleavage and polyadenylation machinery (CPM). Intriguingly, a screen for yeast mutants that increase the formation of Rad52 foci, a marker for recombination-mediated repair, identified seven subunits of the CPM, indicating that defects in transcription termination lead to recombination (Stirling et al., 2012 (Stirling and Hieter 2017). Termination of noncoding RNA genes in yeast is mediated by a complex containing the RNA:DNA helicase Sen1. After binding to the nascent RNA, Sen1 translocate to RNAPII and initiates termination. Mutation of the Sen1 helicase domain results in genome-wide transcription termination defects (Steinmetz et al., 2006), concurrent with transcription-associated genomic instability (Franco-Echevarria, Gonzalez-Polo et al. 2017, Gama-Carvalho, M et al. 2017, Han and Porrua 2017, Leonaite, Han et al. 2017, Roy and Chanfreau 2017). A similar function was described for the human homolog Senataxin (SETX), which promotes transcription termination by exonuclease-mediated (XRN2) degradation of the RNA at G-rich pause sites downstream of the polyadenylation signal (Skourti-Stathaki et al., 2011). Interestingly, numerous termination mutants, including CPM mutants and Sen1/SETX mutants, show increased R-loop levels, in the latter case particularly at transcription termination sites (Mischo et al., 2011; Skourti- Stathaki et al., 2011; Stirling et al., 2012).

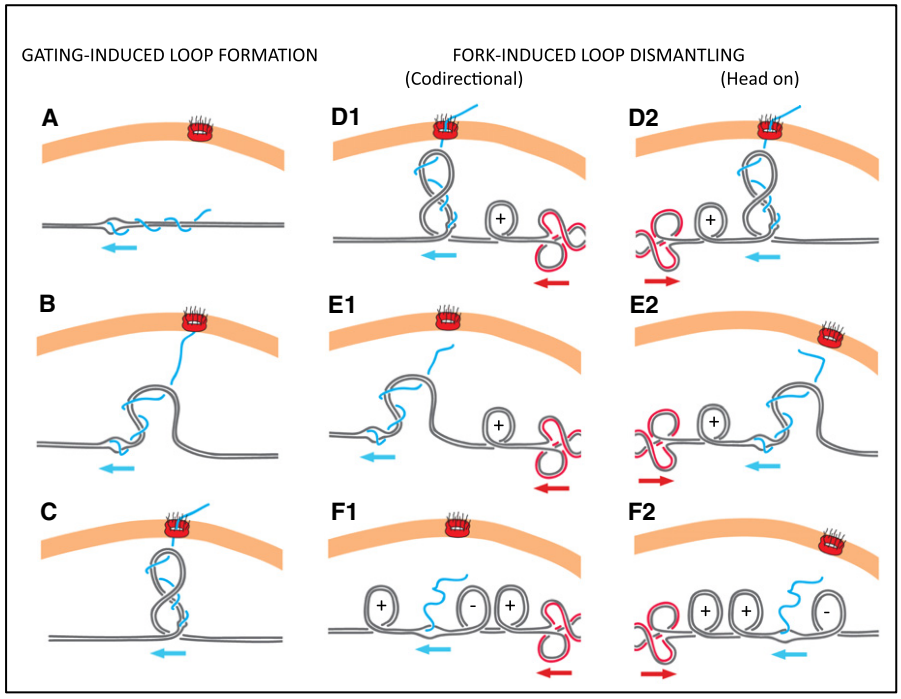
The strong link between transcription termination and R-loop formation may be explained by the notion that inefficient termination increases the presence of a transcript at the 30 end of genes, allowing for unscheduled interactions with the DNA duplex. The formation of stable RNA:DNA hybrids and RNAP complexes in this scenario may pose a stronger transcriptional block, resulting in a higher chance of collisions with replication forks.

Intriguingly, some termination factors may also be used to release transcription complexes ‘‘trapped’’ by a TRC. Sen1 associates directly with replication forks that encounter highly expressed RNAPII genes, suggesting a role for this helicase in coordinating replication with transcription at these sites (Alzu, Bermejo et al. 2012). Importantly, the Sen1 function at replication forks may be conserved, as human SETX forms distinct foci that co-localize with DNA-damage markers in S/G2-phase cells, particularly after the induction of replication stress, and these SETX foci are diminished after RNaseH overexpression. This could indicate a potential role for SETX in resolving R-loops specifically formed during TRCs (Yuce and West 2013).

Interestingly, a recent genome-wide study in fission yeast indicates that Dcr1, but not other components of the RNA interference (RNAi) machinery, can promote the release of RNAPII at TRCs (Castel, Ren et al. 2014). How Dcr1 is specifically recruited to these sites and can distinguish them from other stalled RNAP complexes not involved in TRCs is an unresolved question. Importantly, this link to the RNAi machinery may also exist in human cells, as dicer and other components of this pathway are recruited to double-stranded RNA formed by antisense transcription over R-loops at certain G-rich terminator regions (Skourti-Stathaki et al., 2014).

2.6.5 Gene gating, R-loop Resolution and Replication fork collision.

R-loops are prevalent, dynamic structures throughout the genome of prokaryotic and eukaryotic cells, and in addition to termination sites, they are enriched at telomeres, rDNA, and highly transcribed genes. The causes and consequences of increased R-loop formation have been extensively discussed in other reviews (Santos-Pereira and Aguilera 2015, Sollier and Cimprich 2015, Bhatia, Herrera-Moyano et al. 2017, Lang, Hall et al. 2017)). However, it is important to emphasize here that their accumulation can cause replication- fork stalling. It follows that the mechanisms to suppress or remove RNA: DNA hybrids, including the use of topoisomerases, RNaseH enzymes, endonucleases, and RNA: DNA helicases, can reduce the frequency of TRCs in the genome.



Model 7: the association of promoter and terminator regions establishes Gene Gating and Replication Forks collision in loops. As RNAP initiates transcription, the promoter generates a short nascent RNA chain and keeps rotating around the DNA template. (A–F) As it becomes increasingly longer, the nascent RNA could intertwine with the template DNA (A). Engagement of the nascent RNA by the NPC gating machinery (B) could lead to the formation of gated DNA loops (C). As the replication forks approach gated loops (D1–D2), and dismantled by local checkpoint activation (E1C-E2). Disengagement from the NPC might facilitate the transient formation of twin supercoiled domains (F1-F2). Light blue and red arrows indicate the direction of RNAP and DNAP movement, respectively. **Modified and adapted (Alzu, Bermejo et al. 2012, Bermejo, Lai et al. 2012)**

The coordinated action of type I and type II topoisomerases allows cells to deal with the topological problems that arise when two forks converge during replication termination or when one fork clashes with a transcription bubble in a head-on collision mode Azvolinsky et al., 2009; Brewer and Fangman, 1988; Deshpande and Newlon, 1996 (Azvolinsky et al., 2009; Brewer and Fangman, 1988; Deshpande and Newlon, 1996 Newlon, Collins et al. 1993). The unreplicated DNA becomes very short; rendering it difficult for DNA topoisomerases to bind and remove the last few intertwines. These residual and unsolved intertwines may represent a topological barrier for replication and transcription unless they diffuse into pre-catenanes behind the forks . In *E. coli,* as well as *S. cerevisiae* and *Schizosaccharomyces pombe,* type II topoisomerases are required for timely replication termination and to prevent chromosomal breaks during chromosome segregation (Champoux, 2001; Fachinetti et al., 2010; Wang, 2002), likely by mediating pre-catenane resolution (Wang, 2002; Wang et al., 2008). Prokaryotes, which have only et al., 2009), although this observation might reflect the peculiar DNA-looping organization of RNAPII-transcribed regions (Ansari and Hampsey, 2005; Bermejo et al., 2009; Perkins et al., 2008; Tan-Wong et al., 2009). At least in theory, in a codirectional collision between a fork and a transcribed unit not organized in a loop, the negative supercoiling generated behind the RNAP might adsorb the positive supercoiling generated by the incoming fork, thus facilitating fork progression (Wang, 2002). In the case of tRNA transcription, it is clear that the head-on collision with a fork causes replication pausing (Deshpande and Newlon, 1996). Under these circumstances, fork progression is facilitated by a specialized replisome associated DNA helicase, Rrm3, that likely dislodges the RNAPIII machinery by moving with a 5' to 3' directionality (Ivessa, Zhou et al. 2000, Ivessa, Zhou et al. 2002). It has been proposed that Top1 and Top2 play differential roles in assisting RNAPI progression (French et al., 2011): Top2 is required to relax positive supercoiling in front of the transcription bubble to facilitate its progression, whereas Top1 seems to relax negative supercoiling behind it.

Head-on collisions between replication and transcription generate fork pausing (Liu and Alberts, 1995; Olavarrieta et al., 2002; Wang, 2002). Fork restart can take place through the displacement of the RNAP machinery from the DNA template (Pomerantz and O'Donnell et al., 2008). In vitro, the co-directional collision between replication and transcription barely affects fork progression (Liu and Alberts 1995, Pomerantz and

O'Donnell 2010, Srivatsan, Tehranchi et al. 2010) unless the RNAP is stalled (Dutta et al., 2011). It has been suggested that, occasionally, the replication machinery can use mRNAs to re-prime DNA synthesis after colliding co-directionally with the RNAP (Bates, Boye et al. 1997, Pomerantz and O'Donnell et al., 2010).

2.6.6 Replication-Associated Mechanisms to Overcome Conflicts

Replication stress is defined as the slowing or stalling of replication fork progression and/or DNA synthesis, and various types of natural DNA lesions can lead to replication stress. Strikingly, stalled transcription complexes or transcription-associated RNA:DNA hybrids can also induce the replication stress response. Thus, mechanisms that stabilize or reactivate stalled replication forks can help the cell to over come conflicts with transcription-associated obstacles (Bhatia, Herrera-Moyano et al. 2017, Lang, Hall et al. 2017, Lin and Pasero 2017).

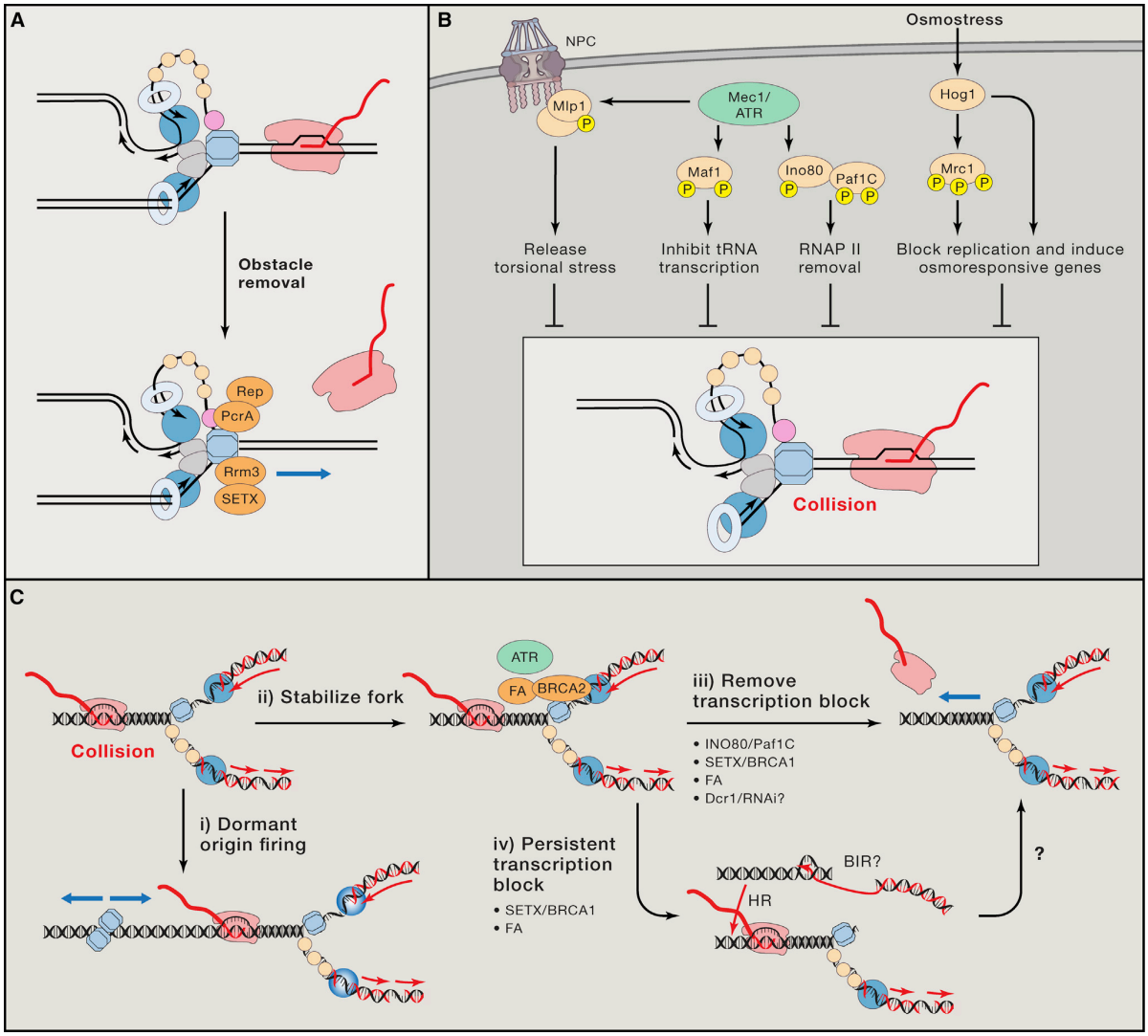
2.6.6.1 Auxiliary Helicases

Auxiliary helicases traveling with replication forks are found in both prokaryotic and eukaryotic cells, and their activities may help the replisome dislodge transcription complexes (Model 9). Notably, these SF1 superfamily helicases may act in distinct ways, whereas UvrD may directly interact with arrested RNAP complexes as part of the TCR pathway (Guy et al., 2009; Gwynn et al., 2013; Merrikh et al., 2015; Iraqui, Kienda et al. 2009). Rrm3, yeast Pif1 family helicase, is also associated with the replisome and facilitates progression through highly transcribed genes (Azvolinsky et al., 2009). Interestingly, RNase H overexpression significantly reduced the association of Rrm3 with these genes, indicating that this helicase accumulates at RNA:DNA hybrids that impair replication fork progression. In addition, the fission yeast Pif1 homolog Pfh1 is enriched at highly transcribed genes, and its absence leads to replication fork stalling (Sabouri, McDonald et al. 2012). As most eukaryotes encode a Pif1 family helicase, the function of these enzymes to promote fork progression across highly transcribed or co-transcriptional non-B DNA structures may be conserved.

2.6.6.2 S-phase Checkpoint

Growing evidence also implicates the ATR kinase pathway in coordinating replication

with transcription (Model 8). In yeast, highly transcribed genes are anchored to the nuclear pore to couple mRNA synthesis with cytoplasmic export. Although such gene gating promotes rapid gene expression, it also creates topological stress and inhibits replication fork progression. In yeast, the ATR homolog, Mec1, and its downstream effector, Rad53, uncouple transcribed genes from nuclear pores by phosphorylating the nucleoporin Mlp1, thereby neutralizing the topological tension generated (Bermejo et al., 2011). Mec1 also responds to replication stress by phosphorylating Maf1, a conserved repressor of tRNA genes. This response inhibits tRNA gene transcription and may therefore prevent interference with replication (Nguyen, Co et al. 2001). In addition, phosphor-proteomic data suggest that Mec1-Rad53 regulates many other proteins involved in transcription and RNA processing in normal S-phase, raising the possibility that Mec1 is needed for the replication of many transcriptional barriers (Bastos de Oliveira et al., 2015). Furthermore, Mec1 acts with the INO80 chromatin-remodeling complex and the PAF1C transcription complex to degrade a subset of chromatin bound RNAPII at genes transcribed near early firing origins (Poli, Gerhold et al. 2016, Poli, Gasser et al. 2017). Finally, R-loop-accumulating mutants in yeast exhibit synthetic growth defects with S-phase checkpoint mutants, suggesting that replication forks stalled at RNA: DNA hybrids rely on check- point-dependent mechanisms to overcome the transcription barrier (Gomez-Gonzalez, Felipe-Abrio et al. 2009). In mammalian cells, the ATR kinase appears to play a related role as it regulates the stability of both ERFS and CFS regions, some of which correspond to R-loop-accumulating or highly transcribed genes (Glover 2006, Casper, Greenwell et al. 2009, Barlow, Faryabi et al. 2013, Glover and Wilson 2013). Together, these studies indicate the importance of a functional S-phase checkpoint in monitoring ongoing replication and negotiating TRCs. Distinctly, checkpoint pathway that may coordinate transcription and replication under conditions of induced transcription. The stress-activated protein kinase Hog1 promotes the activation of hundreds of genes under osmostress. Interestingly, Hog1 phosphorylates Mrc1, a downstream effector of Mec1. This phosphorylation is independent of the Mec1 pathway and delays origin firing to prevent TRCs and transcription-associated recombination during this transcriptional outburst (Duch, Palou et al. 2011). It is tempting to speculate that TRCs increase in these situations, and the mechanisms to avoid and resolve them become particularly important to minimize their effect on genome stability cells.



Model 8: Replication-Associated Mechanisms to Prevent and Resolve TRCs. (A) Accessory helicases including Rep (*E. coli*), PcrA (*B. subtilis*), Rrm3, Sen1 (yeast), or SETX (human) can assist the replicative helicase by dislodging transcription complexes ahead of the replication fork.

(B) The S-phase checkpoint can monitor and respond to replication forks stalled at transcription complexes in eukaryotic cells. The Mec1/ATR kinase may promote fork progression and stability at transcribed genes by phosphorylating the nucleoporin Mlp1, thereby releasing genes from the nuclear pore to reduce topological tension. The checkpoint also controls tRNA gene transcription mediated by the Maf1. The osmostress induced protein kinase Hog1 phosphorylates Mrc1, a downstream component of the Mec1/ATR pathway. In addition, Mec1/ATR, in cooperation with INO80 and PAF1C, can trigger the efficient removal of chromatin- bound RNAPII near early firing origins. NPC, nuclear pore complex.

(C) Replication forks stalled at transcription complexes can resume DNA synthesis by

different fork-restart and DNA-repair pathways. (i) A replication fork stalled at a transcription complex can be rescued by firing of an adjacent dormant origin. Alternatively, replication forks stalled at TRCs may be stabilized by ATR, BRCA2, or the FA pathway (ii). Prolonged stalling of the replication fork may also promote re-annealing of parental strands priming fork reversal. Removal of the transcription block by one or several of the pathways/factors listed can then promote fork restart (iii). If the transcription block persists, this may ultimately lead to fork breakage (iv). Break-induced replication (BIR)- and/or homologous recombination (HR)-dependent repair mechanisms may then be used to overcome the obstacle.

2.6.6.3 Replication Restart and DNA Repair

How can a replication fork stalled at a transcription block overcome the conflict and restart DNA synthesis? Several fork restart and repair mechanisms have been implicated in this important task (Model 9C). Intriguingly, the RNA transcript was used as a primer to restart DNA synthesis after the collisio (Pomerantz and O'Donnell 2010) . It is unclear, however, if such a mechanism exists in vivo, especially if the replisome is challenged with an array of multiple RNAPs. Indeed, in *B. subtilis*, the replication restart protein PriA and the helicase loaders DnaB and DnaD are required to resume replication after resolution of a TRC at the highly transcribed rDNA operon (Merrikh, Zhang et al. 2012, Paul, Million-Weaver et al. 2013, Million-Weaver, Samadpour et al. 2015). Thus, if the replicative helicase is inactivated or disassembled at the conflict site, prokaryotic cells may use these factors to establish a new replication fork and complete DNA synthesis.

In eukaryotes, alternative mechanisms to replication restart may be more important for completing DNA replication. As noted previously, a common mechanism utilized to complete DNA synthesis may involve the firing of a backup origin adjacent to a TRC. Nevertheless, a large body of evidence indicates that overcoming transcription-dependent replication blocks requires the activity of additional factors involved in DNA recombination, the activity of which appears to be particularly important during head-on confrontations (Gottipati et al., 2008; Prado and Aguilera, 2005; Wellinger et al., 2006). The molecular mechanism(s) by which a fork stalled at a transcription complex gives rise to the DSB or ssDNA gap needed to initiate recombination are still unresolved.

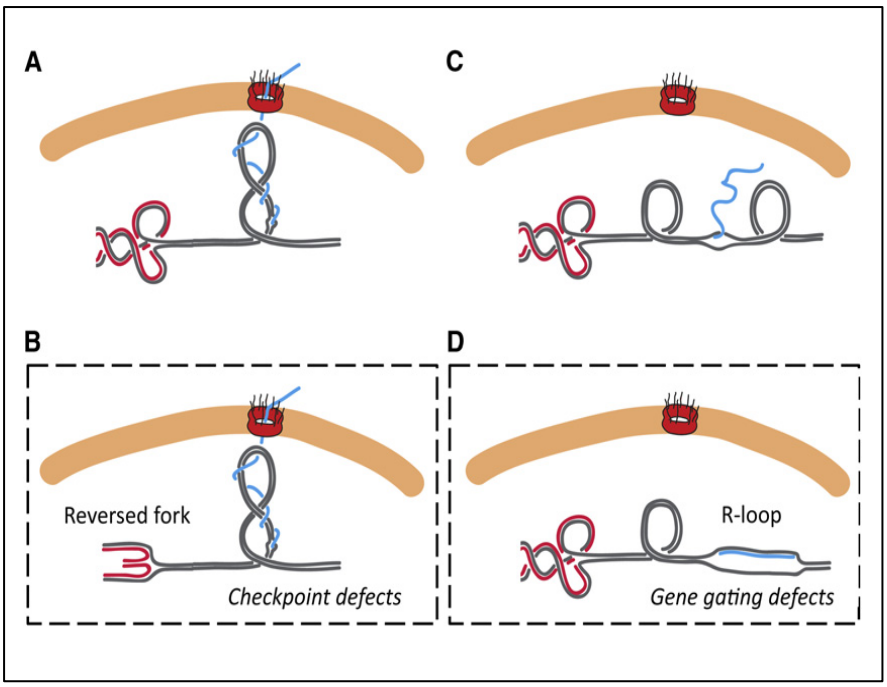
Interestingly, recent studies showing that R-loops accumulate in cells without the recombination repair and tumor suppressor genes BRCA1 and BRCA2 provide a mechanistic connection between recombination and R-loops in higher eukaryotes (Bhatia

et al., 2014; Hatchi, Skourti-Stathaki et al. 2015). In particular, it was shown that BRCA1 interacts with SETX to prevent ssDNA break formation and mutation at certain R-loop-prone transcription termination regions. This finding suggests that BRCA1 may suppress R-loop formation and subsequent processing. How BRCA2 acts at R-loops is less clear. Replication forks stalled at R-loops may be stabilized and restarted by BRCA2, or a BRCA2-dependent recombination event may be necessary to overcome this obstacle (Roy et al., 2011). Interestingly, BRCA2 is also a member of the Fanconi anemia (FA) DNA-repair pathway of interstrand crosslinks, which was recently shown to be activated by R-loop-mediated conflicts between transcription and replication (Bhatia, Barroso et al. 2014, Garcia-Rubio, Perez-Calero et al. 2015, Madireddy, Kosiyatrakul et al. 2016, Garcia-Pichardo, Canas et al. 2017, Munoz-Galvan, Garcia-Rubio et al. 2017)Schwab, Nieminuszczy et al. 2015).

As our understanding of the molecular mechanism(s) by which a fork stalled at a transcription complex can restart is nascent, additional mechanisms are likely to emerge. For example, topological stress or fork-remodeling enzymes could promote fork reversal when forks stall at transcription barriers. This could stabilize the fork structure and allow more time to promote resolution of the transcriptional block. Once resolved, the reversed fork could be remodeled for direct restart. If the block persists, however, restart could be initiated by break formation and recombination-mediated processes like those that act on forks stalled by other means. Similarly, template-switching and bypass pathways could be important for progression past TRCs (Gomez-Gonzalez, Felipe-Abrio et al. 2009). Indeed, some TRCs could be ‘‘tolerated’’ by the cell using the template-switching pathways that are utilized to tolerate some lesions during S-phase. This could be one mechanism to manage the conflicts that inevitably arise at long genes, and it would also allow cells to maintain R-loop structures that may have physiological functions in the cell. The recently identified PrimPol activity could also facilitate fork restart by reinitiating DNA synthesis downstream of TRCs (Gomez-Gonzalez, Felipe-Abrio et al. 2009, Gomez-Gonzalez, Garcia-Rubio et al. 2011). Although speculative, this R-loop-mediated and origin-independent mechanism for re-initiation of DNA synthesis may help to overcome R-loop-mediated TRCs. More direct experiments focusing on the replication intermediates and the fork structure during TRCs will be necessary to determine whether and how TRC-stalled forks differ from those blocked by other lesions.

2.7 Pathological Outcomes of the Topological Interference between Replication and Transcription

Replication forks accumulate torsional energy when paused at termination zones or when they approach transcribed genes. Unless promptly resolved, torsional stress can generate aberrant DNA transitions, leading to genome instability (Branzei and Foiani 2010, Branzei and Foiani 2010, Potenski and Klein 2011) (Model 9). In vitro studies have shown that positive supercoiling in front of a fork can be accommodated by fork reversal through the extrusion and reannealing of nascent DNA strands (Postow et al., 2001b). Reversed forks can also derive from the run-off of hemicatenane structures that likely represent precatenane derivatives (Bermejo et al., 2008; Cotta-Ramusino et al., 2005). Reversed forks are cruciform DNA structures resembling Holliday junctions and, being highly recombinogenic, they can lead to genome rearrangements (Lopes et al., 2001; Sogo et al., 2002). In yeast mutants altered in the Mec1/ATR pathway, replication forks that undergo pausing rapidly collapse into a reversed-fork conformation (Lopes et al., 2001; Sogo et al., 2002). Mec1/ATR-mediated Mlp1 phosphorylation assists replication across gated genes whose architecture hinders fork progression. In checkpoint mutants, the transcribed chromatin remains perinuclear and accumulates torsional stress in the proximity of forks encountering gated genes, thus generating the context for fork reversal (Bermejo et al., 2011).



Model 9. Pathological Events Caused by Replication and Transcription

Interference (A) NPC-associated gene loops can behave as barriers for the diffusion of the torsional stress generated by incoming replication forks. (B and C) In checkpoint-defective cells, persistence of topological barriers at gated genes locally increases positive supercoiling accumulation that, in the context of an unstable replisome, could result in fork reversal (B). In normal cells, twin supercoiled domains might form transiently following the checkpoint-mediated dismantling of gated DNA loops (C). (D) In gene gating-defective mutants, twin supercoiled domains would persist longer, and the underwound DNA helix behind the transcription bubble might favor the annealing of the nascent RNA molecules, thus leading to the formation of R-loops. Dashed boxes mark pathological events challenging genome integrity. **Adapted (Bermejo, Kumar et al. 2012)**

2.8 Replication Barriers Associated with Repeat DNA and Protein–DNA Complexes

RFBs have been reported at rDNA arrays, centromeres, telomeres, mating-type locus, and tRNA genes (Branzei and Foiani 2010, Branzei and Foiani 2010, Liberi and Foiani 2010). In some cases, RFBs may function to coordinate replication and transcription processes and/or to prevent replication slippage at repetitive DNA loci. Other RFBs are genetically programed to establish a site where genomic instability is created under tight cellular control in order to achieve cellular differentiation.

2.8.1. Telomeres

Telomeres are the physical ends of eukaryotic chromosomes. They provide a mechanism for full replication of the chromosomal ends while protecting these ends from DNA degradation and recombination. At the same time, several telomeric features pose challenges to the replication machinery. At telomeres, replication forks proceed in a unidirectional manner from a centromere-proximal origin (Miller, Rog et al. 2006). Although some later reports suggest that replication could also be initiated within the telomeric repeats (Sfeir, Kosiyatrakul et al. 2009, Kurth and Gautier 2010) the unidirectional nature of telomere replication may present a problem for complete replication of chromosomal ends. Furthermore, the repetitive nature of their DNA sequence, the presence of heterochromatin proteins and chromatin remodeling marks,

and the potential to form T-loop structures make telomeres difficult to replicate templates for DNA replication (Gavalda, Santos-Pereira et al. 2016, Geronimo and Zakian 2016, Webb and Zakian 2016, Zaaijer, Shaikh et al. 2016).

2.8.2 rDNA Repeats

Ribosomal DNA (rDNA) is found as tandem repeats localized at discreet locations in the genome. Each eukaryotic rDNA transcription unit contains sequences encoding 16–18S rRNA, 5.8S rRNA, and 25–28S rRNA. The transcription units are separated by the non-transcribed spacers, where replication barriers are located in most eukaryotic species, including yeast, ciliates (*Tetrahymena thermophila*), pea (*Pisum sativum*), frog (*Xenopus laevis*), mouse (*Mus musculus*), and humans. During S phase, these barriers lead to replication fork arrest, which is likely to coordinate transcription, replication, and recombination at these loci (Kim and Wang 1989, Hernandez, Martin-Parras et al. 1993, Ahn, Osman et al. 2005, Krings and Bastia 2005, Krings and Bastia 2006, Bairwa, Zzaman et al. 2010, Bairwa, Mohanty et al. 2011, Mundbjerg, Jorgensen et al. 2015).

2.8.3 Centromeres

Centromeres are large chromatin structures responsible for the proper segregation of chromosomes during mitosis and meiosis. Defects in centromere regulation result in chromosome defect and aneuploidy (Ekwall, Javerzat et al. 1995, Appelgren, Kniola et al. 2003, Enukashvili, Kuznetsova et al. 2003). Centromeres are characterized by an intricate structure that generates obstacles for DNA replication. In contrast, *S. cerevisiae* centromeres are defined by an ~125-bp DNA sequence and termed “point centromeres” because of their simple organization. Replication fork pausing was detected at centromeres of various chromosomes (*CEN1*, *CEN3*, *CEN4* and *CEN6*), thus the ability to promote fork pausing seems to be a general property of *S. cerevisiae* centromeres (Pluta, Mackay et al. 1995, Pidoux and Allshire 2000, Pidoux, Uzawa et al. 2000, Yamagishi, Sakuno et al. 2008)

2.8.4 tRNA Genes and LTR Retro-transposons

Genetic screenings in *S. cerevisiae* identified numerous essential genes involved in preventing spontaneous DNA damage and genome rearrangements (Yuen, Warren et al.

2007, Stirling, Bloom et al. 2011, Stirling, Crisp et al. 2012, Hamza, Tammpere et al. 2015). These include many DNA replication factors involved in different stages of DNA replication processes (initiation: *CDC45*, *DBF4*, *DPB11*, *MCM4*, *MCM5*, *MCM7*, and *PSF2*; elongation: *CDC45*, *DNA2*, *MCM4*, *MCM5*, *MCM7*, *POL2*, *POL30*, *PSF2*, *RFC2*, and *RFC5*; and termination: *UBC9*). Importantly, genome rearrangements were mapped to yeast fragile sites, including *Ty* retro transposons, tRNA genes, early origins of replication, and replication termination sites. These sites are prone to fork stalling, breakage, and chromosomal rearrangements, particularly, when DNA replication is compromised or when checkpoint activation is defective (Myung, Chen et al. 2001, Mieczkowski, Lemoine et al. 2006, Cheng, Vaisica et al. 2012, Saini, Ramakrishnan et al. 2013). Early work in budding yeast identified polar replication pause sites at *Ty1-LTR* and tRNA genes. These sites arrest forks moving in opposite direction to transcription (Newlon, Collins et al. 1993) and may represent fragile sites when DNA replication is compromised, leading to genomic instability. Indeed, when the level of DNA polymerase α is reduced, chromosome translocations were greatly induced due to hyper-recombination at *Ty* element (Parket, Inbar et al. 1995, Rachidi, Barre et al. 1999, Lemoine, Degtyareva et al. 2005, Resnick 2005)

2.8.5 DNA Barriers of Repetitive DNA and Secondary Structures

Inverted repeats (IRs), mirror repeats (MRs), and direct tandem repeats (DTRs) are all common features of eukaryotic genomes that have potential to undergo structural transitions and generate secondary structures (Liquori, Ricker et al. 2001). IRs can form cruciform structures in double-stranded DNA and hairpins wide range of structures that depend on their base composition. The best-studied examples are G-quadruplexes, which are formed by tandem guanidines (Nicolas and Petes 1994, Sanders 2010, Martini, Borde et al. 2011, Zhou, Zhang et al. 2014, Castan, Hernandez et al. 2018).

2.9. Replication stress and fragile site expression

Common fragile sites (CFSs) were first described in 1984 as sites on human metaphase chromosomes that are particularly prone to forming cytogenetically defined chromosomal gaps or breaks following the partial inhibition of DNA synthesis1 (Model 10). The same CFSs were seen in all individuals studied and thus were thought to represent a conserved component of chromosome structure. Interest in CFSs rapidly

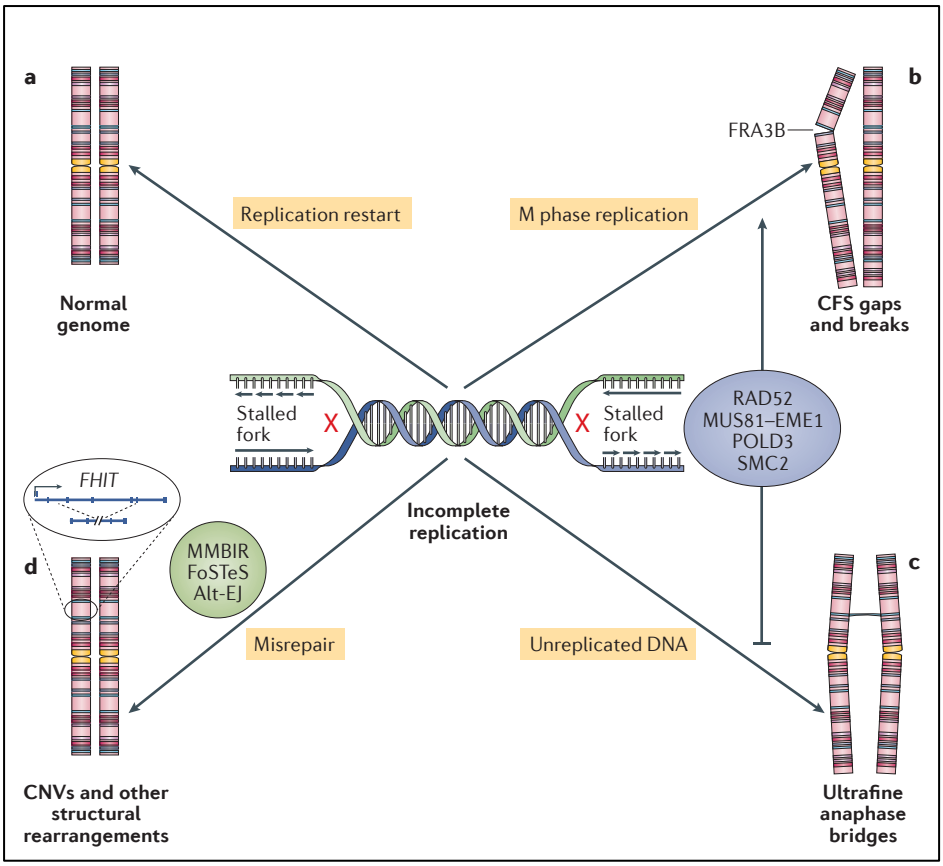
increased for two reasons. First, the agents and conditions that lead to CFS formation (that is, CFS expression) allowed the identification of factors that are involved in the cellular response to perturbed replication known as 'replication stress'. Second, and more prominently, the association of CFSs with recurrent chromosome rearrangements in cancers, including those involving oncogenes, suggested that CFSs could be responsible for these events and could be drivers of tumorigenesis or tumour progression (Rowley 1983, Rowley 1984, Yunis 1984, Nowell, Emanuel et al. 1985, Le Beau 1986, Dal Cin and Sandberg 1989, Rabbitts 1991, Yunis and Tanzer 1993). Notably, these associations were made without the benefit of the human genome sequence or precise mapping of either the chromosome rearrangements or the CFSs. There are few common characteristics associated with CFSs.

2.9.1 CFSs are late replicating due to hard to replicating nature.

Subsequent replication timing studies demonstrated that other CFSs experience similar difficulty in either the progression or the completion of replication (Durkin and Glover 2007). Importantly, late replication is not sufficient to fully define a CFS, as other, stable regions of the genome also replicate late in S phase. Nonetheless, it is clear that late-replicating DNA at CFSs is particularly sensitive to replication inhibitors and has a central role in their instability (Glover 2006).

2.9.2 CFSs are enriched in large genes transcribing even during S phase.

Reports of CFSs extending over several megabases may be influenced by two or more large CFS-associated genes mapping so close together as to be indistinguishable at the cytogenetic level, as was shown for CFSs in the *AUTS2* and *MAGI2* genes on chromosome 7 (Wilson, Arlt et al. 2015). Recent findings, discussed below, offer mechanistic explanations for this interesting association between large gene size and the occurrence of a CFS and suggest that most, if not all, large, actively transcribed, late-replicating genes have the potential to be CFSs.



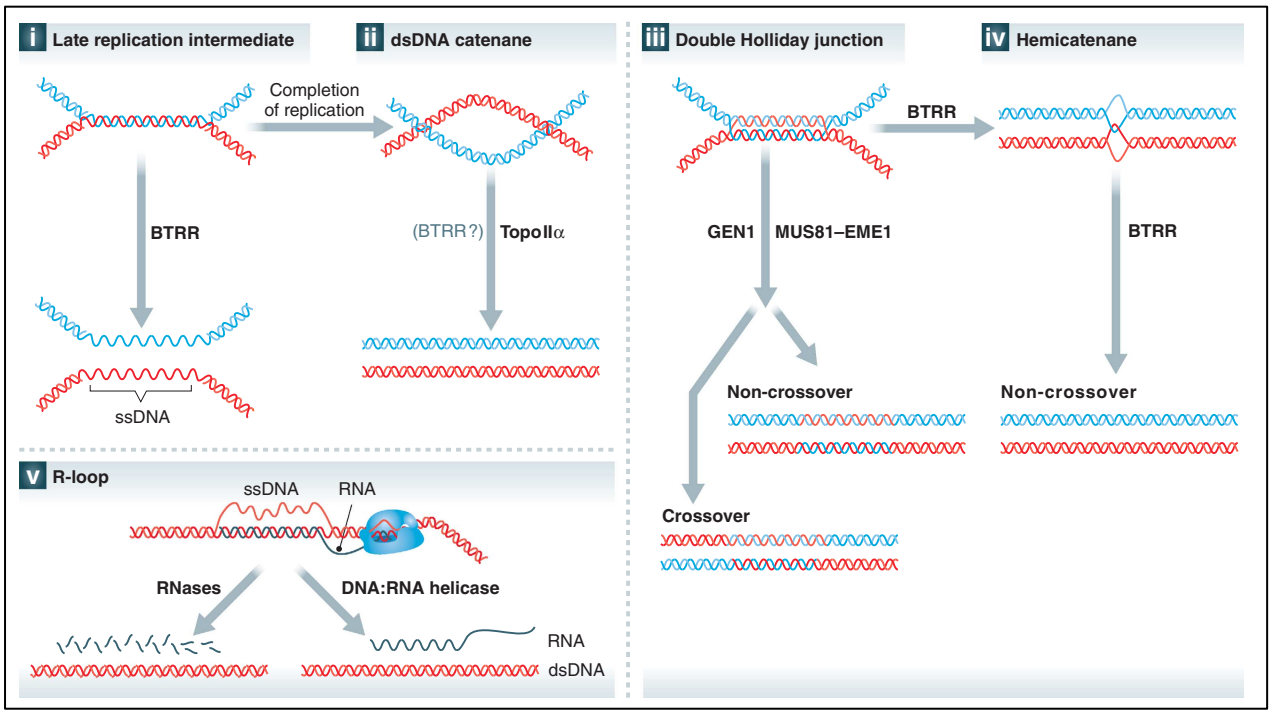
Model 10. Replication stress, genomic instability and fragile sites expression. DNA replication stress during S-phase leads to stalled or collapsed replication forks, which may be resolved in several ways. **A.** Successful restart and completion of replication leads to an intact, normal genome. **B.** If regions of un-replicated DNA (Under-replicated) persist through late S phase, replication may be completed as late as M phase, resulting in an apparent common fragile site (CFS) gap or break due to a lack of normal chromosome condensation. **C.** If the un-replicated DNA is not resolved and persists to anaphase, ultrafine anaphase bridges can form at these sites. **D.** If the stalled or collapsed forks are repaired and restarted through an error-prone mechanism, then genome rearrangements, including copy number variants (CNVs), can occur. Alt-EJ, alternative end joining; *FHIT*, fragile histidine triad; FoSTeS, fork stalling and template switching; MMBIR, microhomology-mediated break-induced replication; POLD3, DNA polymerase δ non-catalytic subunit; SMC2, structural maintenance of chromosomes protein 2. **Modified and adapted (Glover, Wilson et al. 2017)**

2.10 Under-replicated genome in S-phase and Mitosis at CFSs:

To deal with potential problems arising in S-phase (Model 11), cells have evolved efficient checkpoint signaling pathways that become activated following DNA replication stress (Errico and Costanzo 2012, Jones, Mortusewicz et al. 2013). Through these intracellular signaling mechanisms, cells are able to respond in specific ways according to the

particular problem that they encounter (e.g., by activating appropriate repair/tolerance pathways and the firing of additional replication origins). However, as discussed above, these mechanisms may blind, particularly during the terminal steps of DNA replication. So why do cells ever enter mitosis without fully completing S-phase? There are few potential ways to deal with under replicated genomic DNA in S-phase. (1) There may be a fundamental problem associated with DNA replication termination, because the S-phase checkpoint machinery is unable to efficiently detect small regions of un-replicated DNA and gene gating (Dewar and Walter 2017). (2) Certain regions of the genome, particularly those with important structural functions (e.g., centromere and telomeres), are inherently difficult to replicate and to segregate in a coordinated fashion along with the rest of the bulk genomic DNA. Therefore, cells have evolved efficient ways to cope with this inevitable situation, and may in some cases even exploit it to their advantage (Soudet, Jolivet et al. 2014, Jay, Smith et al. 2016, Crefcoeur, Zgheib et al. 2017). (3) The carry-over of incompletely replicated/unresolved chromosomes into mitosis may actually be a fundamental aspect of normal DNA replication at replication fork obstacles cell-cycle progression. This process might fulfill positive and important biological functions, at least in unperturbed cells (Bartek, Bartkova et al. 2007, Bartek, Lukas et al. 2007). (4) Cells may consider mitosis to be a far more hazardous cell-cycle stage than S-phase. Once cells have committed to mitosis, they subsequently proceed as quickly as possible to minimize the possibility of gross chromosomal aberrations (Ganem and Pellman 2012).

The discovery that 'unfinished S-phase business' in mitosis is remarkably prevalent is a relatively new aspect in our understanding of chromosome segregation. However, we are only just beginning to understand how cells maintain genome stability in the face of such persistent, and probably ubiquitous, problems.



Model 11: Examples of DNA structures arising in S-phase under replication stress that may cause problems for chromosome segregation in mitosis unless resolved. A late replication intermediate (**i**), which escapes cleavage by MUS81-EME1 and contains a short stretch of unreplicated ssDNA, can be unwound by the Bloom's complex (depicted as BTRR). As a result of this, the chromosomes may contain regions of ssDNA that persist into mitosis. Fully replicated chromosomes contain dsDNA catenanes (**ii**), forming at replication termination sites. TopoIIa is the main enzyme that can decatenated these DNA entanglements, to produce two fully replicated dsDNA duplexes. In principle, the concerted action of the BTRR complex may also contribute to their decatenation. (Right) A double Holliday junction (**iii**) arises as an intermediate of homologous recombination repair of DNA gaps and breaks in S-phase. This structure can be resolved by the Bloom's complex (depicted as BTRR) in a process known as 'double Holliday junction dissolution', resulting in non-crossover (NCO) dsDNA products. Alternatively, Holliday junctions can be resolved by structure-specific endonucleases, such as MUS81-EME1 or GEN1. Crossover (CO) or NCO dsDNA products are formed depending on the relative orientation of the cleavage and ligation products. A hemicatenane (**iv**) can form at sites of converging DNA replication forks or as an intermediate product in the double Holliday junction dissolution reaction. Hemicatenanes are efficiently resolved by the TopoIIIa component of the Bloom's complex, resulting in NCO dsDNA molecules. (Lower left) An R-loop (**v**), formed during transcription, comprises an DNA:RNA hybrid with a region of displaced ssDNA. Specific DNA:RNA helicases can disrupt R-loops; the RNA transcripts dissociate and the DNA complementary strands are annealed. Alternatively, RNases may digest the RNA transcript. **Modified and adapted from (Mankouri, Huttner et al. 2013)**

2.11. Targeting DNA replication stress for cancer therapy:

The net effect of replicative stress is the stalling of replication forks and the accumulation of ssDNA as previously described RE (Gaillard, Garcia-Muse et al. 2015, Gelot, Magdalou et al. 2015, Gallina, Christiansen et al. 2016, Madireddy, Kosiyatrakul et al. 2016, Irony-Tur Sinai and Kerem 2017). The ssDNA is rapidly coated by ssDNA-binding proteins such as replication protein A (RPA), which then activates the ATR signaling pathway resulting in the subsequent phosphorylation of Chk1 kinase (Costanzo and Gautier 2003). The activity of this pathway is crucial to stabilize stalled forks as well as activate cell cycle S-M checkpoints so as to limit entry into mitosis in the presence of un-replicated DNA (Eykelenboom, Harte et al. 2013). However, under conditions that enhance replication stress, such as in the absence of ATR and Chk1, stalled forks can persist and other replication origins are fired, leading to an exhaustion of deoxynucleotide triphosphate (dNTP) pools, which aggravate replicative stress and further accumulation of non-progressive forks (Fernandez-Capetillo and Nussenzweig 2013, Toledo, Altmeyer et al. 2013). When the amount of ssDNA exceeds the amount of available RPA, the forks may collapse leading to the generation of DNA double strand breaks (DSBs) (Costantino, Sotiriou et al. 2014, Peng, Raghuraman et al. 2014, Kondratova, Watanabe et al. 2015). When these cells are allowed to enter mitosis, the unreplicated chromosomes will trigger cell death through mitotic catastrophe (Canman 2001, Beckta, Dever et al. 2015) .In fact, although replication stress induces genomic instability and fuels tumorigenesis, studies have shown this is only the case when replicative stress occurs at low to mild levels [1,3,18]. High levels of replicative stress, however, may instead induce cancer cell death through mitotic catastrophe and therefore counteract cancer progression (Lecona and Fernandez-Capetillo 2014)(model 12).

To enhance replication stress, several key steps are theoretically subject to manipulation: the entry into S phase; DNA synthesis, replication and repair; and the premature entry into M phase. We will consider conventional approaches such as chemotherapy and radiation, and extend our discussion to emerging novel strategies to enhance replication stress.

Table 1. Therapeutic agents that enhance replicative stress.

Target/mechanism	Compounds	Stage of development
DNA misincorporation/modification	Alkylating agents e.g., cyclophosphamide, temozolamide, etc.	Approved
	Platinum compounds e.g., cisplatin, carboplatin, etc.	Approved
Ribonucleotide reductase	Gemcitabine	Approved
Thymidylate synthetase	5-fluorouracil	Approved
Topoisomerase I	Irinotecan, topotecan	Approved
Topoisomerase II	Etoposide, doxrubicin	Approved
Chk1	UCN-01	Phase I/II. Multiple studies completed
	LY2606368	Phase I/II, one study completed
	AZD7762	Phase I. One completed.
ATR	AZD6738	Phase I, one study completed
PARP1	Olaparib and niraparib	Approved
WEE1	MK-1775	Phase I
MELK	OTS167	Phase I, 2 studies
NAE	MLN4924	Phase I, multiple studies

Model: 12 Therapeutic agents that enhance replicative stress. Adapted from (Zhang, Dai et al. 2016)

2.12 Conclusions and perspectives

CFS gaps and breaks on metaphase chromosomes were discovered more than 35 years ago as the first indicators of the unusually high instability of large, late-replicating genes that also manifests as frequent and, in many cases, unexplained focal CNVs in cancer. We now know that the most frequent and unstable CFSs are enriched within large genes with a paucity of replication origins and that active transcription greatly increases their instability, leading to late or incomplete replication under conditions of replication stress. These perturbations of DNA replication can lead to several different outcomes depending on the resolution of these unreplicated regions including, most importantly for cancer and perhaps normal somatic tissues, CNV formation. In cancer, this relationship is particularly exacerbated because the early stages of oncogenic transformation represent a form of transcription-associated replication stress that can potentiate further genomic instability and CNV formation.

Results: Chapter 1

Tittle: Natural chromosomal pausing sites are endogenous fragile sites prone to accumulate CNVs under replication stress.

One of the earliest observations linking replication stress caused by exogenous and endogenous elements to genomic instability was the appearance of chromosomal breaks on metaphase spreads following treatment of cells with aphidicolin, which inhibits DNA polymerase-α (Glover, Berger et al. 1984). These breaks were observed preferentially at specific chromosomal sites, termed Common Fragile Sites (CFS). Subsequently, comparative genomic hybridization analysis revealed the presence of Gross Chromosomal Rearrangements (GCRs), constituting mainly genomic deletions and amplification, that were mapped to the CFSs. This suggested that chromosomal breaks may result from aberrant DNA replication events (Durkin and Glover 2007).
Fragile sites can be classified into Early CFSs and Late CFSs, depending on their time of occurrence during S-phase (Arlt, Casper et al. 2003, Barlow, Faryabi et al. 2013). Fragile sites can potentially stall or pause replication forks and activate the replication checkpoint and different DNA Repair pathways. Under physiological conditions, endogenous elements could cause fork pausing and stalling, leading to different events in a locus-specific manner. These loci can be classified as Natural chromosomal pausing sites (NCPs), Hard to replicate region and Replication fork barriers (RFBs). The link between NCPs and CFSs expression is poorly understood.

NCPs and RFBs cause replication fork stalling and polar pausing, involve either remodeling or disassembly of the replisome, and can occur with or without DNA breakage (Jaarsma, van der Pluijm et al. 2011, Berti, Ray Chaudhuri et al. 2013, Sirbu, McDonald et al. 2013). Stalled and polar paused forks challenge DNA synthesis and activate the replication checkpoint kinases ATR^{mec1}/ATM^{tel1}. In certain cases, DNA replication is completed by the firing of adjacent dormant origin (Mayle et al., 2015; Nguyen et al., 2015; Yekezare et al., 2013). However, to guard against the possibility that replication fork from dormant origins may also fail, cells deploy homologous recombination (HR) enzymes that occasionally can restart collapsed forks (Lambert et al., 2010; Mohebi et al., 2015; Nguyen et al., 2015; Yeeles et al., 2013). This so-called recombination-dependent replication (RDR) or Break Induced Replication (BIR) ensures

that the DNA is fully replicated prior to chromatid segregation, thereby avoiding mitotic catastrophes.

The presence of under-replicated DNA at NCPs, CFSs and other genomic regions could potentially induce broad changes to chromosome structure and number by interfering with mitosis consequently leading to aneuploidy. Regions of under-replicated DNA may form anaphase bridges as hallmark of replication stress, which interfere with chromosome segregation during mitosis, resulting in DNA damage in the next cell cycle and genomic instability.

Another type of genomic change induced by DNA replication stress is tandem segmental genomic duplication commonly observed following ionizing radiation (IR) or oncogene induced replication stress. The difference may relate to the fact that IR and oncogenes induce fork collapse, whereas aphidicolin and hydroxyurea induce primarily fork stalling. Collapsed forks are processed into one-ended DNA DSBs, which are then repaired specifically by BIR pathway, which is a form of homologous recombination. According to one model, BIR may produce tandem genomic duplications when the collapsed fork being repaired is near a progressing fork (Arlt, Mulle et al. 2009, Hastings, Ira et al. 2009, Hastings, Lupski et al. 2009, Arlt, Ozdemir et al. 2011, Arlt, Rajendran et al. 2012, Arlt, Wilson et al. 2012, Carr and Lambert 2013, Arlt, Rajendran et al. 2014, Costantino, Sotiriou et al. 2014).

In addition to changes in chromosome structure, DNA replication stress has the potential to induce single nucleoutide substitution (SNS) (Howlett, Taniguchi et al. 2005). Stalling or collapse of replication forks results in DNA being single-stranded for protracted periods of time; during this time, damaged bases cannot be repaired efficiently, resulting in SNSs. Single-stranded DNA also arises during repair of collapsed replication forks by BIR because in BIR the two strands of DNA are not coordinately replicated. Thus, in yeast, replication by BIR is associated with about a thousand-fold increase in mutation rates, as compared to normal replication (Anand, Lovett et al. 2013, Saini, Ramakrishnan et al. 2013, Anand, Tsaponina et al. 2014, Sotiriou, Kamileri et al. 2016).

Endogenous NCPs and RFBs are obstacles that pause fork in a polar and transient manner. One can enhance the pausing and stalling using aphidicolin (Aph) or hydroxyurea (HU), which slow down global replication synthesis.

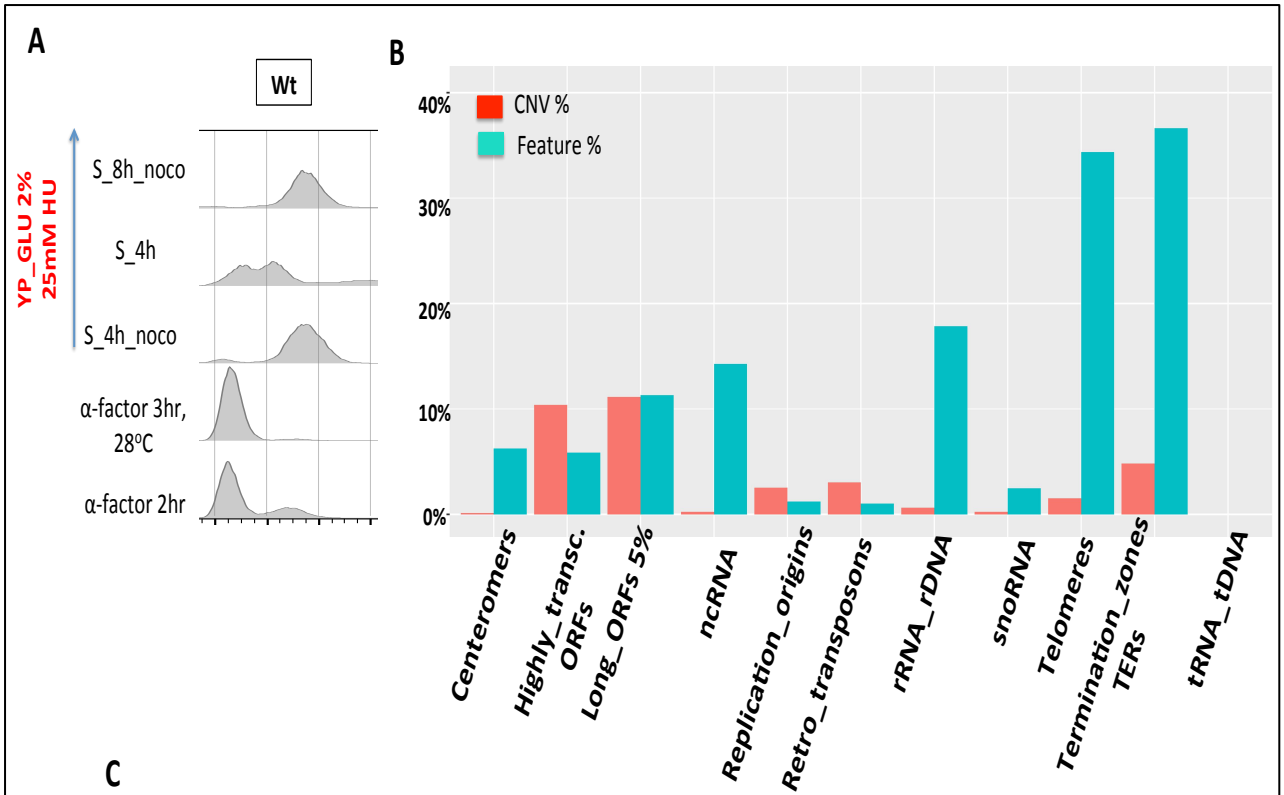
We were interested to find patterns in copy number variation (CNVs), deletion and amplification under mild replication stress in proliferating cells. We utilized next generation sequencing (NGS) and looked for chromosomal structural variants (CSVs) to mark/assign fragile sites. We scored CNV distribution with respect to pausing elements, hard to replicate genomic loci, Fork converging loci (TERs), repeat sequences (rDNA, LTRs, Telomers) and RFBs.

1.2 Genome wide mapping of CNVs under mild replication stress in wild type cells.

We scored for CNV in wild type cells grown for a different number of cell cycles under mild replication stress (25mM HU for 8hours). Our hypothesis was that endogenous fork pausing and stalling are the key source of genomic instability. In our experiments, G1 arrested wild type (MATa) cells were released in S-phase at 30^{o}C with or without 25mM HU for 2 cell cycle divisions. We then added nocodozole to arrest proliferating cells in G2/M phase of cell cycle and purified genomic DNA and processed for NGS. This procedure avoids any biasness in sequencing because of differences in cell cycle stage between strains (Fig. 1.A).

We scored for distribution of total CNVs along 11 different categories of genomic loci referred as features. These features includes regions which have transcriptional activity dependency on RNAP I (rDNA), RNAP II (mRNAs, ncRNA, retro-transposones, centromeres), RNAP III (snoRNAs, tRNAs), repeat regions (rDNA, telomeres, retro-transposones), natural polar fork barrier (tRNA, LTRs, rDNA), non-histone proteins-DNA complex barriers (CEN) and regions with end-replication problems (Telomeres). Apart of these genomic features, we included DNA replication origin (ARSs) and DNA replication termination zones (TERs).

We observed accumulation of CNVs at rDNA (5/28), Telomeres (11/32) and TERs (26/71) with significant $p<0.05$ carrying either deletion or amplification (Fig.1.C). rDNA loci have programmed fork arrest (PFA) elements that pause forks in a polar orientation. Programmed fork arrest at rDNA is essential for faithful replication and segregation of rDNA array. We observed strong accumulation of CNVs, mostly genomic deletion at 5 rDNA features out of 28. PFA has been hypothesized as a mechanism to facilitate replication tyermination at replication termination zones and at telomeress.



C

Type	Ref	Test	TotalCNV	Total Deletion	Total Amplification	Total Features	CNV Overlap	Deletion Overlap	Amplification Overlap	Feature Overlap	P-value
Centromere	wt_4h	wt_8h	789	225	564	16	1	1	0	1	0.17628
HighTranscribingORF	wt_4h	wt_8h	789	225	564	1143	82	79	15	67	0.99307
LongORF_fivepercent	wt_4h	wt_8h	789	225	564	336	88	66	50	38	0.99721
ncRNA	wt_4h	wt_8h	789	225	564	14	2	2	0	2	0.21497
ReplicationOrigin	wt_4h	wt_8h	789	225	564	410	20	20	15	5	0.23112
Reterotransposon	wt_4h	wt_8h	789	225	564	486	24	22	19	5	0.90712
rRNA	wt_4h	wt_8h	789	225	564	28	5	9	0	5	8,30E-07
snoRNA	wt_4h	wt_8h	789	225	564	81	2	2	0	2	0.55602
Telomere	wt_4h	wt_8h	789	225	564	32	12	12	1	11	0.22144
Termination	wt_4h	wt_8h	789	225	564	71	38	29	12	26	0.0012358
tRNA	wt_4h	wt_8h	789	225	564	395	0	0	0	0	1

Figure 1. Mild replication stress accumulates Genome wide CNVs (deletion and amplification) at affecting most of natural chromosomal pausing sites.

A). FACs profile to assess cell cycle progression of wild type strain in 25mM HU.

B). Genome wide distribution of CNVs in wild type strain after 8h (2-cell cycle) in 25mM HU compare to 4hrs (1 cell cycle). X-axis marked with 11 categories of genomic features which cover most of natural chromosomal pausing site RFBs sites and repeat region in genome and

Y-axis: red bar labeled as CNV% (percentage of total 789 CNVs overlap with given feature)

Green bar labeled features% (percentage of given feature overlap with CNVs).

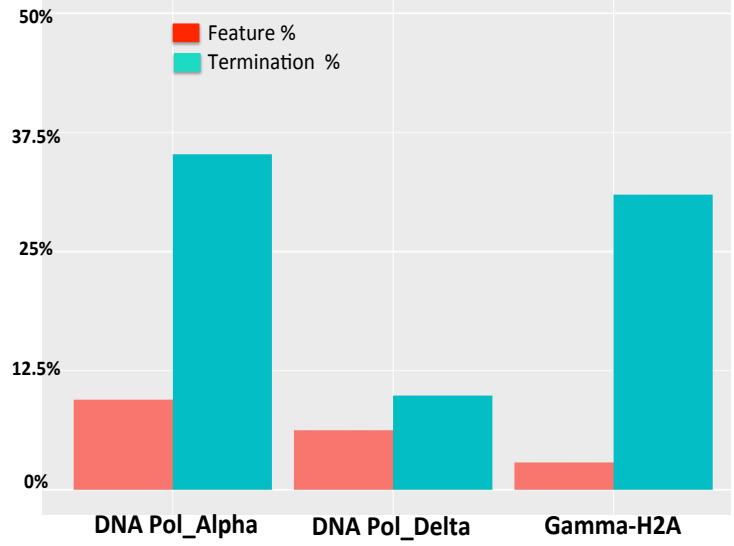
C). Tabular representation of all CNVs in wt_8h_25mMHU, distributed along different genomic features. Total CNVs categories as deletion and amplification, and overlap with different genomic features assess for signification $p < 0.05$. In similar way, we assess how many features appeared to overlap with CNVs, as some features tend to have more then one CNV for one element of feature. Telomeres (11 features) and Termination zones (26 features, deletion $p=0.001235$) showed significant correlation with CNVs distribution.

1.3 Reduced level of DNA Pol α make TERs fragile.

Adjacent and converging forks by generating local replication termination zones, can rescue replication forks, which are stalled or collapsed. Our lab demonstrated that TERs are genetically defined loci and carry endogenous properties of polar fork pausing and PFA.

It is unclear whether HU causes global replication fork pausing and stalling at both lagging and leading strand synthesis. Therefore we decided to explore available studies from (Song, Dominska et al. 2014, Zheng, Zhang et al. 2016) where DNA syntheses of lagging or leading strand were genetically and selectively impaired by reducing DNAP α or DNAP δ, respectively.). Tom Petes's lab scored for different kind of GCRs across genome including deletion, amplification, SNPs, crossover or non-crossover translocation and inversions using dedicated strains for genetic screening.

A



B

Type	Test	Total Features	Termination Total	Feature Overlap	Termination Overlap	P-value	% of TERs
Termination	Gamma-H2A	878	71	25	22	0.94694	30.98%
Termination	DNA Pol_Alpha	286	71	27	25	0.0070006	35.21%
Termination	DNA Pol_Delta	112	71	7	7	0.76123	9.85%

Figure2: Replication Termination Zones are fragile sites.

A). Termination zones overlap with GCR events caused by reduced level of DNA Replication polymerases Alpha (α and δ). Distribution of DNA damage repair (DDR) marker Gamma-H2Ax along TERs in wild type strain.

B). Tabular form of distribution of features described in Fig.2.A. All 3 features tested against Termination Zones (4.5kb mean length), Reduced DNA pol Alpha and delta causes 25 and 7 TERs out of 71 TERs tested against given feature. DDR marker Gamma-H2Ax Chip-Peaks overlap with 22 TERs.

Interestingly, TER fragility showed biasness towards DNA polymerase alpha depletion. Depletion of DNA Pol α significantly increases number of GCR events (27/286) at TERs

and cover 35% (25/71) of total TERs (Fig.2.A) while reduced amount of DNA Pol delta affected only 7 TERs. Extensive RF pausing and stalling at TERs might generate DNA breaks leading to accumulation of DDR signals at TERs. We therefore analyzed the gamma-H2AX CHIP profile obtained under physiological conditions in budding yeast by Rachel et al. 2010. We scored for the presence of significant cluster of peaks of gamma-H2Ax at TERs. Indeed, TERs accumulate significant gamma-H2Ax peaks (Fig 2A,B): 22 TERs overlap with 25 peak clusters out of total 878 peaks. Thus we conclude that TERs are natural polar pausing elements characterized by intrinsic fragility.

1.3. Tel1 and Mec1 control CNVs at natural chromosomal pausing sites, RFBs and TERs.

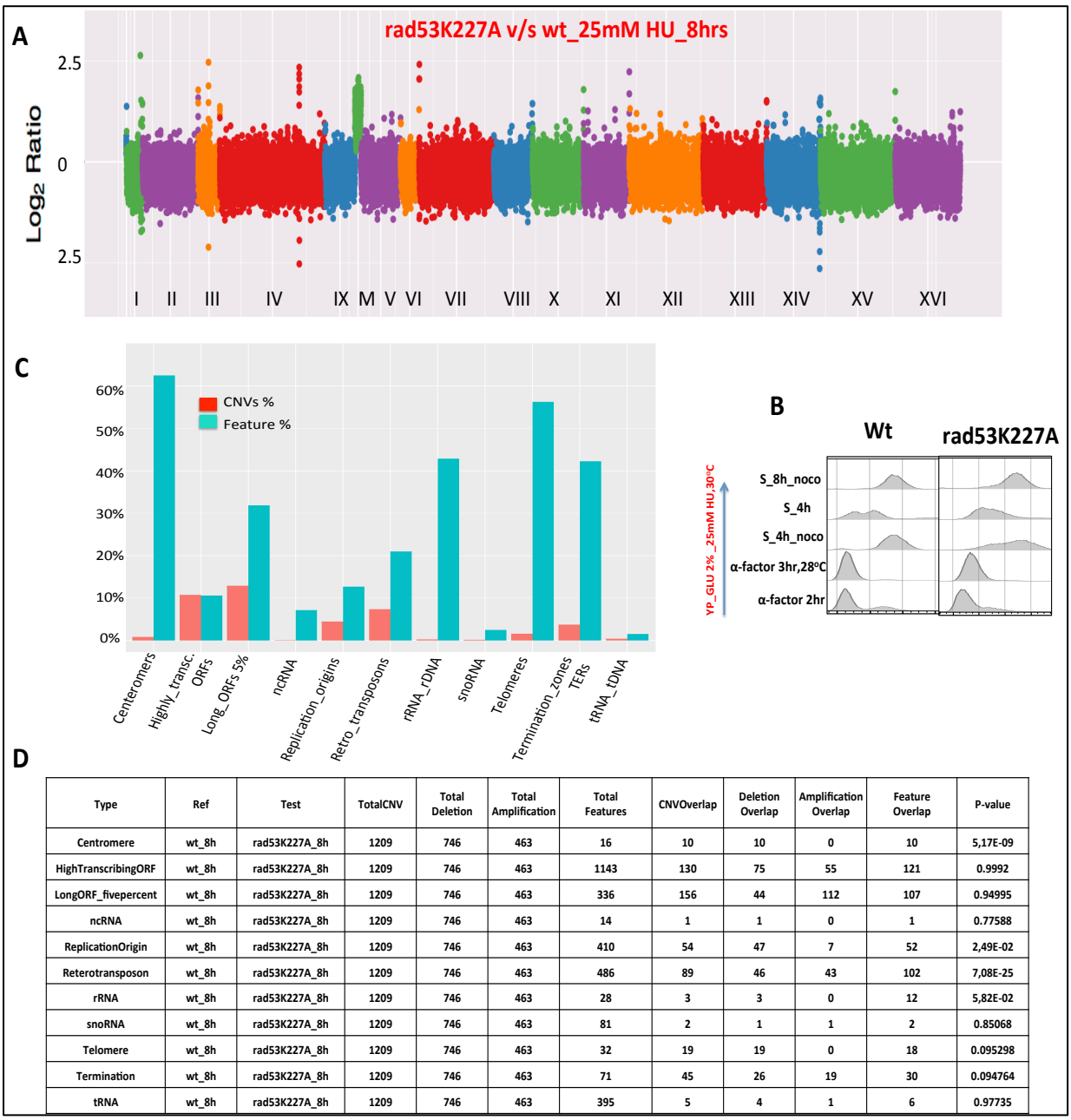
Replication fork integrity is controlled by the replication checkpoint kinases ATR and ATM. In budding yeast Mec1p (ATR) and Tel1p (ATM) activate a cascade of phosphorylation of downstream effector proteins, including Rad53p (CHK1), that control the integrity of stalled and terminal forks, respectively (Lopes, Cotta-Ramusino et al. 2001, Cotta-Ramusino, Fachinetti et al. 2005, Doksani, Bermejo et al. 2009). Mec1, in particular, regulates the architecture of the replication forks, modulates dNTP synthesis via the Dun1p-Sml1p axis, suppresses dormant/late origin firing to avoid depletion of RPA (Rfa1), regulates replisome stability (Cortez 2017) and recruits DNA damage repair proteins on collapsed fork. Programmed fork arrest can be promoted by checkpoint-mediated phosphorylation of the replication fork protection complex subunits Tof1 and Csm3.

Along this notion, we wanted to address whether the replication checkpoint kinases influence the fragility of natural chromosomal fork pausing sites, RFBs and TERs.

1.3.1 Rad53 suppresses CNVs in proliferating cells under replication stress.

To capture spontaneous and key initial GCRs in replication checkpoint deficient cells, we used the kinase- dead allele of Rad53 that retains only 10% kinase activity compared to wild type. Wild type and *rad53-K227A* strains were arrested in G1 and released into S-phase (Fig.3B) and CNVs were mapped along the whole genome by NGS. We captured a total of 1209 CNVs in *rad53-K227A* distributed along the different chromosomes (Fig. 3A) and different RFBs (Fig.3C).

Genome wide Meta analysis showed that the majiority of CNVs are genomic deletions at centrosomes (10/10 CNVs). We captured significant CNVs at 52 replication origins (ARSs) out of total of 410 ARS. Retro-transposones (repeat region, RNA pol II) and rDNA (repeat region, RNA pol I) showed strong correlation with CNVs; CNVs at rDNA loci were mainly deletions. snoRNA and tRNA transcribed by RNA pol III, showed no significant relation with CNVs. Checkpoint mutant strain *rad53-K227A* accumulated CNVs at 18 out of 32 telomeres and 30 out of 71 termination zones (TERs).



Type	Ref	Test	TotalCNV	Total Deletion	Total Amplification	Total Features	CNVOverlap	Deletion Overlap	Amplification Overlap	Feature Overlap	P-value
Centromere	wt_8h	rad53K227A_8h	1209	746	463	16	10	10	0	10	5,17E-09
HighTranscribingORF	wt_8h	rad53K227A_8h	1209	746	463	1143	130	75	55	121	0.9992
LongORF_fivepercent	wt_8h	rad53K227A_8h	1209	746	463	336	156	44	112	107	0.94995
ncRNA	wt_8h	rad53K227A_8h	1209	746	463	14	1	1	0	1	0.77588
ReplicationOrigin	wt_8h	rad53K227A_8h	1209	746	463	410	54	47	7	52	2,49E-02
Reterotransposon	wt_8h	rad53K227A_8h	1209	746	463	486	89	46	43	102	7,08E-25
rRNA	wt_8h	rad53K227A_8h	1209	746	463	28	3	3	0	12	5,82E-02
snoRNA	wt_8h	rad53K227A_8h	1209	746	463	81	2	1	1	2	0.85068
Telomere	wt_8h	rad53K227A_8h	1209	746	463	32	19	19	0	18	0.095298
Termination	wt_8h	rad53K227A_8h	1209	746	463	71	45	26	19	30	0.094764
tRNA	wt_8h	rad53K227A_8h	1209	746	463	395	5	4	1	6	0.97735

Figure 3: Mapping genome wide CNVs in Rad53K227A strain under replication stress.
A). CNVs Rad53K227A compared with wild type (Wt.), represented along all 16 chromosomes. Y axis showed Log ratio of sequencing reads comparison, X axis represent different chromosomes covering different width depending in their size and 5 different colors used to represent 16 chromosomes where different chromosomes appear in same colors too (To avoid any confusion, there is no translocation and gross chromosomal rearrangements represented here).

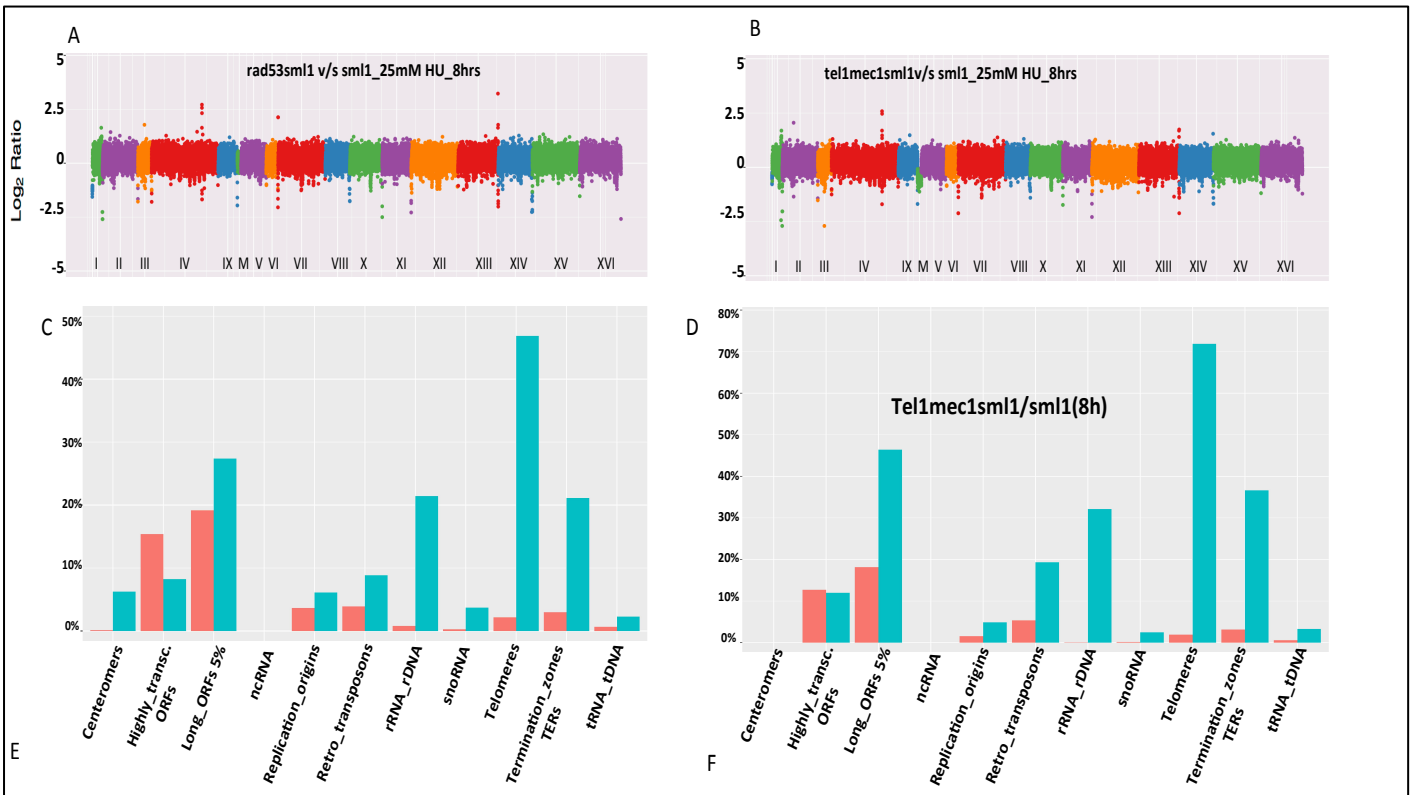
B). FACs profile of the Wt. and Rad53K227A with 25mM HU at 8h and arrested in G2/M with Nocodazole. Meanwhile, took 4h time point with and without Nocodazole to access cell cycle progression.
C). Genome wide distribution of CNVs of Rad53K227A yeast strain. X-axis marked with 11 features which cover most of RFBs sites and repeat region in genome and Y-axis should percentages of total CNVs (1209) overlap with given feature as red bar and percentage of the features marked by CNVs shown as green bar.
D). Tabular representation of all CNVs in Rad53K227A, distributed along different genomic features. Total CNVs categories as deletion and amplification and association with RFBs with p value.

These observations imply that Rad53 affect a wide range of RFBs under replication stress.

1.3.2 *rad53 sml1* and *tel1 mec1 sml1* experiencing mild replication stress (25mM HU) showed major genomic CNVs

To understand the effect of the complete ablation of Rad53 kinase activity on the fragility at natural pausing sites, we used *rad53 sml1* strain. Rad53 deletion has deleterious effect on cell viability that might be caused by extensive genomic instability at endogenous natural pausing sites. Rad53 deletion strains are varying sensitive for dNTP levels and cell viability can be rescued by Sml1p deletion, which is an inhibitor of the RNR enzyme. Sml1p deletion leads to increase in dNTP level and replication fork progression, which rescues cell viability under physiological condition in *RAD53* deleted cells. In order to completely eliminate the replication checkpoint activation, we used the tel1mec1sml1 strain. These strains enabled us to capture genome fragility at endogenous NPS Fig4A and Fig4B respectively.

Checkpoint mutant strain *rad53 sml1* showed significant CNVs accumulation at rDNA, telomeres and TERs (Fig.4C, 4E) but not at replication origins, unlike in rad53-K227A. Interestingly, *tel1 mec1 sml1* strains accumulated CNVs across retro-transposons, rDNA and TERs (Fig.4D, 4F). Remarkably, *rad53-K227A* mutants affected 30 TERs (p=0.0947), *rad53 sml1* 15 TERs (p=0.823) and *tel1 mec1 sml1* 26 TERs.



Type	Ref	Test	Total CNV	Total Deletion	Total Amplification	Total Features	CNV Overlap	Deletion Overlap	Amplification Overlap	Feature Overlap	P-value
rRNA	sml1_8h	rad53sml1	741	688	53	28	6	0	6	6	1,28E-10
Telomere	sml1_8h	rad53sml1	741	688	53	32	16	0	16	15	0.0145
snoRNA	sml1_8h	rad53sml1	741	688	53	81	2	2	0	3	0.6946
Termination	sml1_8h	rad53sml1	741	688	53	71	22	22	0	15	0.82961
Reterotransposon	sml1_8h	rad53sml1	741	688	53	486	29	2	27	43	0.20662
HighTranscribingORF	sml1_8h	rad53sml1	741	688	53	1143	114	111	3	94	0.82405
tRNA	sml1_8h	rad53sml1	741	688	53	395	5	5	0	9	0.95652
Centromere	sml1_8h	rad53sml1	741	688	53	16	1	1	0	1	0.4214
ncRNA	sml1_8h	rad53sml1	741	688	53	14	0	0	0	0	1
LongORF_5%	sml1_8h	rad53sml1	741	688	53	336	142	126	16	92	2,98E-01
ReplicationOrigin	sml1_8h	rad53sml1	741	688	53	410	27	24	3	25	0.35005

Type	Ref	Test	TotalCNV	Total Deletion	Total Amplification	Total Features	CNV Overlap	Deletion Overlap	Amplification Overlap	Feature Overlap	P-value
rRNA	sml1_8h	tel1mec1sml1_8h	1361	1240	121	28	1	0	1	9	0.00325
Telomere	sml1_8h	tel1mec1sml1_8h	1361	1240	121	32	26	1	25	23	0.0008201
snoRNA	sml1_8h	tel1mec1sml1_8h	1361	1240	121	81	2	2	0	2	0.94094
Termination	sml1_8h	tel1mec1sml1_8h	1361	1240	121	71	43	39	4	26	0.70526
Reterotransposon	sml1_8h	tel1mec1sml1_8h	1361	1240	121	486	73	6	67	94	2,23E-05
HighTranscribingORF	sml1_8h	tel1mec1sml1_8h	1361	1240	121	1143	173	167	6	137	0.97491
tRNA	sml1_8h	tel1mec1sml1_8h	1361	1240	121	395	8	6	2	13	0.84773
Centromere	sml1_8h	tel1mec1sml1_8h	1361	1240	121	16	0	0	0	0	1
ncRNA	sml1_8h	tel1mec1sml1_8h	1361	1240	121	14	0	0	0	0	1
LongORF_fivepercent	sml1_8h	tel1mec1sml1_8h	1361	1240	121	336	247	212	35	156	2,66E-07
ReplicationOrigin	sml1_8h	tel1mec1sml1_8h	1361	1240	121	410	21	14	7	20	0.9972

Figure4: Mapping genome wide CNVs in *rad53 sml1* and *tel1mec1 sml1* strains under replication stress.
A, B) Whole Genome sequencing reads (NGS) of *rad53sml1* and *tel1mec1sml1* compared with sml1, represented along all 16 chromosomes. Y axis showed Log ratio of reads comparison, X axis represent different chromosomes covering different width depending in their size and 5 different colors used to represent 16 chromosomes where different chromosomes appear in same colors too.(we don't score for translocation and inversions as GCRs).
C, D). Genome wide distribution of CNVs for *rad53 sml1* (741 CNVs) and *tel1 mec1 sml1* (1361 CNVs). X-axis marked with 11 features which cover most of RFBs sites and repeat region in genome and Y-axis should percentages of total CNVs overlap with given feature as red bar and percentage of the features marked by CNVs shown as green bar.
E, F) Tabular representation of all CNVs *rad53 sml1* (741 CNVs) and *tel1 mec1 sml1* (807 CNVs), distributed along different genomic features and CNVs categorized as Deletion and Amplification.

Hence, the Replication checkpoints protect fork stability during fork conversion at TERs, likely by coordinating a programmed fork arrest and the detachment of gated genes from the nuclear envelope (Bermejo, Capra et al. 2011, Bermejo, Kumar et al. 2012).

1.3.3 Tel1p/Mec1p control the fragility of Replication Termination Zones (TERs).

We employed PFGE to visualize potential DNA breaks at TERs under replication stress in the absence of checkpoint kinases. We first assayed yeast viability using spot assay on YPGlu plates with and without HU at different temperature conditions (Fig5A). While tel1 mutants behaved like wild type cells, *mec1 sml1* and *rad53-K227A* mutants exhibited cell lethality in response to replication stress, as expected. Sml1 deletion rescued the HU sensitivity of Rad53 ablated cells under low HU concentrations.

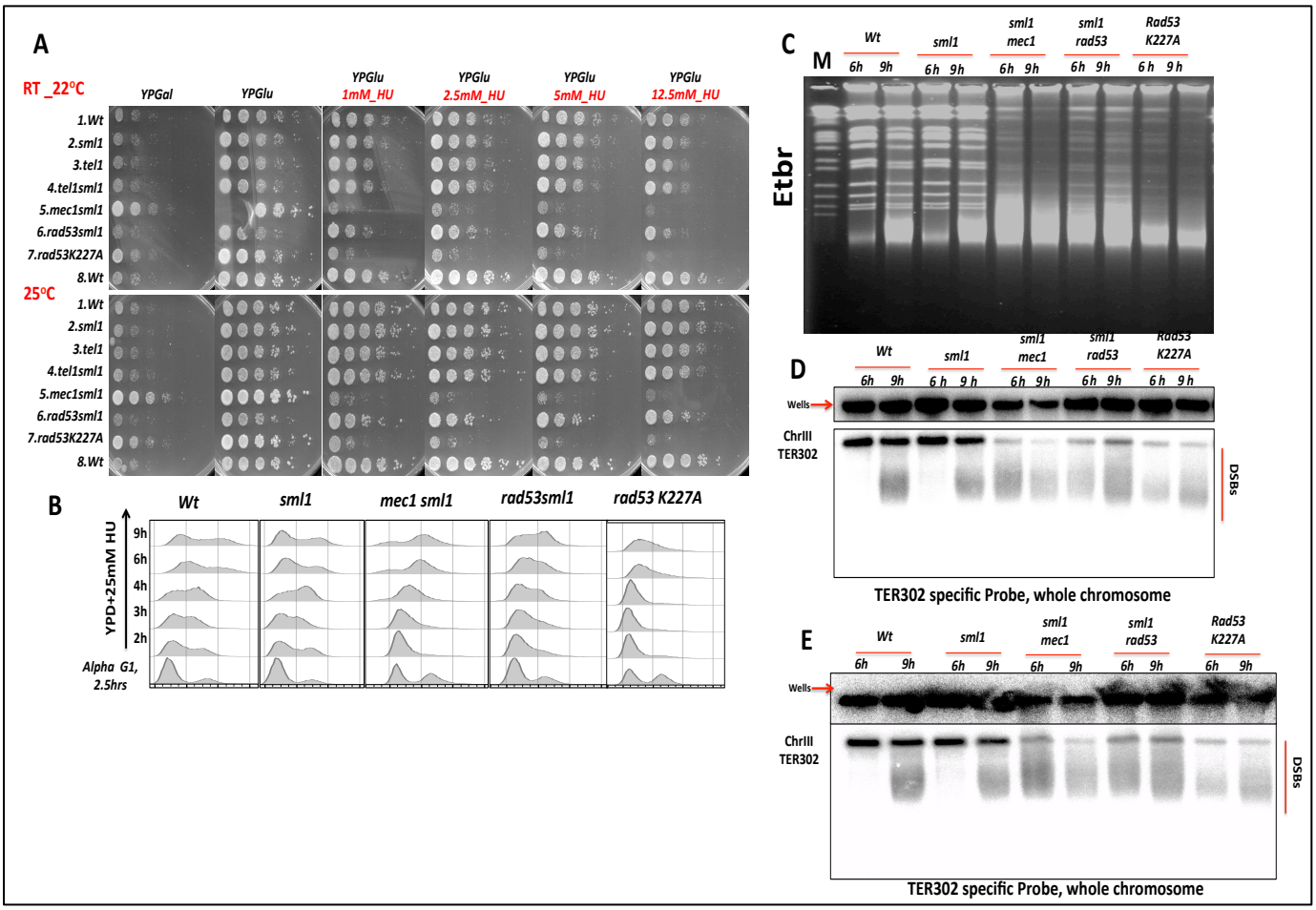


Figure5: Replication Checkpoints (Mec1p/Tel1p) suppresses fragility and higher molecular weight Replication Intermediates at TERs in presence of mild replication stress.

A). Spot assay to assess viability of different mutant strains in Tel1p/Mec1p replication checkpoint pathway. Strains grown over night, and spotted on YPGal and YPGlu plates with mild replication stress 1mM, 2.5mM, 5mM, 12.5mM at RT (22°C) and 25°C.

B). FACs profile of different Checkpoint mutants at mild replication stress. Based on spot assay viability, we picked 3 strains *mec1 sml1, rad53 sml1 and rad53-K227A* along with Wt and sml1 as control. These strains arrested in G1 and released in S-phase in YPGlu+25mM HU, followed till 9hrs-collecting samples for FACs and PFGE for fragility assay at TERs.

C). PFGE based assay for gross chromosomal integrity with staining on Ethidium Bromide (EtBr). Cells from 6h and 9h time point processed and subjected PFGE (20h run) along Marker (M) and stained with EtBr.

D). TERs are fragile in absence of checkpoints proteins in mild replication stress. Gel from Fig.C, processed further and look at specific genomic loci TER302 with specific probe length of 1kb. Two representative southern blots show from

independent experiments (Fig E). Below ChrIII band (detected with probe TER302) and DSBs marked, wells showed retention of Chr III because of X molecules or higher molecular Replication Intermediates at TERs.

We then measured DNA breaks using PFGE (Pulse Field Gel Electrophoresis) across different genotypes in presence of 25mM HU, at different time points of S-phase (Fig 5B). Checkpoint deficient cells completed the bulk of replication in the presence of mild replication stress. However, rad53-*K227A* and *mec1 sml1* remain arrested in G2/M after 9hrs of release, while *rad53 sml1* mutants kept cycling like wild type cells (Fig 5B). EtBr staining of PFGE gels showed differences in chromosomal migration patterns in checkpoint deficient cells compared with wild type cells (Fig 5C). Under-replication of TERs can entangle parental strands leading to the formation of higher molecular weight structure, which cannot migrate further in CHEF gels. We used the TER302 specific probe to visualize the accumulation of replication intermediates (RI) and DNA breaks at TERs. Checkpoint deficient *rad53 sml1, mec1 sml1* and *rad53-K227A* exhibited entangled chromosomes and extensive DNA breaks formation (Fig 5D,E).

1.4 Topological constrain at TERs accumulate replication intermediates and breaks in Replication checkpoint deficient strains under replication stress.

Replication termination zones represent an intense topologically stressed domain as replication and transcription collision causes accumulation of positive supercoiling. We hypothesized that Top2 could influence the integrity of RI at TERs, particularly in the absence of a functional replication checkpoint. We used temperature sensitive *top2-1* mutants in combination with *rad53-K227A* to measure RI at TERs in proliferating cells under mild replication stress.

Spot assay based viability analysis showed that *rad53* and *top2-1* are synthetic sick at different HU concentration and temperature regime (Fig 6A). Interestingly, Top2 inactivation in rad53 mutants resolved chromosome III entanglement at TERs in CHEF (Fig 6C). However, TER fragility was expressed in *top2-1* cells and DNA breakage was enhanced in the *rad53-K227A top2-1* double mutant combination (Fig 6D).

We conclude that in checkpoint defective cells Top2 activity contributes to chromosome entangling and that both Top2 and the replication checkpoint protect TER integrity.

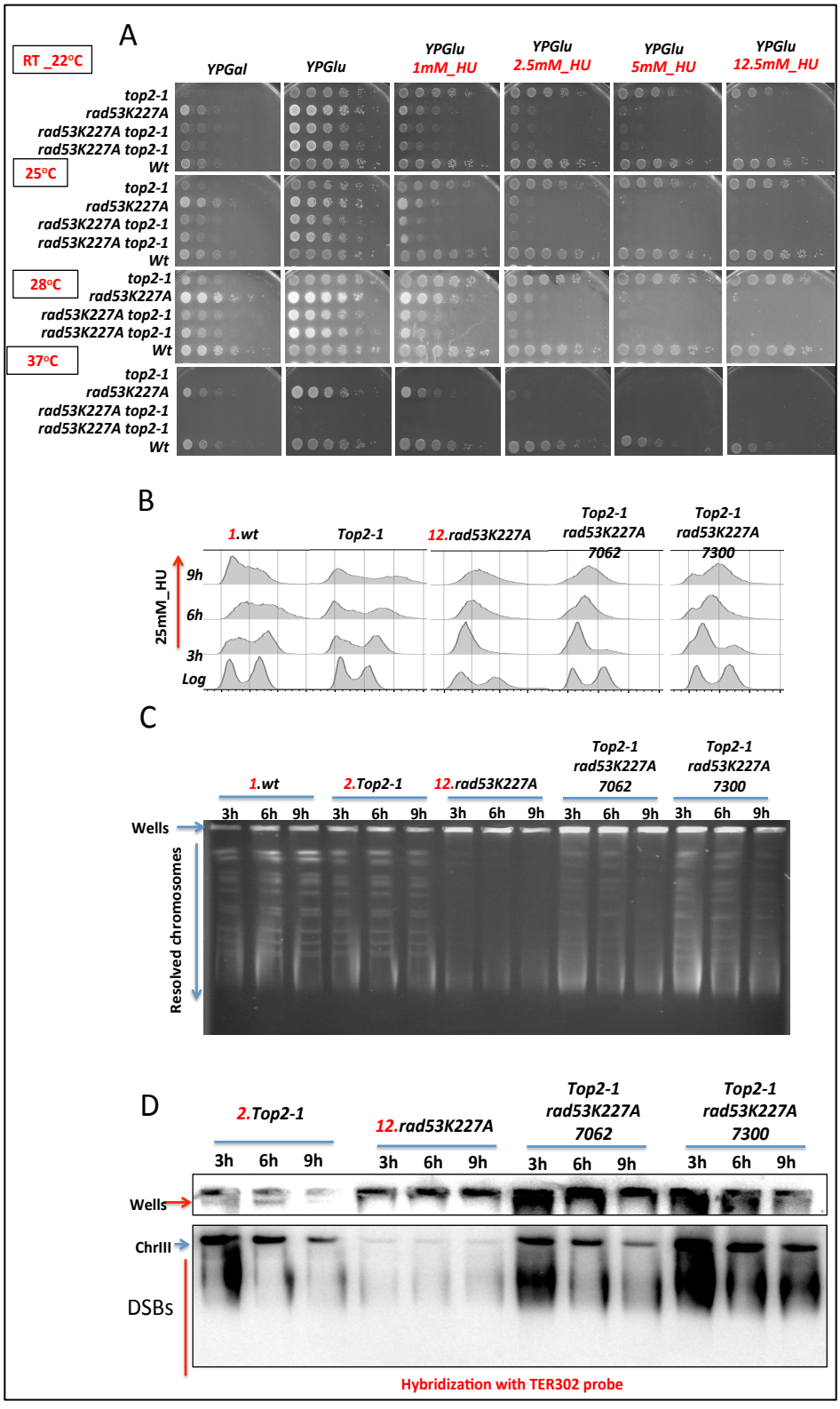


Figure 6: Top2p and Replication Checkpoint proteins interact to suppresses DNA breaks and unusual replication Intermediates at TERs.

A). Spot assay to assess viability of different mutant strains top2-1 (ts) and Rad53K227A along with Wt and *top2-1* Rad53K227A. Strains grown over night, and spotted on YPGal and YPGlu plates with mild replication stress 1mM, 2.5mM, 5mM, 12.5mM at RT-22oC and 25oC, 28oC and 37oC

B). FACs analysis of different strains grown in YPGlu+25mM and samples were collected at different time intervals as indicated for FACs and PFGE.

C). PFGE based assay for gross chromosomal integrity with staining on Ethidium Bromide (EtBr). Cells from 6h and 9h time point processed and subjected PFGE (20h run) along Marker (M) and stained with EtBr.
D). TERs are fragile in absence of checkpoints proteins in mild replication stress. Gel from Fig.C, processed further and look at specific genomic loci TER302 with specific probe length of 1kb. Two representative southern blot show from different experiments (Fig E also). Below ChrIII band (detected with probe TER302) and DSBs marked, wells showed retention of Chr III because of X molecules or higher molecular Replication Intermediates at TERs.

1.5 Conclusion:

The replication checkpoint represents a cancer barrier in response to oncogene induced replication stress (Bartkova, Rezaei et al. 2006, Di Micco, Fumagalli et al. 2006, Durkin, Arlt et al. 2006). We mimicked replication stress using low doses of HU and found that rDNA, telomeres and TERs represent hot spots for CNVs. rDNA, telomeres and TER zones are common features: these are genomic regions that undergo tremendous topological stress and extensive fork pausing, followed by termination. In fact, Top2 assists their replication. These findings indicate that these genomic loci are intrinsically prone to breakage and rearrangements. This is consistent with the finding that TERs have been isolated also in genetic screens aimed at identifying yeast fragile sites (Song, Dominska et al. 2014, Yin, Dominska et al. 2017).

The fragility of these sites is greatly enhanced in checkpoint mutants. This finding likely reflects the observation that in checkpoint defective cells Top2 has aberrant activities leading to DNA break formation (Cha and Kleckner 2002, Hashash, Johnson et al. 2011, Hashash, Johnson et al. 2012). Checkpoint defective cells also exhibited rearrangements at a subset of replication origins. This result may reflect the finding that checkpoint defective mutants experiencing replication stress collapse those forks arising at early origins (Lopes, Cotta-Ramusino et al. 2001). Moreover, we observed strong accumulation of CNVs at transcribed genes in checkpoint mutants, likely due to their inability to uncouple transcription from gene gating, thus leading to topological stress and fork reversal (Bermejo, Capra et al. 2011, Bermejo, Kumar et al. 2012, Bermejo, Lai et al. 2012).

Results: Chapter 2

Tittle: Condensins control the integrity of natural fork pausing elements and TERs.

The condensin complex, along with Topoisomerases II (Top2p), regulates chromatin dynamics during cell cycle-dependent. Condensins are highly conserved from bacteria to humans. In budding yeast the condensin complex is composed of 5 proteins: the coiled coil SMC proteins (Smc2p, and Smc4p), the heat domain containing proteins (Ycg1p and Ycs4) and kleisins domain containing Brn1p (Kinoshita, Kobayashi et al. 2015, Reyes, Serrurier et al. 2015). The localization of condensins is dynamic throughout the cell cycle and spatio-temporal differences exist between different condensins isoforms (Robellet, Vanoosthuyse et al. 2017).

Genome wide CHIP profiles of condensin subunits support an evolutionarily conserved link with transcription in different model organisms (Leonard, Sen et al. 2015, Marbouty, Le Gall et al. 2015, Sutani, Sakata et al. 2015). In particular there is a strong correlation with the transcriptional status of ORFs and its association with the condensin complex. D'Ambrosio et al. (2008) showed that condensins localize at repeat regions including centromeres, sub-telomeres and rDNA but the role of the condensin complex at repeat genomic sequences is still elusive. Genetic data in fission yeast demonstrated a strong interaction (Robellet, Fauque et al. 2014, Bernard and Vanoosthuyse 2015) between SMC subunits and transcriptional factors (TF), which mediates RNA pol I/II/III transcription.
Condensins binding correlates with genes actively transcribed by RNA Pol II during mitosis (Nakazawa et al. 2015; Sutani et al. 2015; Kim et al. 2016). In human cells, condensin I is enriched at the promoters of highly expressed genes. It is absent from the body and/or the 3′ end of genes and its peaks of association are localized around the TSS (Sutani et al. 2015). However, transcription precludes condensins binding to chromatin at highly repeated transcription units, such as sub-telomeric regions. This phenomenon has been convincingly documented in *S. pombe* (Nakazawa et al. 2015;). This observation argues that active transcription could be detrimental for the segregation of chromosomes when condensin is impaired. Thus, the functions of condensin might be both positively and negatively linked to transcription.

We investigated the role of the Condensins in replication termination at different natural fork pausing sites, including TERs.

Results:

2.1 Bnr1 enriches at natural chromosomal pausing sites, highly transcribing ORFs and TERs.

Brn1-PK tagged budding yeast strains were grown in YPGlu and treated to arrest cells at different stages of cell cycle. To measure the localization of Brn1p under replication stress, G1-arrested cells were released in S-phase in presence of 200mM HU for 90 minutes (Fig2.1). Samples were collected at the indicated time-points and processed for ChIP-on-chip.

Brn1p showed a complex genome wide profile. It also localizes at 62 out of total 71 TERs (Fig.2.1B-C).

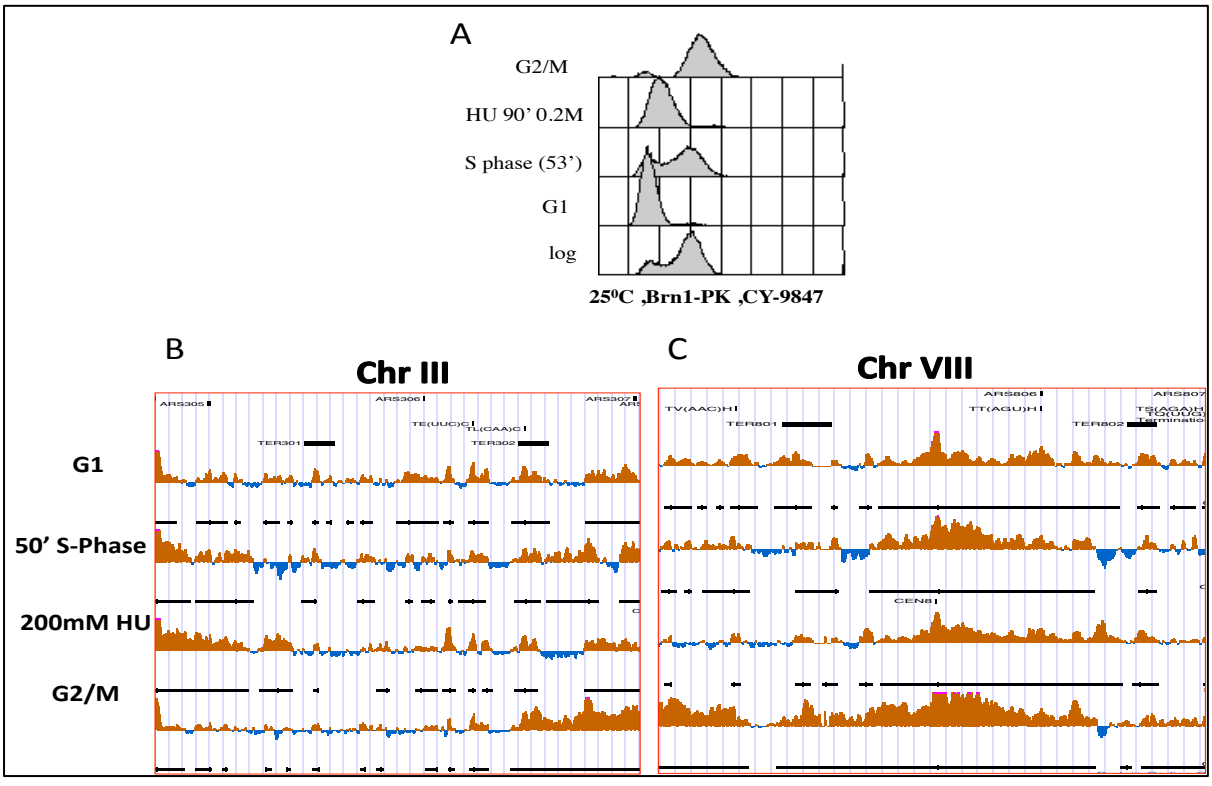


Figure 2.1. Genome-wide association of Brn1p condensin subunit at different cell cycle stages.

A. FACS profiles of different stages of cell cycle of Brn1p-PK strain, samples were collected from respective time-points and subjected to CHIP-chip..

B. Brn1p-PK peaks at ChrIII covering TER301 and TER302 flaked by ARS305 and ARS307. Significant clusters shown with black line below CHIP-Chip profile of cell cycle stages.

C. Significant clusters at ChrVIII, covering TER801 and TER802 along with centromere (CEN8) and tRNA loci.

2.2 Bnr1p interacts with transcribed genes.

We performed a metanalysis of the Brn1 clusters and found that in G1, HU and G2M it preferentially co-localizes at TSS and TTS of transcribed genes (Figure 2.2). This localization resembles the one of Top2 in S phase (Y.Achard and Foiani unpiublished) and likely correlates with the base of chromatin loops containing transcribed genes (Bermejo, Capra et al. 2011, Bermejo, Kumar et al. 2012, Ferrari, Bruhn et al. 2017). This localization is maintained in HU arrested cells replication stress.

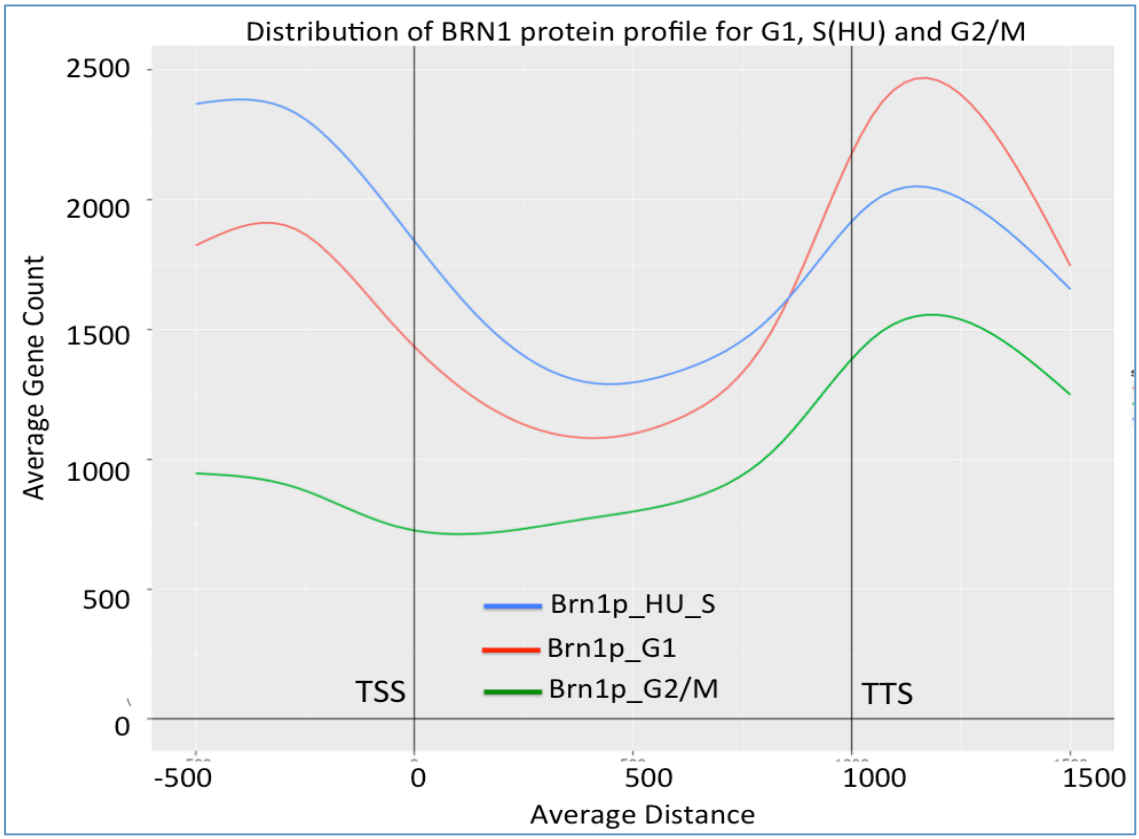
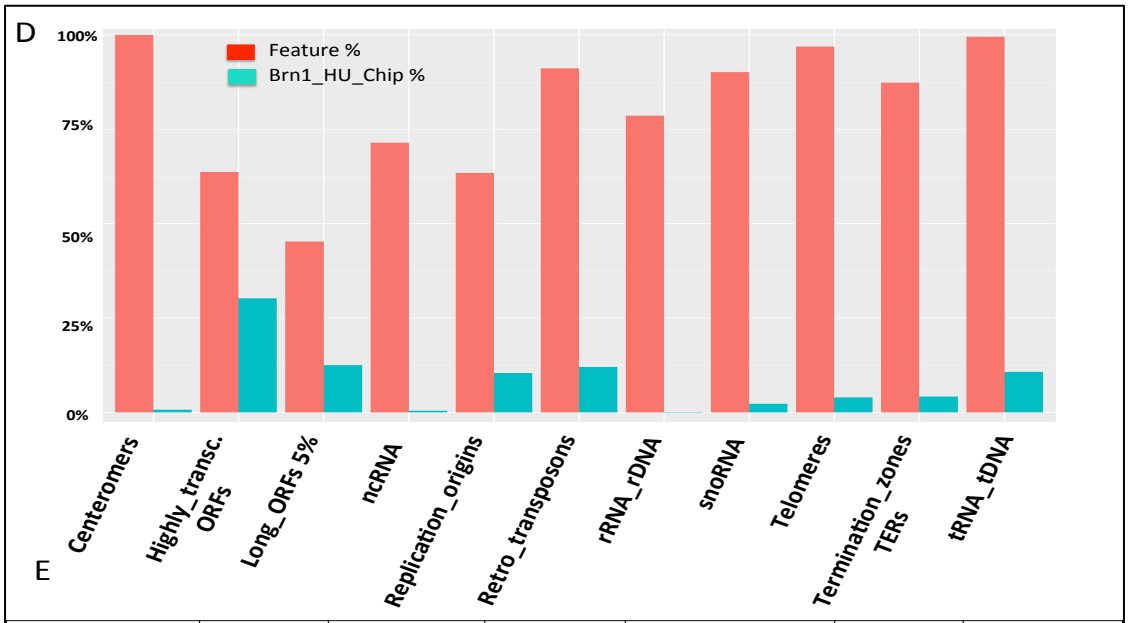


Figure 2.2. Dynamic nature of Brn1p along ORFs forms TSS to TTS.
Red graph labeled (Brn1-p_G1) localization of Brn1p along ORFs in G1 phase. All gene length fit in given window, keeping average ORFs 1000bp where 0 base make Transcription start site (TSS) and 1000 mark Transcription Termination site (TTS). -500 bp from TSS represent promoter and enhancer regions.
Blue graph labeled (Brn1-p_HU_S) S-phase under replication stress scenario.
Green graph labeled (Brn1-p_ G2/M) G2/M phase transition causes change in Brn1p localization at TSS and TTS.

Intriguingly, while Top2 exhibits a binding to TSS and TTS only in S phase (Bermejo, Kumar et al. 2012, Bermejo, Lai et al. 2012), Brn1 seems bound at the same location throughout the cell cycle.

2.3 Brn1p localizes at different natural chromosomal pausing sites including TERs.

To have insight on the role of condensing complex in genomic instability, we focused on Brn1p localization in presence of HU. We scored for association of total peaks 2321 with different genomic features mainly with natural pausing sites and fragile site shown in chapter1.



Type	Test	Brn1_HU_Chip % Total	Total Features	Brn1_HU_peak Overlap	Feature Overlap	P-value
rRNA	BRN1_Hu	2321	28	2	22	9,79E-05
Telomere	BRN1_Hu	2321	32	92	31	1
snoRNA	BRN1_Hu	2321	81	53	73	2,81E-28
Termination	BRN1_Hu	2321	71	97	62	1
Reterotransposon	BRN1_Hu	2321	486	279	443	3,99E-216
HighTranscribingORF	BRN1_Hu	2321	1143	701	728	8,11E-107
tRNA	BRN1_Hu	2321	395	249	393	3,51E-230
Centromere	BRN1_Hu	2321	16	16	16	3,09E-06
ncRNA	BRN1_Hu	2321	14	10	10	0.018273
LongORF_fivepercent	BRN1_Hu	2321	336	290	152	1
ReplicationOrigin	BRN1_Hu	2321	410	242	260	1,87E-33

Figure 2.3. Different natural pausing sites showed increased association with Brn1P under replication stress.
C). Genome wide distribution of Brn1_HU_Chip as indicated (Fig7A). X-axis marked with 11 features which cover most of natural pausing sites and repeat region in genome and Y-axis show percentages of total 2321 peaks overlap with given feature as green bar and percentage of the features marked by Brn1p peaks indicated red bar.
D) Tabular representation of localization of Brn1_HU_Chip peaks along different genomic features with signification p <0.05. In similar way, we assess how many features appeared to overlap with Brn1_HU_Chip.

Brn1p showed strong association with telomeres (31 out of 32), centromeres (16 out of 16) and LTRs (443 out of 486), all these repeat regions are transcribed by RNA pol II. Natural RFBs including rDNA (22 out of 28) and polar fork pausing elements TERs (62 out of 71) showed strong association with condensin complex. RNA pol III mediated transcribed loci tRNA and snoRNA also associated with Brn1p protein (Fig 2.3C,D). Brn1

showed strong association with transcribed loci, which imply potential role of condensin complex at transcribing loci during replication stress.

2.4 Depletion of condensin complex subunits (Ycg1p or Ycs4p) causes chromosomal segregation defects and replication checkpoint activation

Condensins complex components proteins are essential. We therefore generated a degron system for both heat domain-containing subunits Ycg1p and Ycs4p of the complex. The endogenous promoter was replaced with GAL promoter (GAL to GLU degron) and the N terminal was tagged with HA (protein detection) and URL sequence which lead to proteasomal degradation.

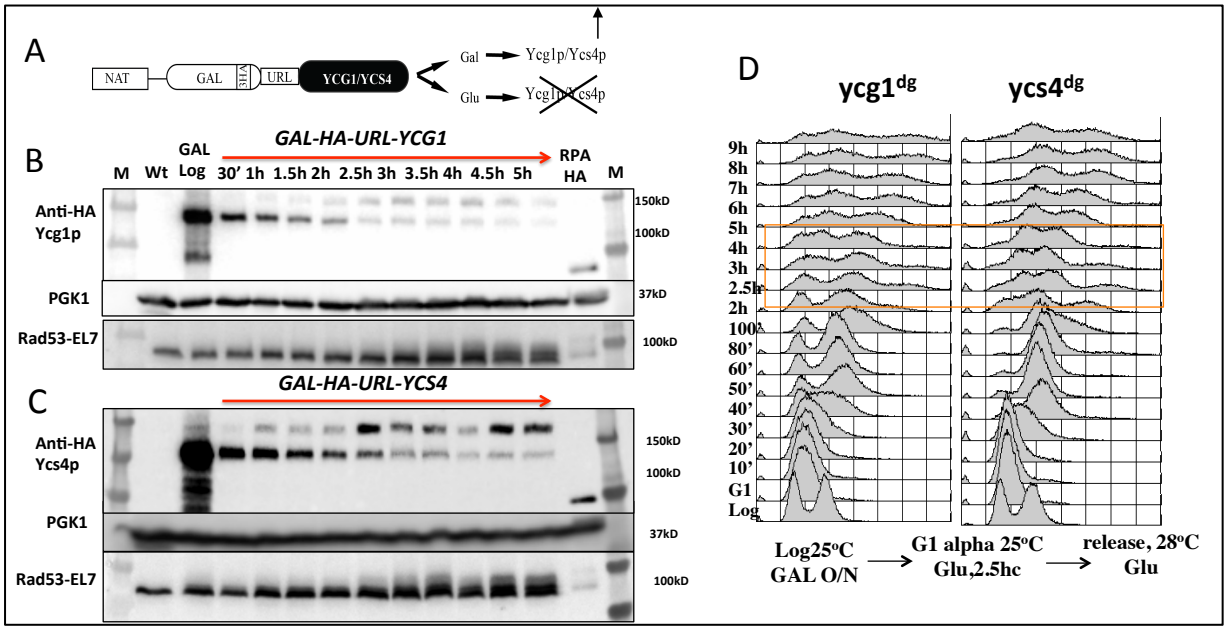


Figure2.4. Depletion of Condensin subunits -Ycg1p and Ycs4p caused segregation defects and replication checkpoint activation.

A. The endogenous promoter of Ycg1/Ycs4 was replaced with GAL promoter, which can be regulated with carbon source. The URL sequence at the N-terminal of YCG1 protein, causes degradation of endogenous protein After YPGal to YPGlu shift

B. YCG1p degron validation from YPGal to YPGlu shown., different time points taken at every 30' time interval and TCA protein extraction to check efficiency of degron system with anti-HA antibody (tagging N-terminal of protein). Checkpoint activation was detected with Anti-Rad53 antibody (phosphorylation appears as low mobility smear) and anti-PGK1 antibody was used as loading control.

C. Degron validation for Condensin complex component, Ycs4p.

D. chromosomal Segregation defect in condensin subunit depleted strains (ycg1^{dg} and ycs4^{dg})

The depletion of Ycs4p and Ycg1p caused Rad53 activation (Fig.2.4B,C) and aberrant FACS profiles likely resulting from segregation defects (Fig.2.4D).

2.5 Mapping genome-wide fragile sites in *Ycg1^{dg} and Ycs4^{dg}* strains in the presence of mild replication stress.

We investigated whether condensins influenced the integrity of natural pausing sites and TERs in presence of mild replication stress.

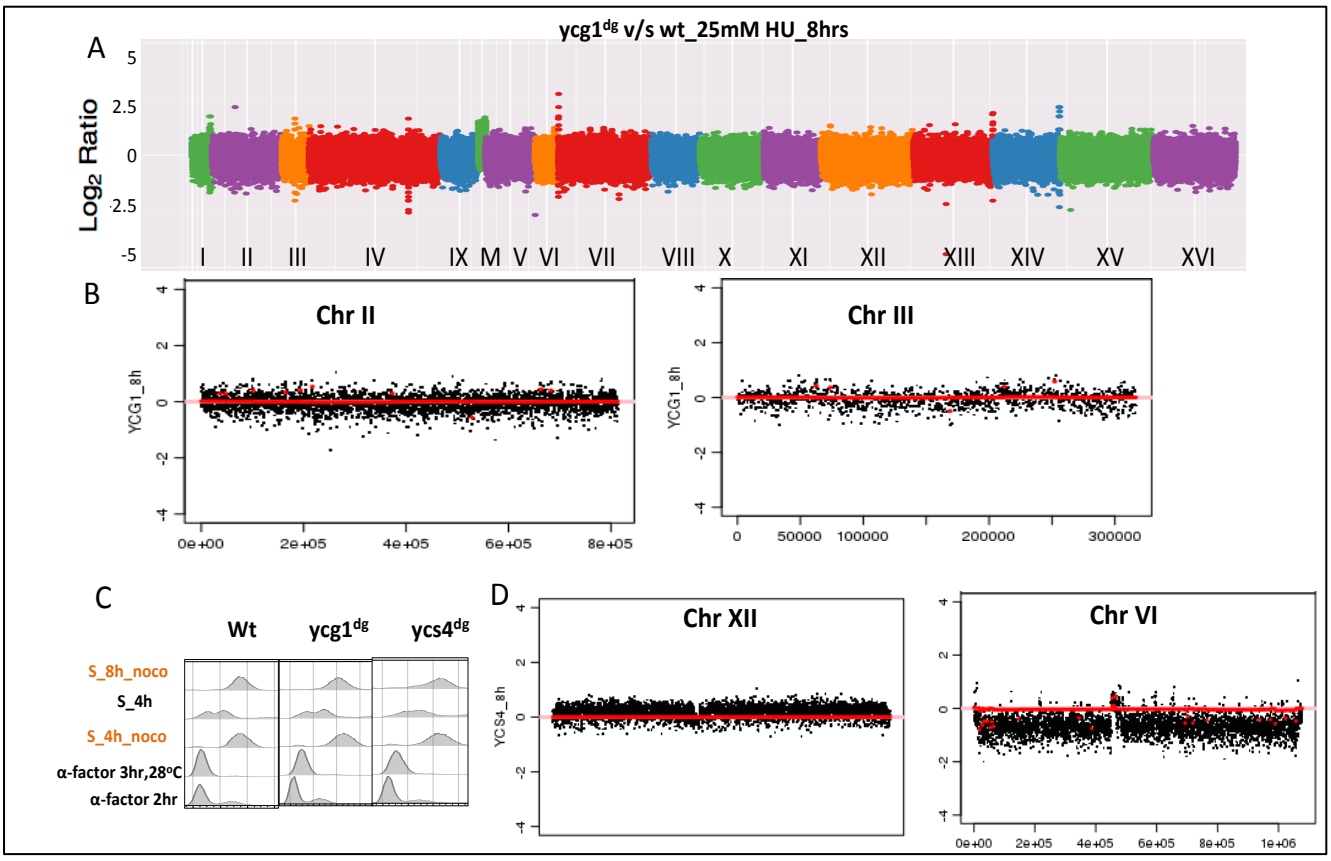
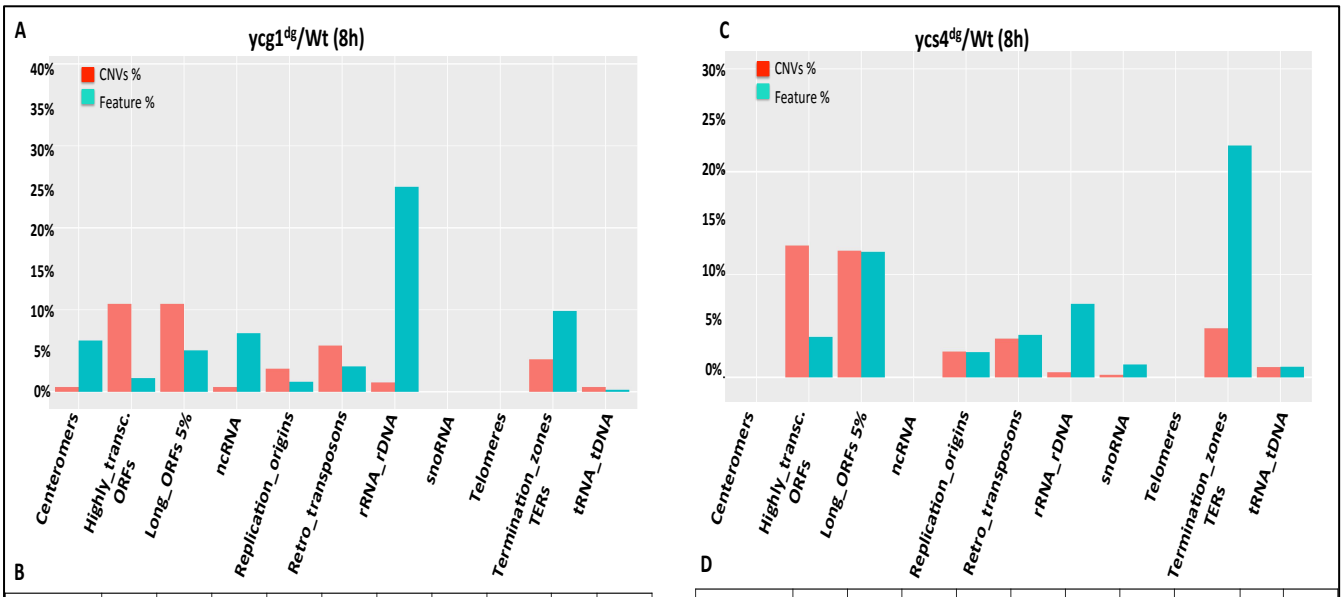


Figure 2.5. Mapping genome wide CNVs in *Ycg1^{dg} and Ycs4^{dg}* strain with mild replication stress.
A). Whole Genome sequencing reads (NGS) of *Ycg1^{dg}* compared with Wild type, represented along all 16 chromosomes. Y axis showed Log ratio of reads comparison, X axis represent different chromosomes. Black arrow marking different region showed far from mean distribution of reads and scored as CNVs. (I don't see the black arrow)
B). CNVs at ChrII and ChrIII, alone showing distribution of reads including strong copy number variation (Deletion and Amplification as well).
C). FACS profiles of wild-type, and *ycg11^{dg}* grown 2 cell cycles (8h) with 25mM HU and arrested in G2/M with Nocodazole. Meanwhile, took 4h time point with and without Nocodazole to assess cell cycle progression.
D). GCRs and CNVs at Chr XII and VI, alone showing distribution of reads including strong copy number variation (Deletion and Amplification too).

Whole genome sequencing data (NGS) from wild type and condensin subunit-depleted strains, represented as log2 ratio, are shown in Fig.2.5 A. Individual chromosomes II and III are shown, where genomic loci with less and more reads compare to average reads marked as red dot above or below the red line representing average reads. These regions

(red dots) represent deleted and amplified loci in proliferating yeast cells under replication stress in the absence of condensin complex (Fig.2.5 B). Apart from CNVs distribution, we were able to capture the typical phenotype of condesin-depleted cells, aneuploidy (Fig.2.5D). In absence of Ycs4p, cells showed gain of chromosome XII and complete loss of ChrVI. CNV distribution along different genomic loci, including natural pausing elements, RFBs and TERs, reflect differential effects of Ycg1p and Ycs4p deletion on genomic landscape. Retro-transposons (RNA pol II-transcribed) and rDNA (RNA pol I-transcribed) loci strongly correlated with CNVs accumulation in the absence of Ycg1 (total CNVs 177) (Fig.2.6A-D). NGS based CNVs did not unmask aneuploidy or other GCRs including translocation, inversion and crossovers. Instead, Ycs4p depletion, besides causing aneuploidy, results also in higher number of CNVs at TERs along with rDNA and LTRs.

Ycs4 depletion accumulates total CNVs (398, 222 del/ 176 amp) distributed over pausing sites, including 16 out of 71 TERs (p=0.035) (Fig.2.6A-D).



B

Type	Test	Total CNV	Total Deletion	Total Amplification	Total Features	CNV Overlap	Deletion Overlap	Amplification Overlap	Feature Overlap	P-value
Centromere	ycg1_8h	177	138	39	16	1	1	0	1	0.091427
HighTranscribingORF	ycg1_8h	177	138	39	1143	19	16	3	19	0.97051
LongORF_5%	ycg1_8h	177	138	39	336	19	5	14	17	0.94748
ncRNA	ycg1_8h	177	138	39	14	1	1	0	1	0.21597
ReplicationOrigin	ycg1_8h	177	138	39	410	5	5	0	5	0.5772
Reterotransposon	ycg1_8h	177	138	39	486	10	0	10	15	0.0034611
rRNA	ycg1_8h	177	138	39	28	2	2	0	7	4,09E-07
snoRNA	ycg1_8h	177	138	39	81	0	0	0	0	1
Telomere	ycg1_8h	177	138	39	32	0	0	0	0	1
Termination	ycg1_8h	177	138	39	71	7	5	2	7	0.37535
tRNA	ycg1_8h	177	138	39	395	1	1	0	1	0.93186

D

Type	Test	TotalCNV	Total Deletion	Total Amplification	Total Features	CNV Overlap	Deletion Overlap	Amplification Overlap	Feature Overlap	P-value
Centromere	ycs4_8h	398	222	176	16	0	0	0	0	1
HighTranscribingORF	ycs4_8h	398	222	176	1143	51	30	21	45	0.47763
LongORF_5%	ycs4_8h	398	222	176	336	49	16	33	41	0.82725
ncRNA	ycs4_8h	398	222	176	14	0	0	0	0	1
ReplicationOrigin	ycs4_8h	398	222	176	410	10	5	5	10	0.22749
Reterotransposon	ycs4_8h	398	222	176	486	15	3	12	20	0.058284
rRNA	ycs4_8h	398	222	176	28	2	2	0	2	0.0020563
snoRNA	ycs4_8h	398	222	176	81	1	0	1	1	0.53814
Telomere	ycs4_8h	398	222	176	32	0	0	0	0	1
Termination	ycs4_8h	398	222	176	71	19	9	10	16	0.035597
tRNA	ycs4_8h	398	222	176	395	4	4	0	4	0.19085

Figure 2.6. Distribution of CNVs along different genomic regions and their significant association with amplifications and deletions in *Ycg1^{dg} and Ycs4^{dg}* strains.

A, C) Genome-wide distribution of CNVs for *Ycg1^{dg}* (177 CNVs) and *Ycs4^{dg}* (398 CNVs). X-axis marked with 11 regions covering most of the RFBs sites and repeat regions in whole genome. Y-axis shows percentages of total CNVs

overlapping with given regions (shown as red bar) and percentages of the regions carrying CNVs (shown as green bar).
B, D) Tabular representations of all CNVs rad53sml1 (741 CNVs) and tel1mec1sml1 (807 CNVs), distributed along different genomic features and CNVs categorized as Deletions and Amplifications.

2.6 TERs are fragile in the absence of Condensin subunits (Ycg1p and Ycs4p).

We then addressed whethe condensins influence DSB formation at TERs, by looking at TER302 using PFGE. We collected samples for 3h and 6h from proliferating cells in the presence of 25mM HU with and without 1mg/ml caffeine, which suppresses checkpoint activation. Interestingly, as reported in chapter 1, wild type cells accumulate basal amount of breaks at TERs under replication stress, which increased, with inhibition of replication checkpoints. We observed that TER302 accumulated more breaks in ycg1^{dg} and ycs4^{dg} strains under mild replication stress compared to wild type (Fig. 2.7). Moreover, in contrast to wild type cells, the fragility at TERs did not increase by caffeine treatment in condensins depleted cells.
These data point at a role of Condensin complex in the formation of local topological domains preserving integrity of TERs (Fig. 2.7).

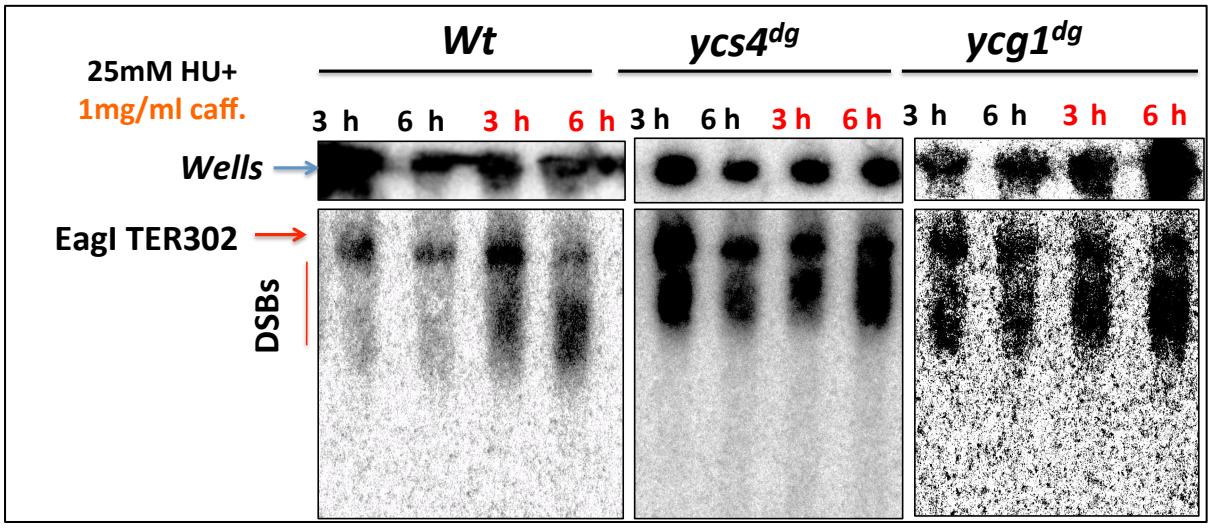


Figure 2.7. DSBs accumulation at TER302 in ycg1^{dg} and ycs4^{dg} stain under replication stress.
G1-arrested cell where released in S-phase in the presence of 25mM HU +/- 1mg/ml Caffeine to inhibit checkpoint activation. Samples at 3h and 6h time-points were collected to perform PFGE-based gross chromosomal integrity assay. A specific probe against TER302 (RNA pol II) was used to look at TER302 fragility in the absence of ycg1^{dg} and ycs4^{dg}. I think you should explain why you do not have the sample before HU treatment, time-point 0h. Moreover, these samples where run on the same gel? Otherwise how can you compare wild-type and mutants?)

2.7 Conclusion:

Our data suggest a role for condensins in transcription-coupled activities. Ongoing transcription would generate nucleosome free regions that may favor condensation activities, particularly considering that condensins are recruited in the proximity of TSS and TTS. Hence, condensing activities must be highly coordinated in order to prevent unscheduled condensation events. Notably, while condensins bind TSS and TTS already in G1, Top2 binds the same regions specifically in S phase (Bermejo, Capra et al. 2009). It is tantalizing to speculate that the checkpoint kinases play a key role in restraining the activities of condensins and Top2 at transcribed genes in S phase, in order to prevent premature condensation. Interestingly, DNA break formation at yeast natural pausing sites following checkpoint inactivation depends on condensins and Top2 (Cha and Kleckner 2002, Hashash, Johnson et al. 2012). In this scenario, TER zones that contain transcribed genes and facilitate fork converging may represent hot spots for condensation.

Our data also suggest that topological stress correlates with the presence of RNA-DNA hybrids. This is consistent with the view that these hybrids have a tendency to form in the proximity of underwound DNA. Whether the RNA-DNA hybrids at negative supercoiled regions play a causative role in generating rearrangements or, rather, they protect the unwound duplex, remains to be elucidated.

Results: chapter 3

Tittle: PIF1 family helicase Rrm3p counteracts the accumulation of RNA-DNA hybrids at natural chromosomal pausing sites and TERs.

DNA helicases facilitate fork movement through obstacles. PIF1 family DNA helicases are present in all eukaryotes (Shimada and Gasser 2012). Most eukaryotes, encode a single Pif1 family DNA helicase, while *Saccharomyces cerevisiae* encodes two, Rrm3p and Pif1p (Ivessa, Zhou et al. 2000). Although Pif1p and Rrm3p are often affecting the same kind of substrates on DNA template, they work in different ways; e.g., Pif1p inhibits telomerase, while Rrm3 promotes semiconservative replication of telomeric DNA (Phillips, Chan et al. 2015). Pif1 is required for stable maintenance of mitochondrial DNA, Okazaki fragment maturation and break induced replication (BIR) (Saini, Ramakrishnan et al. 2013) while Rrm3 is dispensable for these processes. Pif1p also promotes replication and suppresses DNA damage at sequences that can form G-quadruplex structures (Li, Lu et al. 2016). Rrm3 is best known for promoting fork progression at stable protein–DNA complexes as a component of ongoing replication fork, while Pif1 is probably recruited to its sites of action by different mechanism depending on the site of genomic lesion. On the contrary, Rrm3 is involved in global chromosomal replication including rDNA loci (Craven and Petes 1999, Ivessa, Zhou et al. 2000). Rrm3 was discovered as an inhibitor of HR (Homologous Recombination) between the ribosomal DNA as anti-recombinases like Srs2, although this has not be demonstrated for other repetitive sequences (Chung 2014).

There is evidence that leads to a potential new role of Rrm3p at transcribing loci. Absence of Rrm3p alone and with Pif1p cause fork stalling at tRNA genes (RNA pol III) (Osmundson, Kumar et al. 2017, Tran, Pohl et al. 2017) and, moreover Pif1p family helicases resolve transcription mediated R-loop formation at tRNAs and suppresses GCRs depending orientation of collision (HO or CD) between replication and transcription machinery. *Δrrm3* mutants are highly sensitive to Top1p inhibitors (Azam, Lee et al. 2006).

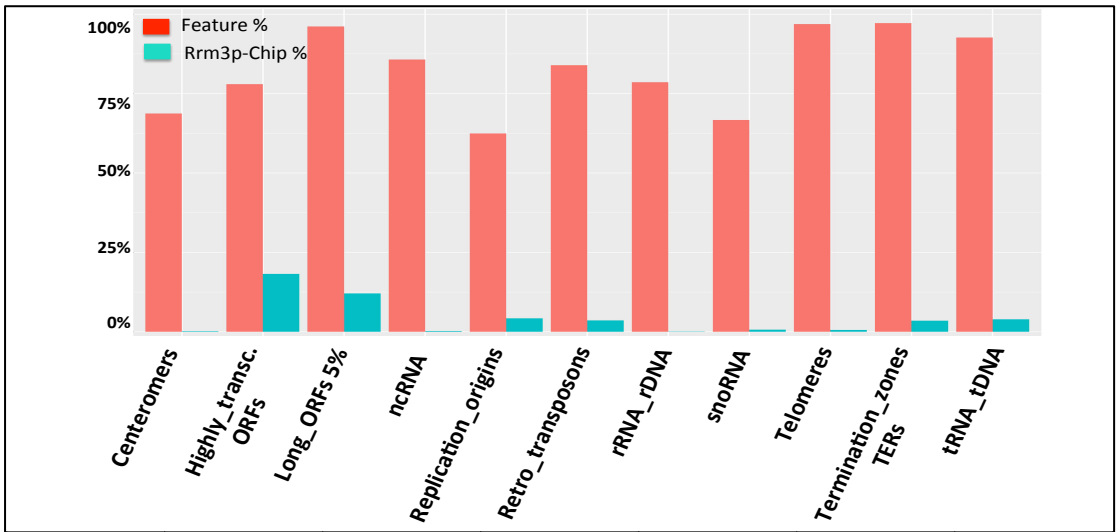
All sites affected by the absence of Rrm3p are assembled into non-nucleosomal protein-DNA complexes implying that Rrm3p acts directly or indirectly to facilitate replication through protein-DNA complexes (Ivessa, Zhou et al. 2000, Ivessa, Zhou et al. 2002,

Ivessa, Lenzmeier et al. 2003). The accumulation of Rrm3p at highly transcribed regions as a consequence of replication fork (RF) stalling suggests that Rrm3p might have a role in the progression of stalled RFs but no evidence has been reported on whether Rrm3p is required for repair of transcription-associated damage too (Munoz-Galvan, Garcia-Rubio et al. 2017, Osmundson, Kumar et al. 2017, Tran, Pohl et al. 2017). Indeed, Rrm3p has been shown to prevent not only transcription-induced RF stalling but also transcription-associated hyper recombination. Rrm3p has a synthetically lethal interaction with many genes involved in HR as well as with *rad3/XPD* Nucleotide Excision Repair (NER) mutation of TFIIH, *rad3-102*, which blocks NER at a post-incision intermediate and causes an extended retention of TFIIH at the damaged DNA, converting bulky adducts to DSBs when reached by the RF (Torres, Schnakenberg et al. 2004). All above observations strongly suggest a role of Rrm3p at transcribing genomic loci, which might be separate from it's classical role as a component of replication fork helping the fork progression along hard to replicate genomic loci. SILAC data showed increased binding of Top2p and Rrm3p to Orc5 suggesting they are located near by origins and regulate DNA synthesis under replication stress with HU (Syed, Desler et al. 2016). Deleting the N-terminal tail of Rrm3 disrupts Orc5 binding and association with origins and causes enhanced DNA synthesis and S phase progression in HU, as well as accumulation of point mutations in normal S-phase under HU treatment. Understanding the mechanism(s) by which Rrm3p helicases affect genome integrity is relevant to human disease, as mutation of mammalian PIF1 family helicases is associated with increased risk of breast cancer and mitochondrial myopathies(Pinter, Aubert et al. 2008, Bochman, Sabouri et al. 2010, Song, Dominska et al. 2014, Byrd and Raney 2017).

In this chapter we performed genome-wide GCRs analyzing Copy number variations CNVs) amplifications and deletions in *Δrrm3* cells under mild replication stress. Our group has shown that Rrm3 mediates transient fork pausing at Replication termination zones-TERs (Having transcribing loci, LTRs and tRNAs motifs as pausing elements). Our Assumption is that pausing / stalling of fork at TERs along with other loci might be a consequence of R-loop mediated blocks of forks in a co-directional or head-on collision. This collision between RF and Transcriptional machinery may lead to DSB accumulation and error prone repair, which can influence the CNVs landscape at TERs.

3.1 RRM3 showed strong binding pattern, at natural chromosomal pausing sites (CPSs) and replication fork barriers (RFBs).

To understand the role of Rrm3p in genomic stability, independently of Replication fork associated function at hard to replicate loci, we first re-analyzed Rrm3p-FLAG Chip data obtained from cell in S-phase (Herrera-Moyano, Mergui et al. 2014). We scored for the binding of Rrm3p-FLAG along 11 different genomic features covering ORFs (Pol II), Replication origins (DNA pol) and rDNA (Pol I) (Fig3.1). Other most natural chromosomal pausing sites, repetitive sequence transcribing with RNA pol II (Centromeres, retro-transposons and telomeres) and RNA pol III mediated transcribing snoRNA and tRNA.



Type	Rrm3p-Chip	Total peaks	Total Features	Peaks Overlap	Feature Overlap	P-value
rRNA	RRM3Protein	6184	28	5	22	1
Telomere	RRM3Protein	6184	32	34	31	1
snoRNA	RRM3Protein	6184	81	41	54	4,73E-03
Termination	RRM3Protein	6184	71	216	69	1
Reterotransposon	RRM3Protein	6184	486	220	408	1,47E-10
HighTranscribing ORF	RRM3Protein	6184	1143	1127	891	5,46E-33
tRNA	RRM3Protein	6184	395	242	366	3,33E-130
Centromere	RRM3Protein	6184	16	11	11	0.0026951
ncRNA	RRM3Protein	6184	14	13	12	0.056783
LongORF_5%	RRM3Protein	6184	336	746	323	1
ReplicationOrigin	RRM3Protein	6184	410	262	256	8,38E-03

Figure 3.1. Rrm3p-FLAG (Chip) binding at different natural chromosomal pausing sites and replication fork barriers under physiological condition. Genome wide meta-analysis of 6184 binding sites of Rrm3p protein and scored significant association with different genomic loci including 11 categories as shown on X-axis. We includes rDNA loci, Telomeres and Replication termination zones along with highly transcribing regions ORFs including longest ORFs (5% of total). Same data represented in tabular form below. (Significant P< 0.05)
Red bar: Percentage of given genomic feature overlap with Rrm3p-FLAG peaks (Here for example TERs 69/71)
Green bar: fraction of Rrm3-FLAG peaks overlaps with given feature. (Here for example at TERs 216/6184)

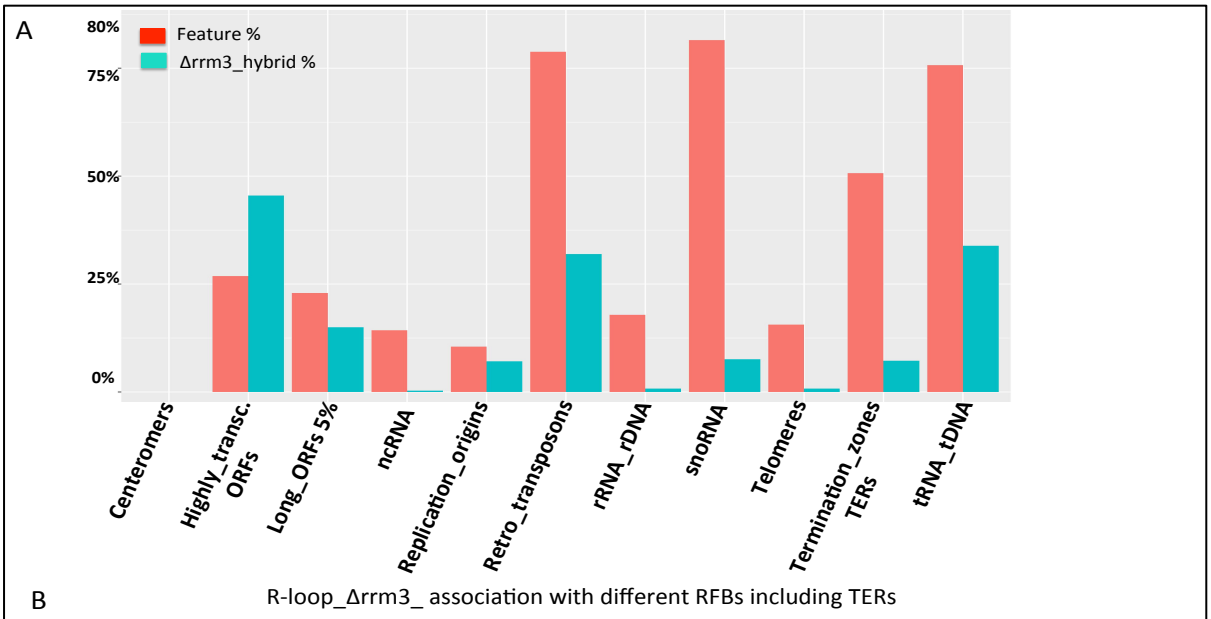
Rrm3-FLAG ChIP-chip peaks associated with highly transcribing ORFs (891out of 1143, p=5.463E-33) but not significantly to the 5% longest ORF (p=1). Replication origins bind Rrrm3p. Other genomic loci including rDNA (22/28), Telomeres (31/32) and TERs

(69/71) bind Rrm3p in S-phase (Fig18). snoRNA , Retro transposons and tRNA showed significant binding with Rrm3p. Hence Rrm3 might regulate transcriptional of loci and suppresses TCR (transcription coupled repaired) and TAR (transcription associated recombination).

3.2 Rrm3 suppresses RNA-DNA hybrid accumulation at different pausing elements.

R-loop causes obstacle to fork progression and generate replication associated genomic instability by fork breakage and DSB accumulation. We speculated, that in *Δrrm3* strains, transcribing loci accumulate R-loop, which impaired fork progression and enhance the transient pausing. Δrrm3 did not show sensitivity to replication stressing agents such as HU and this may reflect its potential role in transcriptional associated DNA damage response caused by R-loop accumulation.

According to our hypothesis, we decided to measure RNA-DNA hybrids accumulation in *rrm3Δ* cells in S-phase using the DRIP-Chip method. We scored for R-loop peaks (620) along 11 genomic features and significance of association. Although replication origins have no transcriptional activity we observe strong binding of Rrm3p (Fig.3.2). We observed that long ORFs (top 5%) neither had significant Rrm3p clusters nor R-loop accumulation although these ORFs are transcriptionally active. We observed the same for rDNA and Telomeres. On the contrary, highly transcribing ORFs showed significant association with Rrm3p binding as well R-loop accumulation in Δrrm3. Centromeres show significant binding (11/16) but absence of R-loops (0/16). Replication Termination (TERs) showed accumulation of R-loops in *rrm3Δ* mutants, likely due to the enhanced fork pausing (69 TERs overlapped with Rrm3p binding profile). snoRNA (RNAP III), retro-transposons (RNAPII) and tRNAs (RNAP III) loci showed strong correlation of Rrm3 helicase binding and R-loop accumulation in *rrm3Δ* (Fig3.2A,B). Hence, the association of Rrm3p to different loci might be transcription associated, and perturbation of this function creates more R-loop-mediated obstacles causing replication fork stalling in *rrm3Δ* mutants.



B R-loop_Δrrm3_ association with different RFBs including TERs

Type	Test	R-loops Total	Total Features	R-loop Overlap	Feature Overlap	P-value
rRNA	rrm3_S_hybrids	620	28	5	5	0.42496
Telomere	rrm3_S_hybrids	620	32	5	5	0.985
snoRNA	rrm3_S_hybrids	620	81	47	66	8,64E-52
Termination	rrm3_S_hybrids	620	71	45	36	7,11E-03
Reterotransposon	rrm3_S_hybrids	620	486	198	383	0
HighTranscribingORF	rrm3_S_hybrids	620	1143	282	307	1,29E-44
tRNA	rrm3_S_hybrids	620	395	210	299	1,53E-261
Centromere	rrm3_S_hybrids	620	16	0	0	1
ncRNA	rrm3_S_hybrids	620	14	2	2	0.51876
LongORF_5%	rrm3_S_hybrids	620	336	93	77	0.95671
ReplicationOrigin	rrm3_S_hybrids	620	410	44	43	0.42915

Figure 3.2. R-loop accumulation at different natural chromosomal pausing sites and Replication termination in absence of rrm3.

A). Genome wide meta-analysis of DRIP-Chip data for R-loop accumulation in Δrrm3. DRIP-Chip experiment performed on S-phase at 40-minute time point. Different significant clusters for R-loop peaks (using S9.6_antibody) subjected to score their association with different genomic loci including 11 categories as shown on X-axis which includes rDNA loci, Telomeres and Replication termination zones along with highly transcribing regions ORFs. Same data represented in tabular form as Fig B. snoRNA, TERs, highly transcribing genes and tRNAs genomic loci accumulate significant R-loops in Δrrm3. (Significant P< 0.05)

Red bar: Percentage of given genomic feature overlap with R-loop peaks.

Green bar: fraction of R-loop peaks overlaps with given feature.

3.3 Transient RNA-DNA hybrid accumulation during S-phase in Δrrm3 at TERs.

After mapping genome wide R-loop profile in S-phase in *Δrrm3* (Fig.3.2), We looked at of R-loop dynamic accumulation at different cell cycle stages. TER303 (LTRs and tRNAs), TER102 (Rbp3) and TER802 (Rbp3) showed enhanced R-loop accumulation in S-phase (late, 50') compared to wild type. Interestingly this accumulation is transient and resolved in G2/M. This is consistent with the dynamic nature of Fork pausing at TERs.

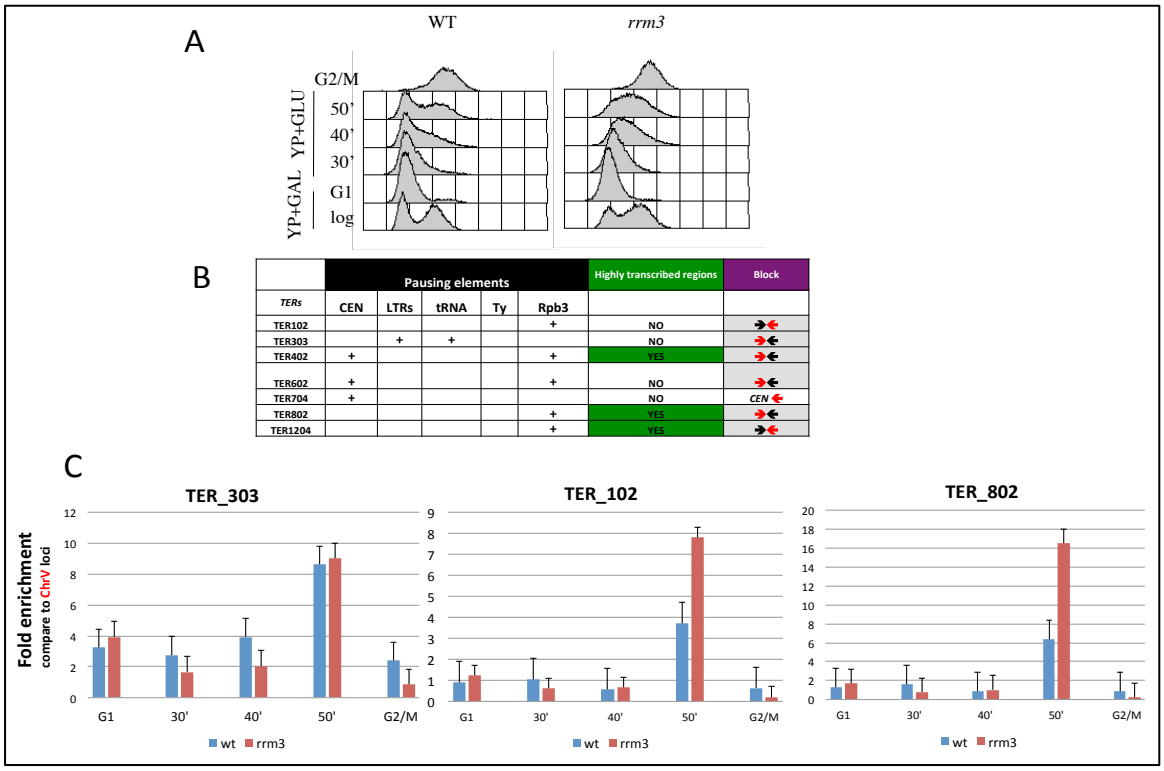


Figure3.3: Transient hybrid accumulation during S-phase in Δrrm3 at TERs

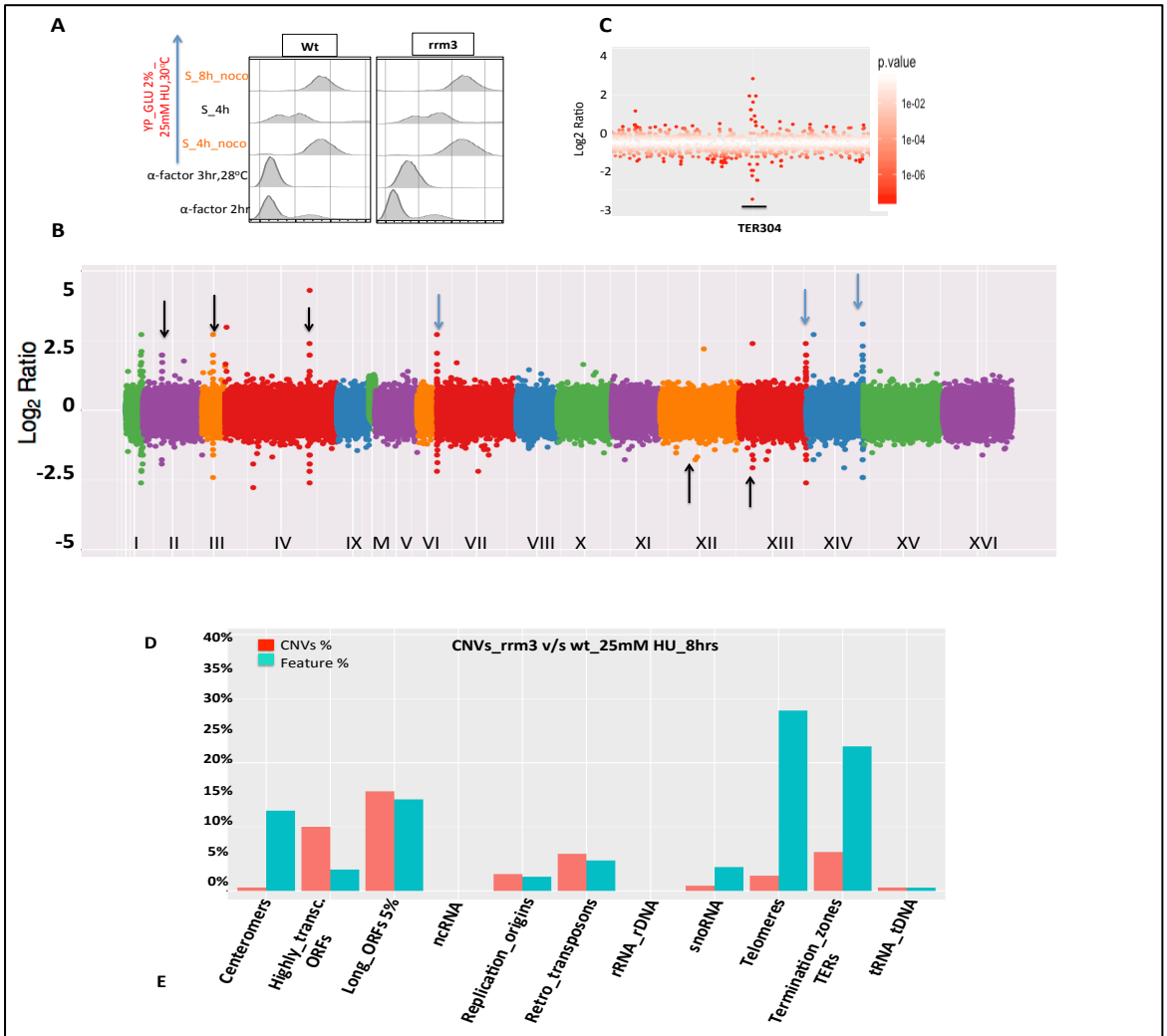
A). FACs profile of wild type and Δrrm3 after G1-released in S-phase with Nocodazole to arrest in G2/M stage of cell cycle. Meanwhile, 30', 40' and 50' time points were collected for FACs and DRIP-qPCR.

B). List of selected TERs out of total 73 TERs in budding yeast for DRIP-qPCR. List composes type of pausing elements (CEN, LTRs, tRNA, Ty, Rbp3 binding), transcriptional statues and block to approaching replication fork.

C). Fold enrichment at different TERs for R-loop during s-phase. Data acquisition done at indicated time points and scored for R-loop accumulation compare to non-transcribing, non R-loop accumulating loci on ChrV in wild type and Δrrm3 (As previous reports).

3.4 Genome wide CNVs analysis in *Δrrm3* strain along natural chromosomal pausing sites, replication fork barriers and TERs.

We speculated that R-loop accumulation could cause longer stalling of replication fork at natural pausing sites leading to Gross chromosomal rearrangements (GCRs). We scored for copy number variation based on whole genome sequencing of wild type and *Δrrm3*. Fig.3.4A shows the FACs profile at 8hrs under 25mM HU and then arrested in G2/M with nocodazole treatment. Interestingly, centromeres, snoRNA, telomeres and Termination zones accumulated a significant number of CNVs. This result is consistent with the binding of Rrm3p and R-loop accumulation in *Δrrm3* cells.



Type	Ref	Test	TotalCNV	Total Deletion	Total Amplification	Total Features	CNV Overlap	Deletion Overlap	Amplification Overlap	Feature Overlap	P-value
Centromere	wt_8h	rrm3_8h	380	230	150	16	2	2	0	2	0.001404
HighTranscribingORF	wt_8h	rrm3_8h	380	230	150	1143	38	23	15	38	0.92587
LongORF_fivepercent	wt_8h	rrm3_8h	380	230	150	336	59	28	31	48	0.13504
ncRNA	wt_8h	rrm3_8h	380	230	150	14	0	0	0	0	1
ReplicationOrigin	wt_8h	rrm3_8h	380	230	150	410	10	7	3	9	0.17349
Reterotransposon	wt_8h	rrm3_8h	380	230	150	486	22	7	15	23	7,49E-01
rRNA	wt_8h	rrm3_8h	380	230	150	28	0	0	0	0	1
snoRNA	wt_8h	rrm3_8h	380	230	150	81	3	2	1	3	0.03387
Telomere	wt_8h	rrm3_8h	380	230	150	32	9	0	9	9	0.028709
Termination	wt_8h	rrm3_8h	380	230	150	71	23	16	7	16	0.00085779
tRNA	wt_8h	rrm3_8h	380	230	150	395	2	2	0	2	0.59916

Figure 3.4: Mapping genome wide CNVs under mild replication stress in Δrrm3 cells.
A). FACs profile of the wild type and Δrrm3 grown two cell cycles (8h) with 25mM HU and arrested in G2/M with nocodazole treatment.
B). Whole Genome sequencing (NGS) of Δrrm3 compared with wild type, represented along all 16 chromosomes. Y axis showed log ratio of reads compared with Δrrm3, X axis represent different chromosomes covering different width depending in their size and 5 different colors used to represent 16 chromosomes where different chromosomes appeared in same colors too (To avoid any confusion, no translocation and conversion represented. For visual representation some CNVs regions marked as black arrow (TERs) and blue arrow (Telomeres).
C). Enlarged view of TER304, showing strong association of copy number variation within TER 304 on ChrIII.
D). Genome wide distribution of CNVs after 8h in 25mM HU Δrrm3 strain. X-axis marked with 11 features which cover most of RFBs sites and repeat region in genome and Y-axis should percentages of total CNVs (380) overlap with given feature as red bar and percentage of the features marked by CNVs in Δrrm3.
E). Tabular representation of all CNVs in Δrrm3_8h_25mMHU, distributed along different genomic features. Total CNVs as deletion and amplification, and overlap with different genomic features with signification p value <0.05.

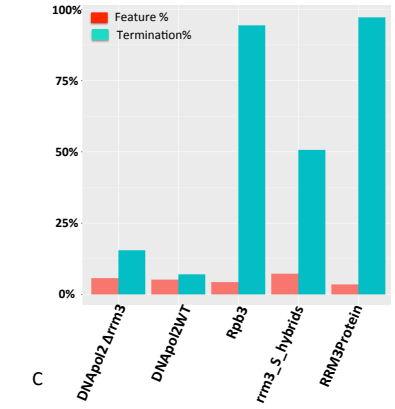
Whole Genome sequencing reads from NGS of *Δrrm3*, compared with wild type, represented along all 16 chromosomes showed different genomic region with deletion and amplification (Fig.3.4B). Replication Termination zones accumulated significant CNVs shown as enlarged view at *TER302* in *Δrrm3* (Fig.3.4C). Genome wide distribution of CNVs in *Δrrm3* strain shown along 11 features which cover most of RFBs sites and repeat region of the genome and Y-axis shows the percentage of total CNVs (380) that overlap with a given genomic feature as red bar. Percentage of the features marked by CNVs represented as green bar in *Δrrm3* (Fig.3.4D). CNVs categories as deletions and amplifications, and we can see overlap with different genomic features. In similar way, we assessed how many features appeared to overlap with CNVs, as some features tend to have more than one CNV for one feature. Centromeres (2 features, deletion p=0.0014) and Termination zones (16 features, deletion p=0.00085) showed significant correlation with CNVs distribution. Genome wide CNVs distribution showed deletion and amplification at telomeres, snoRNA and retro-transposons too, in *Δrm3*.

3.5 Replication termination zones accumulate all features associated with fork pausing and stalling in *Δrrm3* strains.

Replication Termination zones (TERs) are strongly associated with Rrm3p binding and accumulation of R-loops and CNVs in *Δrrm3* strains. We decided to look at different characteristic feature of pausing and stalled fork in *Δrrm3* strain and correlation to replication termination zones (TERs). We scored for Rbp3-Chip (represent RNAP II) (data from Bermego et al. 2009), Rrm3p-Chip protein (data from Herrera-moyano et.al, 2014), DNApol2 enrichment in *Δrrm3* and wild type (data from Azvolinsky et al. 2009) and R-loop enrichment shown as percentage at TERs (71 TERs). Tabular form for the

distribution of features described (Fig.3.5A). All 5 features tested against Termination Zones (4.5kb mean length) where Rpb3 binding covers 67/71 (94%) TERs and RRM3 protein binding at 69/71 (97%) TERs. Rrm3 deletion causes significant accumulation of R-loops at 36/71 (50%) and CNVs accumulation at 16/71 at TERs with p=0.00085. Meta analysis of CNVs in *Δrrm3* is showed (Fig.3.5D). Tabular representation of CNVs overlap with different features, showing significant correlation with Rbp3p binding loci, R-loop prone loci in Δrrm3 and genomic regions where Rrm3p bind.

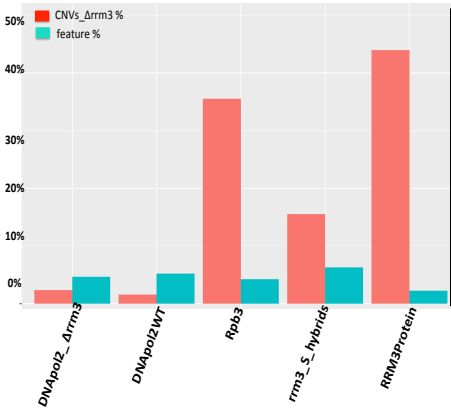
A. Meta analysis of rrm3 mediated pausing at TERs



B. Different Features associated with Termination Zones in context to rrm3 mediated pausing at TERs

Type	Test	Total Features	TerminationTotal	Feature Overlap	Termination Overlap	P-value	% TERs
Termination	DNApol2 _Δrrm3	193	71	11	11	0.1397	15.49%
Termination	DNApol2_Wt	96	71	5	5	0.32897	7.04%
Termination	**Rpb3**	2675	71	116	67	1	**94.36%**
Termination	**rrm3_S_hybrids**	620	71	45	36	7,11E-03	**50.70%**
Termination	**RRM3_Protein**	6184	71	216	69	1	**97.18%**

C



D

Type	Test	Total CNV	Total Deletion	Total Amplification	Total Features	CNV Overlap	Deletion Overlap	Amplification Overlap	Feature Overlap	P-value
DNApol2rrm3del	rrm3_8h	380	230	150	193	9	5	4	9	0.65622
DNApol2WT	rrm3_8h	380	230	150	96	6	1	5	5	0.32515
Rpb3	rrm3_8h	380	230	150	2675	135	87	48	114	0.026698
rrm3_S_hybrids	rrm3_8h	380	230	150	620	59	37	22	39	3,54E-02
RRM3Protein	rrm3_8h	380	230	150	6184	167	92	75	140	0.00054304

Figure 3.5: Different Features associated with functional Rrm3p at TERs.

A. Rbp3 (RNA Pol II), Rrm3p protein, DNApol2 enrichment in Δrrm3 and wild type and R-loop enrichment shown as percentage at TERs (71 TERs). We scored correlation between DNApol2 enrichment in Δrrm3 and Wt (reference), Rbp3 (RNAP II subunit) and Rrm3-chip at TERs. Similarly we look at hybrid distribution at TERs in absence of rrm3 at 40' s-phase.

B. Tabular form for the distribution of features described in FigA. All 5 features tested against Termination Zones (4.5kb mean length) where Rpb3 binding covers 67/71 (94%) TERs and RRM3 protein binding at 69/71 (97%) TERs. Rrm3 deletion causes significant accumulation of R-loops at 36/71 (50%) TERs.

C. CNVs distribution alone different features mentioned in figure A in rrm3 strain.

D. Tabular representation of CNVs overlap with different features, showing significant correlation with Rbp3p binding loci, R-loop prone loci in rrm3 and genomic regions where Rrrm3p bind. (Significant P< 0.05)

3.6 Cell cycle progressions is not impaired in *Δrrm3* mutants

Under physiological condition, *Δrrm3* accumulate the DDR marker gammaH2AX but does not show any viability issues on spot assay at different HU concentration. We assayed cell cycle progression for initial division in the presence of HU after release from G1. FACs profile of *Δrrm3* strains at physiological conditions and with different amount of HU concentration seems to be identical to Wt cells as shown in (Fig 3.6A,B). We compared HU mediated fork stalling (200mM HU, 2hrs) and then recovery in YPGlu media. Again, FACs profile during HU recovery is identical for wild type and *Δrrm3* (Fig 3.6C).

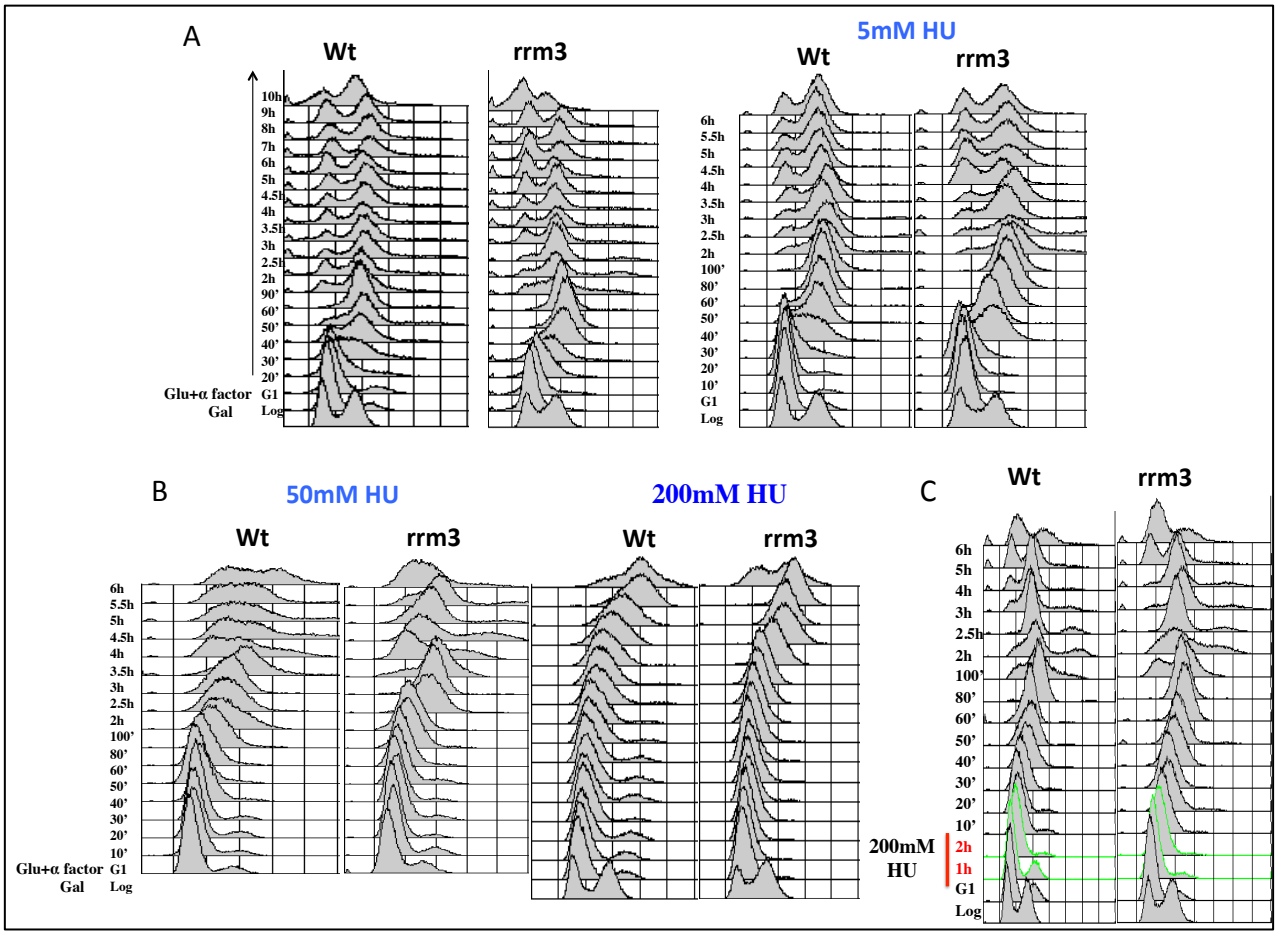


Figure: 3.6. Cell cycle progression profile Δrrm3 strain at physiological condition and replication stress induced by HU.

A and B) Log cells grown in YPGal and arrested with alpha factor in G1, and later released in S-phase with out HU and with low concentration of HU (5mM), high concentration of HU 50mM (Figure. B) And 200mM HU.

C. HU recovery, rrm3 strain released in 200mM HU in s phase for 2hrs and further released from HU in YPGlu medium.

3.7 Termination zone accumulate Unusual Replication intermediates in *Δrrm3*

As Rrm3p associates with replisome components PCNA and Orc5p complex, we checked analyzed replication intermediates accumulation at ARS (replication initiation) and TERs (replication termination). Wild type and *rrm3* cells were arrested in G1 and released in S-phase with 100mM HU (Fig.3.7A). Along with G1, samples were collected at different time points for cell cycle progression and 2D gel analysis using a probe specific to ARS305 (*Eco*RI). 2D gels allowed us to score for the replication bubble arc and any unusual replication intermediates (Fig.3.7B). Origin firing pattern seems to be identical for wild type and *Δrrm3*. From the same Genomic DNA preparation, 10ug of genomic DNA digested with Hind III restriction enzyme to produce 5kb long fragment carrying TER704 (CEN is pausing element). Samples were run on a 2D gel to capture replication intermediates at TER704 in *Δrrm3*, as shown in (Fig.3.7C). Converging forks at TER704 can pause and appear as dots on Y and X molecules along the fork converging arc. Genomic DNA was also digested with *Pst*I enzyme to generate 6kb long fragment and scored for Replication Intermediates at TER603 carrying tRNA as pausing element in *Δrrm3*. We observed enhanced fork pausing signature as spike, representative of X molecules in *Δrrm3* compare to wild type (Data not shown). Hence, Rrm3 seems to specifically affect the replication intrermediates at TERs.

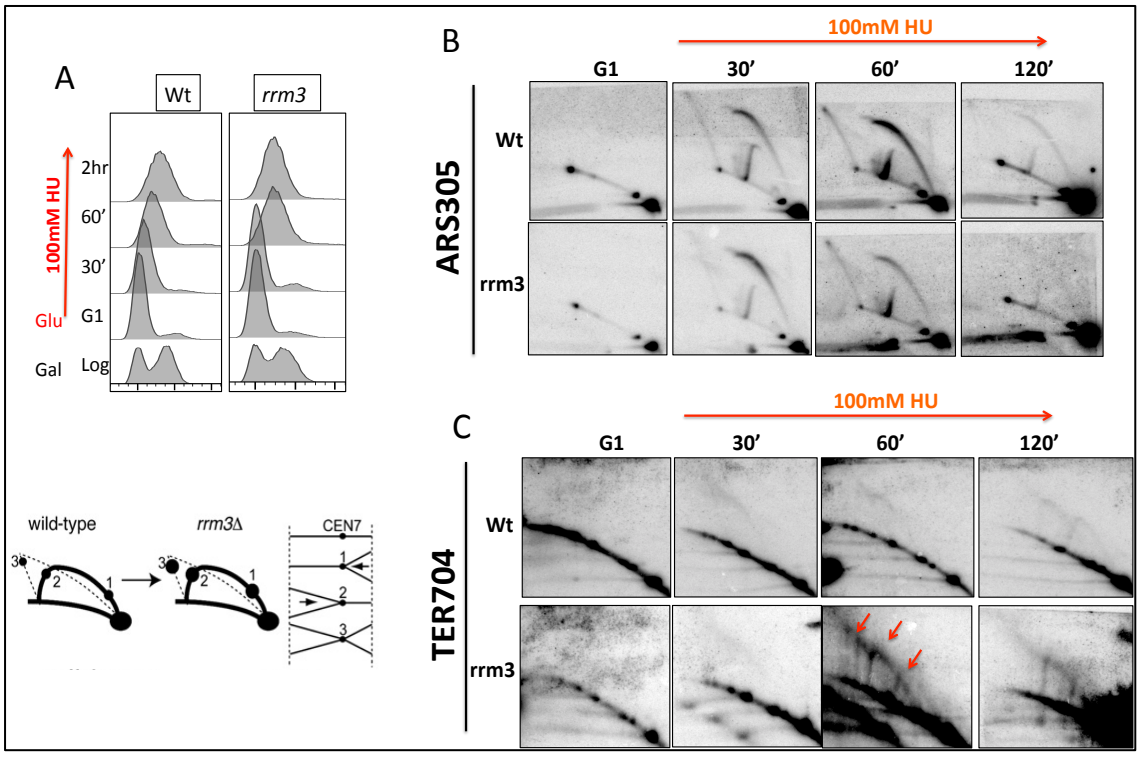


Figure: 3.7. Not Origin firing but Replication termination was impaired in Δrrm3 cells under replication stress. A). FACs profile of wild type and rrm3 cells arrested in G1 and released in S-phase with 100mM HU. Along with G1, B).Psorolen cross-linked in-vivo, genomic DNA was purified and 10ug of it digested with *EcoRI* and subjected for 2D gel analysis. We used probe against ARS305 and scored for the bubble arc and any unusual replication intermediates. C). Genomic DNA preparation for fig.B , 10ug was digested with Hind III restriction enzyme for TER704 (CEN is pausing element) for 2D procedure. Converging forks at TER704 can pause and appear as dots on Y and X molecules arc. Similar way we scored for Replication intermediates at TER603 (Data not shown).

3.8 Rrm3 and Rad53 interact to resolve unusual replication intermediates at TERs and suppress breakages at TERs.

Different studies have shown that *Δrrm3* genetically interacts with intra S-phase checkpoints mutants and homologous recombination HR pathways. Interestingly, survival of different helicases *Δsrs2* and *Δsgs1* depends on functional Rrm3. We explored the role of replication checkpoint proteins at TERs to resolve fork pausing in *Δrrm3*. Spot assay were performed to assess viability of different mutant strains *Δrrm3* and *Δrad53 Δsml1* along with wild type. Strains grown over night, and spotted on YPGal and YPGlu plates with mild replication stress 1mM, 2.5mM, 5mM, 12.5mM at RT (22^{o}C) and 25^{o}C and 28^{o}C. We showed that the viability of *Δrrm3* strain depends on replication checkpoint Rad53 under mild replication stress (Fig. 3.8A).

Different strains grown in YPGlu+25mM and samples were collected at different time intervals as indicated for PFGE and we scored for gross chromosomal breaks and unresolved replication intermediates in different genotypes. Interestingly, *Δrrm3 Δrad53 Δsml1* strains showed less resolved chromosomes (Fig.3.8B). *Δrrm3* and *Δrad53Δsml1* alone showed resolved chromosomes and DSBs accumulation. We therefore conclude that Rad53 and Rrm3 partecipate in the resolution of replication intermediates accumulating at TERs. Moreover, Rrm3 plays a kye role in assisting fork pausing at TERs counteracting aberrant transitions leading to DNA breaks accumulation.

3.9 Conclusion:

Cells lacking the Rrm3p DNA helicase increase replication fork pausing at over 1,000 sites scattered throughout the genome. Depending on the genomic loci, broken replication forks are also readily detected in *rrm3* cells (Ivessa, Zhou et al. 2000, Ivessa, Zhou et al. 2002, Ivessa, Lenzmeier et al. 2003). Here we explored the role of Rrm3 in suppressing R-loop accumulation at natural pausing sites and TERs. From yeasts to humans, R-loops have been suggested to cause DNA damage at RNA Pol II transcribed genes. However, it is unclear whether all R-loops behave similarly, or whether certain loci, in certain genetic backgrounds accumulate genotoxic species of R-loops. Our data

suggest that Rrm3 counteracts the accumulation of RNA-DNA hybrids that may hamper fork progression and integrity.

Rrm3 has been implicated in assisting replication termination (Fachinetti, Bermejo et al. 2010). However, even in the total absence of Rrm3, termination can still occur, although

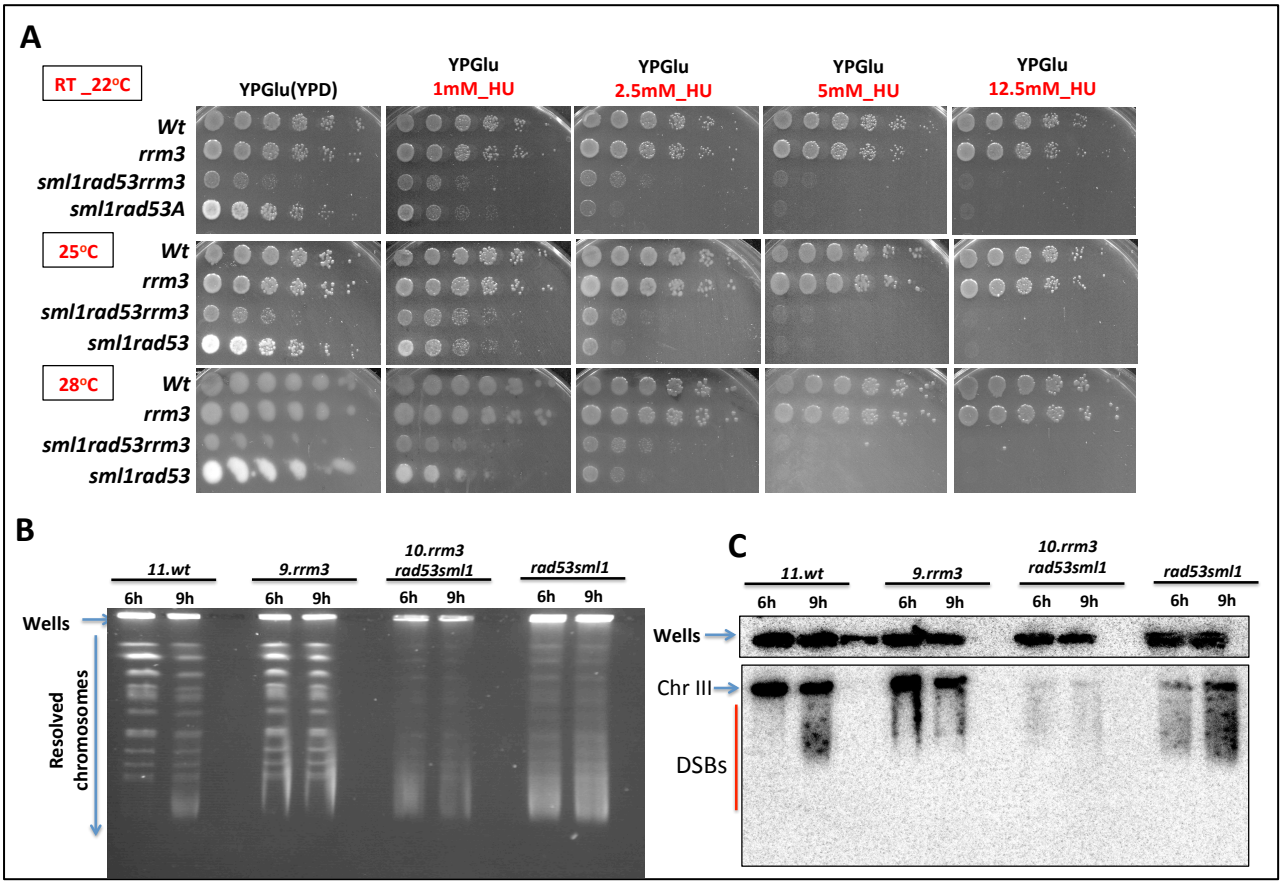


Figure 3.8: Rrm3p and Replication Checkpoint proteins interact to preserve fragility at TERs including Replication intermediates.

A). Spot assay to assess viability of different mutant strains rrm3 and Rad53sml1 along with Wt.. Strains grown over night, and spotted on YPGal and YPGlu plates with mild replication stress 1mM, 2.5mM, 5mM, 12.5mM HU at RT (22oC) and 25oC and 28oC.

B). EtBr staining of PFGE to assess gross chromosomal integrity. Different strains grown in YPGlu+25mM HU and samples were collected at different time intervals as indicated for PFGE.

C). Replication intermediates and fragility (DNA breaks) detected at TER302 using specific probe. ChrIII and DSBs marked along with well showing retention of Chromosome III because of unusual replication intermediate formation at TERs in absence of Replication checkpoint activation, which can be rescued by depleting rrm3.

less efficiently. We speculated that other yet unidentified helicases might substitute for the absence of Rrm3. Rrm3 has been implicated in several processes and exhibits positive and negative genetic interactions with a variety of genome integrity pathways. We speculated that the ideal candidate for substituting Rrm3 in mediating replication termination should be a helicase involved in counteracting RNA-DNA hybrids and interacting genetically with *RRM3*. We therefore focused our studies on Sen1.

Results: chapter 4

Tittle: Senataxin-1 (Sen1p) suppresses genomic copy number variations at transcribing natural chromosomal pausing sites and TERs

In *Saccharomyces cerevisiae*, Sen1, a super- family I RNA/DNA helicase restricts this RNA/DNA hybrids (R loops) formation during transcription by interacting directly with RNA polymerase II. Sen1p mutants exhibit pleiotropic defects in RNA processing and transcription termination. These defects are thought to be associated with Sen1 role in limiting the accumulation of transcription-directed R-loop structures that would otherwise lead to unscheduled recombination events.

Senataxin gene encodes a conserved DNA/RNA helicase with multiple roles in RNA metabolism (Suraweera, Lim et al. 2009). It is found mutated in two severe neurodegenerative disorders ataxia-ocular apraxia type 2 (AOA2) (Moreira, Klur et al. 2004) and amyotrophic lateral sclerosis type 4 (ALS4) (Chen et al., 2004 (Chen, Muller et al. 2014, Pan, Jiang et al. 2014). Yeast Sen1p acts in complex with two RNA-binding proteins Nrd1 and Nab3, to terminate non-polyadenylated RNA species that include small nuclear and small nucleolar RNAs (Lenstra, Tudek et al. 2013) 2001; Ursic et al. (Ursic, DeMarini et al. 1995, Ursic, Himmel et al. 1997, Ursic, Chinchilla et al. 2004), 1997), cryptic unstable transcripts (Arigo et al., 2006; Thiebaut et al., 2006), and aberrant mRNAs (Rondo´ n et al., 2009 (Rondon, Mischo et al. 2009). It has been proposed that, in both yeast and mammals, Senataxin/Sen1 removes R-loops during transcription termination (Mischo et al., 2011; Skourti-Stathaki et al., 2011) and whose pathological accumulation would cause hyper-recombination (Mischo et al., 2011; Stirling et al., 2012).

Apart from transcription termination, recent evidence supports a role for Sen1 in resolving R-loop structures that arise at transcription pause sites. In addition, SETX (Senataxin) depleted cell lines are sensitive to agents that cause DNA damage, in

particular those that introduce oxidative stress and single-strand breaks. These observations led us to further explore the potential links between replication stress, transcription, and the DNA damage response and to determine whether Senataxin plays a role in the processing of R loops that might otherwise lead to genome instability.

Replication forks slow down when they encounter DNA secondary structures, DNA lesions, and DNA-bound proteins (Mirkin and Mirkin, 2007 (Mirkin and Mirkin 2007). Stalled forks are potentially genotoxic because they can be engaged by dangerous recombination activities (Branzei and Foiani, 2010 (Branzei and Foiani 2010, Branzei and Foiani 2010). Transcription is one major physiological obstacle for replication (Aguilera, 2005; Bermejo et al., 2012; Rudolph et al., 2007) and failure to assist fork progression across transcription units leads to DNA damage (Bermejo et al., 2009, 2011; Brewer and Fangman, 1988; Huertas and Aguilera, 2003; Sabouri et al., 2012). In eukaryotes, both head-on and co-directional collisions between replication and transcription occur and hamper fork progression (Azvolinsky et al., 2009; Bermejo et al., 2009; Deshpande and Newlon, 1996). Members of the conserved family of Pif1 DNA helicases facilitate fork progression past protein-DNA barriers, including those at transcribed genes (Azvolinsky et al., 2009; Ivessa et al., 2003; Sabouri et al., 2012; Steinacher et al., 2012). The replication checkpoint contributes to prevent replication and transcription interference by disassembling the RNA polymerase (RNAP) III pre-initiation complex (Clelland and Schultz, 2010) and by counteracting abnormal fork transitions at RNAPII-transcribed genes (Bermejo et al., 2011 (Bermejo, Capra et al. 2011). RNAPII-transcribed genes are organized in chromatin loops (Hampsey et al., 2011 (Laine, Singh et al. 2009), and the S phase architecture of messenger RNA (mRNA) genes depends on DNA topoisomerase II (Bermejo et al., 2009). The THO/TREX-2 complexes couple RNAPII transcription (Go´mez-Gonza´lez et al., 2011) with mRNA export through the nuclear envelope, a process known as gene gating (Blobel, 1985). The ATR checkpoint phosphorylates key nucleoporins to counteract gene gating, thus neutralizing the topological tension generated when forks encounter gated genes (Bermejo et al., 2011).

We speculated a potential role of Sen1p at different transcribing units, which can behave as natural pausing sites. Because DNA and RNA synthesis generates positive supercoiling downstream of DNA and RNA polymerases, head-on collisions between replisomes and

RNAPs are expected to generate tremendous topological constraints (Olavarrieta et al., 2002; Wang, 2002). Negative supercoiling accumulates behind transcription bubbles, whereas replicated chromatids undergo pre-catenation, which is a form of positive supercoiling (Wang, 2002). Unsolved topological constraints lead to the accumulation of dangerous recombinogenic DNA structures. Positive supercoiling can result in fork reversal (Postow et al., 2001), while R-loop formation depends on negative supercoiling accumulation (Drolet, 2006). A growing body of evidence suggests that, in eukaryotes, the DNA-RNA hybrids at R-loops promote chromosomal rearrangements (Gan et al., 2011; Go´ mez-Gonza´ lez et al., 2011; Gottipati et al., 2008; Helmrich et al., 2011; Huertas and Aguilera, 2003; Li and Manley, 2005; Mischo et al., 2011; Paulsen et al., 2009; Tuduri et al., 2009; Wahba et al., 2011). R-loop accumulation is enhanced in the absence of mRNA biogenesis factors and the SR protein SRSF1 (Li and Manley, 2005). These factors sequester nascent transcripts, thus preventing RNA re-annealing to the template. Topoisomerase I (Drolet, 2006; Tuduri et al., 2009), RNase H (Potenski and Klein 2011, Wahba, Amon et al. 2011, Wahba, Costantino et al. 2016), and Senataxin (Sen1 in budding yeast) (Mischo et al., 2011; Skourti-Stathaki et al., 2011; Stirling et al., 2012) are few proteins involved in suppressing R-loop accumulation.

Sen1p previously identified as a physical interactor of the Srs2 recombination DNA helicase (Chiolo et al., 2005 (Chiolo, Carotenuto et al. 2005). We found that Sen1p regulates fragility at different natural fork pausing sites. We observed strong relation of Sen1p binding at pausing elements and R-loop accumulation in absence of Sen1p at these loci. Sen1p suppresses genomic alterations under mild replication stress in proliferating cells, scored as CNVs. We then focused on a novel role of Sen1p at replication termination (TERs). Sen1p associates with TERs and protects the integrity of those forks while encountering highly expressed RNAPII genes at TERs and involved in gene gating. In the absence of Sen1, forks engaging RNAPII-transcribed genes in a head-on conformation accumulate aberrant DNA structures DNA-RNA hybrids (R-loops) that are then processed in genotoxic events. Fork stalling and pausing at transcribing loci might prime unscheduled recombination events, checkpoint activation, and genome instability. Our data indicate a role for Sen1 during chromosome replication in facilitating replisome progression across RNAPII-transcribed genes at TERs and natural pausing sites, thus preventing DNA-RNA hybrid accumulation and GCRs.

4.1 Sen1p is required for recovery from HU.

Senataxin-1 (Sen1p) participates in transcription termination and also functions as a component of replisome to avoid R-loop mediated replication fork stalling at highly transcribing genes. This made us thinking about the unexplored role of Sen1p in fork progression at different natural pausing sites and under replication stress. Under physiological conditions, *sen1-1* mutants accumulate mild DDR marker gammaH2AX, exhibits replication checkpoint activation and show strong viability issues on spot assay even in absence of any external stress. We assayed cell cycle progression for initial division in presence of HU after released from G1. FACs profile of *sen1*^{dg} strains at physiological condition (Fig 4.1B) or in presence of low or high amount of HU seems to be identical to wild type (Fig 4.1A,D). We compared HU mediated fork stalling (200mM HU, 2hrs) and then recovery in YPGlu media. During HU recovery, *sen1*^{dg} showed slight differences in the FACS profiles compared to wild type (Fig 4.1C). After the first cell cycle, sen1^{dg} cells were arrested in G2/M. We assumed that absence of sen1 caused DNA damage response activation.

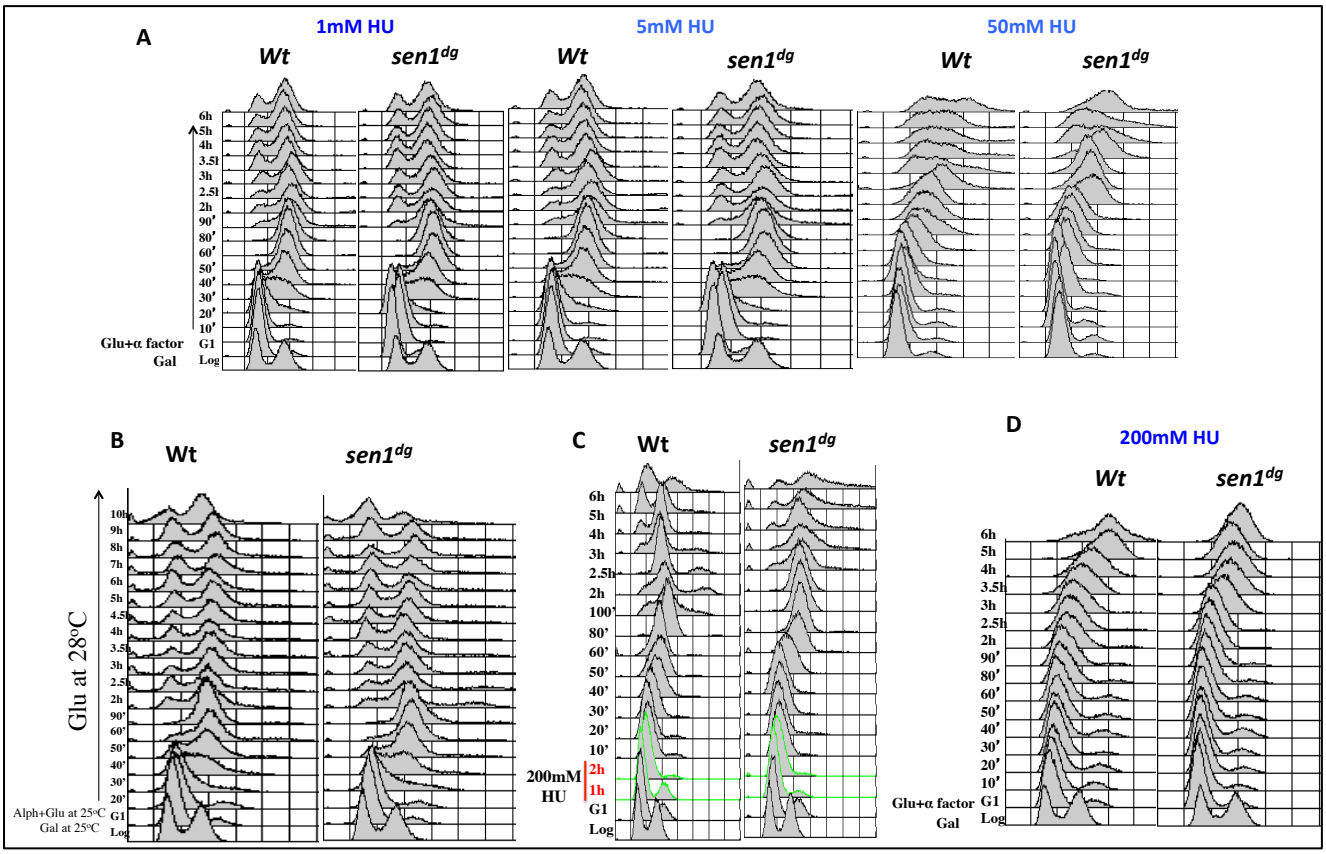


Figure4.1: Cell cycle progression profile of sen1^{dg} strain in physiological condition and replication stress induced by HU.
A. Log cells grown in YPGal and arrested with alpha factor in G1, and later released in S-phase with out HU (B) and different concentration of HU (1,5 50mM), high concentration of HU 200mM (Fig.D)
C. HU recovery, sen1^{dg} strain released in 200mM HU in s phase for 2hrs and further released from HU in YPGlu medium.

4.2 Sen1p expression though-out cell cycle.

We analyzed the Sen1 protein levels during cell cycle progression and we did not observe significant changes during the cell cycle phases.

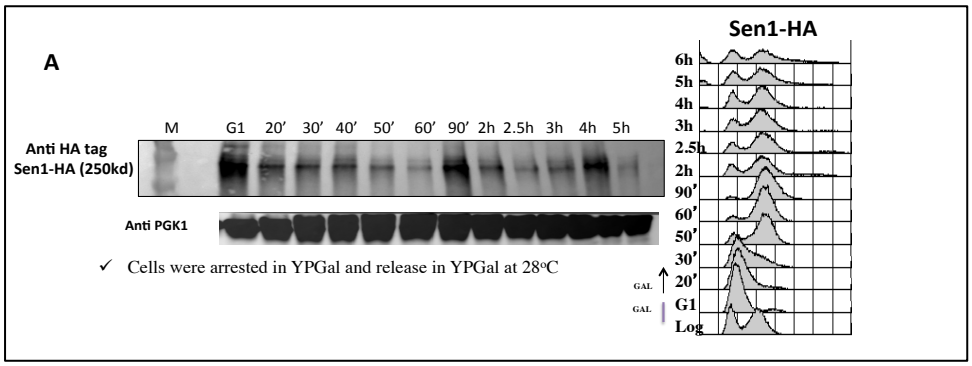


Figure 4.2: Sen1p expression during different stage of cell cycle.
A).Yeast strain where endogenoug protein is tagged at N-terminal, arrested at G1 and release in S-phase . At different time point, samples were collected for FACs profile and TCA exptraction . Anti-HA antibody used to measure expresion of sen1p and PGK1 antibody used for loading control.

4.3 Depletion of Sen1p causes replication checkpoint activation and G2/M arrest under replication stress.

To explore role of Sen1p helicase in preserving fork progression, we scored for replication checkpoint activation in absence of Sen1p. Wild type and *Sen1^{dg}* arrested G1 and released in YPGlu presence and absence of 25mM HU. We observed differential cell cycle progression compare to wild type in 25mM HU (Fig4.3A). We looked at Rad53 activation using antibody FL7 (E9). As expected wild type proliferating cells increased activation of Rad53 checkpoint in presence of mild replication stress. *Sen1^{dg}* showed mild increased checkpoint activation and DDR response already under unperturbed conditions, which suggest a potential role in replication fork integrity. Under mild replication stress, *Sen1^{dg}* enhanced checkpoint activation and gamma-H2Ax also. DDR activation causes G2/M arrest of *Sen1^{dg}* strain.

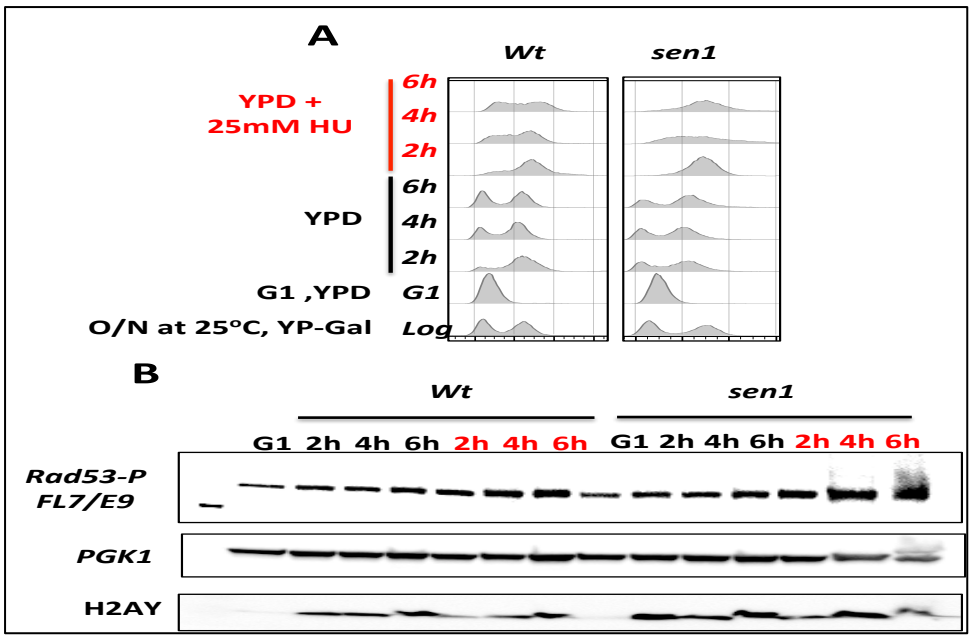


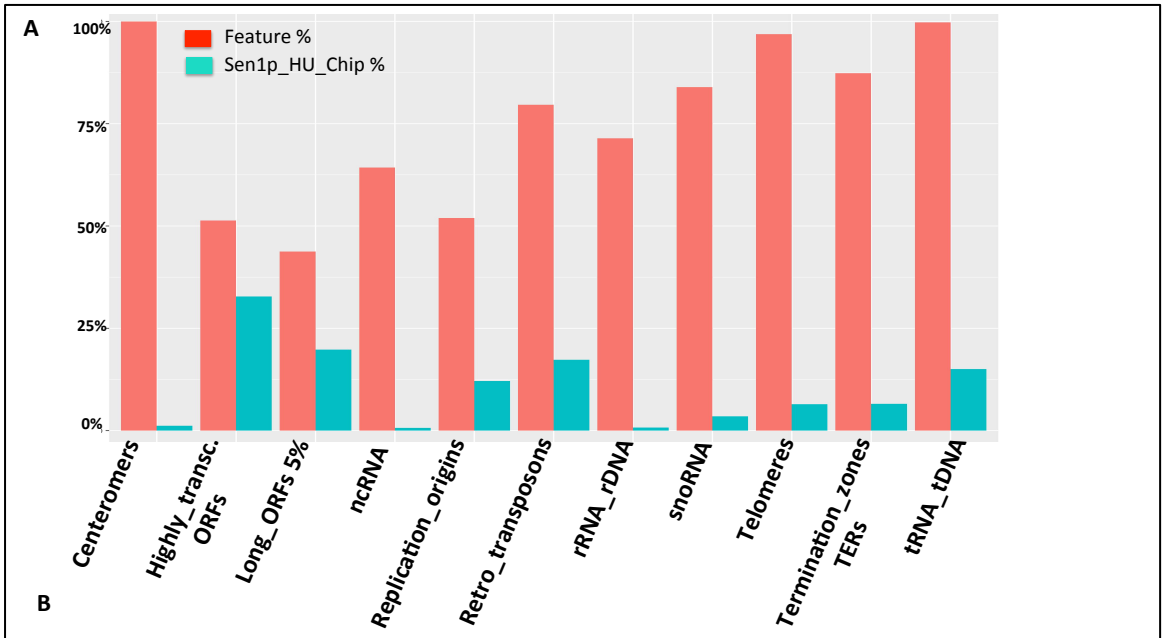
Figure 4.3: sen1^{dg} showed increased Checkpoint activation presence of mild replication stress (25mM HU)

A). FACs profile of wild and sen1^{dg} genotypes, proliferating in YPGlu +/- 25mM HU after synchronized released in S-phase. G1 arrest and S-phase released done in YPGlu medium as required for degron system of Sen1p.

B). Checkpoint activation measured with anti-Rad53-P (FL7/E9) and DNA damage response with Gamma-H2Ax. Anti-PGK1 was used as loading control.

4.4 Different transcribing natural chromosomal pausing sites exhibit enrichment for Sen1p under replication stress.

We therefore focused on Sen1p localization in presence of HU (23°C, 60' in 0.2M HU), which was reported by Amaya Alzu et al, 2012. We scored for association of total peaks 1376 with different genomic features transcribing natural chromosomal pausing sites, RFBs and TERs. These genomic regions are fragile under mild replication stress in checkpoint deficient cells as shown in chapter 1.



Type	Test	Sen1p_HU_Chip % Peaks total	Total Features	Peaks_verlap	Feature Overlap	P-value
rRNA	Sen1_Prot_HU_Sphase	1376	28	10	20	7,78E-08
Telomere	Sen1_Prot_HU_Sphase	1376	32	89	31	2,08E-06
snoRNA	Sen1_Prot_HU_Sphase	1376	81	48	68	8,04E-21
Termination	Sen1_Prot_HU_Sphase	1376	71	90	62	4,42E-02
Reterotransposon	Sen1_Prot_HU_Sphase	1376	486	238	387	9,35E-211
HighTranscribingORF	Sen1_Prot_HU_Sphase	1376	1143	451	587	9,82E-43
tRNA	Sen1_Prot_HU_Sphase	1376	395	207	394	8,64E-226
Centromere	Sen1_Prot_HU_Sphase	1376	16	16	16	1,72E-05
ncRNA	Sen1_Prot_HU_Sphase	1376	14	9	9	0.0097162
LongORF_5%	Sen1_Prot_HU_Sphase	1376	336	272	147	0.00092549
ReplicationOrigin	Sen1_Prot_HU_Sphase	1376	410	167	213	1,88E-13

Figure 4.4: Binding profile of Sen1p protein at different natural pausing sites, RFBs and Replication termination in during S-phase under replication stress.

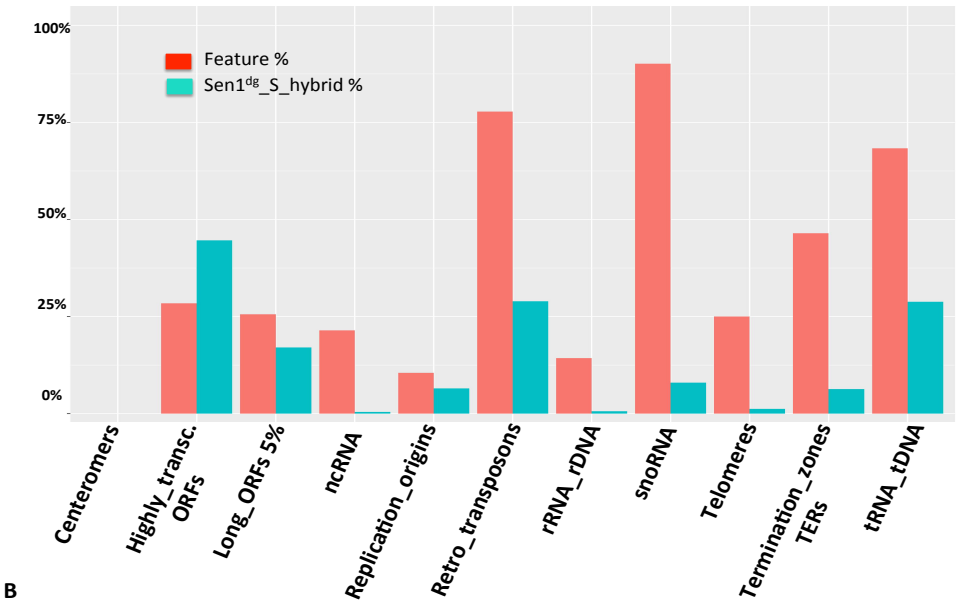
Meta-analysis of Sen1-FLAG Chip data for significant clusters at natural fork pausing genomic loci in presence of HU. Chip experiment performed on S-phase under 200mM HU. Different significant clusters for Sen1p peaks (1376) subjected to score there association with different genomic loci including 11 categories as shown on X-axis which includes rDNA loci, Telomeres and Replication termination zones and highly transcribing ORFs including longest ORFs (5% of total). Same data represented in tabular form as fig B.

We scored for the binding of Sen1p-FLAG along 11 different genomic features covering ORFs (Pol II), Replication origins (DNA pol) and rDNA (Pol I) (Fig4.4) as well as other natural chromosomal pausing sites, repetitive sequence transcribing with RNA pol II (centromeres, retro-transposons and telomeres) and RNA pol III transcribing snoRNA and tRNA. Interestingly, Sen1p-FLAG enriched at highly transcribing ORFs (587/1143) including 5% long ORF (247/336) as well (Fig4.4). Sen1p binds also replication origins (213/410), as it is a component of the replisome. Other fork pausing elements including rDNA (20/28), Telomeres (31/32) and TERs (62/71) showed significant Sen1p-FLAG clusters (Fig4.4).

4.5 Genome wide enrichment of R-loops in the absence of Sen1p.

We measured R-loop accumulation on proliferating sen1^{dg} cells in cell cycle dependent manner, here shown only S-phase (40') using DRIP-Chip method. We scored for R-loop peaks (663) along 11 genomic features and significance of association (Fig4.5). Although replication origins have no transcriptional activity we observed strong binding Sen1p (213/410) but no significant R-loop accumulation in sen1^{dg} (Fig.4.5). We observed that long ORFs (top 5%) showed no significant R-loop accumulation (86/336) although these ORFs are transcriptionally active, we observed the same for rDNA and Telomeres. On the contrary highly transcribing ORFs showed significant association with Sen1p binding as well as R-loop accumulation (325/1143) in sen1^{dg}. Replication Termination (TERs) are prone to accumulate R-loops in sen1^{dg}. snoRNA (RNAP III) and tRNAs (RNAP III) loci showed significant R-loop accumulation in sen1^{dg} (Fig4.5). Hence, Sen1p counteracts R-loop accumulation at different loci, likely to facilitate fork advance.

A



B

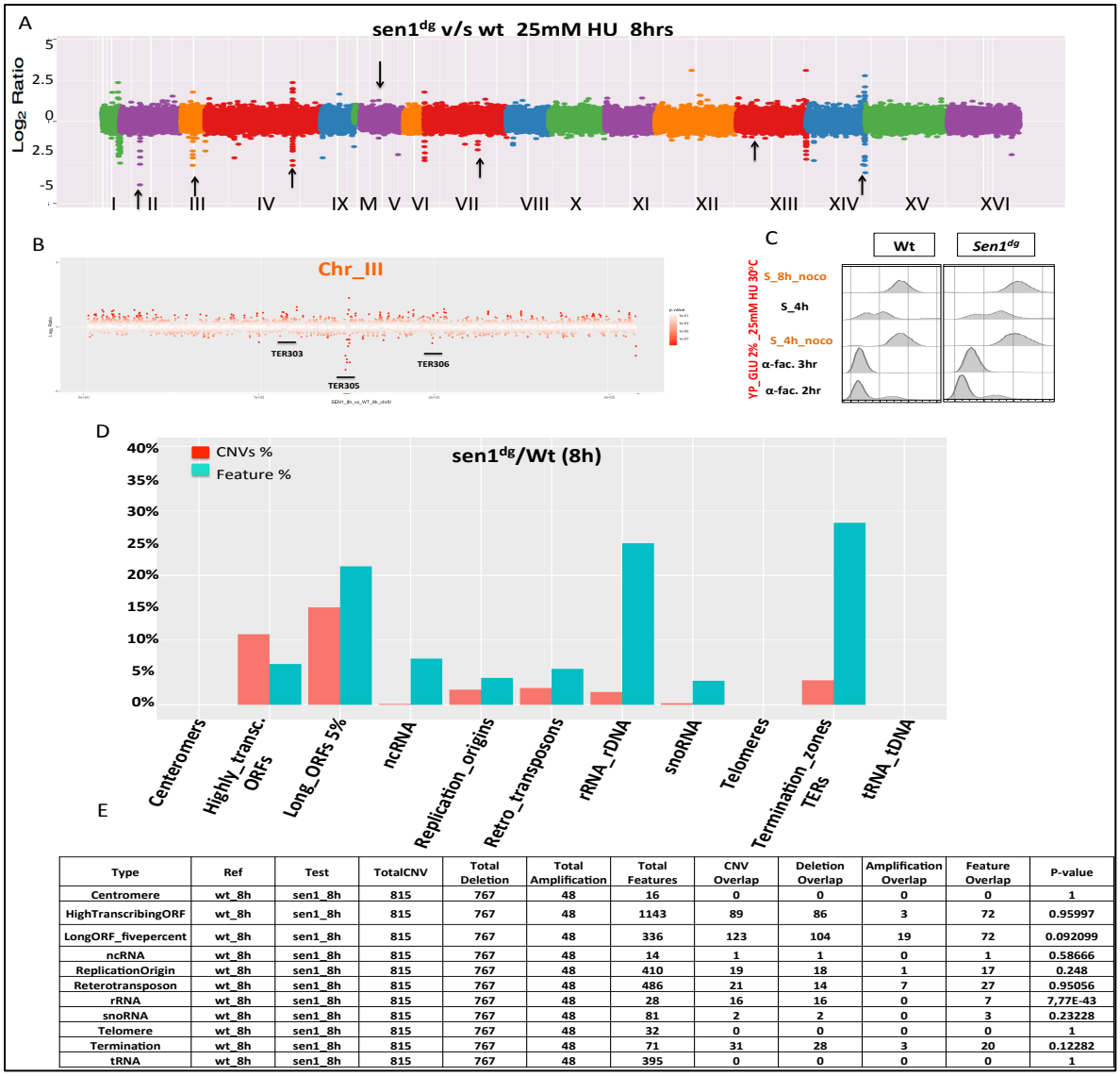
Type	Test	Sen1_S_R-loop Total	Total Features	R-loop Overlap	Feature Overlap	P-value
rRNA	sen1_S_hybrids	663	28	4	4	0.70255
Telomere	sen1_S_hybrids	663	32	8	8	0.88002
snoRNA	sen1_S_hybrids	663	81	53	73	1,55E-61
Termination	sen1_S_hybrids	663	71	42	33	0.0001618
Reterotransposon	sen1_S_hybrids	663	486	192	378	0
HighTranscribingORF	sen1_S_hybrids	663	1143	296	325	2,73E-46
tRNA	sen1_S_hybrids	663	395	191	270	5,39E-199
Centromere	sen1_S_hybrids	663	16	0	0	1
ncRNA	sen1_S_hybrids	663	14	3	3	0.278
LongORF_fivepercent	sen1_S_hybrids	663	336	113	86	0.60077
ReplicationOrigin	sen1_S_hybrids	663	410	43	43	0.68868

Figure 4.5. R-loop accumulation at natural pausing sites, RFBs and Replication termination
Meta-analysis of DRIP-chip data for R-loop accumulation in sen1^{dg}. DRIP-Chip experiment performed on S-phase at 40-minute time point. From Chip data, different significant clusters for R-loop peaks (S9.6_antibody) subjected to score association with different genomic loci including 11 categories as shown on X-axis which includes rDNA loci, Telomeres and Replication termination zones along with highly transcribing regions ORFs including longest ORFs (5% of total). Same data represented in tabular form as fig B. (Significant P< 0.05)

4.6 CNVs mapping in sen1^{dg} under mild replication stress.

We scored for copy number variation based of whole genome sequence of wild type and sen1^{dg} shown in FACS profile at 8hrs with 25mM HU and arrested in G2/M with Nocodazole (Fig.4.6C).

Whole Genome sequencing reads from NGS of sen1^{dg}, compared with wild type, represented along all 16 chromosomes show different genomic region with deletion and amplification (Fig.30A). Replication Termination zones accumulate significant CNVs shown as showed in the enlarged view at TER302 in sen1^{dg} (Fig.30B). Genome wide distribution of CNVs in *sen1^{dg}* strain shown along 11 features which cover most of natural chromosomal fork pausing sites and repeat region in genome and Y-axis represent percentages of total CNVs (815) overlap with given feature as red bar and percentage of the features marked by CNVs in *sen1^{dg}* marked as green bar (Fig.4.6D). Total CNVs categories as deletion and amplification, and overlap with different genomic features assess for signification p value <0.50. Interestingly, snoRNA and Termination zones accumulate significant number of CNVs in strong correlation with Sen1 binding. RFBs at rDNA (2 features, deletion p=0.0014) and Termination zones (16 features, deletion p=0.00085) showed significant correlation with CNVs distribution. Long ORFs and SnoRNA also showed deletions and amplifications in sen1^{dg} under replication stress.



Type	Ref	Test	TotalCNV	Total Deletion	Total Amplification	Total Features	CNV Overlap	Deletion Overlap	Amplification Overlap	Feature Overlap	P-value
Centromere	wt_8h	sen1_8h	815	767	48	16	0	0	0	0	1
HighTranscribingORF	wt_8h	sen1_8h	815	767	48	1143	89	86	3	72	0.95997
LongORF_fivepercent	wt_8h	sen1_8h	815	767	48	336	123	104	19	72	0.092099
ncRNA	wt_8h	sen1_8h	815	767	48	14	1	1	0	1	0.58666
ReplicationOrigin	wt_8h	sen1_8h	815	767	48	410	19	18	1	17	0.248
Reterotransposon	wt_8h	sen1_8h	815	767	48	486	21	14	7	27	0.95056
rRNA	wt_8h	sen1_8h	815	767	48	28	16	16	0	7	7,77E-43
snoRNA	wt_8h	sen1_8h	815	767	48	81	2	2	0	3	0.23228
Telomere	wt_8h	sen1_8h	815	767	48	32	0	0	0	0	1
Termination	wt_8h	sen1_8h	815	767	48	71	31	28	3	20	0.12282
tRNA	wt_8h	sen1_8h	815	767	48	395	0	0	0	0	1

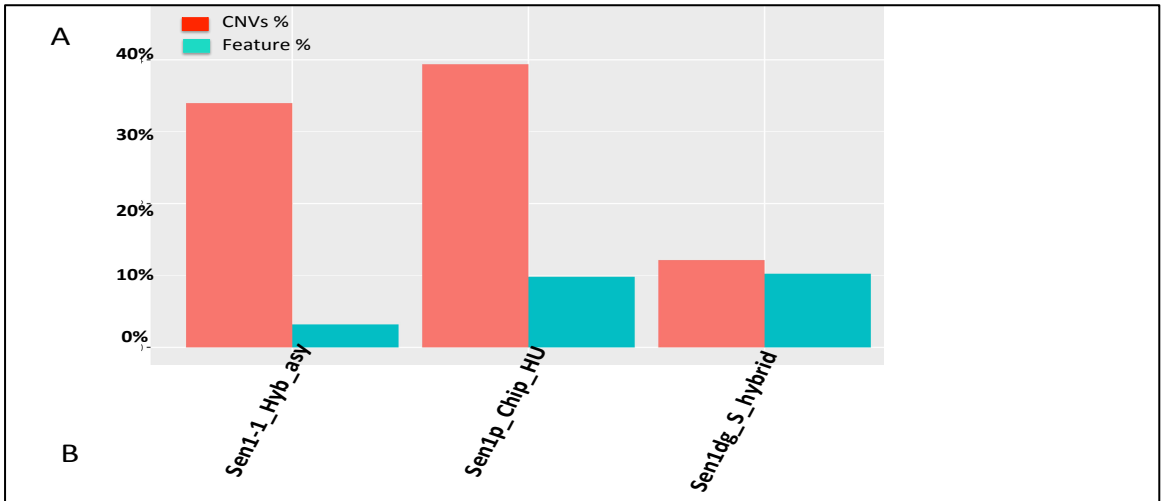
Figure: 4.6 Meta-analysis of genome wide CNVs in *Sen1^{dg}* strain with mild replication stress.
A). Whole Genome sequencing reads (NGS) of *Sen1^{dg}* compared with Wild type, represented along all 16 chromosomes. Y axis showed Log ratio of reads comparison, X axis represent different chromosomes Black arrow marking different region showed dots appeared far from mean distribution of reads.
B). CNVs at chrIII alone showing few TERs marked and have strong copy number variation (Deletions and Amplifications too).
C). FACs profile of the Wild type and *Sen1^{dg}* grown 2 cell cycles (8h) with 25mM HU and arrested in G2/M with nocodazole. Meanwhile, took 4h time point +/- nocodazole to assess cell cycle progression.
D). Genome wide distribution of CNVs after 8h in 25mM HU in *Sen1^{dg}* yeast strain. X-axis marked with 11 features which cover most of natural pausing sites, TERs and repeat region in genome and Y-axis should percentages of total CNVs (815) overlap with given feature as red bar and percentage of the features marked by CNVs shown as green bar.
E). Tabular representation of all CNVs in *Sen1^{dg}*, distributed along different genomic features. Total CNVs categories as deletions and amplifications, and CNVs overlap with different genomic features and vise-versa. Significance p<0.50.

4.7 CNVs in sen1^{dg} strains localize at Sen1-FLAG binding sites and R-loops in sen1^{dg} mutants

We looked at the distribution of CNVs along all the binding sites of Sen1p-FLAG (our lab, section 4.4, R-loop (S-hybrids, sen1dg, 40' S-phase, our lab, and section 4.5) and hybrid

formation in sen1-1 (log cells, Chan et al, 2014, Plos Genetics). Genomic deletions (767/815) are major CNVs in sen1^{dg} cells and showed strong correlation with Sen1p-FLAG binding sites (1376 peaks) where genomic deletion 285 and amplification 36 overlap with 135 peaks Sen1p-FLAG with p <0.05(Fig 4.7B). Hybrid profile of sen1-1 ts allele in log cells from Chan et al, 2014, showed strong correlation with CNVs, as 250 deletion and 27 amplification overlapped with 228 R-loop accumulation prone sites with p=0.003(Fig 4.7B). Interestingly, more stringent S-phase R-loop profile, gives us 663 genomic loci. CNVs distribution showed 79 deletion and 20 amplification overlap with 68 R-loop accumulating regions on sen1^{dg} with p=0.0054 (Fig 4.7B).

We conclude that most of the Sen1p-FLAG binding sites under replication stress, are prone to accumulate R-loop and CNVs in absence of Sen1p.



Type	Ref	Test	Total CNV	Total Deletion	Total Amplification	Total Features	CNV Overlap	Deletion Overlap	Amplification Overlap	Feature Overlap	P-value
Sen1_Hyb	wt_8h	sen1_8h	815	767	48	7150	277	250	27	228	0.0038337
Sen1_Prot_HU_S phase	wt_8h	sen1_8h	815	767	48	1376	321	285	36	135	3,05E-07
sen1_S_hybrids	wt_8h	sen1_8h	815	767	48	663	99	79	20	68	0.0054753

Figure 4.7: CNVs in sen1^{dg} strains are strongly associated with Sen1p-FLAG protein binding sites and R-loop prone genomic loci

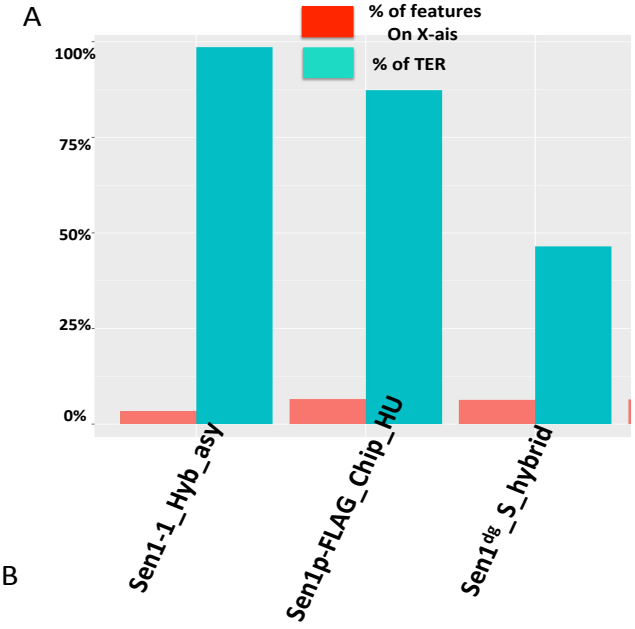
A. CNVs distribution alone different features associated with Sen1p including Binding profile of Sen1p-FLAG in presence of HU and R-loop prone loci from our lab marked as sen1^{dg}_S_hybrids and Chan et al, 2014 marked as Sen1-1_hyb_asy.

B. Tabular representation of CNVs overlap with different features, showing significant correlation p<0.05.

4.8 Termination Zones accumulate R-loops in sen1^{dg} strains.

We observed strong association of Sen1p-FLAG peaks to TERs in S-phase (60', 200mM HU) under replication stress. 62 out of 71 TERs accumulate binding of Sen1p with *p=0.002.* TERs accumulate R-loop 33/71 and 70/71 in sen1^{dg} and *sen1-1* respectively.

A



B

Type	Test	Total Features	Termination Total	Feature Overlap	Termination Overlap	P-value	% TERs
Termination	Sen1-1_Hyb_asy	7150	71	243	70	1	98.59%
Termination	Sen1p-FLAG_HU	1376	71	90	62	4,42E-02	87.32%
Termination	sen1^{dg}_S_hybrids	663	71	42	33	0.0001618	46.47%

Figure 4.8: replication termination zones (TERs) are strongly associated with Sen1p-FLAG protein binding and R-loop prone genomic loci in sen1^{dg}

A. Percentage of TERs (Green bar) showed overlapped with Sen1p-FLAG binding sites and R-loop accumulation in sen1^{dg} and *sen1-1*.

B. Tabular representation of data, significant correlation with given features and termination zones with p-value and %TERs..

4.9 TERs are fragile in sen1^{dg} strains under replication stress.

We tested the cell viability on spot assay for degron system sen1^{dg} and different clones of temperature sensitive allele of Sen1p shown as *sen1-1.* We used different mild concentration of HU and temperature conditions that cause deactivation of Sen1p in the mutant ts background (Fig.4.9A). Depletion of Sen1p and heat inactivation causes cell death on spot assay. We therefore explored genomic instability events during the first and second cell cycle in absence of active sen1p in presence of mild replication stress 25mM HU (Fig.4.9B). Cell cycle progression shown with FACS profile where all sen1-1 ts alleles arrest in G2/M stage of cell cycle but sen1^{dg} kept cycling (Fig.4.9B). We checked activation of replication checkpoint with Rad53 phosphorylation and gamma-H2Ax (data now shown). We observed enhanced Rad53-p and gamma-H2Ax in the temperature

sensitive alleles that account for the G2/M arrest; however, this was not the case in sen1^{dg}. We did not observe dramatic differences at the level of EtBr staining after running PFGE in the different strains. Resolved chromosome could be easily scored with individual bands along with marker in all the genetic backgrounds analyzed.

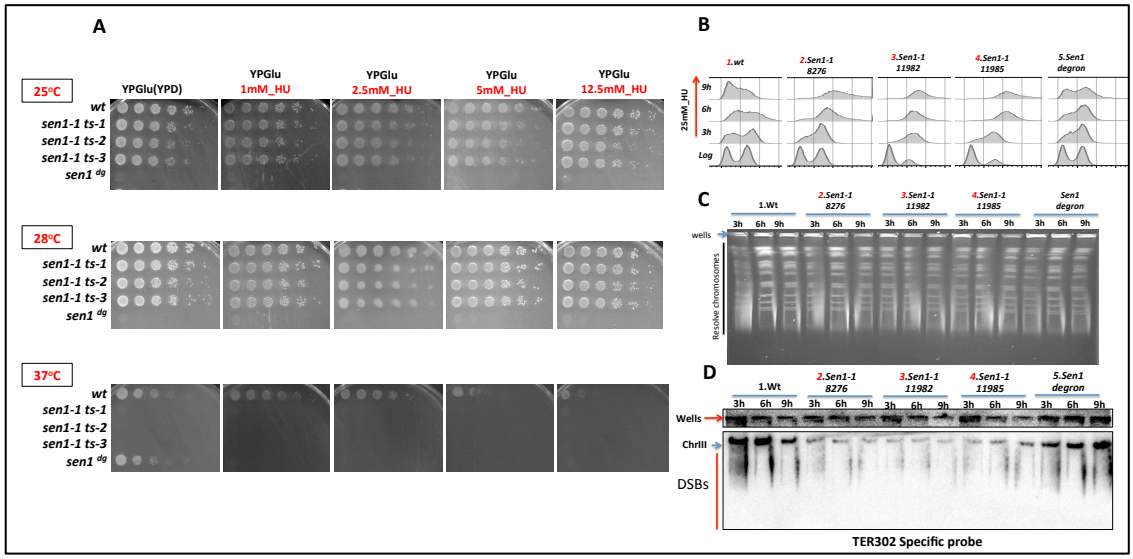


Figure4.9: Sen1p preserve fragility at TERs including Replication intermediates.
A). Spot assay to assess viability of different mutant strains, temperature sensitive alleles of Sen1p (*sen1-1* ts), Sen1^{dg} (degron system GAL to GLU) along with wild type. Strains grown over night, and spotted on YPGal and YPGlu plates with mild replication stress 1mM, 2.5mM, 5mM, 12.5mM at RT-22oC and 25oC and 28oC.
B). FACs analysis of different strains grown in YPGlu+25mM and samples were collected at different time intervals as indicated for FACs and PFGE.
C). Etbr staining of PFGE to assess gross chromosomal integrity. PFGE plugs prepared from different time points after Log cells grown in YPGal, were shifted to YPGlu+25mM HU.
D). Replication intermediates and fragility (DNA breaks) detected at TER302 using specific probe. ChrIII and DSBs marked along with wells showing retention of Chromosome III because of unusual replication intermediate formation at TERs in absence of Sen1p or temperature sensitive allele sen1-1.

We looked at chromosomal fragility at TERs by southern blot using specific probe for TER302. Again, as shown in chapter 1, even wild type cells accumulate mild breaks at TERs with HU and the breaks increase increase during the course of HU treatment toward 9h. Temperature sensitive alleles (ts) *sen1-1* accumulates replication intermediates (RI), which remain in wells and resolve less as individual chromosome. sen1^{dg} accumulates more breaks at TERs and less unresolved RIs.

4.10 Sen1p suppresses breaks at TERs during mitotic phase of cell cycle under replication stress.

To explore cause to genomic fragility at TERs in sen1^{dg}, we look at breaks in cell cycle dependent manner. As shown in figure Fig.4.10, We arrested wild type and *sen1^{dg}* in G1 and released in YPGlu in presence or absence of 25mM HU (100mM for sen1^{dg}) with

nocodazole to arrest in G2/M. Further cells were released from nocodazole arrest and followed as indicated in FACs profile till 8hrs (Fig.4.10A).

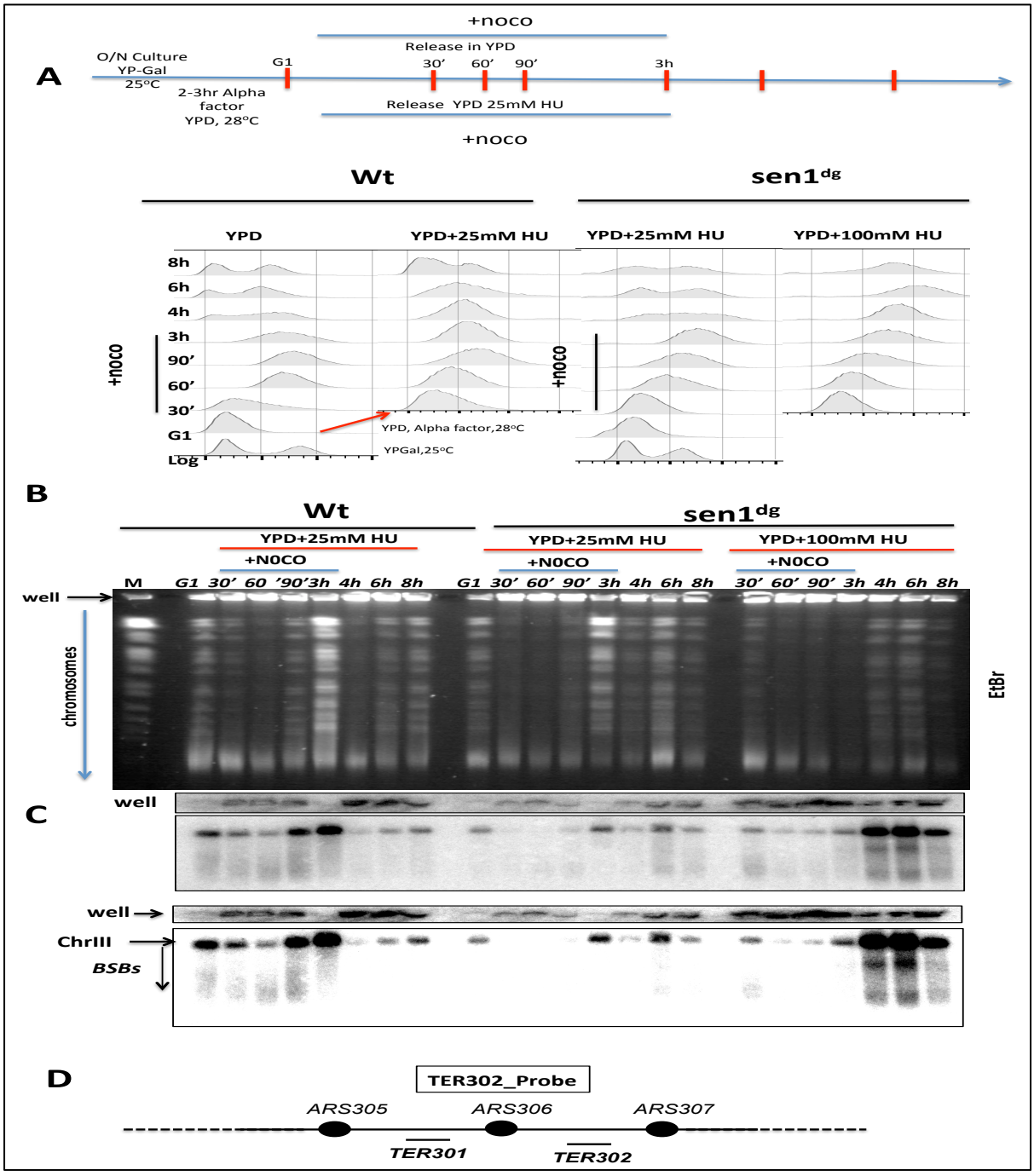


Figure 4.10: Sen1p suppresses breaks at TERs during mitotic phase of cell cycle under mild replication stress
A). FACs analysis of wild type and sen1^{dg} different strains grown in YPGlu+25mM and samples were collected at different time intervals as indicated for FACs and PFGE.
B). Etbr staining of PFGE to assess gross chromosomal integrity. PFGE plugs prepared from different time points after Log cells grown in YPGal, were shifted to YPGlu+25mM HU.

C). Replication intermediates and fragility (DNA breaks) detected at TER302 using specific probe. ChrIII and DSBs marked along with wells showing retention of Chromosome III because of unusual replication intermediate formation at TERs in absence of Sen1p activation.
D). Representation of TER320 with surrounding

Gross chromosomal integrity checked using PFGE. Replication mediated chromosomal entanglement during S phase is clear under 25mM HU in wild type and *sen1^{dg}* too. It is identical between G1 and S phase till nocodazole arrest. Interestingly after nocodazole released (G2/M released) *sen1^{dg}* cells accumulated breaks at TER302 (Fig.4.10C, Lower image is same but with higher contrast).

4.11 Conclusion

While both Rrm3 and Sen1 have been shown to travel with the replication machinery, Sen1 has also a role in transcription termination (Ivessa, Zhou et al. 2002, Arndt and Reines 2015, Fasken, Laribee et al. 2015, Martin-Tumasz and Brow 2015, Porrua and Libri 2015, Rossi, Ajazi et al. 2015, Syed, Desler et al. 2016, Brambati, Zardoni et al. 2017). Moreover, Sen1 has been recently implicated in preventing the accumulation of RNA-DNA hybrids (Alzu, Bermejo et al. 2012).

While the understanding of the exact roles of Rrm3 and Sen1 at replication termination will require further investigations, we can conclude from our results that the absence of both helicases causes the accumulation of aberrant replication termination intermediates characterized by the presence of ss-DNA tracts. We speculate that these ss-DNA tracts may represent scars of RNA-DNA hybrids as, during the EM procedure RNA species are degraded. Hence, the failure of completing replication termination might be influenced by the inability to remove stable hybrids. This would cause the accumulation of topologically complex termination structures that would be engaged by condensation activities.

Chapter 5

Title: Rrm3 and Sen1 assist replicon fusion at Termination Zones

The results described in the precious chapters suggest that both Rrm3 and Sen1 assist replication termination at TERs. We therefore explored the fate of TERs in double mutant combinations using a variety of approaches.

5.1 Double mutant *sen1^{dg}* rrm3Δ exhibit a first cell cycle arrest in G2/M.

sen1-1 (*ts*-allele)(Alzu et al., 2012) and rrm3 deletion exhibit synthestic genetic interactions (Fig. 5.1B). Two parental haploid strains, carrying the *sen1-1* and *rrm3* mutation, were crossed and then a heterozygous diploid was subjected to sporulation and tetrad dissection (Joanna Niska PhD thesis). Spores were kept at a semi-permissive temperature of 30°C in which *sen1-1* single mutant spores were still viable. Conversely, we found that the double mutants were unviable (Fig. 5.1C). This observation lead us to investigate both Rrm3p and Sen1p helicases in terms of DNA replication through natural chromosomal pausing sites, RFBs and TERs. We used the degron system to conditionally deplete Sen1 (Fig. 5.1D, see Chapter 4). The depletion of Sen1 under physiological conditions causes cell lethality. We followed cell cycle progression using FACS, *sen1^{dg}* and *rrm3Δ* showed identical FACs profiles compared to Wild type, but the double mutant arrested in G2/M after the bulk DNA replication was completed (Fig. 5.1A). Interestingly, under physiological conditions the double mutants progressed S-phase faster than the wild type and the two single mutant strains.

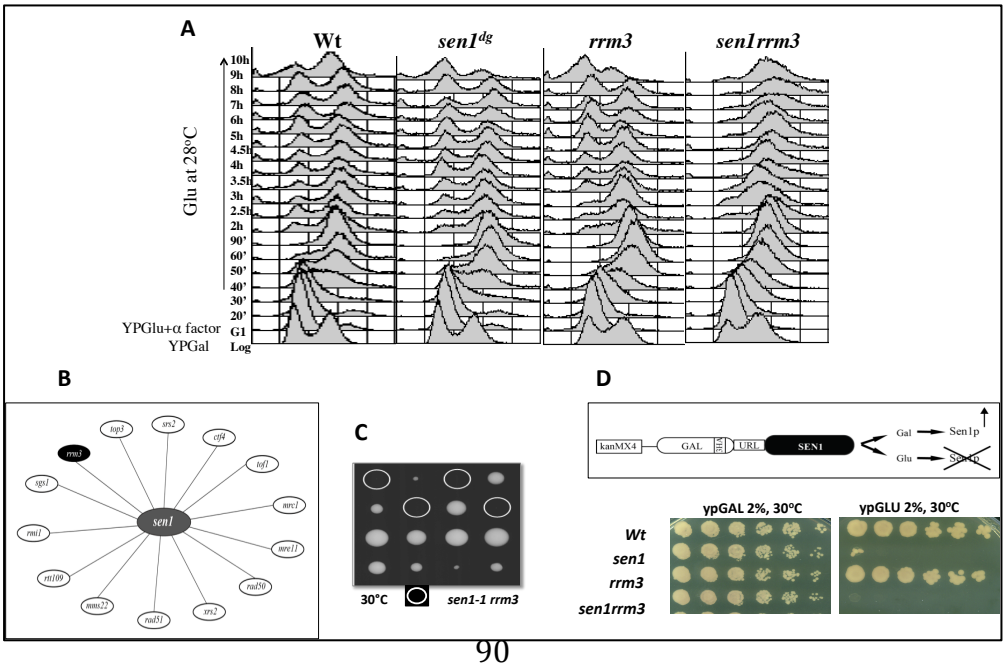


Figure 5.1: Double mutant *sen1^{dg}* rrm3Δ showed G2/M arrest immediately after the first cell cycle under physiological condition.
A) Cell cycle by FACs profile, showed G2/M arrest after the first S-phase. Wild type, sen1^{dg}, rrm3Δ and *sen1^{dg}* rrm3Δ arrested in G1 YPGlu medium. Samples were taken at the indicated time points and subjected to FACs using PI dye.
B) Osprey map for synthetically lethal interaction of sen1-1 (Alzu et al. 2012).
C) Tetrad dissection at 30^{o}C of diploid strains of sen1-1 and rrm3Δ. Circles mark double mutant genotype showing lethal interaction.
D) Degron system for the essential gene Sen1p and spot assay showing viability defect in absence of Sen1p in single mutant or double mutant.

5.2 Double mutant sen1^{dg}rrm3Δ showed arrest from metaphase to anaphase with lagging chromosomes mimicking anaphase bridges

Previous work performed in our lab showed that G2/M arrested double mutant *sen1^{dg}*rrm3Δ has a defect in incorporating Brdu (thymidine analogue) along with natural chromosomal pausing sites and TERs (Joanna Niska Phd thesis). To understand the effect of under-replicated genomes in mitosis, we looked at the G2/M arrest with tubulin and DAPI staining during cell cycle progression. A representative image of 4h for *sen1^{dg}*rrm3Δ is shown in Fig.5.2. We observed DAPI positive entities along the tubulin spindle axis, a typical marker of anaphase bridges and lagging chromosomes. Fig. 5.2(A, B) shows G1 arrested cells released in S-phase and followed at indicated time points and score for cells in metaphase and anaphase with tubulin spindle elongation. We observed a normal metaphase to anaphase transition and further cell cycle progression in the wild type, but in the double mutant a major arrest happened during the metaphase (Fig. 5.2B). We observed a strong accumulation of lagging chromosomes in the anaphase arrested cells for *sen1^{dg}*rrm3Δ, even at 2h, 4h and 6h after the release from G1 arrest.

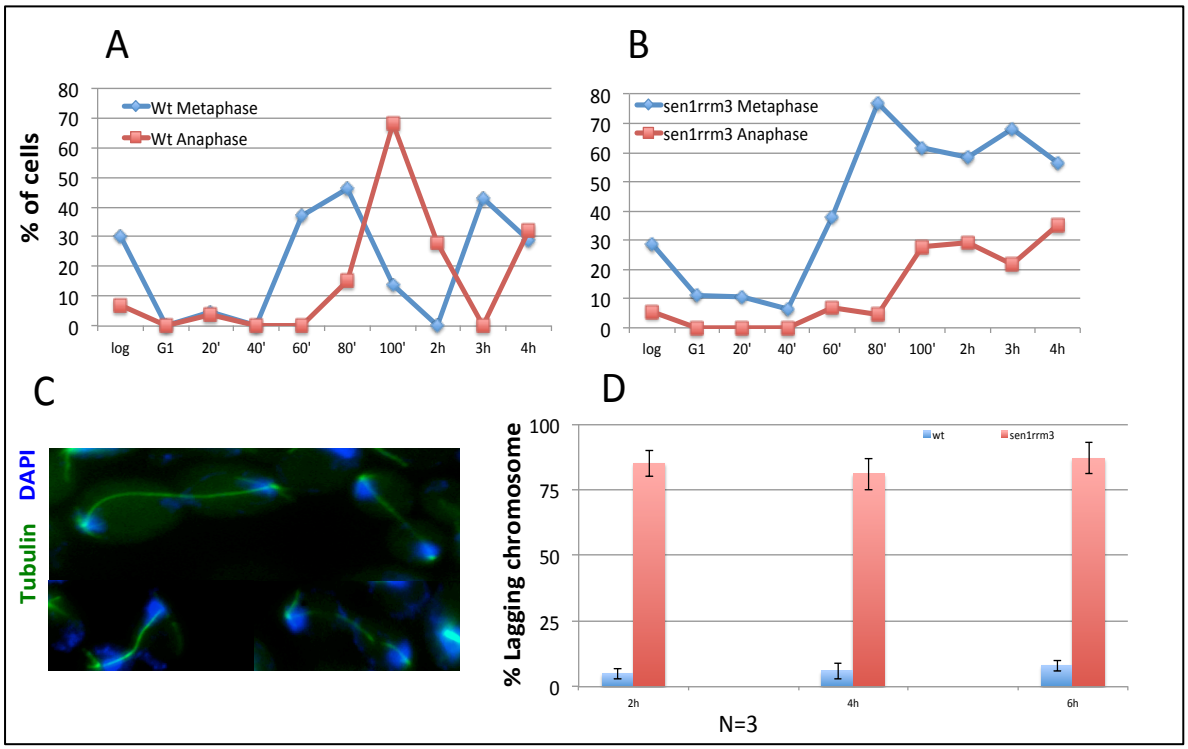


Figure 5.2: Double mutant sen1^{dg}rrm3Δ shows an arrest from metaphase to anaphase transition with lagging chromosomes, mimicking anaphase bridges phenotype.

A) Percentage of metaphase and anaphase cells in Wild type during cell cycle progression. G1 arrested cells are released and samples collected at different time points (x-axis) for FACs and Tubulin staining with DAPI. Metaphase and anaphase cells were counted manually and plotted as percentage of total cells (y-axis).

B) Percentage of metaphase and anaphase cells in double mutant sen1^{dg}rrm3Δ strain.

C) Representative image of tubulin (green) and DAPI (blue) staining of the 4hr double mutant sen1^{dg}rrm3Δ strain.

D) Percentage of anaphase cells carrying lagging chromosome in sen1^{dg}rrm3Δ strains at indicated time points.

5.3 sen1^{dg}rrm3Δ do not alter replication initiation at ARSs.

We synchronized cells in G1 with alpha factor in YPGlu medium to deplete Sen1 and released cells in the S-phase. We used 2D gels to assess any defect in origin firing and unusual structural formation at ARS, which might lead to a defective segregation phenotype. Wild type, *sen1^{dg}*, *rrm3* and *sen1^{dg}rrm3Δ* are arrested in G1 and released in S-phase. Samples were collected at 2h, 4h and 6h for FACs (Fig.5.3A) and PFGE assay. We used ARS305 specific probes for southern blot analysis. Any abnormal fork transition along ARS305 might lead to higher retention in wells and accumulate more breaks below the ChrIII band marked in Figure 5.3B. We did not observe any difference in structure accumulation in double mutant compared to wild type and single mutants (Fig. 5.3B).

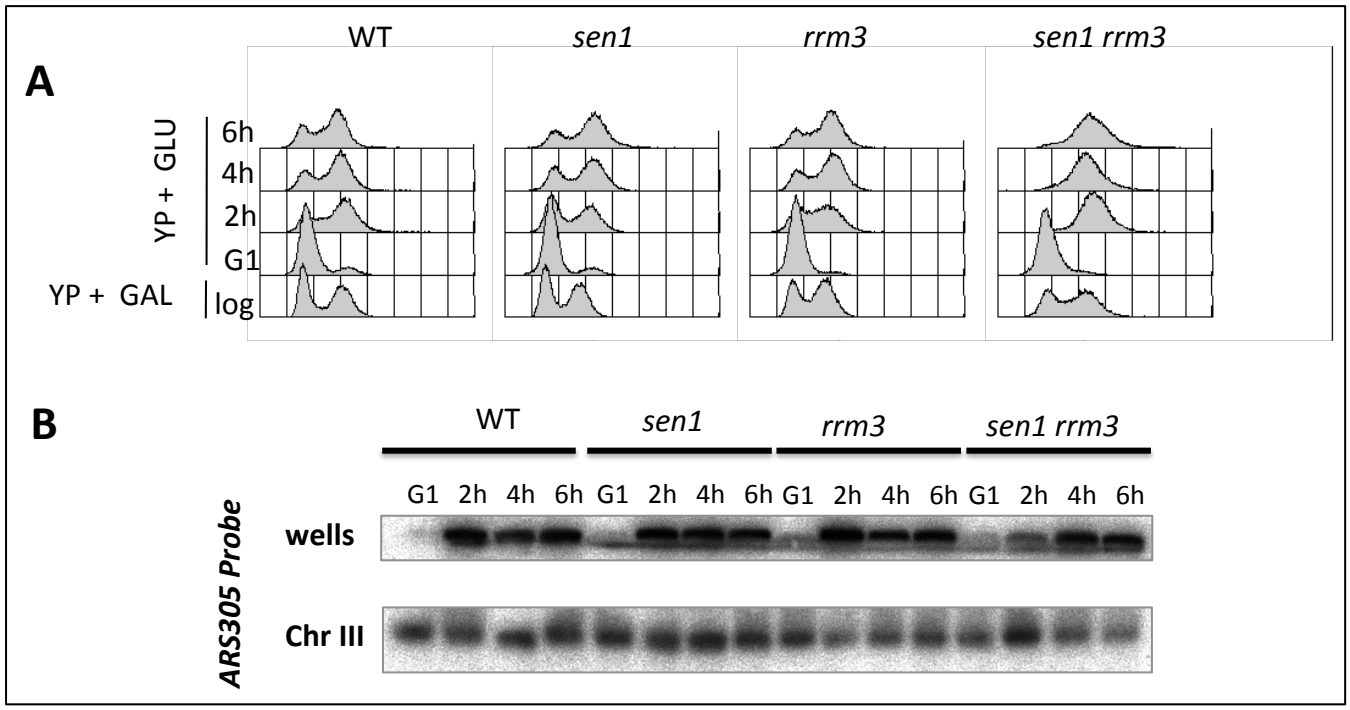


Figure5.3: No aberrant replication intermediates accumulation at ARS during gross chromosomal replication in sen1^{dg}rrm3Δ.

A) FACs profile for the PFGE experiment. After G1 arrest with alpha factor, different strains are released in YPGlu and samples are collected at 2h, 4h and 6h along with Log and G1 phase. Samples processed for PI staining followed cell cycle progression with FACs.

B) PFGE plugs run 24 hrs and southern blot to capture replication intermediates with ARS302 specific probes. Cropped part of full PFGE represented showing region of interest, wells where chromosomes are accumulated because of higher molecular structure and intact chromosome migrated as individual band marked as ChrIII.

5.4 Double mutant *sen1^{dg}rrm3Δ* strains accumulate unresolved replication termination intermediates

Double mutants sen1^{dg}rrm3Δ showed metaphase and anaphase arrest. Late replicating regions including fragile sites (NCPs, RFBs) and TERs might be the most affected loci. We looked at chrIII TER302 in *EagI* fragment after digestion of PFGE plugs. Wild type and sen1^{dg}rrm3 were both arrested in G1 YPGal and released in S-phase in YPGlu, and then samples were collected for PFGE and FACS profile. The double mutant compared to wild type showed more G2/M arrests in FACs profiles (Fig.5.4A) and a large amount of unresolved replication intermediates causing an accumulation of TER302 in the wells (Fig.5.4B). In both strains EagI fragments were intact, as there is no smear below the EagI fragments.

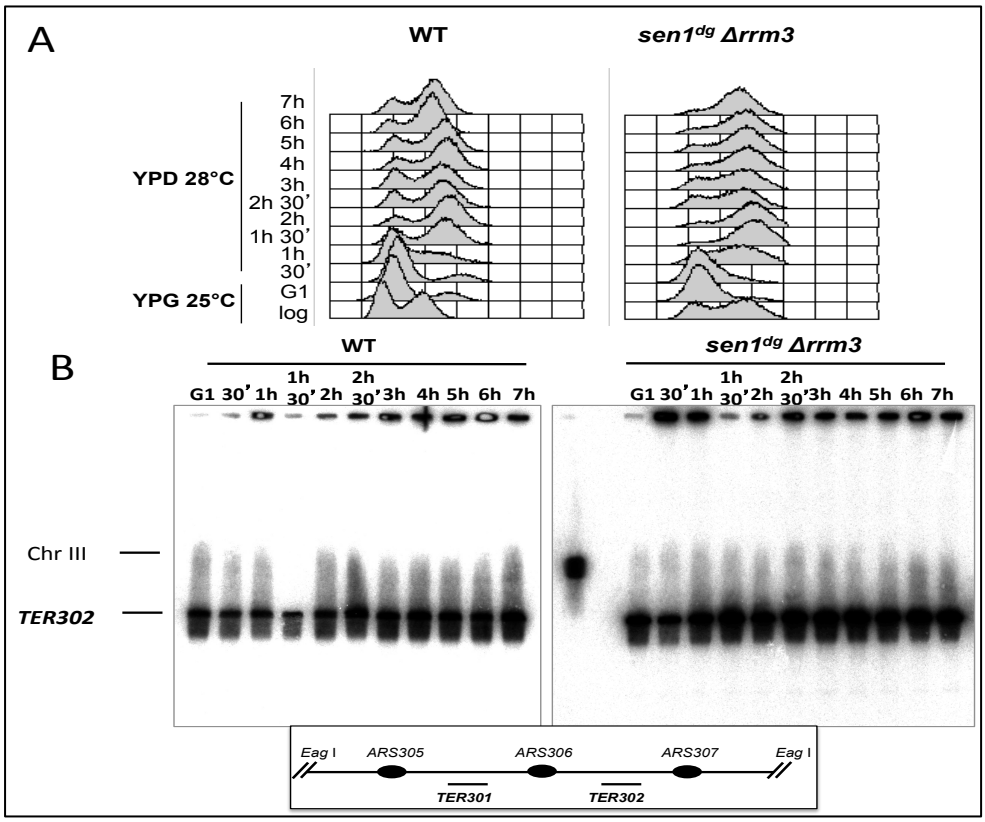


Figure 5.4: Double mutant sen1^{dg}rrm3Δ strains accumulate replication termination intermediates during physiological cell cycle.

A) Cell cycle progression after arrest in G1 with alpha factor and released in YPGlu medium. Samples were collected at the indicated time points for FACs and for PFGE analysis.

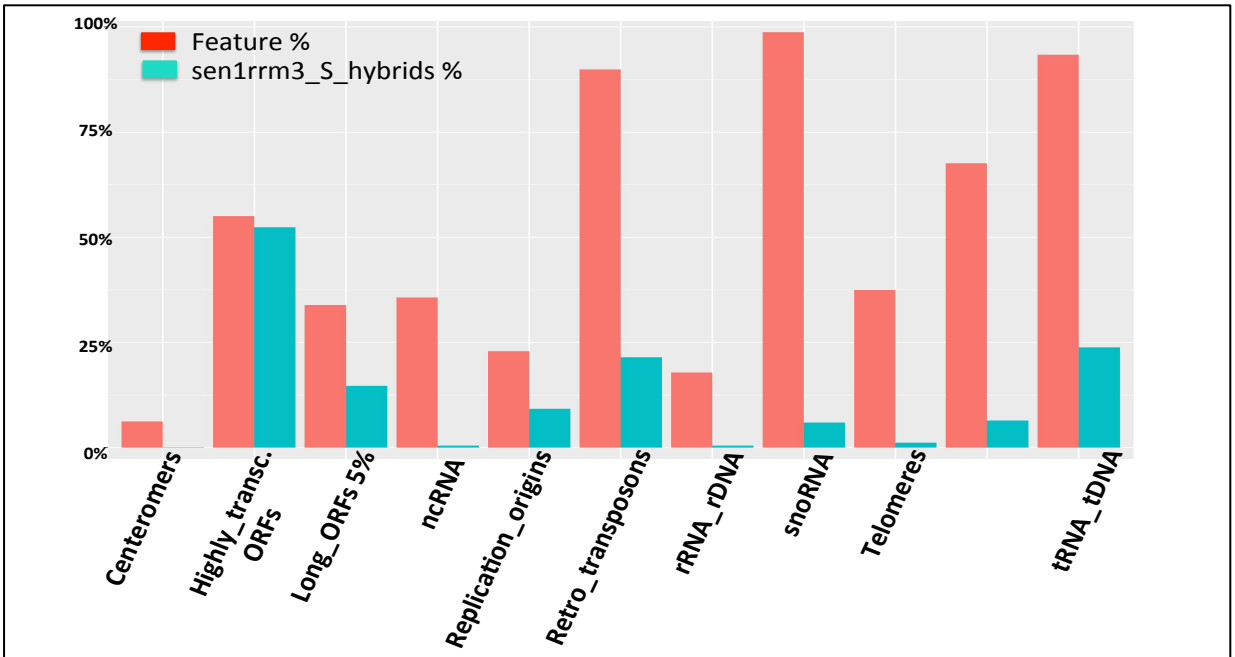
B) PFGE analysis at different time points for WT and *sen1^{dg}Δrrm3* of replication intermediates at TER302 on chrIII, after plugs were digested with Eag1 enzyme. EagI fragment hybridized using radiolabeled probe for TER302 within 110Kb long fragments. At the bottom, represented Eag1 fragment carrying 3 ARSs (305,306,307) which flank TER301 and TER302.

5.5 *sen1^{dg}rrm3Δ* mutants accumulate RNA-DNA hybrids at different chromosomal pausing sites, RFBs and TERs.

We speculated based on the binding pattern of Rrm3 and Sen1 along all transcriptionally active pausing elements, that the double mutant *sen1^{dg}rrm3Δ* helicase might be unable to suppress RNA-DNA hybrids accumulations.

Therefore we measured R-loop accumulations in *sen1^{dg}rrm3Δ* cells in S-phase using DRIP-Chip. We score for R-loop peaks (1006) along 11 genomic features and by the association significance. As replication origins have no transcriptional activity, no R-loop accumulation was found in *sen1^{dg}rrm3Δ* (Fig.5.5A, B). We observed that long ORFs (top 5%) did not accumulate RNA-DNA hybrids although these ORFs are transcriptionally active. We observed the same for rDNA and Telomeres. On contrary, highly transcribed

ORFs (629/1143) showed significant RNA-DNA hybrids accumulation in *sen1^{dg}rrm3Δ*. Centromeres show no significant association with R-loop accumulation (1/16). TERs showed a significant accumulation of R-loops (48/71) in *sen1^{dg}rrm3Δ*, which might cause enhanced fork pausing and lead to fork remodeling and under-replicated genomic regions. snoRNA (RNAP III), retro-transposons (RNAPII) and tRNAs (RNAP III) loci showed a strong correlation with RNA-DNA hybrids accumulation in *sen1^{dg}rrm3Δ* (Fig5.5A,B). This reflects a functional association of Sen1 and Rrm3 around different loci affecting transcriptional products during RNAP and DNAP collision. A perturbation of this function creates more RNA-DNA hybrid obstacles causing defective replication fork stalling in *sen1^{dg}rrm3Δ*. In the following part of the study, we will focus on TERs considering natural pausing elements lead to polar fork pausing.



Type	Test	hybrids Total	Total Features	hybrids Overlap	Feature Overlap	P-value
rRNA	sen1rrm3_S_hybrids	1006	28	5	5	0.93205
Telomere	sen1rrm3_S_hybrids	1006	32	12	12	0.97744
snoRNA	sen1rrm3_S_hybrids	1006	81	60	80	4,40E-55
Termination	sen1rrm3_S_hybrids	1006	71	65	48	2,68E-05
Reterotransposon	sen1rrm3_S_hybrids	1006	486	216	437	0
HighTranscribingORF	sen1rrm3_S_hybrids	1006	1143	527	629	3,15E-164
tRNA	sen1rrm3_S_hybrids	1006	395	240	369	5,04E-268
Centromere	sen1rrm3_S_hybrids	1006	16	1	1	0.94852
ncRNA	sen1rrm3_S_hybrids	1006	14	5	5	0.20989
LongORF_fivepercent	sen1rrm3_S_hybrids	1006	336	148	114	1
ReplicationOrigin	sen1rrm3_S_hybrids	1006	410	93	94	0.11937

Figure 5.5. R-loop accumulation at TERs and different natural chromosomal pausing sites in *sen1^{dg}rrm3Δ* during S-phase.

A) Meta-analysis of DRIP-Chip data for R-loop accumulation in sen1^{dg}rrm3Δ. DRIP-Chip (S9.6) experiment is performed on S-phase at 40-minute time point. RNA-DNA hybrid association with different genomic loci scores for significant clusters for R-loop peaks. The 11 loci are shown on X-axis and include rDNA loci, Telomeres and Replication termination zones, and highly transcribing regions.
B) The same data in tabular form. snoRNA, TERs, highly transcribing genes and tRNAs genomic loci accumulate significant R-loops in sen1^{dg}rrm3Δ.

5.6 DRIP-pPCR captures transient RNA-DNA hybrids accumulation at TERs during S-phase in absence of Sen1p and Rrm3p

Further we wanted to understand the dynamic nature of RNA-DNA hybrids accumulation in *sen1^{dg}rrm3Δ*.

We employ DRIP-qPCR to quantify R-loop accumulation along different 7 TERs carrying different kind of pausing elements as summarized in Fig.5.6B. Wild type and *sen1^{dg}rrm3Δ* strains were released in YPGlu and collected at different time points (Fig.5.5A). Quantitative DRIP-qPCR showed a strong accumulation of R-loops at different TERs including TER802 (RNA pol II), TER303 (RNA pol III), TER704 (CEN) and TER1204 (RNA pol II) (Fig.5.6C). This R-loop accumulation is transient and might be resolved later in the G2/M phase by unknown mechanisms. A transient accumulation of R-loops might lead to a perturbed fork conversion at TERs and cause fork remodeling because of topology stress in *sen1^{dg}rrm3Δ*.

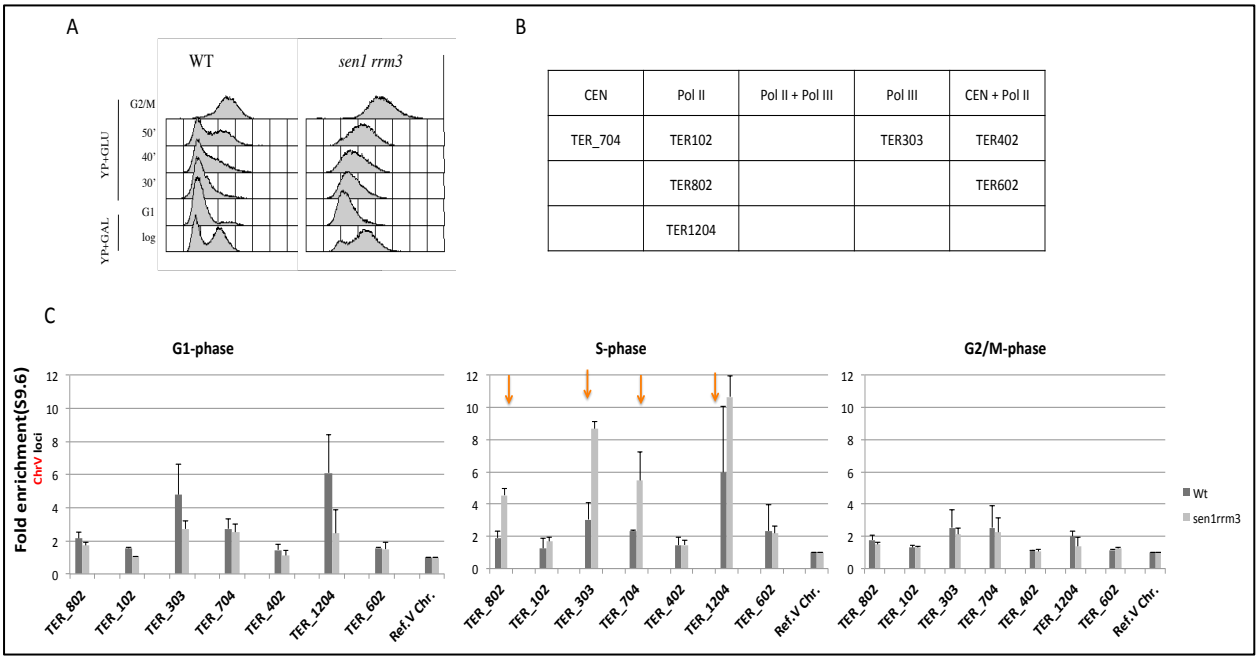


Figure 5.6: DRIP-pPCR captures transient R-loop accumulations at TERs during the S-phase in absence of Sen1p and Rrm3p.
A) FACs profile of Wild type and sen1rrm3 used for DRIP-qPCR experiments. Log cells are grown in YPGal and arrested in G1 with alpha factor. They are further released in YPGlu with Nocodazole and collected at 30', 40', 50' along with G1 and G2/M. 200ml culture from each time point subjected to genomic DNA purification without RNAs treatment.

B) The list of all 7 TERs, along with different associated features. The TERs are subjected to quantify R-loop accumulation with qPCR.
C) R-loop accumulation during G1, S phase (40') and G2/M in Wild type and sen1^{dg}rrm3Δ for all selected 7 TERs overlap with different kind of pausing elements.

5.7 Common interactors between Sen1 and Rrm3 helicase indicates different pathways might be involved in replication fork metabolism at TERs

We looked for common genetic interactors between Sen1 and Rrm3. Deletion of these gene can affect the viability of both individual strains Δrrm3 and sen1^{dg} as synthetic lethal interaction. We observed different mutants being involved in replication fork metabolism that appeared as common interactors.

1. Sgs1-Top3p-Rmi1p complex. STR complex proteins are involved in DNA catenation/de-catenation, template switch and HR, cohesion establishment during S-phase (by ctf18-RFC complex and Mrc1p), they play a role in genomic integrity maintenance, relax single strand negativity supercoiled DNA and regulate mitotic recombination.
2. Replication fork protection complex (Tof1-Mrc1-Csm3) and MMS21, which play a main role at paused and stalled replication forks as replication-pausing checkpoint complex. These proteins are involved in stabilizing helicases and polymerases (DNAP2) at fork and cohesion establishment at stalled forks. This complex mimic mammalian tipin1-timeless-claspin complex, which is an important activity at fork converging regions like TERs.
3. MRX (Mre11-RAD50-Xrs2) complex protein is involved in double strand break repair, meiotic recombination, and telomere maintenance and checkpoint activation.
4. BIR modulators (structure specific nucleases), which includes Mus81p, Mms4p, Srs2p, Rad51 and Rad52. Structure-specific Mms4p-Mus81p endonuclease and cleaves branched DNA, is involved in DNA repair, replication fork stability, joint molecule formation/resolution during meiotic recombination, promotes template switching during break-induced replication (BIR) and causes non-reciprocal translocations (NRTs); helix-hairpin-helix protein; phosphorylation of non-catalytic subunit Mms4p by Cdc28p and Cdcp during mitotic cell cycle activates function of Mms4p-Mus81p.

As speculated, at TERs and natural pausing sites an extensive stalling and topological constrains can remodel fork and might compromise replication fork protection complex activities (Tof1-Mrc1-Csm3). This may lead to double strand DNA breaks, which needed to process by MRX complex to favor HR similar activity to generate D-loop for BIR. Break

Induced Replication (BIR) can be supported by Template-Switch activity (STR complex - Sgs1-Top3p-Rmi1p). The STR complex has the potential to resolve BIR mediated crossovers and the process needs cohesion to keep the sister chromatids in close proximity. We speculated a close coordination between these process and fork conversion during replication termination.

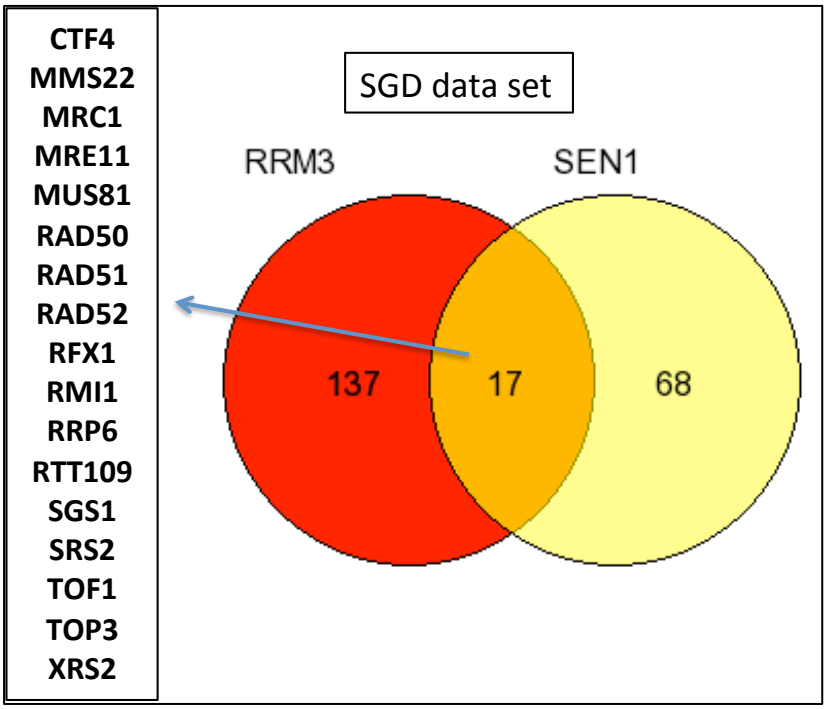


Figure 5.7: Common interactors between Sen1 and Rrm3 helicases indicated that different pathways are involved in the replication fork metabolism.
We used interactome data from SGD and bioGRID database for Sen1 and Rrm3 and scored common interactors. Categories analysis indicated STR complex, MRX complex, replication fork protection complex and BIR pathway along cohesion establishment.

5.8 Origin firing is not affected in *sen1^{dg}rrm3Δ* strain under replication stress

We synchronized Wild type and sen1^{dg}rrm3Δ in G1 released in S-phase in presence of 100mM HU. We collected samples at the indicated time points and subjected for detection of replication intermediates at ARS302 using 2D gel method employed in lab (Materials and Methods). We did not see any aberrant RI structure at ARS305 in absence of sen1^{dg}rrm3Δ and the 2D pattern appears to be comparable to wild type (Fig.5.8B, C)

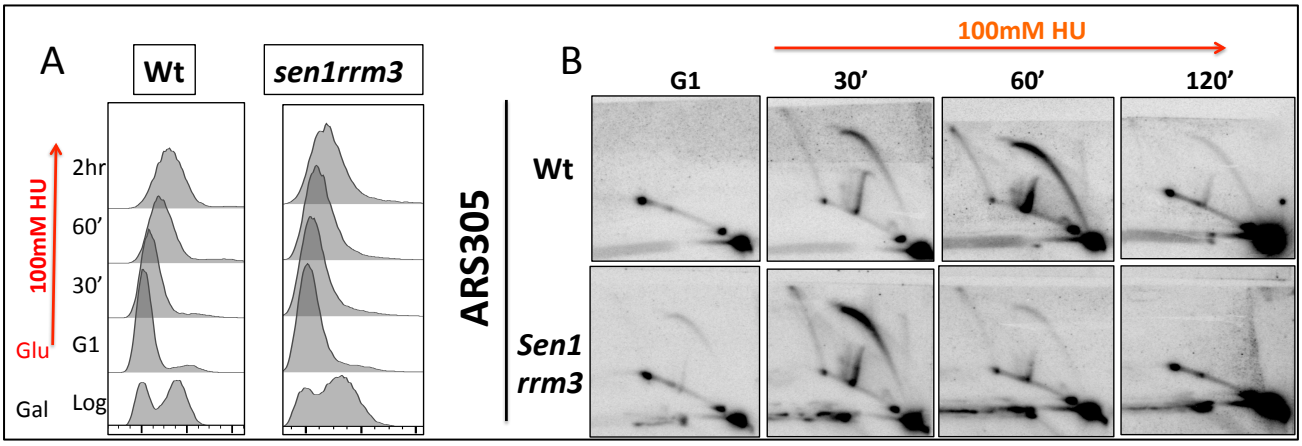


Figure 5.8: Origin firing at ARS305 was not impaired in absence of sen1^{dg}rrm3Δ under replication stress.

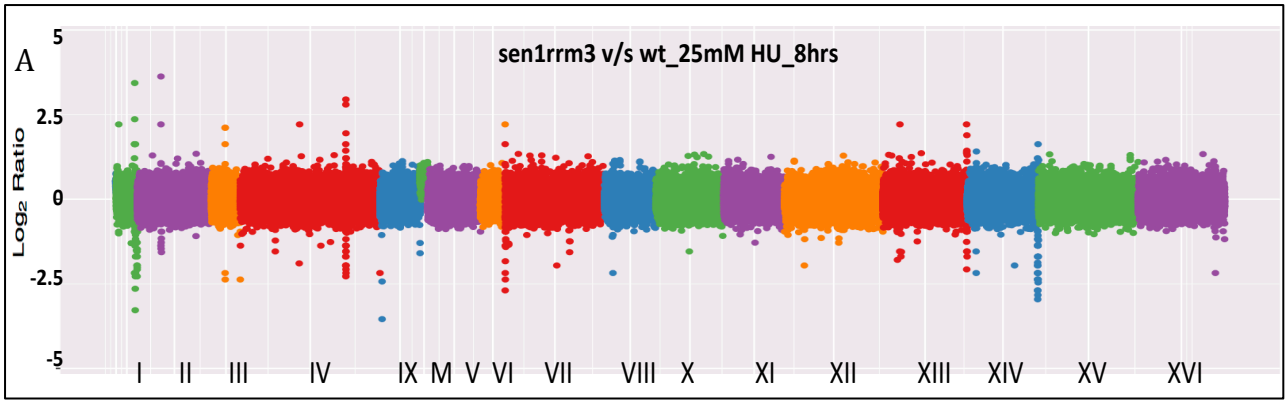
A) FACs profile of the Wild type and sen1^{dg}rrm3Δ. Cells are arrested in G1 and released in S-phase with 100mM HU. Along with G1, samples were collected at different time points for cell cycle progression and 2D gel analysis.

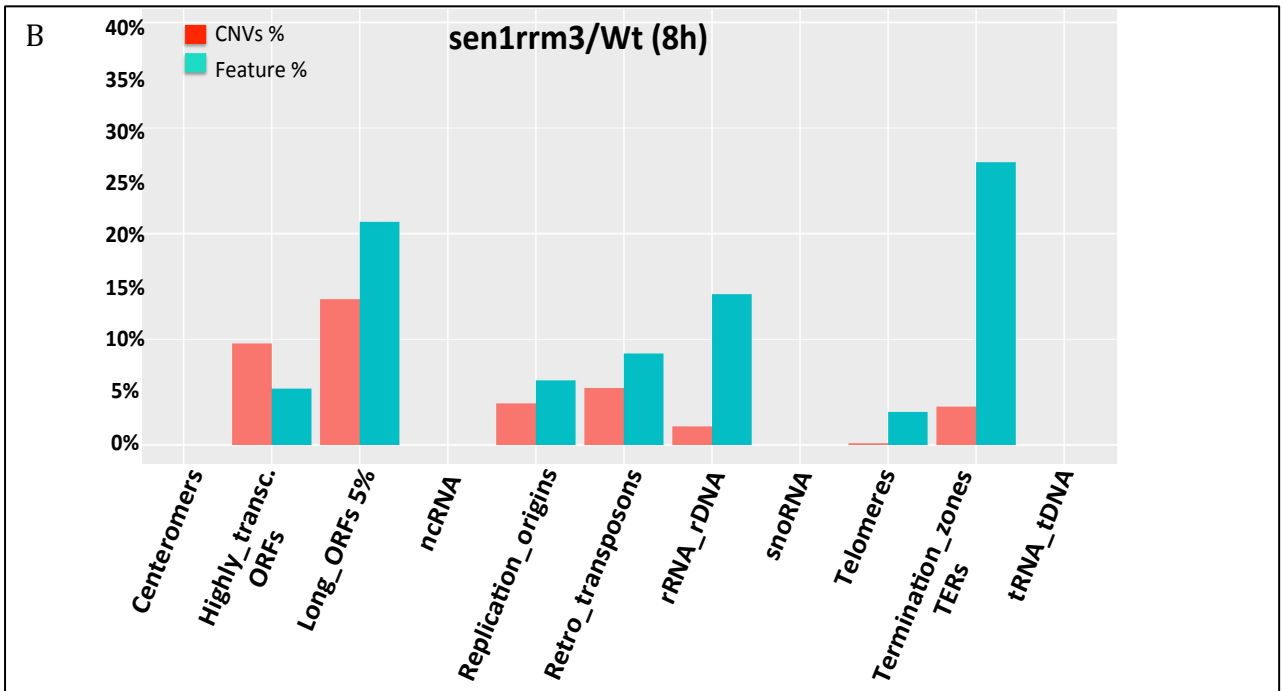
B) Psorolen crosslinked (in-vivo), genomic DNA was purified and 10ug digested with EcoRI and subjected for 2D gel analysis. We used a probe against ARS305 and scored for replication intermediates between 1N and 2N genomic DNA spots, which is the signature of the replication fork bubble migration during S-phase progression.

5.9 sen1^{dg}rrm3Δ mutants accumulate copy number variations

We scored for CNVs based on whole genome sequencing of wild type and sen1^{dg}rrm3, at 8hrs with 25mM HU and arrested in G2/M with Nocodazole. Interestingly, TERs, rDNA loci and long ORFs accumulate a significant number of CNVs.

Whole genome sequencing reads from NGS of sen1^{dg}rrm3Δ compared with the wild type, represented along all 16 chromosomes show different genomic regions with deletion and amplification (Fig.5.9A). Replication termination zones accumulate significant CNVs, which might correlate with R-loop accumulation and the under-replicated nature of TERs. Fig. 5.9B shows the genome wide distribution of CNVs in *sen1^{dg}rrm3Δ* strain along 11 features, which cover most of the RFBs sites and repeated regions in the genome. The y-axis shows the percentage of the total number of CNVs (688) that overlap with the given features (as red bars). The percentage of the features marked by CNVs is shown in green for *sen1^{dg}rrm3*. Total CNVs categories like deletion and amplification, and overlap with different genomic features assess for signification p <0.05. TERs (19/71) major genomic deletion with p=0.235) and rDNA loci (4/28) major genomic deletion with p=1.72E-34) showed significant correlation with CNVs distribution.





Type	Ref	Test	Total CNV	Total Deletion	Total Amplification	Total Features	CNV Overlap	Deletion Overlap	Amplification Overlap	Feature Overlap	P-value
Centromere	wt_8h	sen1rrm3_8h	688	624	64	16	0	0	0	0	1
HighTranscribingORF	wt_8h	sen1rrm3_8h	688	624	64	1143	66	63	3	61	0.99406
LongORF_fivepercent	wt_8h	sen1rrm3_8h	688	624	64	336	95	72	23	71	0.47961
ncRNA	wt_8h	sen1rrm3_8h	688	624	64	14	0	0	0	0	1
ReplicationOrigin	wt_8h	sen1rrm3_8h	688	624	64	410	27	26	1	25	0.00035881
Reterotransposon	wt_8h	sen1rrm3_8h	688	624	64	486	37	18	19	42	9,11E-01
rRNA	wt_8h	sen1rrm3_8h	688	624	64	28	12	12	0	4	1,72E-34
snoRNA	wt_8h	sen1rrm3_8h	688	624	64	81	0	0	0	0	1
Telomere	wt_8h	sen1rrm3_8h	688	624	64	32	1	0	1	1	0.99993
Termination	wt_8h	sen1rrm3_8h	688	624	64	71	25	21	4	19	0.23515
tRNA	wt_8h	sen1rrm3_8h	688	624	64	395	0	0	0	0	1

Figure **5.9: Mapping genome wide CNVs under mild replication stress in sen1^{dg}rrm3Δ.**
A) Whole Genome sequencing (NGS) of sen1^{dg}rrm3Δ compared with Wild type, represented along all 16 chromosomes. The y-axis shows the log ratio of the reads compared with sen1^{dg}rrm3Δ. The x-axis represent different chromosomes covering different width depending of their size. The 5 different colors represent different chromosomes but different chromosomes can share the same colors (To avoid any confusion, there is no translocation and conversions as gross chromosomal rearrangements represented here).
B) Genome wide distribution of CNVs after 8h in 25mM HU for sen1^{dg}rrm3Δ. The x-axis shows 11 features that cover most of the RFBs sites and repeated region in the genome. The y-axis shows the percentage of the total CNVs (688) overlapping with the given feature as red bar. The percentage of the features marked by CNVs are show as green bars in sen1^{dg}rrm3Δ.

C) Tabular representation of all CNVs in sen1^{dg}rrm3Δ_8h_25mMHU, distributed along different genomic features. Total CNVs as deletion and amplification, and overlap with different genomic features p value <0.05.

5.10 Mild replication stress accumulates DSBs at TERs in sen1^{dg}rrm3Δ during the S-phase

To explore the cause of genomic fragility at TERs in *sen1^{dg}rrm3Δ*, we looked at breaks in a cell cycle dependent manner. We arrested wild type and *sen1^{dg} rrm3Δ* in G1 and released in YPGlu in absence or presence of 25mM HU with nocodazole to arrest in G2/M. Then cells were released from nocodazole arrest and followed as indicated in FACs profile Fig.5.10A.

We checked gross chromosomal integrity using PFGE and EtBr staining (Fig.5.10C), which showed a different pattern of chromosomal segregation depending on the cell cycle stage. During S-phase replication mediated chromosomal entanglement is present in wild type and *sen1^{dg}rrm3Δ* in presence of 25mM HU. Interestingly, during S-phase progression in mild replication stress, causes breaks at TER302 (Fig.5.10B). Earlier we observed an accumulation of unusual replication intermediates, which causes retention of TERs in wells under-physiological condition and leads to G2/M arrest. Here the mild replication stress decreases the accumulation of slow migrating replication intermediates that accumulate in wells, as consequences of breaks at TERs, ChrIII is well resolved with DSBs accumulation.

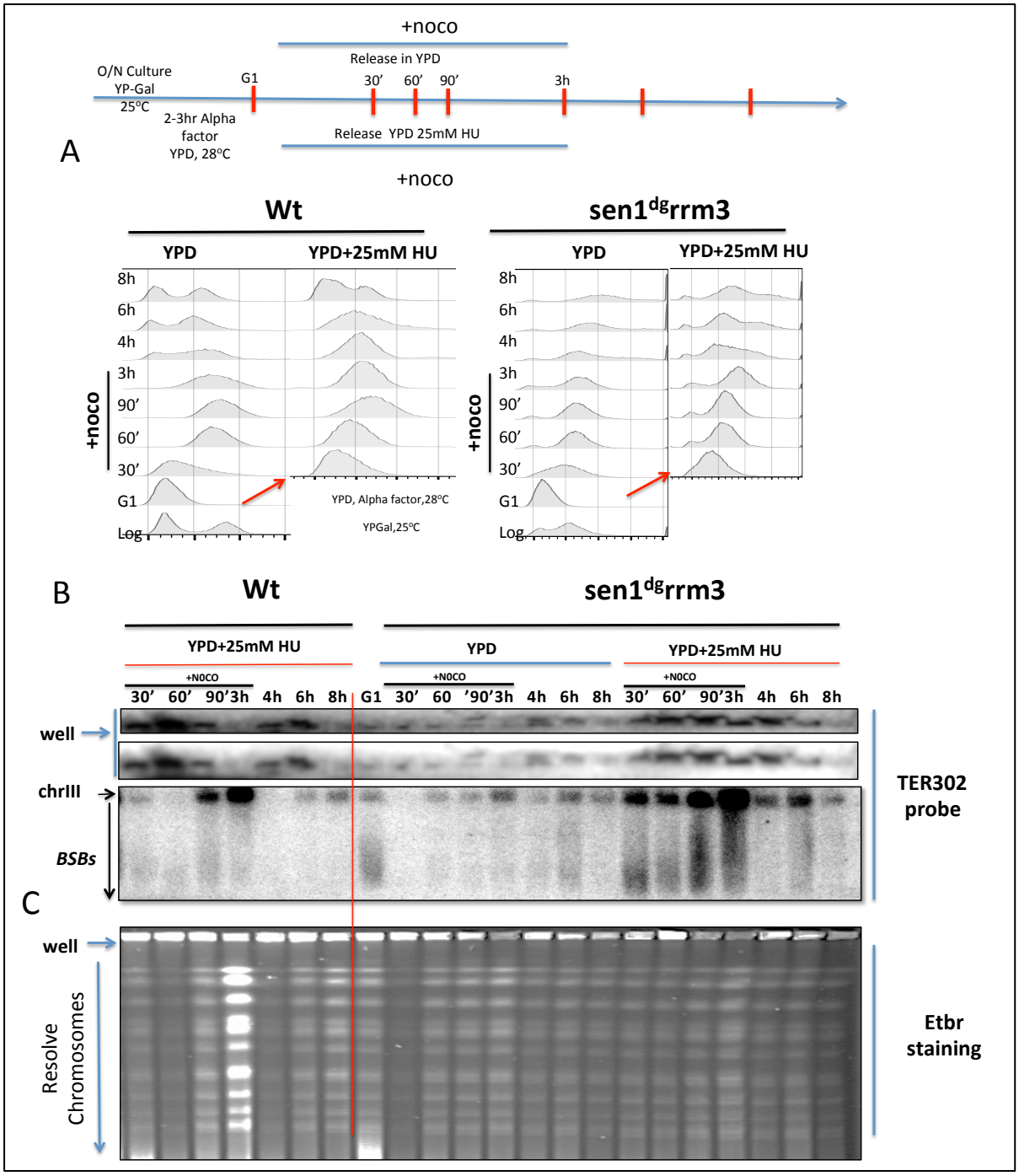


Figure 5.10: Mild replication stress accumulates DSBs at TERs in sen1^{dg}rrm3Δ during S-phase of cell cycle.
A) FACs analysis of Wild type and sen1^{dg}rrm3Δ. Different strains grown in YPGlu+25mM. Samples were collected at different time intervals as indicated for FACs and PFGE.
B) Replication intermediates and fragility (DNA breaks) detected at TER302 using specific probes. ChrIII and DSBs marked along with wells showing retention of Chromosome III because of replication intermediate formation at TERs and massive breaks during S-phase progression under mild replication stress.
C) EtBr staining of PFGE gel to assess gross chromosomal integrity. PFGE plugs prepared at different time points after Log cells grown in YPGal, were shifted to YPGlu+25mM HU.

5.11 Characterization of replication intermediates in *sen1^{dg}rrm3Δ* by EM.

We wanted to explore potential unusual replication intermediates in *sen1^{dg}rrm3Δ* compare to wild type during the cell cycle progression, which might lead to G2/M arrest and under-replicated DNA at TERs. We used single molecule analysis approach on replication intermediates using TEM (Transmission electron microscopy)(Neelsen & Lopes, 2015; Neelsen, Zanini, Herrador, & Lopes, 2013; Ray Chaudhuri et al., 2012).
We used *in vivo* psoralen cross linking, alkyldimethylbenzylammonium chloride (BAC) spreading of purified naked genomic DNA, platinum rotatory shadowing and transmission electron microscopy (TEM) to analyse the fine ultrastructure of DNA replication intermediates (RIs) generated after a single S-phase without Rrm3 and Sen1. To maximize the concentration of RIs per genome cell cultures of the wild type and *sen1^{dg}* strains were pre-synchronized in Nocodazole and released in the presence of alpha factor. Sen1 shut off was induced during the release from G2 into G1-phase when galactose in the medium was substituted by glucose. Wild type and *sen1^{dg}* cells where released into S-phase at 20°C-23°C and RIs were analysed by TEM at 45' minutes from the G1 release, a condition that was previously reported to be suitable for the study of DNA replication termination intermediates (TERs)(Fachinetti et al., 2010). The synchrony of the cells was controlled by FACS analysis and complete degradation of Sen1 was checked by western blot (data not shown). We found that 80% of RIs isolated in wild type cells were normal DNA replication forks with absent of very short stretches of ssDNA (>200 nts) at the fork branching points, 4% were TERs characterized by a double Y structure with absence of ssDNA at the two branching points of the TER molecule, 2% were reversed forks and 6% were hemicatenanes, which are specific types of X-molecules not stabilized by homologous pairings and characterized by the presence of four branches of different dimension (Figure 3A). Sen1 ablation led to a drop in the percentage of normal forks to 60% and to an increase in the percentage of TERs (16%), reversed forks (4%) and hemi-catenanes (12%). Importantly on top of 45 TERs analysed in *rrm3 sen1* cells 10 molecules showed extended stretches of ssDNA (>300 nts) very close to the fork fusion point of the molecule. These TERs molecules with extended regions of ssDNA at the fork fusion point were not present in the wild type cells.

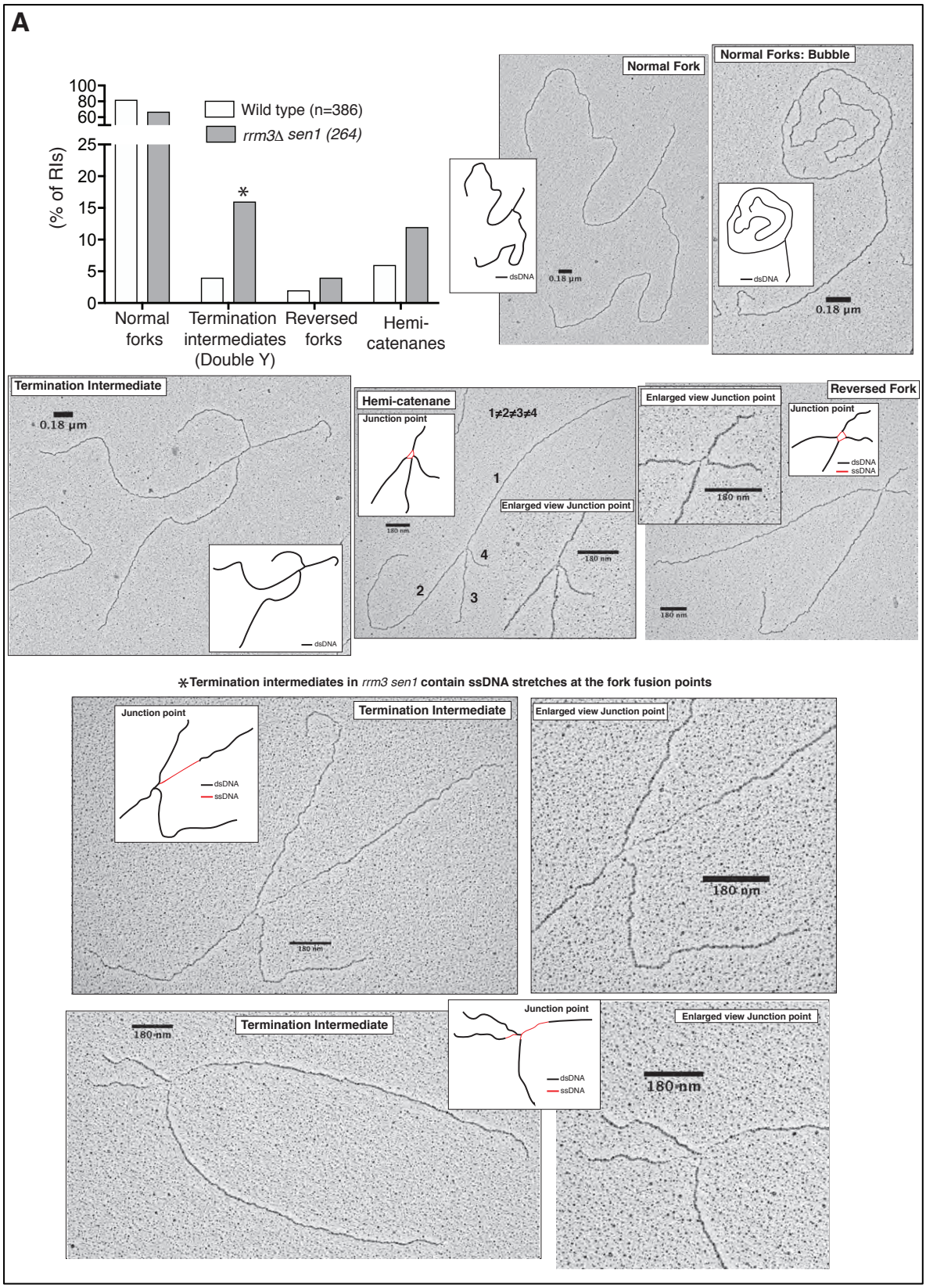


Figure 5.11. sen1 rrm3 cells accumulate TERs with long ssDNA regions at the fork fusion point. **A)** Chart showing the percentages of RIs identified at 45' minutes from the G1 release into S-phase in wild type and *sen1^{dg}rrm3* cells. In wild type (n=386) and *sen1^{dg}rrm3* (n=264) numbers of molecules analysed in two independent experiments. Representative TEM pictures of each category of RIs analysed. An enlarged view of the junction point and a schematic

representation of the molecule is reported with ssDNA in red and dsDNA in black. A scale bar of 180 nm (corresponding to 500 bp) is reported for each picture. For the hemicatenane the four branches of the X-molecule that have different dimensions are numbered

5.12 Depletion of Condensin complex subunits Ycg1p and Ycs4p rescues cell cycle arrest of sen1^{dg} rrm3Δ

We speculate, that in double mutant sen1^{dg}rrm3Δ the high amount of topological constrains at different natural pausing sites (including TERs), might lead to chromatin binding of Top2p and Condensin complex. The accumulation of R-loops can cause loading of Condensin by H3S10 phosphorylation. As shown in Chapter 2, transcriptional activity might load Condensin complex, which can be very dynamic, depending on the cell cycle stage and HU mediated replication stress. To check this, we depleted Condensin subunits using Gal to Glu degron system (Chapter 2) in double mutant sen1^{dg}rrm3Δ. All strains were arrested in G1 and released in S-phase and followed by a FACs for 10hrs.

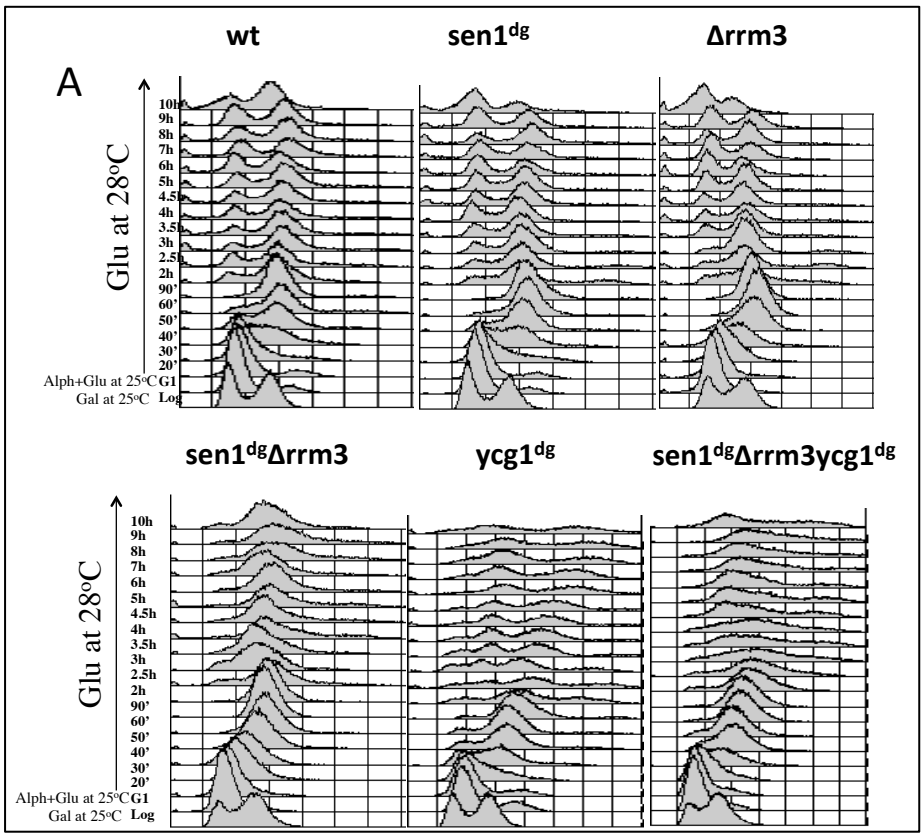


Figure 5.12: Depletion of Condensin complex subunits Ycg1p and Ycs4p rescues physiological cell cycle arrest of sen1^{dg}rrm3Δ.

Different strains are grown over night at 25°C in YPGal and arrested at G1 phase using alpha factors in YPGlu medium. Arrested cells are washed with YPGlu medium and released in the S-phase at 28°C. Samples are collected for assessing cell cycle progression from 20' onwards till 10hrs at different time points. We compared the cell cycle progression of sen1^{dg}rrm3Δ double mutant with the single genotypes sen1^{dg} and rrm3Δ along with the Wild type and triple combination sen1^{dg}rrm3Δycg1^{dg} or sen1^{dg}rrm3Δycs4^{dg}. (sen1^{dg} ,ycg1^{dg} and ycs4^{dg} were depleted using GAL to GLU degron system)

As mentioned before, the FACS profile of sen1^{dg} and rrm3Δ is identical to the Wild type. Double mutant sen1^{dg}rrm3Δ and ycg1^{dg} showed G2/M arrest and uneven segregations of chromosomes, respectively. Interestingly, the depletion of Ycg1p in the double mutant rescued G2/M arrest (Fig 5.12). We concluded that double mutant sen1^{dg}rrm3Δ causes premature condensation at TERs and impairment of fork fusion at TERs.

5.13 Depletion of Condensins subunit Ycg1p or Ycs4p rescues G2/M arrest and resolves unusual replication intermediates at TERs in sen1^{dg}rrm3Δ

We checked unresolved replication intermediates accumulation in triple mutants assuming that the depletion of Condensine resolves unusual structures at TERs in sen1^{dg}rrm3Δ, which tend to accumulate in the wells (Fig.5.13B). Double mutant sen1^{dg}rrm3Δ showed under-replicated TERs and accumulation of R-loops, which might cause the attachment of the sister DNA strands and lead to lagging chromosomes in the anaphase. Late replicating regions, including fragile sites (NCPs, RFBs) and TERs, might be the most affected loci. We looked at TER302 in *EagI* fragment after digestion of PFGE plugs. Wild type, sen1^{dg}rrm3Δ along with ycg1^{dg}, triple mutant sen1^{dg}rrm3Δycg1^{dg} and sen1^{dg}rrm3Δycs4^{dg} were arrested in G1 YPGlu and released in S-phase in YPGlu, collecting samples for PFGE and FACs profile (Fig.5.13A). Double mutant sen1^{dg}rrm3Δ compared to wild type showed a huge amount of unusual replication intermediates causing the accumulation of TER302 in wells over the course of 6hrs (Fig.5.13C).

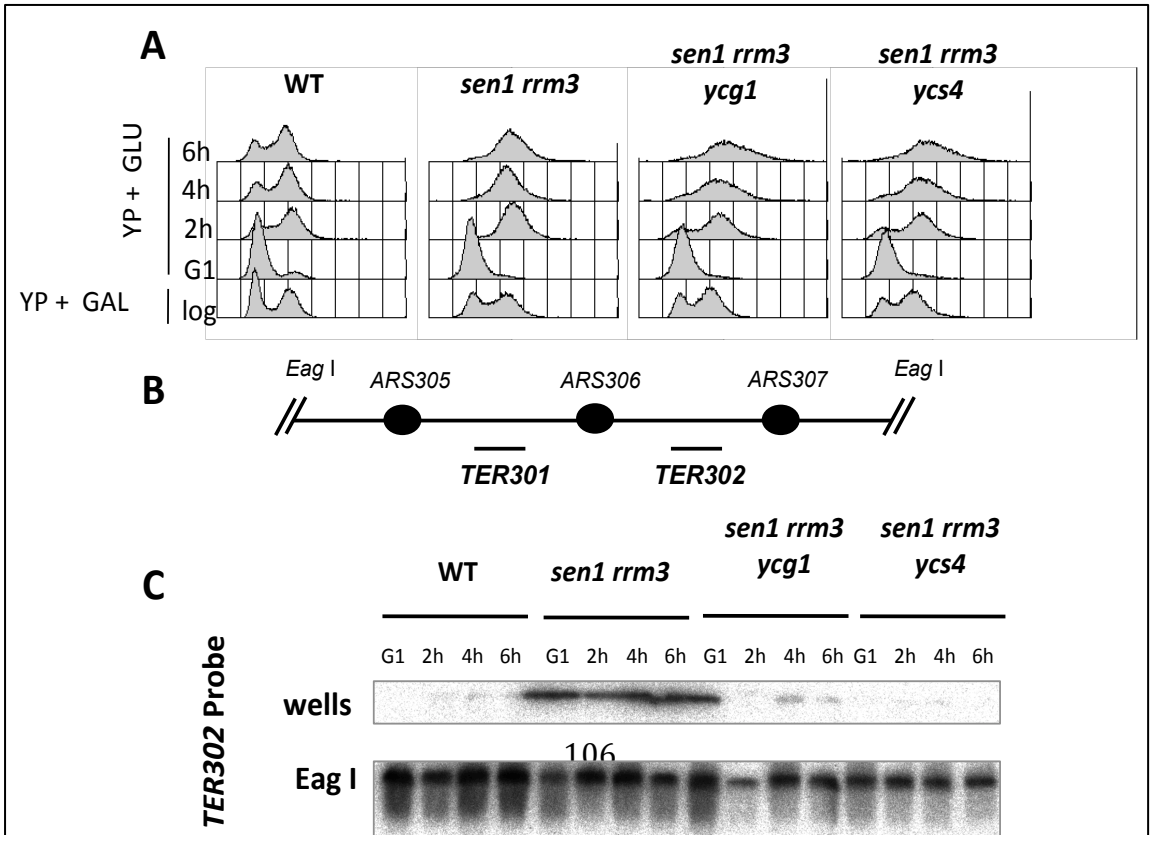


Figure 5.13: Condensin subunits Ycg1p and Ycs4p caused accumulation of aberrant replication intermediates at TERs in sen1^{dg}rrm3Δ.
A) FACs profile for Wild type and sen1^{dg}rrm3Δ with triple mutant sen1^{dg}rrm3Δycg1^{dg}/sen1^{dg}rrm3Δycs4^{dg}. Log cells in YPGal arrested at G1 with alpha factor for 3hrs and released in YPGlu medium. Different time points at 2h, 4h and 6h were taken for FACs and PFGE experiments.
B) Representation of the 110kb long fragment from Chr III after digestion with Eag1. This region contains 3 ARS (305, 306 and 307) and 2 TERs (301 and 302). We are using a probe specific to TER302 to determine the accumulation of replication intermediates in the EagI fragment.
C) PFGE experiment in different strains at different time points G1, 2h, 4h, and 6h. TER302 specific probes are used to detect replication intermediates in EagI fragment. Compared to wild type, sen1^{dg}rrm3Δ accumulates slow moving structures accumulated in wells, reduced on depleting Ycg1 or Ycs4 in double mutant.

In all the strains the *EagI* fragment maintained its integrity, as there is no detectable smear below the EagI fragment (Fig.5.13C). Both subunits of the Condensin complex in combination with double mutant *sen1^{dg}rrm3Δycg1^{dg}* or *sen1^{dg}rrm3Δycs4^{dg}* showed a rescue of the entangked intermediates at TERs. We concluded, that a premature loading of Condensin during S-phase progression causes G2/M arrest in double mutants. This event might also cause premature condensation and entanglement of partially replicated structures.,

5.14 Absence of Condensins suppresses R-loop accumulation at TERs in sen1^{dg}rrm3Δ

We decided to look at the fate of RNA transcripts in the triple mutant (*sen1^{dg}rrm3Δycg1^{dg}*) along with the double mutant strain in proliferating cells under physiological condition.

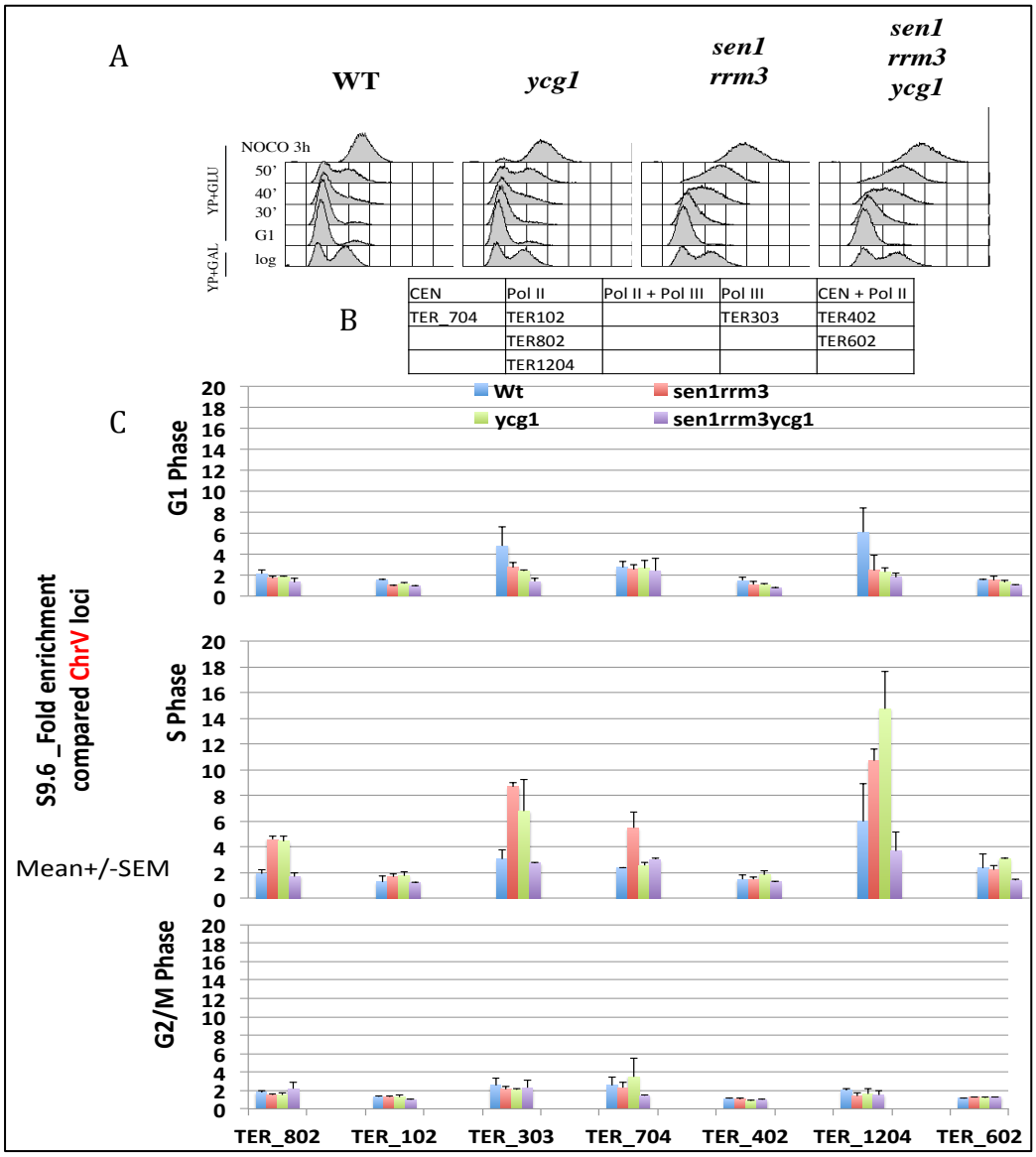


Figure 5.14.1 : DRIP-pPCR captures transient R-loop accumulations at TERs during S-phase in sen1^{dg}rrm3Δ, but is rescued by depletion of Ycg1p.

A) FACs profile of Wild type and sen1^{dg}rrm3Δ used for DRIP-qPCR experiments. Log cells are grown in YPGal and arrested in G1 with alpha factor, are released in YPGlu with Nocodazole and collected at 30', 40', 50', along with G1 and G2/M. 200ml cultures for each time point were subjected to genomic DNA purification without RNAs treatment and CHIP by S9.6 antibody.

B) List of 7 different TERs with different associated features. TERs are used to quantify R-loop accumulation with qPCR.

C) R-loop accumulation during G1, S phase (40') and G2/M in Wild type and sen1rrm3 for all 7 TERs, which cover most of the different pausing elements at TERs.

We employ DRIP-qPCR to quantify R-loop accumulation along 7 TERs carrying different kind of pausing elements as summarized in Fig.52B. Wild type, *sen1^{dg}rrm3Δ, ycg1^{dg}* and *sen1^{dg}rrm3Δycg1^{dg}* strains were released in YPGlu and collected at different time points at indicated in Fig.5.14A. The quantitative DRIP-qPCR showed a strong accumulation of R-loops at different TERs including TER802 (RNA pol II), TER303 (RNA pol III) and TER1204 (RNA pol II) (Fig.5.6C) in *sen1^{dg}rrm3Δ*. This RNA-DNA hybrid accumulation is

transient and accumulated in Condensin depleted Ycg1^{dg} only. Triple mutants sen1^{dg}rrm3Δycg1^{dg} did not accumulate R-loops (Fig.5.14.1C). Transient accumulation of R-loops might lead to fork perturbations at TERs and fork remodeling because of topological stress, which is likely enhanced by unscheduled condensing-mediated chromatin compaction.

We investigated the rescue of cell viability defect in double mutant when Ycg1p is depleted. We did not observe any rescue on spot assay in triple mutant sen1^{dg}rrm3Δycg1^{dg} or sen1^{dg}rrm3Δycs4^{dg} compared to the double sen1^{dg}rrm3Δ (Fig 5.14.2A,B).

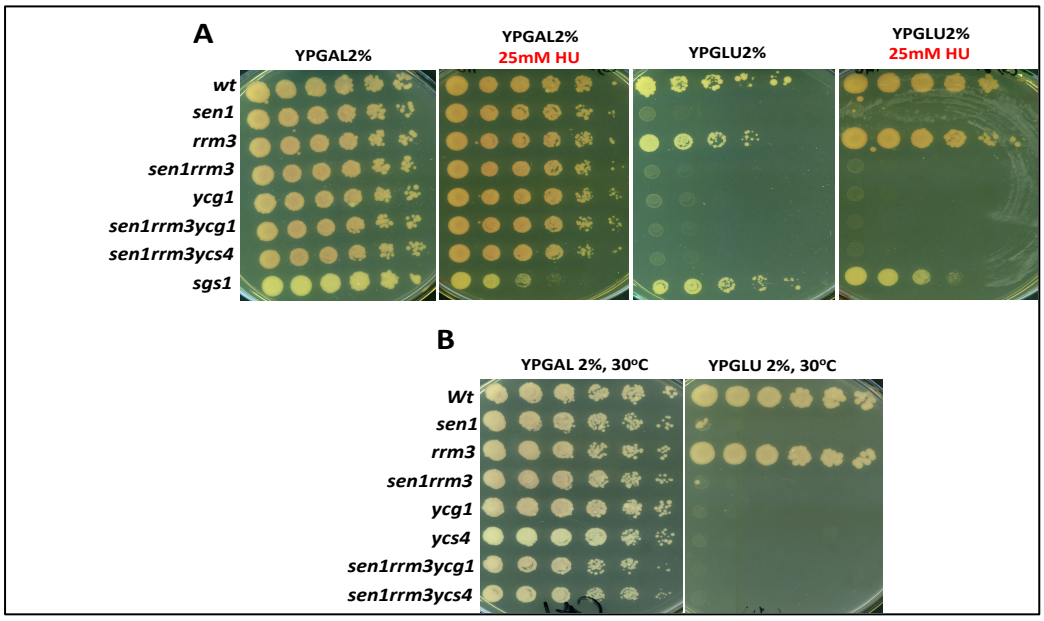


Figure 5.14.2: Spot assay based viability in different genotypes.
A) Spot assay on YPGal and YPGlu plates +/- 25mM HU. All plates were kept at 28°C for 2 days. Wild type, sen1^{dg}, rrm3Δ and sen1^{dg}rrm3Δ mutant were grown over night grown culture in YPGal and spotted as indicated on different plates.
B) *sen1^{dg}rrm3Δ* along with single mutants and triple mutant, on YPGal and YPGlu plates at 30°C.

5.15 Absence of Condensins suppresses DSBs accumulation at TERs in double mutant sen1^{dg}rrm3Δ under mild replication stress.

We collected samples for 3h and 6h from cycling cells in 25mM HU with and without 1mg/ml caffeine, which suppresses checkpoint activation. Interestingly, Condensin complex depleted cells accumulate breaks at TERs under replication stress (Chapter 2), which did not increase with the inhibition of checkpoint activation. In the triple mutant

(*sen1^{dg}rrm3Δycg1^{dg}* or *sen1^{dg}rrm3Δycs4^{dg}*) the basal breakage is equal to *ycg1^{dg}* and *ycs4^{dg}*, and enhanced compared to double mutant sen1^{dg}rrm3Δ. DSBs breaks were rescued for Condensin subunit depleted strains when Sen1 and Rrm3 helicase are not functional (Fig. 5.15A). Adding caffeine did not enhance the fragility at TERs for the wild type. Fig.5.15C shows the quantification of DSBs accumulation as percentage of the total loading in each lane, for different strains in EagI fragment.

We conclude that the Condensin complex generates topological stress and DNA breaks when Sen1 and Rrm3 are depleted..

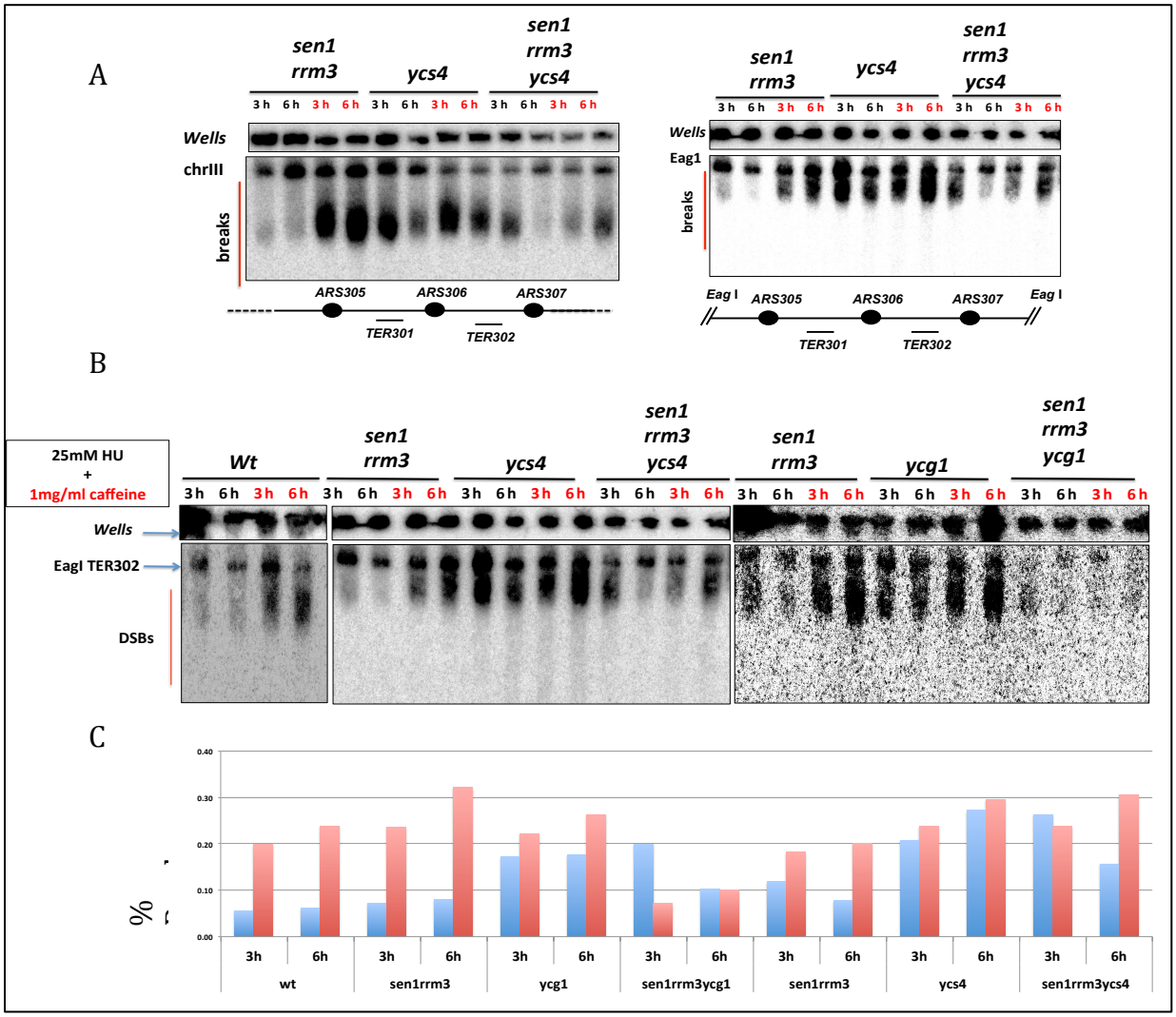


Figure 5.15: Absence of Condensin complex suppresses DSBs accumulation at TERs in double mutant sen1^{dg}rrm3Δ under mild replication stress, and epistasis interaction with replication checkpoints.

A) Breaks accumulated in double mutant sen1^{dg}rrm3Δ and in combination with ycs4 in cycling cells in 25mM HU in absence and presence of 1mg/ml caffeine. Left: whole chromosome fragility at TER302 region. Right: fragility in Eag1 fragment of ChrIII and probe against TER302.

B) Breakage accumulation in EagI fragment in Wild type, sen1^{dg}rrm3Δ and double mutant in combination with Condensin subunits Ycg1p and Ycs4p.

C) Quantification of figure B, at percentage of breakages below EagI fragment, along all genotypes.

5.16 Conclusion

Protein-DNA complexes mediate polar fork arrest in prokaryotic replicons as well in eukaryotes at ribosomal DNA loci. Site-specific replication fork arrest occurs in yeast (Linskens and Huberman, 1988), plants (Hernandez, Martin-Parras et al. 1993), frogs (Wiesendanger et al., 1994) and humans (Daly, Newlon et al. 1993). Replication fork barriers (RFBs) ensure the proper coordination between replication and transcription.

Polar fork pausing has been recently described at TERs to ensure proper replicon fusion (Fachinetti et al., 2010). 58/71 *TER*s have well conserved pause sites in other yeasts. We note that *CEN*s also assist termination but they were excluded from these analyses because they rapidly diverged in evolution (Henikoff et al., 2001). Therefore, evolution has preserved *TER*-containing pause sites integrity.

We showed that Sen1 and Rrm3 defective cells accumulating Lagging chromosomes in anaphase arrested cells and several studies in mammalian cells have shown that DNA replication stress generates DAPI-negative ultra-fine bridges (UFBs) of DNA connecting daughter nuclei during mitosis (Chan et al., 2009). As a consequence of UFBs formation, sister chromatids are interlinked creating the potentiality for generating DNA breakage and rearrangements. It has been suggested that UFBs generate where termination occurs, particularly following replication stress. In humans the Fanconi anaemia proteins FANCD2 and FANC1 and the BLM (Bloom syndrome) helicase have been involved in the metabolism of UFBs (REF).

4. Materials and methods

4.1 S. cerevisiae strains.

Strains are listed in Table 1. All the strains used are isogenic derivatives of W303-1A (Thomas and Rothstain, 1989). Deletion strains were generated using PCR-base gene disruption strategy (Wach et al., 1994), while rad53 mutants were constructed integrating a rad53-K227A-KanMX4 cassette into the RAD53 locus. All the strains used for the experiments were mating type a.

Table 1. Genotypes of the strains used in this study.

Strain	Genotype	Source
SY2080	*Mat***a** *ade2-1 trp1-1 leu2-3,112 his3-11,15 ura3 can1-100 GAL PSI+ RAD5+*	H. Klein
CY11007	*Mat***a** *ade2-1 trp1-1 leu2-3,112 his3-11,15 ura3 can1-100 GAL PSI+ RAD5+ ura3::URA3/GPD-TK(7X)*	M. Foiani lab
CY10731	*Mat***a** *ade2-1 trp1-1 leu2-3,112 his3-11,15 ura3 can1-100 GAL PSI+ RAD5+ rrm3::HIS3MX6*	M. Foiani lab
CY11008	*Mat***a** *ade2-1 trp1-1 leu2-3,112 his3-11,15 ura3 can1-100 GAL PSI+ RAD5+ rrm3::HIS3MX6 ura3::URA3/GPD- TK(7X)*	M. Foiani lab
CY8702	*Mat***a** *ade2-1 trp1-1 leu2-3,112 his3-11,15 ura3 can1-100 GAL PSI+ RAD5+ sen1::GAL-URL-3HA-SEN1-KANMX6*	M. Foiani lab
CY10300	*Mat***a** *ade2-1 trp1-1 leu2-3,112 his3-11,15 ura3 can1-100 GAL PSI+ RAD5+ sen1-G1747D-HIS3*	G. Libri
CY11009	*Mat***a** *ade2-1 trp1-1 leu2-3,112 his3-11,15 ura3 can1-100 GAL PSI+ RAD5+ sen1::GAL-URL-3HA-SEN1-KanMX6 ura3::URA3/GPD-TK(7X)*	M. Foiani lab
CY11224	*Mat***a** *ade2-1 trp1-1 leu2-3,112 his3-11,15 ura3 can1-100 GAL PSI+ RAD5+ rad51::HPH*	M. Foiani lab
CY11893	*Mat***a** *ade2-1 trp1-1 leu2-3,112 his3-11,15 ura3 can1-100 GAL PSI+ RAD5+ rrm3::HIS3MX6 rad51::HPH*	M. Foiani lab
CY11746 **CY10715**	*Mat***a** *ade2-1 trp1-1 leu2-3,112 his3-11,15 ura3 can1-100 GAL PSI+ RAD5+ sen1::GAL-URL-3HA-SEN1-KANMX6 rad51::HPH* *Mat***a** *ade2-1 trp1-1 leu2-3,112 his3-11,15 ura3 can1-100 GAL PSI+ RAD5+ sen1::GAL-URL-3HA-SEN1-KANMX6 rrm3::HIS3MX6*	M. Foiani lab M. Foiani lab
CY11010	*Mat***a** *ade2-1 trp1-1 leu2-3,112 his3-11,15 ura3 can1-100 GAL PSI+ RAD5+ sen1::GAL-URL-3HA-SEN1-KanMX6 rrm3::HIS3MX6 ura3::URA3/GPD-TK(7X)*	M. Foiani lab
CY11894	*Mat***a** *ade2-1 trp1-1 leu2-3,112 his3-11,15 ura3 can1-100 GAL PSI+ RAD5+ sen1::GAL-URL-3HA-SEN1-KANMX6 rrm3::HIS3MX6 rad51::NAT*	M. Foiani lab

CY10300	*Mat***a** *ade2-1 trp1-1 leu2-3,112 his3-11,15 ura3 can1-100 GAL PSI+ RAD5+sen1-G1747D-HIS3*	G. Liberi
CY12093	*Mat***a** *ade2-1 trp1-1 leu2-3,112 his3-11,15 ura3 can1-100 GAL PSI+ RAD5+ rad9::hph ura3::URA3/GPD-TK(7X)*	M. Foiani lab
CY12095	*Mat***a** *ade2-1 trp1-1 leu2-3,112 his3-11,15 ura3 can1-100 GAL PSI+ RAD5+ rrm3::HIS3MX6 rad9::hph ura3::URA3/GPD-TK(7X)*	M. Foiani lab
CY12096	*Mat***a** *ade2-1 trp1-1 leu2-3,112 his3-11,15 ura3 can1-100 GAL PSI+ RAD5+sen1::GAL-URL-3HA-SEN1-KanMX6rad9::hph ura3::URA3/GPD-TK(7X)*	M. Foiani lab
CY12117	*Mat***a** *ade2-1 trp1-1 leu2-3,112 his3-11,15 ura3 can1-100 GAL PSI+ RAD5+ sen1::GAL-URL-3HA-SEN1-KanMX6rrm3::HIS3MX6 rad9::hph ura3::URA3/GPD-TK(7X)*	M. Foiani lab

4.2 Growth media and buffers composition for *S. cerevisiae*

YP 1% Yeast extract

2% bactopeptone

pH 5.4

YP agar YP + 2% agar (DIFCO)

YPD YP + 2% glucose

YPD agar YPD + 2% agar

SC 0.67% yeast nitrogen base (YNB, DIFCO w/o AA)

2% glucose

amino acids as required

SC agar SC + 2% agar

VB sporulation media NaAc$3H_2O$ 1.36%, KCl 0.19%

(+ 1.5% agar) NaCl 0.12% , $MgSO_47H_2O$ 0.074%

4.3 Buffers

Laemmli buffer 3X: Tris 0.187 M, SDS 6%, β-Mercaptoethanol 15%, Glycine 30%, BPB 0.003%

SDS-PAGE running buffer 5X: Glycine 2 M, Tris 0.25 M, SDS 0.02 M, pH 8.3

SSC 20X: NaCl 3 M, Sodium Citrate 0.3 M, pH 7.5

TBE 10X: Tris borate 0.9 M, EDTA 0.02 M

TBS 10X: NaCl 1.5 M, Tris 0.5 M, pH 8.0

TAE 50X: Tris-acetate 0.04 M, EDTA 0.001 M

TE 1X: Tris-HCl 10 mM, EDTA 1 mM, pH 7.4

4.4 Yeast transformation (PCR cassette or plasmid)

The main procedure used is described by (Gietz et al., 1995). Exponentially growing cells are treated for 30 min with Lithium Acetate (LiAc) 0.1 M in TE 1X. A 50 µl aliquot, corresponding to 10^8 cells, is incubated at 30°C with 2-5 µg of PCR-amplified linear DNA cassette or 1 µg of plasmid DNA and 20 µg of ssDNA carrier for at least 30 min. 5 volumes of freshly prepared 40% PEG-4000 are added and cells are incubated for 30 min at 30°C. DMSO is added to a final concentration 10% of the final volume, what is followed by 15-20 minutes of heat-shock at 42°C. The cells are centrifuged at low speed (3000 rpm) and if they carry a *KAN* or *NAT* marker, they are re-suspended in YPD or YPG medium and subjected to 4-5 hours recovery and then plated on selective plates.

4.5 Cell cycle arrest

There are commercially available substrates that allow blocking the cell cycle at the specific phases. In this thesis I used the α-Factor pheromone, that blocks the cells in G1, and nocodazole, which depolymerizes the microtubules and arrests the cells in pro-metaphase.

α-Factor (G1 arrest) – This pheromone is produced by *Saccharomyces cerevisiae "*α" cells and by inducing mating genes expression arrests "a" cells in G1 phase. The growth of "a" cells is polarized towards the mating partner and cells undergo morphological elongation into pear-shaped "shmoos". Exponentially growing cells are treated with 4 µg/ml (3

μg/ml + 1 μg/ml added after 1 hour 30 minutes) of the synthetic peptide α-Factor (Primm). When approximately 90% of cells show the shmooing phenotype, cells are centrifuged and washed with YP in order to wash the α-Factor away and release the cells in fresh medium.

Nocodazole (G2 arrest) – It is an anti-neoplastic agent, which by depolymerizing microtubules, arrest cycling cells in G2/M phase. Nocodazole-treated cells do enter mitosis but cannot form metaphase spindles. Cells are arrested in G2/M phase by the addition of 10 μg/ml of Nocodazole (Sigma-Aldrich) dissolved in DMSO. The arrest is maintained for 3 hours by re-adding 5 μg/ml of Nocodazole or 10 μg/ml, to maintain the arrest for a longer time.

4.6 Total protein extract with TCA

The yeast protein extraction is performed using TCA as described by (Reid and Schatz, 1982). 108 cells samples are collected, centrifuged at 4°C at 4000 rpm, washed with 1 ml of TCA 20% and transferred to a 2 ml tube. The pellet is re- suspended in 100 μl of TCA 20% and an equal volume of glass beads (425-600 μm, Sigma-Aldrich) is added leaving a layer of a supernatant over the beads. Cells are broken by continuous vortexing for 7-10 minutes. 200 μl of TCA 5% is added and the lysate is transferred to a new 1.5 ml tube and centrifuged for 10 minutes at 3000 rpm at RT. The pellet is re-suspended in 100 μl of Laemmli Buffer 1X. The pH is neutralized with 50 μl of Tris Base 2M (the colour needs to turn from yellow to blue). The protein extract is boiled for at least 3 minutes and centrifuged for 10 minutes at 3000 rpm at RT. The supernatant is collected and the protein extract is subjected to SDS-PAGE analysis.

4.7 Western blot protocol (SDS-PAGE)

Proteins are separated by their molecular weight in the denaturing conditions using gel electrophoresis in polyacrylamide gels. The concentration of acrylamide determines the resolution of the gel. The polyacrylamide gel consists of two parts: running and stacking. The lower the acrylamide concentration is in the running part of the gel, the better the resolution of big molecular weight proteins becomes. The protein migration is performed in a SDS-PAGE running buffer. The procedure is described by (Laemmli, 1970). Proteins

with a known molecular weight serve as a marker. The gel with separated proteins is transferred on a nitrocellulose filter (Whatman Protrane, Nitrocellulose Transfer Membrane, Pore size 0.45 μm) O/N at 0.2 Ampere in a transfer buffer (Glycin 1%, Tris-HCl 0.02 M, Methanol 20%). After the transfer the filter is washed with TBST 1X and coloured with Ponceau S staining solution (Ponceau S 1gr, acetic acid 50 ml, up to 1000 ml ddH_2O) that enables the visualization of the total protein extract. The filter is washed again with TBST and then is incubated for at least 30 minutes with milk 4% in TBST. The primary antibody is added and incubated for 2 h at RT. The membrane is washed 3X for 10 minutes in TBST and the filter is incubated with secondary antibody for 1 hour at RT. After the hybridization the filter is washed again 3X for 10 minutes with TBST. Finally, the membrane is incubated for 5 minutes at RT with SuperSignal West Femto Chemiluminescent Substrate (Thermo Scientific) and the signal is developed using ChemiDoc (Bio- Rad, Molecular Imager ChemiDoc XRS+). The dilutions of the primary and secondary antibodies used as standard protocols in laboratory. H2AX phosphorylated Serine 129 at histone H2A, phosphorylated Rad53p, HA-tagged Sen1p and expressed level of PGK1p (loading control). Due to different protein sizes, adequate acrylamide concentration is used to separate the proteins. The antibodies used for western blots are the monoclonal anti-FLAG M2 from SIGMA (F1804), the 22C5 monoclonal antibody from Invitrogen (A6457) for Pgk1, the polyclonal Clb2 (y-180) antibody from Santa Cruz Biotechnology, the mouse monoclonal anti-MYC (9E10), the mouse monoclonal anti-HA (12CA5).

4.8 FACS (Fluorescence activated cell sorter) analysis

0.5-2 x107 cells were fixed with 70% ethanol. Cells were treated with 2 mg/ml RNAse A (Sigma) in Tris-HCl 50 mM pH 7.5 for at least 1hour at 37°C. Cells were then stained with Propidium Iodide (Sigma) 50 μg/ml in FACS Buffer solution (180 mM Tris-HCl pH 7.5; 190 mM NaCl; 70 mM MgCl2). A 1:10 dilution in Tris-HCl 50mM pH 7.5 was sonicated for 6'' and analyzed in Becton Dickinson FACScan for FL2H fluorescence. Alternatively, after RNase A treatment, cells were treated with Proteinase K (Roche) 1mg/ml for 30' at 50°C. Cells were than resuspended in Tris-HCl 50 mM pH 7.5. A 1:10 dilution in sytox green staining solution (1 μM sytox green in Tris-HCl 50 mM pH 7.5), sonicated for 6'' and analyzed in Becton Dickinson FACScan for FL1H fluorescence.

4.9 Spot assay

Stationary phase grown cells were counted and 10 fold serial dilutions were spotted onto YPDA, YPDA containing HU at the indicated concentrations, SC or 5-FOA plates. The plates were then incubated for 2-4 days at the indicated temperatures and scanned.
5-FOA plates (200 ml): 1) 4 gr of Agar are dissolved in 100 ml of water and then autoclaved. 2) Prepare a mix with:

- 1,4 gr YNB
- 200 mg FOA (1 g/L)
- 10 mg Ura (50 mg/L)
- 8 ml Glucose 50%
- 2 ml Ade 5 mg/ml
- 2 ml His 5 mg/ml
- 2 ml Trp 5 mg/ml
- 2 ml Leu 5 mg/ml 3) Add water to 100 ml final volume and let this mix to dissolve. 4) Then filter it and warm at 65°C. 5) Put together agar+water and the mix containing FOA and Ura (final 200 ml) and pour the plates (10).

4.10 DAPI and tubulin staining

10^7 cells were fixed with 1 ml of EtOH 70% for 30'. Cell were treated with (1mg/ml) Zymolase in osmotic solution to prepare spheroplast for 5-15' at RT. Cells were than washed twice with PBS 1X (137 mM NaCl, 10 mM Na2HPO4, 1.76 mM KH2PO4, 2.7 mM KCl, pH 7.4) and stored at 4°C. Cells were pelleted, applied on glass slides and fixed with acetone and ethanol combination later incubated with Mouse anti tubulin antibody followed by secondary antibody (FITC-anti-Mouse). Immediate before IF imaging on confocal microscopy DAPI 0.5 µg/ml added for 20 minuts and analyzed using Hoest and FITC filters.

4.11 ChIP-on-chip

The ChIP-on-chip technique uses the DNA obtained by chromatin immunoprecipitation (ChIP) and PCR amplification as a probe for hybridization to DNA chips, allowing the detection of protein binding to chromosomal DNA at a resolution of 300 bp. Protein-

DNA complexes are crosslinked by formaldehyde treatment, chromatin is then sheared by sonication to obtain suitable protein-DNA fragments and immune-precipitation is carried out with specific antibodies. Two fractions are obtained: IP, enriched in the protein of interest, and SUP, which contains non-immunoprecipitated DNA and is used as a hybridization control. Crosslink is reversed, samples are treated with proteinase K and RNase to extract DNA. DNA fractions are amplified by tagged-random PCR, DNAse digested and labeled with biotin. Enriched and non-enriched DNA pools are probed to independent chips and, after staining, washing and scanning, signal intensities of each locus for IP and SUP hybridized arrays are compared, providing a measurement of the protein-DNA association along the entire genome. (Katou et al., 2006).

S.cerevisiae oligonucleotide microarrays were provided by Affymetrix (*S.cerevisiae* Tiling 1.0R, P/N 900645). Proteins ChIP-chip analysis were carried out as described (Bermejo et al., 2009b), employing anti-Flag monoclonal antibody M2 (Sigma-Aldrich) and anti-PK SV5-Pk1 antibody (AbD Serotec). ChIP-on-chip experiment were performed after HU 200 mM or Nocodazole 20 μg/ml treatment, to analyze, respectively, chromatin enrichment of a given protein in S phase or in G2/M. Analysis of the data was performed using TAS (Affymetrix) and MAT software.

Solutions :

PBS 1X

TBS 1X

TE 1X: 10 mM Tris-HCl pH 8.0, 1 mM EDTA

Laemmli Buffer 2X

PBS/BSA: PBS 1X containing 5 mg/ml Bovine Serum Albumin

Lysis Buffer: Hepes-KOH pH 7.5 50 mM, NaCl 140 mM, EDTA 1 mM, Triton-X100 1%, Na-deoxycholate 0.1% (autoclaved)

Wash Buffer: Tris-HCl pH 8.0 10 mM, LiCl 250 mM, NP-40 0.5%, Na-deoxycholate 0.5%, EDTA 1 mM (autoclaved)

Elution Buffer: Tris-HCl pH 8.0 50 mM, EDTA10 mM, SDS 1%

TE -1% SDS: Tris-HCl pH 8.0 10 mM, EDTA1 mM, SDS 1%

10X One-Phor-All-Buffer: Tris-Acetate pH7.5 100 mM, Mg-Acetate 100 mM, K-Acetate 500 mM

Magnetic beads preparation (Protein A)

1. Transfer 60 µl of magnetic beads (Dynabeads, Invitrogen) in a 1.7-ml prelubricated Costar tube

2. Place the tube in a magnetic grid and aspirate the supernatant with a vacuum pump.

3. Wash beads twice as follows with 0.5 ml of ice cold PBS/BSA

4. Resuspend the beads in 60 µl of PBS/BSA and add 20 µg of anti-Flag monoclonal antibody M2 or anti-PK SV5 antibody

5. Incubate with rotation overnight at $4^{o}C$

6. Immediately before use, remove the antibody containing solution; wash twice with ice- cold PBS/BSA and resupend in 60 µl of PBS/BSA (15 µl of magnetic beads are added to each 0.4 ml Lysis Buffer aliquot)

Chromatin extracts preparation and immunoprecipitation

1. Collect 100 ml of culture at the concentration of $1*10^{7}$ cells/ml

2. Transfer the culture into two 50-ml centrifuge tubes containing formaldehyde to a 1% final concentration

3. Incubate at room temperature for 30 minutes gently shaking by rotation

4. Wash cells twice with 20 ml of ice-cold TBS 1X; after the last washing step discard the supernatant and carefully remove the remaining liquid with a vacuum pump

5. Resuspend each pellet in 0.8 ml of Lysis Buffer supplemented with 1 mM PMSF (Phenylmethanesulphonyl fluoride) and antiproteolytic cocktail (Complete protease

inhibitor tablets, Roche) immediately before use

6. Transfer 0.4 ml Lysis Buffer aliquots into 2-mL O-ring screw-cap tubes add glass beads (Sigma) up to 1 mm below the buffer's meniscus (approximately 1 ml of beads)

7. Break cells with a multibeads shocker (Yasui-kikai, Osaka, Japan) using the following pattern: 60 min total time (1 min shaking / 1 min pause) at 2500 rpm and 4 °C Breakage time can be extended if broken cells are not over 90% of the total (cell breakage can be assessed by analyzing a small aliquot of the lysate by phase contrast microscopy)

8. Recover the cell lysate

9. Centrifuge the extracts at 13400 g for 1 min at 4°C. Add a 5 µl aliquot of the soluble fraction to 5 µl of 2X Laemmli Buffer for Western blot analysis of IP efficiency (Western blot detection of this fraction indicates the proportion of protein that is not associated to chromatin after the formaldehyde crosslink)

10. Discard the supernatant containing the soluble protein fraction and add 0.45 ml of Lysis Buffer supplemented to 1 mM PMSF and 1X Antiproteolytic Cocktail) without resuspending the pellet

11. Shear chromatin by applying 5 sonication cycles of 15 sec at 1.5 tune; after each sonication cycle, pellet the chromatin by centrifuging at 2300 g for 1 min at 4 °C

12. After the final sonication cycle, centrifuge the sheared DNA at 16000 g for 5 min at 4°C and transfer the supernatant to a new 1.7-ml prelubricated tube.

Add a 5 µl aliquot of this Whole Cell Extract (WCE) to 5 µl of 2X Laemmli Buffer for Western blot analysis

13. Add previously washed antibody-bound magnetic beads (15 µl per tube) and incubate on a rotating wheel at 4°C ON

<u>Beads washing and crosslink reversal</u>

1. Place beads-containing tubes in a magnetic grid and wait until the beads attach to the magnet leaving a clear supernatant.

2. Transfer 5 µl of the supernatant to a 1.5 ml microcentrifuge tube to be used as hybridization control (SUP)

3. Transfer another 5 µl to a tube containing 5 µl of 2X Laemmli Buffer for Western blot analysis of IP efficiency.

4. Wash the beads as follows:

a. twice with 1 ml of ice cold Lysis Buffer (without antiproteolytics)

b. twice with 1 ml of ice cold Lysis Buffer supplemented with 360mM NaCl

c. twice with 1 ml of ice cold Wash Buffer

d. once with 1 ml of ice cold TE 1X pH 8

5. Remove the TE 1X with a micropipette in order to avoid beads aspiration and centrifuge the beads at 800 g for 3 min at 4 °C

6. Add 40 µl of Elution Buffer to each tube and incubate at 65 °C for 10 min

7. Centrifuge the tubes for 1 min at 16000 g at RT

8. Place the tubes back in the magnetic grid and transfer 5 µl in a tube containing 5 ml of 2X Laemmli Buffer

9. For the Western blot analysis of IP efficiency boil the samples at 95 °C for 30 min prior to SDS-PAGE

10. Transfer the remaining IP fractions (35-40 µl) to new 1.5-ml microcentrifuge tubes containing 4 volumes (140-160 µl) of TE-1% SDS

11. Add 95 µl of TE-1% SDS to the SUP fraction (collected on step 2)

12. Incubate overnight at 65 °C in order to reverse the crosslink

<u>DNA purification</u>

1. Consolidate the samples by pulse-spinning and add 25 µl of TE to the IP sample containing 175 µl 2. Add:

- 89.5 µl of TE, 3 µl of glycogen (20 mg/ml) and 7.5 µl of Proteinase K (50 mg/ml) to the IP samples

- 44.75 µl of TE, 1.5 µl of glycogen (20 mg/ml) and 3.75 µl of Proteinase K (50 mg/ml) to the SUP sample 3. Mix, without vortexing, and incubate at 37 °C for 2 hours 4. Pulse-spin to consolidate the samples and add:

- 12 µl of a 5M NaCl stock to the IP samples

- 6 µl of a 5M NaCl stock to the SUP samples

5. Extract twice by adding an equal volume of phenol/chlorophorm/isoamylalcohol pH 8.0 (300 µl for the IP samples and 150 µl for SUP samples)

6. Vortex and spin at 13400 g for 5 min at RT.

7. Add 2 volumes of cold 100% ethanol (600 µl for the IP samples and 300 µl for the SUP samples), vortex and incubate at -20 °C for at least 20 min (can be extended up to ON)

8. Centrifuge at 13400 g for 10 minutes at 4 °C

9. Discard the supernatant using a Gilson pipette and wash with 1 ml of cold 80% ethanol

10. Centrifuge at 13400 g for 10 minutes at 4 °C

11. Discard the supernatant and spin again; discard the remaining ethanol with a gel loading tip and let the pellet air-dry 12. Resuspend the pellet in 30 µl of TE containing 10 mg of RNase A (stock 10 mg/ml) 13. Incubate 1h at 37 °C

14. Consolidate the samples by pulse spinning

15. Pool two 30 µl IP samples together to obtain two 60 µl samples and purify the IP/SUP DNA using a PCR purification kit following the manufacturer's instructions (QIAquick PCR purification kit, QIAGEN)

16. Elute the DNA with 50 µl of EB buffer

17. Pool the two 50 µl IP samples together and precipitate the DNA by adding:

- 5 µl of 3M Sodium Acetate, 2 µl of glycogen (20 mg/ml) to the IP SAMPLE
- 2.5 µl of 3M Sodium Acetate, 1 µl of glycogen (20 mg/ml) to the SUP SAMPLE

18. Add 2.5 volumes of cold 100% ethanol (267.5 µl to the IP samples and 133.75 µl to the SUP samples)

19. Incubate at -20 °C for at least 20 min (can be extended up to ON)

20. Centrifuge at 13400 g for 10 minutes at 4 °C

21. Discard supernatant using a Gilson pipette and wash with 0.5 ml of cold 70% ethanol
22. Centrifuge at 13400 g for 10 minutes at 4° C

23. Discard the supernatant using a Gilson pipette and spin again; discard the remaining ethanol with a gel loading tip

24. Leave 5' at 37° C and resuspend the pellet in 10 µl of bidistilled water

25. Vortex then pulse-spin for three times to recover the precipitate

DNA amplification

1. Use WGA2 GenomePlex Complete Genome Amplification (WGA) Kit (Sigma) and follow the manufacturer's instructions from the *Library Preparation* step on:

a) Add 2 µl of 1X Library preparation Buffer to each sample

b) Add 1 µl of Library stabilization solution

c) Vortex thoroughly, consolidate by centrifugation and place in thermal cycler at 95° C for 2 minutes

d) Cool the sample on ice, consolidate the sample by centrifugation and return to ice

e) Add 1 µl Library Preparation Enzyme, vortex thoroughly and centrifuge briefly

f) Place the sample in a thermal cycler and incubate as follows:

16° C for 20 minutes /24° C for 20 minutes /37° C for 20 minutes /75° C for 5 minutes

/4° C hold

g) Centrifuge briefly the samples and amplify them immediately or store at -20° C

2. Amplification step

A master mix may be prepared by adding the following reagents:

Nuclease-free water: 48.5 µl

10X Amplification Master Mix: 7.5 µl

Reaction from step g): 14.0 µl

WGA DNA Polymerase: 5 µl

Vortex thoroughly, centrifuges briefly, and begins thermocycling.

Initial Denaturation: 95° C for 3 minutes

Perform 14 cycles as follows:

Denature: 94° C for 15 seconds

Anneal/Extend: 65° C for 5 minutes

After cycling is complete, maintain the reactions at 4°C or store at -20°C

- Pulse-spin the samples

- Check the amplified DNA by loading a 2.5 µl aliquot of the reaction in a 1.2% agarose gel; a smear ranging from 100-1000 bp should be observed.

- Concentrate the DNA with YM30 Microcon cartridges (Millipore): Add to the sample 400 µl of bidistilled water

Centrifuge at 14000g for 8 min

Discard the eluted material and add 500 µl of bidistilled water

Centrifuge at 14000g for 8 min

Check the concentrate volume, that should be less than 41.75 µl

Collect the concentrate centrifuging at 1000g for 3'

Arrange the concentrate volume up to 41.75 µl

- Measure the DNA concentrations by spectrometry at 260 nm (using a Nanodrop)

DNAse digestion

1. Prepare a DNAse reaction mix as follows (for 13 samples):

ddH2O	14.8 µl
10X One-Phor-All-Buffer plus	2 µl
25mM CoCl2	1.2
DNAse I 1U/ml (Invitrogen)	2 µl

2. Add to each sample:

10X One-Phor-All-Buffer plus	4.85 µl
25mM CoCl2	2.9 µl
DNAse I reaction mix	1.5 µl

3. Vortex, pulse-spin and incubate at 37° C for 30''; then transfer the samples at to 95°C for 15' (in a thermocycler)

DNA labeling

1. Spin the samples and transfer them into new 1.5ml-microcentrifuge tubes

2. Add:

5µl of TdT reaction buffer

1µl Biotin-N11-ddATP (Perkin)

1µl terminal transferase (Roche)

3. Vortex, pulse-spin and incubate at 37° C for 1 hour

Hybridization and analysis of the data

Hybridization, washing, staining, and scanning were performed according to the manufacturer's instructions (Affymetrix).

Primary data analyses were carried out using the Affymetrix microarray Suite version 5.0 software to obtain hybridization intensity, fold change value, change p value and detection of p value for each locus.

Evaluation of the significance of protein cluster distributions within the different genomic areas and protein-binding correlations was performed by confrontation to the model of the null hypothesis distribution generated by a Montecarlo-like simulation. The significance of the overlap between proteins clusters was evaluated as in (Bermejo et al., 2009a; Gonzalez-Huici et al., 2014).

4.12 DRIP with DNA: RNA hybrids precipitation

Before GIP procedure:

Protein A or Protein G Magnetic beads preparation:

- Transfer 20 µl of magnetic beads in a 1.7-ml prelubricated tube.
- Place the tube in a magnetic grid and aspirate the supernatant with a vacuum pump.
- Wash the beads twice as follows: re-suspend the magnetic beads in 0.5 ml of ice cold PBS/BSA by removing the tube from the magnetic grid and gently shaking.
- Place the tube back in the magnetic grid, wait until the beads attach to the magnet leaving a clear solution and aspirate the supernatant with a vacuum pump.
- Add 7.5 µg of S9.6 antibody. Incubate with rotation overnight at 4˚C.

Immediately before use, remove the antibody containing solution; wash twice with ice-cold PBS/BSA and proceed with GIP.

GIP with DNA: RNA hybrids precipitation procedure:

1) Extract the DNA with QIAGEN GENOMIC DNA ISOLATION KIT (Cat. No. 19060) without RNase A treatment. Re-suspend each sample in 300 µl of 1X TE pH 8.

2) Shear the BrdU containing DNA by sonication to a length of 200-1000 bp using the Bandelin UW2070 sonicator. You can use the following parameters:

   Power 20%

   20 seconds/pulse

   6 pulses

3) Precipitate 300 µg of the genomic material in a pre-lubricated eppendorf tube with Na Acetate, glycogen and ice-cold Ethanol 100% (see 5.17). Precipitate at -20°C O/N.

4) Wash the precipitate with Ethanol 70% and re-suspend in 50 µl of ddH2O. To re-suspend: vortex and centrifuge at 11600 x g for 1 minute, 3 times.

5) Add 400 µl of FA-1 buffer (0.1% SDS, 1% Triton X100, 10 mM HEPES pH 7.5, 0.1% Na Deoxycholate, 275 mM NaCl; filter), mix.

6) Add 20 µl of washed beads with S9.6 antibody bound. Leave the reaction for 90 minutes at 4°C.

7) Collect 200 µl of IP SUPERNATANT (SUP) in an Eppendorf tube. Leave on ice.

8) Wash the beads as follows (see 5-17):

   - 2X with 1ml of ice-cold ChIP Lysis buffer
   - 2X with 1 ml of ice-cold ChIP Lysis buffer +500 mM NaCl
   - 2X with 1 ml of ice-cold ChIP Washing buffer
   - 1X with 1ml of ice-cold 1X TE pH 8.0

9) Remove the TE with a micropipette in order to avoid beads aspiration. Centrifuge the beads at 800x g for 3 minutes at 4°C. Place the tubes on the magnet and thoroughly remove the remaining liquid with the vacuum pump.

10) Elute the beads with 50 µl of ChIP Elution buffer (see 5.17). Re-suspend the beads by pipetting up and down. Incubate for 10 minutes at 65°C mixing.

11) Centrifuge the tubes for 1 minute at 16000x g at RT. Move the eluate in a new Eppendorf tube.

12) In a new Eppendorf tube, add 5 µl of IP SUPERNATANT from #7 to 45 µl of ChIP Elution buffer.

13) Add to both the IP and SUP tubes 49 µl of TE 1X pH 8.0 and 1 µl of Proteinase K (Proteinase K stock: 50 mg/ml in 50% glycerol). Mix without vortexing.

. 14) Leave for 2 hours at 37°C without mixing.

. 15) Purify the IP/SUP DNA using a PCR purification kit (Qiagen) following the manufacturer's instructions. Elute the DNA with 50 µl of EB buffer.

16) To both the IP and SUP tubes add 50 µl of EB buffer (up to 100 µl). Precipitate with Na Acetate, glycogen and ice-cold Ethanol 100%. Precipitate at -20°C O/N.

17) Wash the precipitate with ice-cold Ethanol 70% and re-suspend in 29 µl of TE 1X + 1 µl of RNase A (stock: 10 mg/ml). Leave the samples for 1 hour at 37°C. To re-suspend: vortex and centrifuge at 11600 x g for 1 minute, 3 times.

18) Add to both the IP and SUP tubes 70 µl of TE 1X. Purify using Qiagen columns using standard protocol. Elute with 50 µl of EB buffer and add 50 µl of EB buffer up to 100 µl. Precipitate with Na Acetate, glycogen and ice-cold Ethanol 100%. Precipitate at -20°C O/N.

19) Wash the precipitate with ice-cold Ethanol 70% and re-suspend in 10 µl of ddH2O. To re-suspend: vortex and centrifuge at 11600 x g for 1 minute, 3 times.

20) Continue with WGA protocol (see 3.11 CHIP protocol).

4.13 GIP analyses and statistical methods

Data from all GIP experiments were analyzed using a modified version of the Tiling Array Suite software (TAS) from Affymetrix. Clusters from TAS data were identified as ranges within the chromosome respecting the following conditions:

i) Estimated signal (IP/SUP binding ratio) positive in the whole range; ii) change P-value of the Wilcoxon signed rank test < 0.2 in the whole range, except for segments within the range shorter than 600 bp; iii) size of the region at least 600bp. The peak of each cluster has been defined as the genomic position within the cluster with the highest estimated signal. Evaluation of the significance of the presence of BrdU and S9.6 antibody binding peaks were performed by confrontation against a null hypothesis model generated with a Montecarlo-like simulation. For each data set (binding clusters of a specific protein or set of pausing elements), 1000 randomizations of the positions of the features were produced, maintaining unchanged the number and size of the genomic areas covered within each chromosome; the number of peaks and features with random positions within the *TER*s was then counted and taken as score for each iteration. The distribution of these random scores was validated to be approximately normal (jSkewj < 0.25 and jKurtosis excessj < 0.25), and then the average and standard deviation for this distribution were taken as null hypothesis.

The increase or decrease ratios for the scores of the actual positions with respect to the expected value for the null hypothesis (defined as the average score of random attempts) was then calculated, and the p values for the drift were estimated as Standard Normal CDF of actual_meanj deviation.

4.14 In-vivo psoralen crosslinking of the DNA

Psoralen efficiently intercalates in the double strand DNA and upon irradiation with ultraviolet (UV) light (366 nm) forms covalent crosslinks between pyrimidines of opposite strands. Psoralen derivatives easily penetrate the membranes of living cells and Trimethylpsoralen (TMP) is the most commonly used for in vivo crosslinking of DNA (Wellinger and Sogo, 1998).

Material and solutions: -

- Psoralen solution: 0.2 mg/ml Trioxalen (SIGMA) in 100% Ethanol. Keep in the dark. Dissolve by stirring overnight at 4°C. Store at -20°C.
- 6 well plates (FALCON)
- UV stratalinker (Stratagene), 365 nm and 265 nm UV bulbs

Procedure:

1. 2 x 10^9 cells (200 ml from a 1 x 10^7 cells/ml culture) were collected.

2. Block cells by treating with sodium azide (0.1% final) and 5 min or more on ice.

3. Pellet the cells and wash with 20 ml of ice-cold water.

4. Re-suspend in 5 ml of ice-cold water and transfer in a 6 well plate (1sample/well)

5. Keep the 6 well dish always on ice while performing psoralen-crosslinking.

6. Add 300 µl of psoralen solution, mix well and incubate for 5 minutes (on ice)

7. Mix again within the 5 minutes and irradiate for 10 minutes (on ice) in a Stratalinker (Stratagene) with 365 nm UV bulbs, at a distance of 2-3 centimeters from the bulbs.

8. Repeat steps 6-7 for three more times. (Cover with aluminum wrap during incubation with psoralen to keep samples as much as possible in the dark).

9. Transfer cells in falcon tubes and wash the dish with 5 ml of ice- cold water to collect all cells

10. Pellet the cells and proceed with DNA extraction.

Before blotting, revert the crosslinking by irradiating the gel for 10 minutes with 265 nm UV lamps in a Stratalinker (Stratagene). It's not necessary to place the gels very close to the UV bulbs.

4.15 Genomic DNA extraction with the Qiagen genomic Kit

Materials and Solutions: Solutions Y1, G2, QBT, QC and QF are supplied with the Qiagen Kit:

- Buffer Y1 (Yeast Lysis Buffer) 1 M Sorbitol, 100 mM EDTA, 14 mM β-mercaptoethanol (supplemented with 500 µl/sample of zymolyase solution)

- 10 mg/ml Zymolyase, 1000 U/ml (Seikagaku Biobusiness)

- Buffer G2 (Digestion Buffer) 800 mM guanidine HCl, 30 mM Tris-HCl pH 8.0, 30 mM EDTA pH 8.0, 5% Tween 20, 0.5% Triton X-100

- Buffer QBT (Equilibration Buffer) 750 mM NaCl, 50 mM MOPS pH 7.0, 15% Isopropanol, 0.15% Triton X-100

- Buffer QC (Wash Buffer) 1 M NaCl, 50 mM MOPS pH 7.0, 15% Isopropanol

- Buffer QF (Elution Buffer) 1.25 M NaCl, 50 mM Tris-HCl pH 8.5, 15% Isopropanol

- 10 mg/ml RNase A, DNase free (Sigma-Aldrich)

- 20 mg/ml Proteinase K (Roche)

- Isopropanol

- Cold 70% Ethanol

- 10 mM Tris-HCl pH 8.0

- Corex glass tubes

Procedure

1) Start from 2 X 10^9 cells (200 ml of a culture 1 X 10^7 cells/ml).

2) Collect samples in a JA-14 Beckman tubes, block the cells with 0.1% of Sodium Azide (final concentration), keep at least 5 minutes in ice, centrifuge at 6000-8000 rpm for 5 minutes and washed with 20 ml of ice- cold water.
3) Transfer the cells in a 50 ml Falcon tube, re-suspend in 5 ml of Y1 buffer and incubate for 10-30 minutes at 30°C (spheroplasting).
4) Collect the spheroplasts by centrifugation at 4000 rpm for 10 minutes at 4°C.
5) Discard supernatant and re-suspend the spheroplasts in 4 ml of G2 buffer (cell breaking).
6) Add 100 µl of RNase A and incubate at least 20 minutes at 37°C.
7) Add 200 µl of Proteinase K and incubate for 2 hours at 50°C (the lysate should become clear upon proteinase K treatment). To increase the yield of extracted DNA, re-add 100 µl of Proteinase K and incubate O/N at 30°C.
8) Centrifugate the lysate for 10 minutes at 4000 rpm at 4°C.
9) Dilute the supernatant in an equal volume (4 ml) of QBT buffer.
10) Load the diluted supernatant on the Qiagen tip 100G-anion exchange
Column, pre-equilibrated with 4 ml of QBT buffer. 11) Wash twice with 7.5 ml of QC buffer. 12) Elute with 5 ml QF buffer in a corex glass tube. 13) Precipitate with 3.5 ml of isopropanol and centrifugate at 8500 rpm for 10 minutes in a Beckman JS 13.1 swinging bucket rotor. 14) Wash the pellet with 1 ml of ice-cold Ethanol 70%. 15) Re-suspend the pellet in 250 µl of 10 mM Tris-HCl pH 8.0 and store at 4°C.

Quantification of genomic preps

Concentration of DNA and DNA:RNA genomic preps are measured by NanoDrop. At the wavelength of 260 nm, 1.5 µl of genomic sample is subjected to the concentration quantification. If DNA and DNA:RNA concentration is higher than 200 ng/µl and 2000 ng/µl respectively, the samples are diluted and re- quantified.

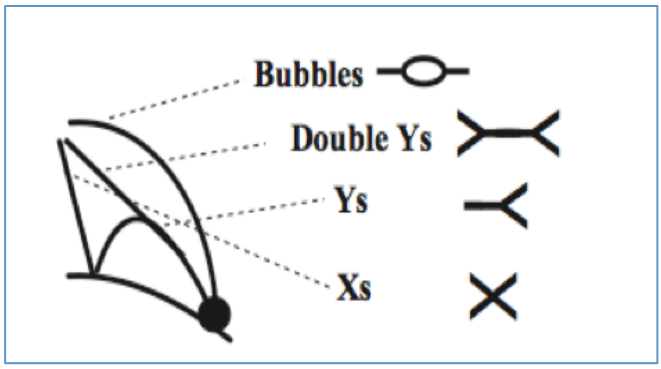
4.16 Analysis of replication intermediates by two-dimensional agarose gel electrophoresis (2D gel)

Replication of a DNA fragment generates a variety of structures that differ from each

other by mass and shape. For instance, passively replicated DNA assumes a characteristic "Y" shape due to the unwinding of a single double helix in two newly replicated templates. When the DNA fragment contains an origin of replication, the two fork molecules are bound in a "bubble" like structures that enlarges with the progression of replication and results in two linear DNA molecules when forks proceed outside the fragment. Recombination intermediates that link two newly replicated DNA molecules assume instead an "X" shape due to the presence of a physical link between them. Neutral-neutral two-dimensional agarose gel electrophoresis (2D gel) technique allows separation and identification of branched DNA molecules according to their mass and shape complexity (Bell and Byers, 1983; Bell and Byers, 1983). This technique further developed by Brewer and Fangman (Brewer and Fangman, 1987) has been used to map origins of DNA replication in yeast chromosomes and to study replication and recombination related DNA structures in many organisms.

The principle on which the method is based consists on the fact that differences in shape can affect, under specific conditions, the electrophoretic mobility of DNA molecules of equal mass. Restriction fragments are therefore separated through a first dimension gel, in conditions that emphasize the mass differences and minimize the contribution of shape to the mobility (low agarose concentration, low voltage, no ethidium bromide).

Subsequently, each sample lane is cut out and separated by the second dimension gel, where DNA runs orthogonally with respect to the first dimension gel. The second gel, on the contrary, is run under conditions that maximize the contribution of the shape to the mobility by means of a delay of complex structures during migration (high agarose concentration, high voltage and in the presence of ethidium bromide). As a result of the consecutive electrophoretic runs, each DNA structure assumes in the two dimensional area a specific position dictated by the unique combination of mass and shape. Moreover, molecules of the same nature (e.g. replication forks), undergo transitions that define specific continuous patterns, the most often encountered arcs been confirmed by electron microscopy (Kuzminov et al., 1997; Kuzminov et al., 1997). The migration patterns of the major DNA structures arising during replication origin firing, replication fork progression, pausing and recombination are depicted in the following scheme (Model 3.1). 2D gel electrophoresis was performed as described in (Branzei et al., 2006; Branzei et al., 2008).



Model 4.1: Schematic representation of the replication and repair intermediates analyzed by 2D gel electrophoresis. In the scheme the signals corresponding to bubbles, Y-arcs, double Y-arcs and X shaped molecules are indicated. Adapted from (Branzei et al., 2008).

Digestion of DNA:

1. Digest 10-20 µg of genomic DNA in 150 µl final volume containing:

- 1X BSA

- 1X enzyme buffer

- 100-120 units of each restriction enzyme (half of the amount is added after 30 min of incubation at 37°C).

2. Digest for 6h to overnight at 37oC.

3. Add 1/8V(19 µl) KAc 2.5 M pH=6 (autoclaved) and 1V (169 µl) of Isopropanol 100% at RT

4. Invert tube delicately

5. Cfg. a 14000rpm for 10 min at RT

6. Wash with 0.5ml Ethanol 75%

7. Discard supernatant, fast spin and remove the remaining supernatant with a yellow tip.

Resuspend in 20 µl TE 1X autoclaved. Leave from 1-2 hours at 30°C to resuspend with gentle shaking.

Digestions for 2D gel analysis were done using the following enzymes purchased from NEB BioLabs:

. - NcoI: ARS305

. - HindIII and PstI: TER302

. - EcoRI: TER704

. 1st dimension electrophoresis:

. 1. Pour 0.35% agarose gel (Low EEO agarose, without EtBr in 500 ml TBE1X*)* at 4oC.

. 2. Add 5 µl of loading dye 20X to the digested DNA that is dissolved in 20 µl of TE. Load the DNA leaving one free lane between each sample.

. 3. Run gels at 50V at room temperature (15-24 hours, depending on the size of the fragment of interest).

. 2nd dimension electrophoresis:

. 1. Stain gel in 500 ml of TBE 1X containing 15 µl EtBr 10 mg/ml in a plastic tray for about 30'. Using the 1Kb marker as reference, cut the gel in order to keep only the fragment(s) of interest. Then cut between the lanes in order to obtain individual slices for each sample.

. 2. Arrange the slices in a new tray allowing 10-12 cm of space for the second dimension migration.

. 3. Pour the second dimension gel at room temperature (0.9% low EEO agarose, 1X TBE, 15 µl EtBr) and wait 30 min for complete solidification.

. 4. For each gel prepare 2 L of cold TBE 1X supplemented with 60 µl EtBr.

. 5. Run the electrophoresis at 4°C with the following settings: 180V, max 140 mA, 7-9h (time depends on the size of the fragment of interest)

. Southern blot:

. 1. Transfer gels to glass trays and treat as follows with agitation:

. - HCl 0.25 N (1 x 7min**)**

. - Denaturing solution (0.5 M NaOH, 1.5 M NaCl) (1 x 20 min)

. - Blot#2 (1 M ammonium acetate, 0.02 M NaOH; prepared fresh) (1 x 20min)

. 2. Equilibrate genescreen membrane in SSC 10x.

. 3. Build southern blot transfer with the following order: 3M paper, gel, genescreen membrane, wet 3M paper, dry 3M paper, towels transfer and 1kg weight on the top.

. 4. At the end of the transfer dry the membranes with clean 3 M paper and crosslink the DNA by UV irradiation (autocrosslinking program, with 265 nm UV lamps on *Stratalinker*).

. Probes : Oligonucleotides used to amplify the probes by PCR and used for 2D gels and PFGE.

. **ARS305**

. ARS305F: CTCCGTTTTTAGCCCCCCGTG

. ARS305R: GATTGAGGCCACAGCAAGACCG

. Alternativerly for ARS305 -a 3 kb BamHI (38606 bp) –NcoI (41670 bp) fragment containing origin of replication *ARS305* (39159 – 39706 bp).

TER302 chromosome III from 91974 to 93001 bp. Amplified with oligos:

. TER302Fw: GAAGGTTCAACATCAATTGATTGATTCTGCCGCCATGATC

. TER302Rv: GCTTCCCTAGAACCTTCTTATGTTTTACATGCGCTGGGTA

. **TER704 :** chromosome VII from 496097 to 497366 bp. Amplified with oligos:

. TER704Fw: TGTGCACATCTTGCCCATTA

. TER704Rv: GCCTCTATCACTGCAAAGTG

***TER102* probe**, chromosome I from 153316 to 154434 bp. Amplified with oligos:

TER102 Fw: TCTGCGCCAAGCAAAGATTC

TER102 Rv : TTTCCTTGCGTCTGATTCGG

***TER603* probe**, chromosome VI from 183324 to 184552 bp. Amplified with oligos:

TER603 Fw : GAATGCCCGAGCCCTAAAAA

TER603 Rv: ATGTGAGCCATCTGGAAAGG

***TER802* probe**, chromosome VIII from 126307 to 127436 bp. Amplified with oligos:

TER802 Fw: CTGAGACAAAGTCTTTCCAG

TER802 Rv : CGAAAGCCTTCTTGACGACT

.

. **Southern blot method: Hybridization of the filters with probe during 2D/PFGE protocols.**

. 1. Add 30 ml of Perfecthyb plus solution (Sigma) to the tubes and warm-up at 65°C for 30 min.

. 2. Wash filter with 10X SCC, then position them in the hybridization tube Incubate at 65°C for at least 1 hour, until probe is ready.

. 3. Prepare the radioactive probe using prime-a-gene labelling kit (Promega). Boil the DNA with water for 10min before adding the rest of the reagents.

. - 50 ng of DNA

. - 30.4 ml H20

. - 10 ml Buffer

. - 2 ml BSA

. - 0.7 ml of dATP, dTTP, dGTP solutions

. - 3-5 units of Klenow DNA polymerase

. - 50 µcurie of radioactive a-dCTP

. Incubate at RT for at least 1 hour to allow incorporation of the radioactive nucleotides in

the DNA fragments.

. 4. Clean DNA from unbounded dCTP using the G50 column (1st centrifuge 3000 rpm 1', change tube, add reaction, wait 1-2' and spin again).

. 5. Boil the labeled DNA (the flow through) and ssDNA for 10 min and add them to the hybridization tube.

. 6. Incubate the tubes at 65°C for at least 6 h in constant rotation prior to washing.

. Washing of the filters:

. 1. Prepare for each tube 500ml *Washing Solution I* and 1000 ml *Washing Solution II*

.	*Washing solution I (65°C)*		*Washing Solution II (42°C)*	
.	*SSC 2x*	*50ml SSC 20x*	*SSC 0.1x*	*5ml SSC 20x*
.	*SDS 1%*	*25ml SDS 20%*	*SDS 0.1%*	*5ml SDS 20%*
.	*Final volume*	*500ml H2O*	*Final volume*	*1000ml H2O*

2. Wash the filters in the following order:

50 ml *Wash Sol. I* at 65°C in tube	10 min, tube rotation
450 ml *Wash Sol. I* at 65°C in tube	15 min with agitation
500 ml *Wash Sol. II* at 42°C in a tray	15 min with agitation
500 ml *Wash Sol. II* a 42°C in a tray	15 min with agitation

3. Dry the filters with 3M paper, cover with saran wrap and expose to a storage phosphor screen in an appropriate cassette.

. **4.17 PFGE procedure:**

. Pulse Field Gel Electrophoresis (PFGE) is a technique that enables the resolution of DNA molecules up to several million base pairs in length (Birren et al., 1989; Lai et al., 1989).

. Solutions:

. 1% Pulse Field Certified Agarose (PFCA), BIO-RAD #162-0137

. SCE Solution: 1 M Sorbitol, 0.1 M Sodium Citrate, 0.06 M EDTA pH 8.0

. Solution I: SCE, 0.2% β-mercaptoethanol, 1 mg/ml Zymolyase (100 U/ml)

. Solution II: 0.5 M EDTA pH 8.0, 0.1% Sarkosyl, 1 mg/ml Proteinase K

. Preparation of the DNA plugs:

. Melt 1% PFCA and store in a both at 50°C.

. Re-suspend the cells in Solution I (50 µl for each plug).

. Add an equal volume of 50°C molten PFCA and mix with a pipette.

. Fill plug-cast (BIOR-RAD) with cell/agarose mix (approximately 90 µl per plug).

. Leave the cast for 20 minutes at RT and 10 minutes at 4°C.

. Eject the plugs in a 50 ml Falcon tube and cover them with Solution I (~ 0.5 ml for plug.

. Leave at 37°C for 1 hour.

. Gently remove Solution I and wash the plugs with an abundant volume of 0.5 M EDTA pH 8.0.

. Re-suspend the plugs with Solution II (0.5 ml/plug) and incubate O/N at 37°C.

. Discard the Solution II and wash 3 times with an abundant volume of 1X TE pH 8.0.

. Transfer the plugs in a new 50 ml falcon tube and wash for 2 hours with 1X TE pH 8.0 on a rotating wheel.

. Transfer the plugs that you do not analyse in a 50 ml falcon tube and cover them with 1X TE pH 8.0. The plugs can be stored indefinitely at 4°C.

. Transfer the plugs that you wish to analyse in an Eppendorf tube and equilibrate them for 1 hour in the running buffer of the gel (0.5 X TBE) on a rotating wheel.

. Electrophoresis is performed on a 1% pulse field agarose gel for 16 hours at 200 V with 60 sec pulses followed by 90 sec pulses in 0.5 X TBE at 14°C (Gene Navigator System, Amersham).

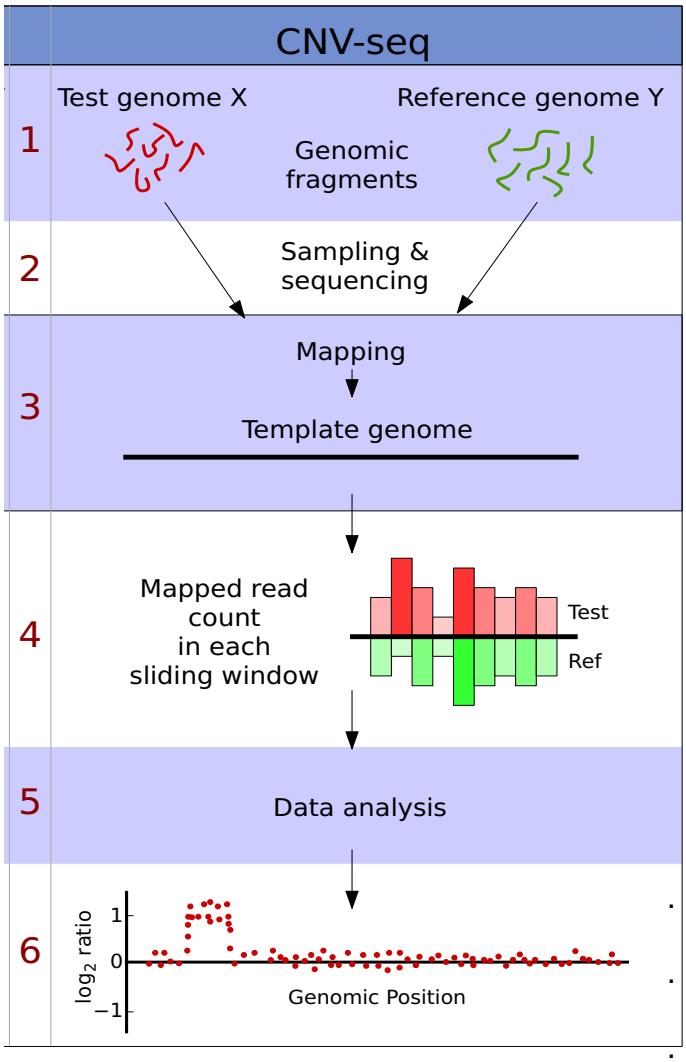
. The gel is then coloured with 0.3 µg /ml Ethidium Bromide for 30 min and then subjected to Southern blot. The membrane is then hybridized with a radiolabeled probe against specific region on the chromosome.

.

.

. **4.18 Scoring Copy number variation with Next generation sequencing**

. DNA copy number variation (CNV) has long been known as a source of genetic variation, but its importance has only been recognized recently



Model 4.2: adapted and modified from (Chao Xie and Martti Tammi. CNV-seq, a new method to detect copy number variation using high-throughput sequencing. *BMC Bioinformatics*, 10(1):80, Mar 2009.)

. 1. Starting material in case of CNV-seq is genomic fragments from two wt and reference condition 2. In CNV-seq the fragments are samples and sequenced. 3. Genomic fragments, In CNV-seq the mapping is performed by sequence alignment. 4. In CNV-seq the number of mapped reads are counted directly. 5. Data analysis, including estimation of copy number ratios, confidence values, etc. 6. Output of the results.

. <u>Genomic DNA preparation:</u>

Genomic DNA extraction with the Qiagen genomic Kit as mentioned in 3.15. Further genomic DNA was sonicated to the medium length of 100-150 bp and proceeded for one end NGS using Ion Proton sequencing platform.

<u>For Ion Proton</u>

Libraries for were prepared following the manufacturer protocols for genome sequencing with the Ion Proton sequencer (Thermo Fisher Scientific/Life Technologies).

Briefly 1ug of fragmented DNA was end repaired and adapter ligated using the KAPABiosystems® Library Prep kir for Ion Torrent™ (KAPABiosystems, inc) and adapter barcode KAPA for Ion Torrent 1-16 .

After adapter ligation each sample was size selected using AMPure XP Bead (Beckman Coulter, inc). An amplification reaction was set up in a final volume of 50ul .

A SPRI cleanup with a 1.5X Bead:DNA ratio was performed post amplification and final libraries were eluted in 25ul.

Libraries were quantified on Qubit fluorometer with HS DNA (Thermo Fisher Scientific/Life Technologies) and checked for size on an Agilent Bioanalyzer with HS DNA kit (Agilent, Santa Clara, CA).

Each size selected library was diluted according to the final concentration of 11 pM and clonally amplified using the Ion Proton™ Hi-Q™Template Kit (Thermo Fisher Scientific/Life Technologies) with IonOneTouch 2 instrument (Thermo Fisher Scientific/Life Technologies) .

After emulsion PCR, DNA positive ISPs were recovered and enriched according to standard protocols with the IonOneTouch ES Instrument (Thermo Fisher Scientific/Life Technologies).

A sequencing primer was annealed to DNA positive ISPs and the sequencing polymerase bound, prior to loading of ISPs into Ion P1 sequencing chips.

Sequencing of the samples was conducted according to the Ion Proton™ Hi-Q Sequencing Kit Protocol. One P1 sequencing chips with 10 libraries were loaded and run on an Ion Proton sequencer.

Scoring for copy number variations (CNVs)

. The following steps are used to process the Copy number variation data generated from ion proton system:

. The quality check is performed for raw data using FASTX-Toolkit [1], with minimum 30 percentage of read containing above 20 quality score are filtered and considered further for the analysis.

. Alignment is performed using tmap [2] software, where yeast reference genome 2011 version (sacCer3) is used to align the filtered raw reads to obtain the bam file. The aligned bam files are then sorted using the samtools.

. The best-hit file is generated which contains the best mapping location of each read from the alignment file. The cnv-seq [3] package in R is used to call the CNVs by comparing the best hit file of wild-type (Reference) with respective to best hit file of knock down (Test) conditions. The cnv-seq calculates the sliding window size based on the log2 threshold (0.6) and p-value (0.001) given by the user. For each calculated window, the number of mapped hits is counted, normalized and ratio is calculated with respective to reference in order to obtain CNVs.

. The CNVs for each knocked down conditions are compared with the functional sites such as Termination, replication origin, high transcribing ORFs, fragile sites, hybrids and protein sites etc. Fisher exact test from bedtools [4] is used to calculate the p-value using CNVs and functional sites along with the respective chromosome lengths. Customized python and R-scripts are used for the graph generation and statistical calculations.

. http://hannonlab.cshl.edu/fastx_toolkit/index.html

. https://github.com/iontorrent/TMAP

. CNV-seq, a new method to detect copy number variation using high-throughput sequencing

. http://bedtools.readthedocs.io/en/latest/content/tools/fisher.html

.

.

5. Discussion:

Mechanisms driving genomic instability in cancer are matter of intense interest. Genome instability is without a doubt one of the hallmarks of cancers and has a causative role not only on cancer onset but also on cancer progression. It is also becoming clear that most of the events causing genome instability arise in response to replication stress. In particular, S phase transcription can easily lead to genotoxicity, due to the interference with fork progression (Negrini, Gorgoulis et al. 2010, Macheret and Halazonetis 2015). Common fragile sites (CFSs) are chromosomal regions known as hotspots for breakage and chromosomal rearrangements under DNA replication stress (Tsantoulis, Kotsinas et al. 2008, Ying, Minocherhomji et al. 2013). They are preferentially unstable in pre-cancerous lesions and during cancer development (Mazouzi, Velimezi et al. 2014). A common feature of CFCs is to stall replication forks, eventually leading to aberrant fork transitions and fork collapse (GCRs)(Sarni and Kerem 2016). The link between natural chromosomal pausing sites (NCPs), CFSs expression and genome rearrangements (GCRs) is poorly understood and needs mechanistic studies (GCRs)(Casper, Nghiem et al. 2002, Arlt, Xu et al. 2004). Genomic deletions and amplifications are very common features in cancer cells and often overlap with CFSs.

Prolonged fork pausing and stalling at CFSs can lead to replication defects and DDR activation (Aguilera and Garcia-Muse 2013).

This study aims at elucidating the key factors and pathways protecting the integrity of CFSs using yeast as a model system. Our working hypothesis is that the topological stress building up on replicating chromosomes, when forks encounter transcription, when forks merge at termination, or as a result of unscheduled condensation events, may cause fork collapse. Our expectation is that CFSs are hot spots for topological stress.

.

5.1. Checkpoint kinases counteract fragility of endogenous natural pausing elements and TERs.

The replication checkpoint represents a cancer barrier in response to oncogene induced replication stress (Bartkova, Rezaei et al. 2006, Di Micco, Fumagalli et al. 2006, Durkin, Arlt et al. 2006). We mimicked replication stress using low doses of HU and found that rDNA, telomeres and TERs represent hot spots for CNVs. rDNA, telomeres and TER zones are common features: these are genomic regions that undergo tremendous topological stress and extensive fork pausing, followed by termination. In fact, Top2 assists their replication. These findings indicate that these genomic loci are intrinsically prone to breakage and

rearrangements. This is consistent with the finding that TERs have been isolated also in genetic screens aimed at identifying yeast fragile sites (Song, Dominska et al. 2014, Yin, Dominska et al. 2017).

The fragility of these sites is greatly enhanced in checkpoint mutants. This finding likely reflects the observation that in checkpoint defective cells Top2 has aberrant activities leading to DNA break formation (Cha and Kleckner 2002, Hashash, Johnson et al. 2011, Hashash, Johnson et al. 2012). Checkpoint defective cells also exhibited rearrangements at a subset of replication origins. This result may reflect the finding that checkpoint defective mutants experiencing replication stress collapse those forks arising at early origins (Lopes, Cotta-Ramusino et al. 2001). Moreover, we observed strong accumulation of CNVs at transcribed genes in checkpoint mutants, likely due to their inability to uncouple transcription from gene gating, thus leading to topological stress and fork reversal (Bermejo, Capra et al. 2011, Bermejo, Kumar et al. 2012, Bermejo, Lai et al. 2012).

It is possible that when forks collapse, specialized replication-coupled repair pathways may take over, leading to further rearrangements. This could be the case for MM-BIR (Micro-homology Mediated Break Induced Replication) at transcribing loci and for IFSA (Inter-Fork Strand Annealing) at repeat regions (Costantino, Sotiriou et al. 2014, Vasianovich, Harrington et al. 2014). Such fork failures would be expected to occur more often when cells experience global replication stress (Arlt, Rajendran et al. 2012), as all forks would be impacted. Fork stalling biased by obstacle on leading and lagging strands might cause single-fork failure, if the lesion burden were low. If a collapsed fork is not rescued, another nearby fork might engage in restart mechanisms that would find another region to use as the template, thus leading to template switching replication, or trigger break induced replication (BIR) (Hastings, Ira et al. 2009, Ruff, Donnianni et al. 2016, Sotiriou, Kamileri et al. 2016, Morrow, Nguyen et al. 2017).

TER zones are characterized by the presence of transcription loops that cause polar replication pausing. These topological structures are simplified in S phase by Top2 activity that acts at the base of the loops (Bermejo, Capra et al. 2011). On the other hand, the coupling between mRNA transcription and mRNA export generates further topological complexity. In this scenario, termination zones represent “the perfect storm” for incoming forks. The function of the checkpoint kinases is therefore critical at TERs, as they will have to control Top2 activity and inhibit the mRNA export, in order to detach transcribed chromatin from the nuclear envelope.

5.2 Condensin complex control fragility at natural chromosomal pausing sites and TERs.

Our data suggest a role for condensins in transcription-coupled activities. Ongoing transcription would generate nucleosome free regions that may favor condensation activities, particularly considering that condensins are recruited in the proximity of TSS and TTS. Hence, condensing activities must be highly coordinated in order to prevent unscheduled condensation events. Notably, while condensins bind TSS and TTS already in G1, Top2 binds the same regions specifically in S phase (Bermejo, Capra et al. 2009). It is tantalizing to speculate that the checkpoint kinases play a key role in restraining the activities of condensins and Top2 at transcribed genes in S phase, in order to prevent premature condensation. Interestingly, DNA break formation at yeast natural pausing sites following checkpoint inactivation depends on condensins and Top2 (Cha and Kleckner 2002, Hashash, Johnson et al. 2012). In this scenario, TER zones that contain transcribed genes and facilitate fork converging may represent hot spots for condensation.

Our data also suggest that topological stress correlates with the presence of RNA-DNA hybrids. This is consistent with the view that these hybrids have a tendency to form in the proximity of under-wound DNA. Whether the RNA-DNA hybrids at negative supercoiled regions play a causative role in generating rearrangements or, rather, they protect the unwound duplex, remains to be elucidated.

5.3. Rrm3 is required for fork protection at natural pausing sites and TERs.

Cells lacking the Rrm3p DNA helicase increase replication fork pausing at over 1,000 sites scattered throughout the genome. Depending on the genomic loci, broken replication forks are also readily detected in *rrm3* cells (Ivessa, Zhou et al. 2000, Ivessa, Zhou et al. 2002, Ivessa, Lenzmeier et al. 2003). Here we explored the role of Rrm3 in suppressing R-loop accumulation at natural pausing sites and TERs. From yeasts to humans, R-loops have been suggested to cause DNA damage at RNA Pol II transcribed genes. However, it is unclear whether all R-loops behave similarly, or whether certain loci, in certain genetic backgrounds accumulate genotoxic species of R-loops. Our data suggest that Rrm3 counteracts the accumulation of RNA-DNA hybrids that may hamper fork progression and integrity.

Rrm3 has been implicated in assisting replication termination (Fachinetti, Bermejo et al. 2010). However, even in the total absence of Rrm3, termination can still occur, although less efficiently. We speculated that other yet unidentified helicases might substitute for the

absence of Rrm3. Rrm3 has been implicated in several processes and exhibits positive and negative genetic interactions with a variety of genome integrity pathways. We speculated that the ideal candidate for substituting Rrm3 in mediating replication termination should be a helicase involved in counteracting RNA-DNA hybrids and interacting genetically with *RRM3*. We therefore focused our studies on Sen1.

5.4. Sen1 prevents R-loop accumulation at TERs and collaborates with Rrm3 in mediating replication termination.

While both Rrm3 and Sen1 have been shown to travel with the replication machinery, Sen1 has also a role in transcription termination (Ivessa, Zhou et al. 2002, Arndt and Reines 2015, Fasken, Laribee et al. 2015, Martin-Tumasz and Brow 2015, Porrua and Libri 2015, Rossi, Ajazi et al. 2015, Syed, Desler et al. 2016, Brambati, Zardoni et al. 2017). Moreover, Sen1 has been recently implicated in preventing the accumulation of RNA-DNA hybrids (Alzu, Bermejo et al. 2012).

While the understanding of the exact roles of Rrm3 and Sen1 at replication termination will require further investigations, we can conclude from our results that the absence of both helicases causes the accumulation of aberrant replication termination intermediates characterized by the presence of ss-DNA tracts. We speculate that these ss-DNA tracts may represent scars of RNA-DNA hybrids as, during the EM procedure RNA species are degraded. Hence, the failure of completing replication termination might be influenced by the inability to remove stable hybrids. This would cause the accumulation of topologically complex termination structures that would be engaged by condensation activities.

5.5. Programmed fork pausing and resolution of R-loops are key processes for TER integrity

Protein-DNA complexes mediate polar fork arrest in prokaryotic replicons as well in eukaryotes at ribosomal DNA loci. Site-specific replication fork arrest occurs in yeast (Linskens and Huberman, 1988), plants (Hernandez, Martin-Parras et al. 1993), frogs (Wiesendanger et al., 1994) and humans (Daly, Newlon et al. 1993). Replication fork barriers (RFBs) ensure the proper coordination between replication and transcription.

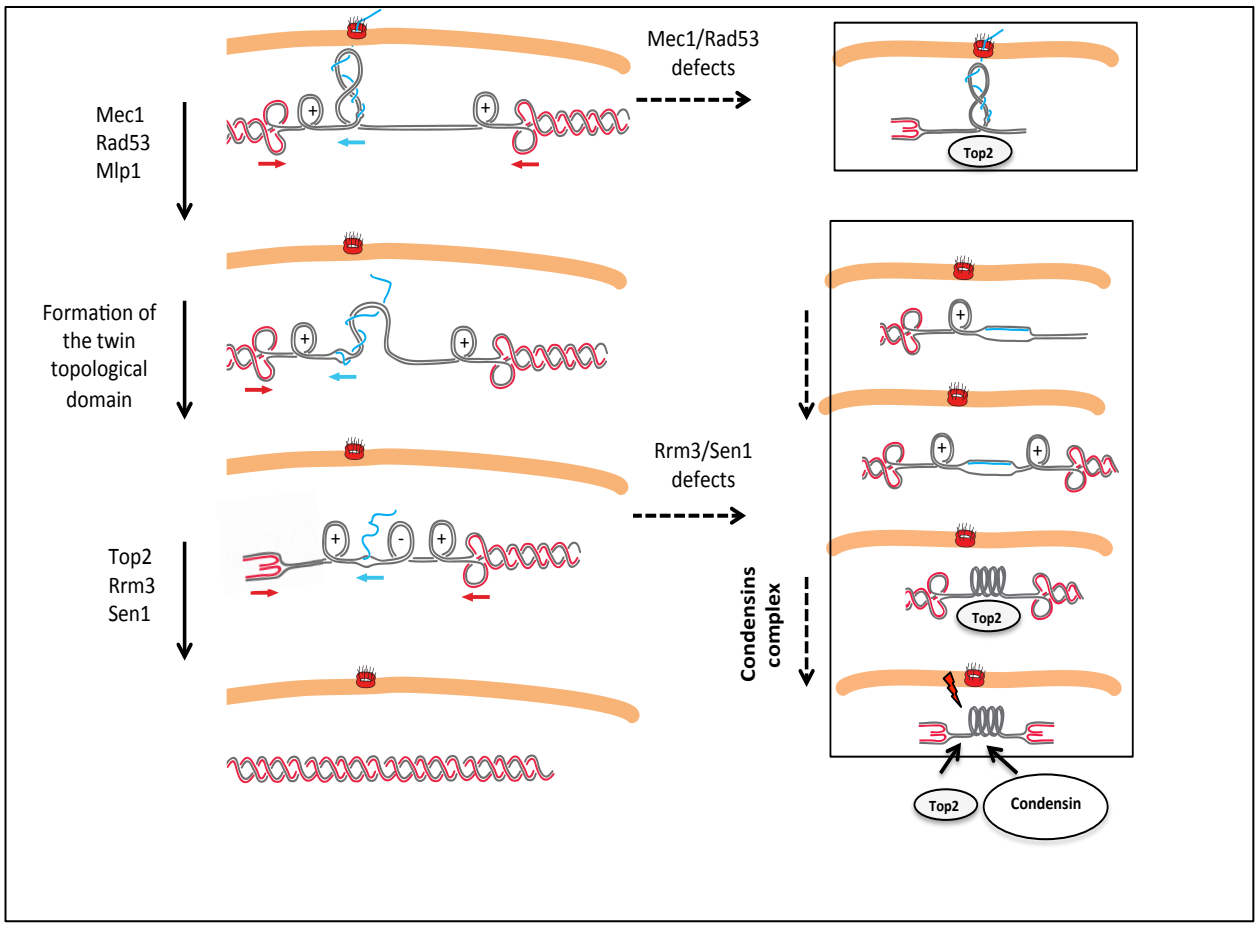
Polar fork pausing has been recently described at TERs to ensure proper replicon fusion (Fachinetti et al., 2010). 58 out of 71 *TER*s have well conserved pause sites in other yeasts. We note that *CEN*s also assist termination but they were excluded from these analyses because

they rapidly diverged in evolution (Henikoff et al., 2001). Therefore, evolution has preserved *TER*-containing pause sites integrity.

We showed that Sen1 and Rrm3 defective cells accumulating Lagging chromosomes in anaphase arrested cells and several studies in mammalian cells have shown that DNA replication stress generates DAPI-negative ultra-fine bridges (UFBs) of DNA connecting daughter nuclei during mitosis (Chan et al., 2009). As a consequence of UFBs formation, sister chromatids are interlinked creating the potentiality for generating DNA breakage and rearrangements. It has been suggested that UFBs generate where termination occurs, particularly following replication stress. In humans the Fanconi anaemia proteins FANCD2 and FANC1 and the BLM (Bloom syndrome) helicase have been involved in the metabolism of UFBs (REF).

How and whether the transcription apparatus is dismantled at TERs remains still elusive. Conflicts arising from replication and transcription collisions are inevitable. Head-on clashes between transcription and replication machineries pose additional problem due to the high topology complexity ahead of the fork (Bermejo et al., 2012). Positive supercoiling, R- loops, non-B-DNA structures formation and DNA damage may easily affect the integrity of TERs.

Based on our observations we propose a model for replication termination (Model 5.1). In Wt cells those forks clashing with the polar fork barrier represented by transcribed units transiently pause. The checkpoint machinery then detaches RNA species from the nuclear envelope. This is achieved through the phosphorylation of the Mlp1 nucleoporin (Bermejo, Capra et al. 2011, Bermejo, Kumar et al. 2012, Bermejo, Lai et al. 2012). This event generates the so-called twin topological domain at the transcribed units. It is unclear which is the fate of the transcription machinery. It is possible that the concerted action of Rrm3 and Sen1 remove transcription factors in front of the forks. These two helicases, in any case make sure that the RNA species re-anneal with the template. In checkpoint mutants, the topological stress accumulated due to the inability to detach transcribed chromatin from the nuclear envelope would cause fork reversal and aberrant Top2 activities. In the absence of Rrm3 and Sen1, RNA species would form hybrids with the template, although this situation might be transient as condensins and Top2 activity may soon take over generating unscheduled condensation events.



Model 5.1: Different steps of events at TERs preserving genomic integrity.

In checkpoint mutants, the topological stress accumulated due to the inability to detach transcribed chromatin from the nuclear envelope would cause fork reversal and aberrant Top2 activities. In the absence of Rrm3 and Sen1, RNA species would form hybrids with the template, although this situation might be transient as condensins and Top2 activity may soon take over generating unscheduled condensation events. The model represents replication fork fusion at *TER* with a gene gating as a threat for replication fork progression. Direction of replication forks (red) and transcribed mRNA (blue) are depicted by the arrows. The left panel represents a physiological situation with functional checkpoint genes (Mec1 and Rad53) and replicative helicases (Sen1 and Rrm3). The right panel refers to a pathological situation in the absence of functional Mec1/Rad53 or defective Sen1 and Rrm3. Shown unscheduled condensation by condensins and Top2 activity at TERs.

6. References:

Ahn, J. S., F. Osman and M. C. Whitby (2005). "Replication fork blockage by RTS1 at an ectopic site promotes recombination in fission yeast." EMBO J **24**(11): 2011-2023.

Alzu, A., R. Bermejo, M. Begnis, C. Lucca, D. Piccini, W. Carotenuto, M. Saponaro, A. Brambati, A. Cocito, M. Foiani and G. Liberi (2012). "Senataxin associates with replication forks to protect fork integrity across RNA-polymerase-II-transcribed genes." Cell **151**(4): 835-846.

Aparicio, O. M., D. M. Weinstein and S. P. Bell (1997). "Components and dynamics of DNA replication complexes in S. cerevisiae: redistribution of MCM proteins and Cdc45p during S phase." Cell **91**(1): 59-69.

Appelgren, H., B. Kniola and K. Ekwall (2003). "Distinct centromere domain structures with separate functions demonstrated in live fission yeast cells." J Cell Sci **116**(Pt 19): 4035-4042.

Araki, H., S. H. Leem, A. Phongdara and A. Sugino (1995). "Dpb11, which interacts with DNA polymerase II(epsilon) in Saccharomyces cerevisiae, has a dual role in S-phase progression and at a cell cycle checkpoint." Proc Natl Acad Sci U S A **92**(25): 11791-11795.

Arlt, M. F. and T. W. Glover (2010). "Inhibition of topoisomerase I prevents chromosome breakage at common fragile sites." DNA Repair (Amst) **9**(6): 678-689.

Arning, L., L. Schols, H. Cin, M. Souquet, J. T. Epplen and D. Timmann (2008). "Identification and characterisation of a large senataxin (SETX) gene duplication in ataxia with ocular apraxia type 2 (AOA2)." Neurogenetics **9**(4): 295-299.

Bairwa, N. K., B. K. Mohanty, R. Stamenova, M. J. Curcio and D. Bastia (2011). "The intra-S phase checkpoint protein Tof1 collaborates with the helicase Rrm3 and the F-box protein Dia2 to maintain genome stability in Saccharomyces cerevisiae." J Biol Chem **286**(4): 2445-2454.

Bairwa, N. K., S. Zzaman, B. K. Mohanty and D. Bastia (2010). "Replication fork arrest and rDNA silencing are two independent and separable functions of the replication terminator protein Fob1 of Saccharomyces cerevisiae." J Biol Chem **285**(17): 12612-12619.

Barlow, J. H., R. B. Faryabi, E. Callen, N. Wong, A. Malhowski, H. T. Chen, G. Gutierrez-Cruz, H. W. Sun, P. McKinnon, G. Wright, R. Casellas, D. F. Robbiani, L. Staudt, O. Fernandez-Capetillo and A. Nussenzweig (2013). "Identification of early replicating fragile sites that contribute to genome instability." Cell **152**(3): 620-632.

Bartek, J., J. Bartkova and J. Lukas (2007). "DNA damage signalling guards against activated oncogenes and tumour progression." Oncogene **26**(56): 7773-7779.

Bartek, J., J. Lukas and J. Bartkova (2007). "DNA damage response as an anti-cancer barrier: damage threshold and the concept of 'conditional haploinsufficiency'." Cell Cycle **6**(19): 2344-2347.

Bates, D. B., E. Boye, T. Asai and T. Kogoma (1997). "The absence of effect of gid or mioC transcription on the initiation of chromosomal replication in Escherichia coli." Proc Natl Acad Sci U S A **94**(23): 12497-12502.

Baxter, J. and J. F. Diffley (2008). "Topoisomerase II inactivation prevents the completion of DNA replication in budding yeast." Mol Cell **30**(6): 790-802.

Beckta, J. M., S. M. Dever, N. Gnawali, A. Khalil, A. Sule, S. E. Golding, E. Rosenberg, A. Narayanan, K. Kehn-Hall, B. Xu, L. F. Povirk and K. Valerie (2015). "Mutation of the BRCA1 SQ-cluster results in aberrant mitosis, reduced homologous recombination, and a compensatory increase in non-homologous end joining." Oncotarget **6**(29): 27674-27687.

Bell, S. P. and B. Stillman (1992). "ATP-dependent recognition of eukaryotic origins of DNA replication by a multiprotein complex." Nature **357**(6374): 128-134.

Bermejo, R., T. Capra, V. Gonzalez-Huici, D. Fachinetti, A. Cocito, G. Natoli, Y. Katou, H. Mori, K. Kurokawa, K. Shirahige and M. Foiani (2009). "Genome-organizing factors Top2 and Hmo1 prevent chromosome fragility at sites of S phase transcription." Cell **138**(5): 870-884.

Bermejo, R., Y. Doksani, T. Capra, Y. M. Katou, H. Tanaka, K. Shirahige and M. Foiani (2007). "Top1- and Top2-mediated topological transitions at replication forks ensure fork progression and stability and prevent DNA damage checkpoint activation." Genes Dev **21**(15): 1921-1936.

Bermejo, R., A. Kumar and M. Foiani (2012). "Preserving the genome by regulating chromatin association with the nuclear envelope." Trends Cell Biol **22**(9): 465-473.

Bermejo, R., M. S. Lai and M. Foiani (2012). "Preventing replication stress to maintain genome stability: resolving conflicts between replication and transcription." Mol Cell **45**(6): 710-718.

Bhatia, V., S. I. Barroso, M. L. Garcia-Rubio, E. Tumini, E. Herrera-Moyano and A. Aguilera (2014). "BRCA2 prevents R-loop accumulation and associates with TREX-2 mRNA export factor PCID2." Nature **511**(7509): 362-365.

Bhatia, V., E. Herrera-Moyano, A. Aguilera and B. Gomez-Gonzalez (2017). "The Role of Replication-Associated Repair Factors on R-Loops." Genes (Basel) **8**(7).

Branzei, D. and M. Foiani (2009). "The checkpoint response to replication stress." DNA Repair (Amst) **8**(9): 1038-1046.

Branzei, D. and M. Foiani (2010). "Leaping forks at inverted repeats." Genes Dev **24**(1): 5-9.

Branzei, D. and M. Foiani (2010). "Maintaining genome stability at the replication fork." Nat Rev Mol Cell Biol **11**(3): 208-219.

Brill, S. J., S. DiNardo, K. Voelkel-Meiman and R. Sternglanz (1987). "DNA topoisomerase activity is required as a swivel for DNA replication and for ribosomal RNA transcription." NCI Monogr(4): 11-15.

Brill, S. J., S. DiNardo, K. Voelkel-Meiman and R. Sternglanz (1987). "Need for DNA topoisomerase activity as a swivel for DNA replication for transcription of ribosomal RNA." Nature **326**(6111): 414-416.

Canman, C. E. (2001). "Replication checkpoint: preventing mitotic catastrophe." Curr Biol **11**(4): R121-124.

Casper, A. M., P. W. Greenwell, W. Tang and T. D. Petes (2009). "Chromosome aberrations resulting from double-strand DNA breaks at a naturally occurring yeast fragile site composed of inverted ty elements are independent of Mre11p and Sae2p." Genetics **183**(2): 423-439, 421SI-426SI.

Castan, A., P. Hernandez, D. B. Krimer and J. B. Schvartzman (2018). "DNA Catenation Reveals the Dynamics of DNA Topology During Replication." Methods Mol Biol **1703**: 75-86.

Castel, S. E., J. Ren, S. Bhattacharjee, A. Y. Chang, M. Sanchez, A. Valbuena, F. Antequera and R. A. Martienssen (2014). "Dicer promotes transcription

termination at sites of replication stress to maintain genome stability." Cell **159**(3): 572-583.
Cerritelli, S. M. and R. J. Crouch (2009). "Ribonuclease H: the enzymes in eukaryotes." FEBS J **276**(6): 1494-1505.
Cheng, E., J. A. Vaisica, J. Ou, A. Baryshnikova, Y. Lu, F. P. Roth and G. W. Brown (2012). "Genome rearrangements caused by depletion of essential DNA replication proteins in Saccharomyces cerevisiae." Genetics **192**(1): 147-160.
Conde, F. and P. A. San-Segundo (2008). "Role of Dot1 in the response to alkylating DNA damage in Saccharomyces cerevisiae: regulation of DNA damage tolerance by the error-prone polymerases Polzeta/Rev1." Genetics **179**(3): 1197-1210.
Costantino, L., S. K. Sotiriou, J. K. Rantala, S. Magin, E. Mladenov, T. Helleday, J. E. Haber, G. Iliakis, O. P. Kallioniemi and T. D. Halazonetis (2014). "Break-induced replication repair of damaged forks induces genomic duplications in human cells." Science **343**(6166): 88-91.
Costanzo, V. and J. Gautier (2003). "Single-strand DNA gaps trigger an ATR- and Cdc7-dependent checkpoint." Cell Cycle **2**(1): 17.
Crefcoeur, R. P., O. Zgheib and T. D. Halazonetis (2017). "A Model to Investigate Single-Strand DNA Responses in G1 Human Cells via a Telomere-Targeted, Nuclease-Deficient CRISPR-Cas9 System." PLoS One **12**(1): e0169126.
Cuvier, O., S. Stanojcic, J. M. Lemaitre and M. Mechali (2008). "A topoisomerase II-dependent mechanism for resetting replicons at the S-M-phase transition." Genes Dev **22**(7): 860-865.
D'Ambrosio, C., G. Kelly, K. Shirahige and F. Uhlmann (2008). "Condensin-dependent rDNA decatenation introduces a temporal pattern to chromosome segregation." Curr Biol **18**(14): 1084-1089.
D'Ambrosio, C., C. K. Schmidt, Y. Katou, G. Kelly, T. Itoh, K. Shirahige and F. Uhlmann (2008). "Identification of cis-acting sites for condensin loading onto budding yeast chromosomes." Genes Dev **22**(16): 2215-2227.
Dal Cin, P. and A. A. Sandberg (1989). "Chromosomal aspects of human oncogenesis." Crit Rev Oncog **1**(2): 113-126.
Dewar, J. M. and J. C. Walter (2017). "Mechanisms of DNA replication termination." Nat Rev Mol Cell Biol **18**(8): 507-516.
DiNardo, S., K. Voelkel and R. Sternglanz (1984). "DNA topoisomerase II mutant of Saccharomyces cerevisiae: topoisomerase II is required for segregation of daughter molecules at the termination of DNA replication." Proc Natl Acad Sci U S A **81**(9): 2616-2620.
Dominguez-Sanchez, M. S., S. Barroso, B. Gomez-Gonzalez, R. Luna and A. Aguilera (2011). "Genome instability and transcription elongation impairment in human cells depleted of THO/TREX." PLoS Genet **7**(12): e1002386.
Duch, A., G. Palou, Z. O. Jonsson, R. Palou, E. Calvo, J. Wohlschlegel and D. G. Quintana (2011). "A Dbf4 mutant contributes to bypassing the Rad53-mediated block of origins of replication in response to genotoxic stress." J Biol Chem **286**(4): 2486-2491.
Durkin, S. G. and T. W. Glover (2007). "Chromosome fragile sites." Annu Rev Genet **41**: 169-192.
Ekwall, K., J. P. Javerzat, A. Lorentz, H. Schmidt, G. Cranston and R. Allshire (1995). "The chromodomain protein Swi6: a key component at fission yeast centromeres." Science **269**(5229): 1429-1431.

El Hage, A., S. L. French, A. L. Beyer and D. Tollervey (2010). "Loss of Topoisomerase I leads to R-loop-mediated transcriptional blocks during ribosomal RNA synthesis." Genes Dev **24**(14): 1546-1558.

Elledge, S. J. (1996). "Cell cycle checkpoints: preventing an identity crisis." Science **274**(5293): 1664-1672.

Enukashvili, N. I., I. S. Kuznetsova and O. I. Podgornaia (2003). "[The mammalian centromere organization]." Tsitologiia **45**(3): 255-270.

Errico, A. and V. Costanzo (2012). "Mechanisms of replication fork protection: a safeguard for genome stability." Crit Rev Biochem Mol Biol **47**(3): 222-235.

Eykelenboom, J. K., E. C. Harte, L. Canavan, A. Pastor-Peidro, I. Calvo-Asensio, M. Llorens-Agost and N. F. Lowndes (2013). "ATR activates the S-M checkpoint during unperturbed growth to ensure sufficient replication prior to mitotic onset." Cell Rep **5**(4): 1095-1107.

Fachinetti, D., R. Bermejo, A. Cocito, S. Minardi, Y. Katou, Y. Kanoh, K. Shirahige, A. Azvolinsky, V. A. Zakian and M. Foiani (2010). "Replication termination at eukaryotic chromosomes is mediated by Top2 and occurs at genomic loci containing pausing elements." Mol Cell **39**(4): 595-605.

Falaschi, A. (2009). "Binding of DNA topoisomerases I and II to replication origins." Methods Mol Biol **582**: 131-143.

Fernandez-Capetillo, O. and A. Nussenzweig (2013). "Naked replication forks break apRPArt." Cell **155**(5): 979-980.

Fierro-Fernandez, M., P. Hernandez, D. B. Krimer, A. Stasiak and J. B. Schvartzman (2007). "Topological locking restrains replication fork reversal." Proc Natl Acad Sci U S A **104**(5): 1500-1505.

Foiani, M., G. Liberi, G. Lucchini and P. Plevani (1995). "Cell cycle-dependent phosphorylation and dephosphorylation of the yeast DNA polymerase alpha-primase B subunit." Mol Cell Biol **15**(2): 883-891.

Franco-Echevarria, E., N. Gonzalez-Polo, S. Zorrilla, S. Martinez-Lumbreras, C. M. Santiveri, R. Campos-Olivas, M. Sanchez, O. Calvo, B. Gonzalez and J. M. Perez-Canadillas (2017). "The structure of transcription termination factor Nrd1 reveals an original mode for GUAA recognition." Nucleic Acids Res **45**(17): 10293-10305.

Gaillard, H., T. Garcia-Muse and A. Aguilera (2015). "Replication stress and cancer." Nat Rev Cancer **15**(5): 276-289.

Gallina, I., S. K. Christiansen, R. T. Pedersen, M. Lisby and V. H. Oestergaard (2016). "TopBP1-mediated DNA processing during mitosis." Cell Cycle **15**(2): 176-183.

Gama-Carvalho, M., L. G.-V. M, R. P. F, F. Besse, J. Weis, A. Voigt, J. B. Schulz and J. De Las Rivas (2017). "Linking amyotrophic lateral sclerosis and spinal muscular atrophy through RNA-transcriptome homeostasis: a genomics perspective." J Neurochem **141**(1): 12-30.

Ganem, N. J. and D. Pellman (2012). "Linking abnormal mitosis to the acquisition of DNA damage." J Cell Biol **199**(6): 871-881.

Garcia-Pichardo, D., J. C. Canas, M. L. Garcia-Rubio, B. Gomez-Gonzalez, A. G. Rondon and A. Aguilera (2017). "Histone Mutants Separate R Loop Formation from Genome Instability Induction." Mol Cell **66**(5): 597-609 e595.

Garcia-Rubio, M. L., C. Perez-Calero, S. I. Barroso, E. Tumini, E. Herrera-Moyano, I. V. Rosado and A. Aguilera (2015). "The Fanconi Anemia Pathway Protects Genome Integrity from R-loops." PLoS Genet **11**(11): e1005674.

Garg, P., C. M. Stith, N. Sabouri, E. Johansson and P. M. Burgers (2004). "Idling by DNA polymerase delta maintains a ligatable nick during lagging-strand DNA replication." Genes Dev **18**(22): 2764-2773.
Gavalda, S., J. M. Santos-Pereira, M. L. Garcia-Rubio, R. Luna and A. Aguilera (2016). "Excess of Yra1 RNA-Binding Factor Causes Transcription-Dependent Genome Instability, Replication Impairment and Telomere Shortening." PLoS Genet **12**(4): e1005966.
Gelot, C., I. Magdalou and B. S. Lopez (2015). "Replication stress in Mammalian cells and its consequences for mitosis." Genes (Basel) **6**(2): 267-298.
Geronimo, C. L. and V. A. Zakian (2016). "Getting it done at the ends: Pif1 family DNA helicases and telomeres." DNA Repair (Amst) **44**: 151-158.
Giannattasio, M. and D. Branzei (2017). "S-phase checkpoint regulations that preserve replication and chromosome integrity upon dNTP depletion." Cell Mol Life Sci **74**(13): 2361-2380.
Glover, T. W. (2006). "Common fragile sites." Cancer Lett **232**(1): 4-12.
Glover, T. W. and T. E. Wilson (2013). "Breaking news on fragile sites in cancer." Cancer Cell **23**(2): 137-139.
Glover, T. W., T. E. Wilson and M. F. Arlt (2017). "Fragile sites in cancer: more than meets the eye." Nat Rev Cancer **17**(8): 489-501.
Gomez-Gonzalez, B., I. Felipe-Abrio and A. Aguilera (2009). "The S-phase checkpoint is required to respond to R-loops accumulated in THO mutants." Mol Cell Biol **29**(19): 5203-5213.
Gomez-Gonzalez, B., M. Garcia-Rubio, R. Bermejo, H. Gaillard, K. Shirahige, A. Marin, M. Foiani and A. Aguilera (2011). "Genome-wide function of THO/TREX in active genes prevents R-loop-dependent replication obstacles." EMBO J **30**(15): 3106-3119.
Guy, L. and C. A. Roten (2004). "Genometric analyses of the organization of circular chromosomes: a universal pressure determines the direction of ribosomal RNA genes transcription relative to chromosome replication." Gene **340**(1): 45-52.
Hamza, A., E. Tammpere, M. Kofoed, C. Keong, J. Chiang, G. Giaever, C. Nislow and P. Hieter (2015). "Complementation of Yeast Genes with Human Genes as an Experimental Platform for Functional Testing of Human Genetic Variants." Genetics **201**(3): 1263-1274.
Han, Z. and O. Porrua (2017). "Helicases as transcription termination factors: Different solutions for a common problem." Transcription: 1-7.
Hartwell, L. H. and M. B. Kastan (1994). "Cell cycle control and cancer." Science **266**(5192): 1821-1828.
Hartwell, L. H. and T. A. Weinert (1989). "Checkpoints: controls that ensure the order of cell cycle events." Science **246**(4930): 629-634.
Hatchi, E., K. Skourti-Stathaki, S. Ventz, L. Pinello, A. Yen, K. Kamieniarz-Gdula, S. Dimitrov, S. Pathania, K. M. McKinney, M. L. Eaton, M. Kellis, S. J. Hill, G. Parmigiani, N. J. Proudfoot and D. M. Livingston (2015). "BRCA1 recruitment to transcriptional pause sites is required for R-loop-driven DNA damage repair." Mol Cell **57**(4): 636-647.
Hernandez, P., L. Martin-Parras, M. L. Martinez-Robles and J. B. Schvartzman (1993). "Conserved features in the mode of replication of eukaryotic ribosomal RNA genes." EMBO J **12**(4): 1475-1485.
Iraqui, I., G. Kienda, J. Soeur, G. Faye, G. Baldacci, R. D. Kolodner and M. E. Huang (2009). "Peroxiredoxin Tsa1 is the key peroxidase suppressing genome

instability and protecting against cell death in Saccharomyces cerevisiae." PLoS Genet **5**(6): e1000524.
Irony-Tur Sinai, M. and B. Kerem (2017). "DNA replication stress drives fragile site instability." Mutat Res.
Ivessa, A. S., J.-Q. Zhou and V. A. Zakian (2000). "The Saccharomyces Pif1p DNA Helicase and the Highly Related Rrm3p Have Opposite Effects on Replication Fork Progression in Ribosomal DNA." Cell **100**(4): 479-489.
Ivessa, A. S., J. Q. Zhou, V. P. Schulz, E. K. Monson and V. A. Zakian (2002). "Saccharomyces Rrm3p, a 5' to 3' DNA helicase that promotes replication fork progression through telomeric and subtelomeric DNA." Genes Dev **16**(11): 1383-1396.
Iyer, D. R. and N. Rhind (2017). "The Intra-S Checkpoint Responses to DNA Damage." Genes (Basel) **8**(2).
Iyer, D. R. and N. Rhind (2017). "Replication fork slowing and stalling are distinct, checkpoint-independent consequences of replicating damaged DNA." PLoS Genet **13**(8): e1006958.
Jay, K. A., D. L. Smith and E. H. Blackburn (2016). "Early Loss of Telomerase Action in Yeast Creates a Dependence on the DNA Damage Response Adaptor Proteins." Mol Cell Biol **36**(14): 1908-1919.
Jones, R. M., O. Mortusewicz, I. Afzal, M. Lorvellec, P. Garcia, T. Helleday and E. Petermann (2013). "Increased replication initiation and conflicts with transcription underlie Cyclin E-induced replication stress." Oncogene **32**(32): 3744-3753.
Ju, B. G., V. V. Lunyak, V. Perissi, I. Garcia-Bassets, D. W. Rose, C. K. Glass and M. G. Rosenfeld (2006). "A topoisomerase IIbeta-mediated dsDNA break required for regulated transcription." Science **312**(5781): 1798-1802.
Ju, B. G. and M. G. Rosenfeld (2006). "A breaking strategy for topoisomerase IIbeta/PARP-1-dependent regulated transcription." Cell Cycle **5**(22): 2557-2560.
Kamimura, Y., Y. S. Tak, A. Sugino and H. Araki (2001). "Sld3, which interacts with Cdc45 (Sld4), functions for chromosomal DNA replication in Saccharomyces cerevisiae." EMBO J **20**(8): 2097-2107.
Kawasaki, Y., S. Hiraga and A. Sugino (2000). "Interactions between Mcm10p and other replication factors are required for proper initiation and elongation of chromosomal DNA replication in Saccharomyces cerevisiae." Genes Cells **5**(12): 975-989.
Kim, H. D., J. Choe and Y. S. Seo (1999). "The sen1(+) gene of Schizosaccharomyces pombe, a homologue of budding yeast SEN1, encodes an RNA and DNA helicase." Biochemistry **38**(44): 14697-14710.
Kim, R. A. and J. C. Wang (1989). "Function of DNA topoisomerases as replication swivels in Saccharomyces cerevisiae." J Mol Biol **208**(2): 257-267.
Kim, R. A. and J. C. Wang (1989). "A subthreshold level of DNA topoisomerases leads to the excision of yeast rDNA as extrachromosomal rings." Cell **57**(6): 975-985.
Kondratova, A., T. Watanabe, M. Marotta, M. Cannon, A. M. Segall, D. Serre and H. Tanaka (2015). "Replication fork integrity and intra-S phase checkpoint suppress gene amplification." Nucleic Acids Res **43**(5): 2678-2690.
Kouzine, F., A. Gupta, L. Baranello, D. Wojtowicz, K. Ben-Aissa, J. Liu, T. M. Przytycka and D. Levens (2013). "Transcription-dependent dynamic supercoiling is a short-range genomic force." Nat Struct Mol Biol **20**(3): 396-403.

Krings, G. and D. Bastia (2005). "Sap1p binds to Ter1 at the ribosomal DNA of Schizosaccharomyces pombe and causes polar replication fork arrest." J Biol Chem **280**(47): 39135-39142.
Krings, G. and D. Bastia (2006). "Molecular architecture of a eukaryotic DNA replication terminus-terminator protein complex." Mol Cell Biol **26**(21): 8061-8074.
Kumar, D., J. Viberg, A. K. Nilsson and A. Chabes (2010). "Highly mutagenic and severely imbalanced dNTP pools can escape detection by the S-phase checkpoint." Nucleic Acids Res **38**(12): 3975-3983.
Kurth, I. and J. Gautier (2010). "Origin-dependent initiation of DNA replication within telomeric sequences." Nucleic Acids Res **38**(2): 467-476.
Labib, K. and G. De Piccoli (2011). "Surviving chromosome replication: the many roles of the S-phase checkpoint pathway." Philos Trans R Soc Lond B Biol Sci **366**(1584): 3554-3561.
Lang, K. S., A. N. Hall, C. N. Merrikh, M. Ragheb and H. Merrikh (2017). "Head-on replication-transcription collisions lead to formation of life threatening R-loops."
Le Beau, M. M. (1986). "Chromosomal fragile sites and cancer-specific rearrangements." Blood **67**(4): 849-858.
Lecona, E. and O. Fernandez-Capetillo (2014). "Replication stress and cancer: it takes two to tango." Exp Cell Res **329**(1): 26-34.
Lee, S. H., G. E. Siaw, S. Willcox, J. D. Griffith and T. S. Hsieh (2013). "Synthesis and dissolution of hemicatenanes by type IA DNA topoisomerases." Proc Natl Acad Sci U S A **110**(38): E3587-3594.
Lemoine, F. J., N. P. Degtyareva, K. Lobachev and T. D. Petes (2005). "Chromosomal translocations in yeast induced by low levels of DNA polymerase a model for chromosome fragile sites." Cell **120**(5): 587-598.
Leonaite, B., Z. Han, J. Basquin, F. Bonneau, D. Libri, O. Porrua and E. Conti (2017). "Sen1 has unique structural features grafted on the architecture of the Upf1-like helicase family." EMBO J **36**(11): 1590-1604.
Leonard, J., N. Sen, R. Torres, T. Sutani, A. Jarmuz, K. Shirahige and L. Aragon (2015). "Condensin Relocalization from Centromeres to Chromosome Arms Promotes Top2 Recruitment during Anaphase." Cell Rep **13**(11): 2336-2344.
Liang, C., M. Weinreich and B. Stillman (1995). "ORC and Cdc6p interact and determine the frequency of initiation of DNA replication in the genome." Cell **81**(5): 667-676.
Liberi, G. and M. Foiani (2010). "The double life of Holliday junctions." Cell Res **20**(6): 611-613.
Lin, Y. L. and P. Pasero (2017). "Transcription-Replication Conflicts: Orientation Matters." Cell **170**(4): 603-604.
Liquori, C. L., K. Ricker, M. L. Moseley, J. F. Jacobsen, W. Kress, S. L. Naylor, J. W. Day and L. P. Ranum (2001). "Myotonic dystrophy type 2 caused by a CCTG expansion in intron 1 of ZNF9." Science **293**(5531): 864-867.
Liu, B. and B. M. Alberts (1995). "Head-on collision between a DNA replication apparatus and RNA polymerase transcription complex." Science **267**(5201): 1131-1137.
Liu, L. F. and J. C. Wang (1987). "Supercoiling of the DNA template during transcription." Proc Natl Acad Sci U S A **84**(20): 7024-7027.
Madireddy, A., S. T. Kosiyatrakul, R. A. Boisvert, E. Herrera-Moyano, M. L. Garcia-Rubio, J. Gerhardt, E. A. Vuono, N. Owen, Z. Yan, S. Olson, A. Aguilera, N. G.

Howlett and C. L. Schildkraut (2016). "FANCD2 Facilitates Replication through Common Fragile Sites." Mol Cell **64**(2): 388-404.
Mankouri, H. W., D. Huttner and I. D. Hickson (2013). "How unfinished business from S-phase affects mitosis and beyond." EMBO J **32**(20): 2661-2671.
Marini, F., A. Pellicioli, V. Paciotti, G. Lucchini, P. Plevani, D. F. Stern and M. Foiani (1997). "A role for DNA primase in coupling DNA replication to DNA damage response." EMBO J **16**(3): 639-650.
Martini, E., V. Borde, M. Legendre, S. Audic, B. Regnault, G. Soubigou, B. Dujon and B. Llorente (2011). "Genome-wide analysis of heteroduplex DNA in mismatch repair-deficient yeast cells reveals novel properties of meiotic recombination pathways." PLoS Genet **7**(9): e1002305.
Mayan-Santos, M. D., M. L. Martinez-Robles, P. Hernandez, J. B. Schvartzman and D. B. Krimer (2008). "A redundancy of processes that cause replication fork stalling enhances recombination at two distinct sites in yeast rDNA." Mol Microbiol **69**(2): 361-375.
Mechali, M. (2010). "Eukaryotic DNA replication origins: many choices for appropriate answers." Nat Rev Mol Cell Biol **11**(10): 728-738.
Merchant, A. M., Y. Kawasaki, Y. Chen, M. Lei and B. K. Tye (1997). "A lesion in the DNA replication initiation factor Mcm10 induces pausing of elongation forks through chromosomal replication origins in Saccharomyces cerevisiae." Mol Cell Biol **17**(6): 3261-3271.
Merrikh, H., Y. Zhang, A. D. Grossman and J. D. Wang (2012). "Replication-transcription conflicts in bacteria." Nat Rev Microbiol **10**(7): 449-458.
Mieczkowski, P. A., F. J. Lemoine and T. D. Petes (2006). "Recombination between retrotransposons as a source of chromosome rearrangements in the yeast Saccharomyces cerevisiae." DNA Repair (Amst) **5**(9-10): 1010-1020.
Miller, K. M., O. Rog and J. P. Cooper (2006). "Semi-conservative DNA replication through telomeres requires Taz1." Nature **440**(7085): 824-828.
Million-Weaver, S., A. N. Samadpour and H. Merrikh (2015). "Replication Restart after Replication-Transcription Conflicts Requires RecA in Bacillus subtilis." J Bacteriol **197**(14): 2374-2382.
Mimura, S., T. Masuda, T. Matsui and H. Takisawa (2000). "Central role for cdc45 in establishing an initiation complex of DNA replication in Xenopus egg extracts." Genes Cells **5**(6): 439-452.
Mundbjerg, K., S. W. Jorgensen, J. Fredsoe, I. Nielsen, J. M. Pedersen, I. B. Bentsen, M. Lisby, L. Bjergbaek and A. H. Andersen (2015). "Top2 and Sgs1-Top3 Act Redundantly to Ensure rDNA Replication Termination." PLoS Genet **11**(12): e1005697.
Munoz-Galvan, S., M. Garcia-Rubio, P. Ortega, J. F. Ruiz, S. Jimeno, B. Pardo, B. Gomez-Gonzalez and A. Aguilera (2017). "A new role for Rrm3 in repair of replication-born DNA breakage by sister chromatid recombination." PLoS Genet **13**(5): e1006781.
Myung, K., C. Chen and R. D. Kolodner (2001). "Multiple pathways cooperate in the suppression of genome instability in Saccharomyces cerevisiae." Nature **411**(6841): 1073-1076.
Nakazawa, N., K. Sajiki, X. Xu, A. Villar-Briones, O. Arakawa and M. Yanagida (2015). "RNA pol II transcript abundance controls condensin accumulation at mitotically up-regulated and heat-shock-inducible genes in fission yeast." Genes Cells **20**(6): 481-499.

Newlon, C. S., I. Collins, A. Dershowitz, A. M. Deshpande, S. A. Greenfeder, L. Y. Ong and J. F. Theis (1993). "Analysis of replication origin function on chromosome III of Saccharomyces cerevisiae." Cold Spring Harb Symp Quant Biol **58**: 415-423.

Newlon, C. S. and J. F. Theis (1993). "The structure and function of yeast ARS elements." Curr Opin Genet Dev **3**(5): 752-758.

Nguyen, V. Q., C. Co and J. J. Li (2001). "Cyclin-dependent kinases prevent DNA re-replication through multiple mechanisms." Nature **411**(6841): 1068-1073.

Nick McElhinny, S. A., D. A. Gordenin, C. M. Stith, P. M. Burgers and T. A. Kunkel (2008). "Division of labor at the eukaryotic replication fork." Mol Cell **30**(2): 137-144.

Nicolas, A. and T. D. Petes (1994). "Polarity of meiotic gene conversion in fungi: contrasting views." Experientia **50**(3): 242-252.

Nowell, P. C., B. S. Emanuel, J. B. Finan, J. Erikson and C. M. Croce (1985). "Chromosome alterations in oncogenesis." Haematol Blood Transfus **29**: 253-260.

Olavarrieta, L., P. Hernandez, D. B. Krimer and J. B. Schvartzman (2002). "DNA knotting caused by head-on collision of transcription and replication." J Mol Biol **322**(1): 1-6.

Parket, A., O. Inbar and M. Kupiec (1995). "Recombination of Ty elements in yeast can be induced by a double-strand break." Genetics **140**(1): 67-77.

Paul, S., S. Million-Weaver, S. Chattopadhyay, E. Sokurenko and H. Merrikh (2013). "Accelerated gene evolution through replication-transcription conflicts." Nature **495**(7442): 512-515.

Pedersen, J. M., J. Fredsoe, M. Roedgaard, L. Andreasen, K. Mundbjerg, M. Kruhoffer, M. Brinch, M. H. Schierup, L. Bjergbaek and A. H. Andersen (2012). "DNA Topoisomerases maintain promoters in a state competent for transcriptional activation in Saccharomyces cerevisiae." PLoS Genet **8**(12): e1003128.

Peng, J., M. K. Raghuraman and W. Feng (2014). "Analysis of ssDNA gaps and DSBs in genetically unstable yeast cultures." Methods Mol Biol **1170**: 501-515.

Pidoux, A. L. and R. C. Allshire (2000). "Centromeres: getting a grip of chromosomes." Curr Opin Cell Biol **12**(3): 308-319.

Pidoux, A. L., S. Uzawa, P. E. Perry, W. Z. Cande and R. C. Allshire (2000). "Live analysis of lagging chromosomes during anaphase and their effect on spindle elongation rate in fission yeast." J Cell Sci **113 Pt 23**: 4177-4191.

Pike, J. E., P. M. Burgers, J. L. Campbell and R. A. Bambara (2009). "Pif1 helicase lengthens some Okazaki fragment flaps necessitating Dna2 nuclease/helicase action in the two-nuclease processing pathway." J Biol Chem **284**(37): 25170-25180.

Pluta, A. F., A. M. Mackay, A. M. Ainsztein, I. G. Goldberg and W. C. Earnshaw (1995). "The centromere: hub of chromosomal activities." Science **270**(5242): 1591-1594.

Poli, J., S. M. Gasser and M. Papamichos-Chronakis (2017). "The INO80 remodeller in transcription, replication and repair." Philos Trans R Soc Lond B Biol Sci **372**(1731).

Poli, J., C. B. Gerhold, A. Tosi, N. Hustedt, A. Seeber, R. Sack, F. Herzog, P. Pasero, K. Shimada, K. P. Hopfner and S. M. Gasser (2016). "Mec1, INO80, and the PAF1 complex cooperate to limit transcription replication conflicts through RNAPII removal during replication stress." Genes Dev **30**(3): 337-354.

Pomerantz, R. T. and M. O'Donnell (2010). "Direct restart of a replication fork stalled by a head-on RNA polymerase." J Vis Exp(38).
Pommier, Y., Y. Sun, S. N. Huang and J. L. Nitiss (2016). "Roles of eukaryotic topoisomerases in transcription, replication and genomic stability." Nat Rev Mol Cell Biol **17**(11): 703-721.
Popuri, V., J. Huang, M. Ramamoorthy, T. Tadokoro, D. L. Croteau and V. A. Bohr (2013). "RECQL5 plays co-operative and complementary roles with WRN syndrome helicase." Nucleic Acids Res **41**(2): 881-899.
Postow, L., N. J. Crisona, B. J. Peter, C. D. Hardy and N. R. Cozzarelli (2001). "Topological challenges to DNA replication: conformations at the fork." Proc Natl Acad Sci U S A **98**(15): 8219-8226.
Postow, L., C. Ullsperger, R. W. Keller, C. Bustamante, A. V. Vologodskii and N. R. Cozzarelli (2001). "Positive torsional strain causes the formation of a four-way junction at replication forks." J Biol Chem **276**(4): 2790-2796.
Potenski, C. J. and H. L. Klein (2011). "R we there yet? R-loop hazards to finishing the journey." Mol Cell **44**(6): 848-850.
Pursell, Z. F., I. Isoz, E. B. Lundstrom, E. Johansson and T. A. Kunkel (2007). "Yeast DNA polymerase epsilon participates in leading-strand DNA replication." Science **317**(5834): 127-130.
Rabbitts, T. H. (1991). "Translocations, master genes, and differences between the origins of acute and chronic leukemias." Cell **67**(4): 641-644.
Rachidi, N., P. Barre and B. Blondin (1999). "Multiple Ty-mediated chromosomal translocations lead to karyotype changes in a wine strain of Saccharomyces cerevisiae." Mol Gen Genet **261**(4-5): 841-850.
Ramamoorthy, M., T. Tadokoro, I. Rybanska, A. K. Ghosh, R. Wersto, A. May, T. Kulikowicz, P. Sykora, D. L. Croteau and V. A. Bohr (2012). "RECQL5 cooperates with Topoisomerase II alpha in DNA decatenation and cell cycle progression." Nucleic Acids Res **40**(4): 1621-1635.
Resnick, M. A. (2005). "Reduced replication: a call to ARMS." Cell **120**(5): 569-570.
Robellet, X., V. Vanoosthuyse and P. Bernard (2017). "The loading of condensin in the context of chromatin." Curr Genet **63**(4): 577-589.
Roberts, R. W. and D. M. Crothers (1992). "Stability and properties of double and triple helices: dramatic effects of RNA or DNA backbone composition." Science **258**(5087): 1463-1466.
Roche, K. C. and N. F. Lowndes (2007). "An investigation into 53BP1 complex formation." Adv Exp Med Biol **604**: 47-57.
Roedgaard, M., J. Fredsoe, J. M. Pedersen, L. Bjergbaek and A. H. Andersen (2015). "DNA Topoisomerases Are Required for Preinitiation Complex Assembly during GAL Gene Activation." PLoS One **10**(7): e0132739.
Rouzeau, S., F. P. Cordelieres, G. Buhagiar-Labarchede, I. Hurbain, R. Onclercq-Delic, S. Gemble, L. Magnaghi-Jaulin, C. Jaulin and M. Amor-Gueret (2012). "Bloom's syndrome and PICH helicases cooperate with topoisomerase IIalpha in centromere disjunction before anaphase." PLoS One **7**(4): e33905.
Rowley, J. D. (1983). "Consistent chromosome abnormalities in human leukemia and lymphoma." Cancer Invest **1**(3): 267-280.
Rowley, J. D. (1984). "Biological implications of consistent chromosome rearrangements in leukemia and lymphoma." Cancer Res **44**(8): 3159-3168.
Roy, K. and G. F. Chanfreau (2017). "A global function for transcription factors in assisting RNA polymerase II termination." Transcription: 1-6.

Russell, B., S. Bhattacharyya, J. Keirsey, A. Sandy, P. Grierson, E. Perchiniak, J. Kavecansky, S. Acharya and J. Groden (2011). "Chromosome breakage is regulated by the interaction of the BLM helicase and topoisomerase IIalpha." Cancer Res **71**(2): 561-571.

Sabouri, N., K. R. McDonald, C. J. Webb, I. M. Cristea and V. A. Zakian (2012). "DNA replication through hard-to-replicate sites, including both highly transcribed RNA Pol II and Pol III genes, requires the S. pombe Pfh1 helicase." Genes Dev **26**(6): 581-593.

Saini, N., S. Ramakrishnan, R. Elango, S. Ayyar, Y. Zhang, A. Deem, G. Ira, J. E. Haber, K. S. Lobachev and A. Malkova (2013). "Migrating bubble during break-induced replication drives conservative DNA synthesis." Nature **502**(7471): 389-392.

Salas-Armenteros, I., C. Perez-Calero, A. Bayona-Feliu, E. Tumini, R. Luna and A. Aguilera (2017). "Human THO-Sin3A interaction reveals new mechanisms to prevent R-loops that cause genome instability." EMBO J.

Sanders, C. M. (2010). "Human Pif1 helicase is a G-quadruplex DNA-binding protein with G-quadruplex DNA-unwinding activity." Biochem J **430**(1): 119-128.

Santos-Pereira, J. M. and A. Aguilera (2015). "R loops: new modulators of genome dynamics and function." Nat Rev Genet **16**(10): 583-597.

Schwab, R. A., J. Nieminuszczy, F. Shah, J. Langton, D. Lopez Martinez, C. C. Liang, M. A. Cohn, R. J. Gibbons, A. J. Deans and W. Niedzwiedz (2015). "The Fanconi Anemia Pathway Maintains Genome Stability by Coordinating Replication and Transcription." Mol Cell **60**(3): 351-361.

Sfeir, A., S. T. Kosiyatrakul, D. Hockemeyer, S. L. MacRae, J. Karlseder, C. L. Schildkraut and T. de Lange (2009). "Mammalian telomeres resemble fragile sites and require TRF1 for efficient replication." Cell **138**(1): 90-103.

Singh, D. K., V. Popuri, T. Kulikowicz, I. Shevelev, A. K. Ghosh, M. Ramamoorthy, M. L. Rossi, P. Janscak, D. L. Croteau and V. A. Bohr (2012). "The human RecQ helicases BLM and RECQL4 cooperate to preserve genome stability." Nucleic Acids Res **40**(14): 6632-6648.

Sissi, C., E. Vazquez, A. Chemello, L. A. Mitchenall, A. Maxwell and M. Palumbo (2010). "Mapping simocyclinone D8 interaction with DNA gyrase: evidence for a new binding site on GyrB." Antimicrob Agents Chemother **54**(1): 213-220.

Skourti-Stathaki, K., K. Kamieniarz-Gdula and N. J. Proudfoot (2014). "R-loops induce repressive chromatin marks over mammalian gene terminators." Nature **516**(7531): 436-439.

Sollier, J. and K. A. Cimprich (2015). "Breaking bad: R-loops and genome integrity." Trends Cell Biol **25**(9): 514-522.

Sollier, J., C. T. Stork, M. L. Garcia-Rubio, R. D. Paulsen, A. Aguilera and K. A. Cimprich (2014). "Transcription-coupled nucleotide excision repair factors promote R-loop-induced genome instability." Mol Cell **56**(6): 777-785.

Soudet, J., P. Jolivet and M. T. Teixeira (2014). "Elucidation of the DNA end-replication problem in Saccharomyces cerevisiae." Mol Cell **53**(6): 954-964.

Sperling, A. S., K. S. Jeong, T. Kitada and M. Grunstein (2011). "Topoisomerase II binds nucleosome-free DNA and acts redundantly with topoisomerase I to enhance recruitment of RNA Pol II in budding yeast." Proc Natl Acad Sci U S A **108**(31): 12693-12698.

Srivatsan, A., A. Tehranchi, D. M. MacAlpine and J. D. Wang (2010). "Co-orientation of replication and transcription preserves genome integrity." PLoS Genet **6**(1): e1000810.

Stillman, B., S. P. Bell, A. Dutta and Y. Marahrens (1992). "DNA replication and the cell cycle." Ciba Found Symp **170**: 147-156; discussion 156-160.

Stirling, P. C., M. S. Bloom, T. Solanki-Patil, S. Smith, P. Sipahimalani, Z. Li, M. Kofoed, S. Ben-Aroya, K. Myung and P. Hieter (2011). "The complete spectrum of yeast chromosome instability genes identifies candidate CIN cancer genes and functional roles for ASTRA complex components." PLoS Genet **7**(4): e1002057.

Stirling, P. C., M. J. Crisp, M. A. Basrai, C. M. Tucker, M. J. Dunham, F. A. Spencer and P. Hieter (2012). "Mutability and mutational spectrum of chromosome transmission fidelity genes." Chromosoma **121**(3): 263-275.

Stirling, P. C. and P. Hieter (2017). "Canonical DNA Repair Pathways Influence R-Loop-Driven Genome Instability." J Mol Biol **429**(21): 3132-3138.

Tanaka, T. and K. Nasmyth (1998). "Association of RPA with chromosomal replication origins requires an Mcm protein, and is regulated by Rad53, and cyclin- and Dbf4-dependent kinases." EMBO J **17**(17): 5182-5191.

Toledo, L. I., M. Altmeyer, M. B. Rask, C. Lukas, D. H. Larsen, L. K. Povlsen, S. Bekker-Jensen, N. Mailand, J. Bartek and J. Lukas (2013). "ATR prohibits replication catastrophe by preventing global exhaustion of RPA." Cell **155**(5): 1088-1103.

Tsurimoto, T. and B. Stillman (1991). "Replication factors required for SV40 DNA replication in vitro. II. Switching of DNA polymerase alpha and delta during initiation of leading and lagging strand synthesis." J Biol Chem **266**(3): 1961-1968.

Tuduri, S., L. Crabbe, C. Conti, H. Tourriere, H. Holtgreve-Grez, A. Jauch, V. Pantesco, J. De Vos, A. Thomas, C. Theillet, Y. Pommier, J. Tazi, A. Coquelle and P. Pasero (2009). "Topoisomerase I suppresses genomic instability by preventing interference between replication and transcription." Nat Cell Biol **11**(11): 1315-1324.

Wang, J. C. (2002). "Cellular roles of DNA topoisomerases: a molecular perspective." Nat Rev Mol Cell Biol **3**(6): 430-440.

Watt, P. M., E. J. Louis, R. H. Borts and I. D. Hickson (1995). "Sgs1: a eukaryotic homolog of E. coli RecQ that interacts with topoisomerase II in vivo and is required for faithful chromosome segregation." Cell **81**(2): 253-260.

Webb, C. J. and V. A. Zakian (2016). "Telomerase RNA is more than a DNA template." RNA Biol **13**(8): 683-689.

Weinert, T. and L. Hartwell (1989). "Control of G2 delay by the rad9 gene of Saccharomyces cerevisiae." J Cell Sci Suppl **12**: 145-148.

Weinreich, M., C. Liang and B. Stillman (1999). "The Cdc6p nucleotide-binding motif is required for loading mcm proteins onto chromatin." Proc Natl Acad Sci U S A **96**(2): 441-446.

Wilson, T. E., M. F. Arlt, S. H. Park, S. Rajendran, M. Paulsen, M. Ljungman and T. W. Glover (2015). "Large transcription units unify copy number variants and common fragile sites arising under replication stress." Genome Res **25**(2): 189-200.

Yamagishi, Y., T. Sakuno, M. Shimura and Y. Watanabe (2008). "Heterochromatin links to centromeric protection by recruiting shugoshin." Nature **455**(7210): 251-255.

Yuce, O. and S. C. West (2013). "Senataxin, defective in the neurodegenerative disorder ataxia with oculomotor apraxia 2, lies at the interface of transcription and the DNA damage response." Mol Cell Biol **33**(2): 406-417.

Yuen, K. W., C. D. Warren, O. Chen, T. Kwok, P. Hieter and F. A. Spencer (2007). "Systematic genome instability screens in yeast and their potential relevance to cancer." Proc Natl Acad Sci U S A **104**(10): 3925-3930.

Yunis, J. J. (1984). "Fragile sites and predisposition to leukemia and lymphoma." Cancer Genet Cytogenet **12**(1): 85-88.

Yunis, J. J. and J. Tanzer (1993). "Molecular mechanisms of hematologic malignancies." Crit Rev Oncog **4**(2): 161-190.

Zaaijer, S., N. Shaikh, R. K. Nageshan and J. P. Cooper (2016). "Rif1 Regulates the Fate of DNA Entanglements during Mitosis." Cell Rep **16**(1): 148-160.

Zhang, J., Q. Dai, D. Park and X. Deng (2016). "Targeting DNA Replication Stress for Cancer Therapy." Genes (Basel) **7**(8).

Zhang, T., J. R. Paulson, M. Bakhrebah, J. H. Kim, C. Nowell, P. Kalitsis and D. F. Hudson (2016). "Condensin I and II behaviour in interphase nuclei and cells undergoing premature chromosome condensation." Chromosome Res **24**(2): 243-269.

Zhou, R., J. Zhang, M. L. Bochman, V. A. Zakian and T. Ha (2014). "Periodic DNA patrolling underlies diverse functions of Pif1 on R-loops and G-rich DNA." Elife **3**: e02190.

Zou, L. and B. Stillman (1998). "Formation of a preinitiation complex by S-phase cyclin CDK-dependent loading of Cdc45p onto chromatin." Science **280**(5363): 593-596.

Arlt, M. F., Casper, A. M., & Glover, T. W. (2003). Common fragile sites. *Cytogenet Genome Res, 100*(1-4), 92-100. doi:10.1159/000072843

Barlow, J. H., Faryabi, R. B., Callen, E., Wong, N., Malhowski, A., Chen, H. T., . . . Nussenzweig, A. (2013). Identification of early replicating fragile sites that contribute to genome instability. *Cell, 152*(3), 620-632. doi:10.1016/j.cell.2013.01.006

Bermejo, R., Capra, T., Jossen, R., Colosio, A., Frattini, C., Carotenuto, W., . . . Foiani, M. (2011). The replication checkpoint protects fork stability by releasing transcribed genes from nuclear pores. *Cell, 146*(2), 233-246. doi:10.1016/j.cell.2011.06.033

Bermejo, R., Kumar, A., & Foiani, M. (2012). Preserving the genome by regulating chromatin association with the nuclear envelope. *Trends Cell Biol, 22*(9), 465-473. doi:10.1016/j.tcb.2012.05.007

Berti, M., Ray Chaudhuri, A., Thangavel, S., Gomathinayagam, S., Kenig, S., Vujanovic, M., . . . Vindigni, A. (2013). Human RECQ1 promotes restart of replication forks reversed by DNA topoisomerase I inhibition. *Nat Struct Mol Biol, 20*(3), 347-354. doi:10.1038/nsmb.2501

Cortez, D. (2017). Proteomic Analyses of the Eukaryotic Replication Machinery. *Methods Enzymol, 591*, 33-53. doi:10.1016/bs.mie.2017.03.002

Cotta-Ramusino, C., Fachinetti, D., Lucca, C., Doksani, Y., Lopes, M., Sogo, J., & Foiani, M. (2005). Exo1 processes stalled replication forks and counteracts fork reversal in checkpoint-defective cells. *Mol Cell, 17*(1), 153-159. doi:10.1016/j.molcel.2004.11.032

Doksani, Y., Bermejo, R., Fiorani, S., Haber, J. E., & Foiani, M. (2009). Replicon dynamics, dormant origin firing, and terminal fork integrity after double-strand break formation. *Cell, 137*(2), 247-258. doi:10.1016/j.cell.2009.02.016

Durkin, S. G., & Glover, T. W. (2007). Chromosome fragile sites. *Annu Rev Genet, 41*, 169-192. doi:10.1146/annurev.genet.41.042007.165900

Glover, T. W., Berger, C., Coyle, J., & Echo, B. (1984). DNA polymerase alpha inhibition by aphidicolin induces gaps and breaks at common fragile sites in human chromosomes. *Hum Genet, 67*(2), 136-142.

Howlett, N. G., Taniguchi, T., Durkin, S. G., D'Andrea, A. D., & Glover, T. W. (2005). The Fanconi anemia pathway is required for the DNA replication stress response and for the regulation of common fragile site stability. *Hum Mol Genet, 14*(5), 693-701. doi:10.1093/hmg/ddi065

Jaarsma, D., van der Pluijm, I., de Waard, M. C., Haasdijk, E. D., Brandt, R., Vermeij, M., . . . van der Horst, G. T. (2011). Age-related neuronal degeneration: complementary roles of nucleotide excision repair and transcription-coupled repair in preventing neuropathology. *PLoS Genet, 7*(12), e1002405. doi:10.1371/journal.pgen.1002405

Lopes, M., Cotta-Ramusino, C., Pellicioli, A., Liberi, G., Plevani, P., Muzi-Falconi, M., . . . Foiani, M. (2001). The DNA replication checkpoint response stabilizes stalled replication forks. *Nature, 412*(6846), 557-561. doi:10.1038/35087613

Sirbu, B. M., McDonald, W. H., Dungrawala, H., Badu-Nkansah, A., Kavanaugh, G. M., Chen, Y., . . . Cortez, D. (2013). Identification of proteins at active, stalled, and collapsed replication forks using isolation of proteins on nascent DNA (iPOND) coupled with mass spectrometry. *J Biol Chem, 288*(44), 31458-31467. doi:10.1074/jbc.M113.511337

Song, W., Dominska, M., Greenwell, P. W., & Petes, T. D. (2014). Genome-wide high-resolution mapping of chromosome fragile sites in Saccharomyces cerevisiae. *Proc Natl Acad Sci U S A, 111*(21), E2210-2218. doi:10.1073/pnas.1406847111

Zheng, D. Q., Zhang, K., Wu, X. C., Mieczkowski, P. A., & Petes, T. D. (2016). Global analysis of genomic instability caused by DNA replication stress in Saccharomyces cerevisiae. *Proc Natl Acad Sci U S A, 113*(50), E8114-E8121. doi:10.1073/pnas.1618129113